Valorisation of paper waste sludge using pyrolysis processing

by

Angelo Mark Christopher Juan Johan Ridout

Dissertation presented for the Degree

of

DOCTOR OF PHILOSOPHY
(Chemical Engineering)

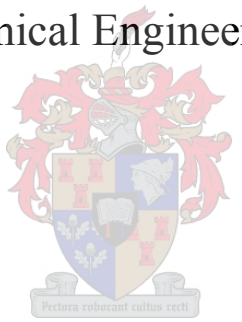

in the Faculty of Engineering
at Stellenbosch University

Supervisor
Prof. Johann Görgens

Co-Supervisor
Dr. Marion Carrier

March 2016

Declaration

By submitting this dissertation electronically, I declare that the entirety of the work contained therein is my own, original work, that I am the sole author thereof (save to the extent explicitly otherwise stated), that reproduction and publication thereof by Stellenbosch University will not infringe any third party rights and that I have not previously in its entirety or in part submitted it for obtaining any qualification.

Signature: …… Date: ……

This dissertation includes one original paper published in a peer reviewed journal and three unpublished publications. The development and writing of the papers (published and unpublished) were the principal responsibility of myself and, for each of the cases where this is not the case, a declaration is included in the dissertation indicating the nature and extent of the contributions of co-authors.

Abstract

Due to depleting fossil fuel reserves and environmental concerns over global warming, alternate sources such as renewable energy are required. One such renewable energy source is biomass which includes plant matter, agricultural residues and industrial wastes. Of interest in this study is the industrial waste paper waste sludge (PWS) which is generated in large quantities by the pulp and paper industry. PWS is mainly landfilled which is costly and environmentally unfriendly, and thus alternative methods of valorisation such as thermochemical and/or biochemical conversion needs to be considered. The thermochemical process of pyrolysis thermally decomposes biomass, in the absence of oxygen, into products of bio-oil, char and non-condensable gas which have various beneficial applications. Alternatively, biochemical conversion of PWS into bioethanol using fermentation can be used as an initial step, followed by pyrolytic conversion of its fermentation residues (FR).

The global objective of this PhD project was to assess the full potential of alternative pyrolysis processes, at varying key operating conditions, as part of a biorefinery to maximise the conversion of PWS and its FR, containing variable amount of organic material, into energy, chemical and biomaterial resources. In addition, statistical analysis of the product yields and quality were performed to reveal new mechanistic insights.

The first part of the study considered the maximisation of the bio-oil yield from low and high ash PWS (8.5 and 46.7 wt.%) using fast pyrolysis (FP) processing. To do this, both reactor temperature and pellet size were optimised using a 2-way linear and quadratic model. Maximum bio-oil yields of 44.5 and 50.0 daf, wt.% were obtained at an intermediate pellet size of ~5 mm and optimum reactor temperatures of 400 and 340 ^{o}C for the low and high ash PWS, respectively. In addition to the above, a thermogravimetric study was implemented to gain insights in the

thermodynamic mechanisms behind the increase in bio-oil yield with larger pellet sizes. Results indicated that fewer secondary tar cracking reactions were prevalent due to lower mass transfer limitations leading to greater yields of bio-oil.

Vacuum, slow and fast pyrolysis processes were assessed and compared, at varying reactor temperatures and pellet sizes, for their ability to maximize the gross energy conversion (EC) from the raw PWS to the liquid and solid products. A 2-way linear and quadratic model was used for the statistical approach. Comparison of the overall EC, as a combination of the solid and liquid products, revealed that FP was between 18.5 and 20.1 % higher for low ash PWS (LAPWS), and 18.4 to 36.5 % higher for high ash PWS (HAPWS) when compared to slow and vacuum pyrolysis. This finding was mainly attributed to the higher production of organic condensable compounds during FP for both PWS. The calorific values displayed by the vacuum pyrolysis (VP) tarry phase and FP bio-oil for both PWSs, as well as the LAPWS char, were high (~18 to 23 $MJ.kg^{-1}$) highlighting their potential for industrial energy applications.

The capability of vacuum, slow and fast pyrolysis to selectively drive the conversion of raw PWS into chemicals (primarily glycolaldehyde and levoglucosan) and biomaterials (sorption medium or biochar) was assessed. Product yields were optimised according to reactor temperature and pellet size (2-way linear and quadratic model) and their variability quantified using principal component analysis (PCA). Results indicated that the high heating applied by FP significantly promoted depolymerisation and/or fragmentation reactions leading to higher yields of most organic compounds, particularly levoglucosan for both LAPWS (1.5 daf, wt.%) and HAPWS (3.7 daf, wt.%). The char biomaterial displayed by both PWSs were ultra-microporous, and the application of VP significantly enhanced the sorptive properties of the LAPWS char.

Sequential PWS fermentation for bioethanol production (separate study), followed by pyrolytic conversion of the FR using alternative processes at varying reactor temperatures, was performed to

maximise the recovery of energy, of which the performance was compared to stand-alone pyrolysis. The recovery of energy was maximised by coupling PWS fermentation and FR fast pyrolysis, resulting in gross ECs of between ~75 and 88% for the LAPWS, and ~41 and 48 % for the HAPWS. These gross ECs were up to ~10 % higher in comparison to those attained for stand-alone pyrolysis of PWS. The greater availability of lignin in FR, after fermentation, led to bio-oil products that were phenols-rich.

In summary, the present study pointed out the promising potential of pyrolysis processing of PWS/FR as part of a biorefinery for production of fuels, chemicals and biomaterials resources. FP maximised the organic liquid and levoglucosan yields as well as the gross EC from PWS. Sequential fermentation of PWS coupled with FP of FR maximised the gross ECs, which were higher in comparison to stand-alone PWS pyrolysis ECs. To confirm which process option is best in terms of overall energy efficiency and economics additional modelling and economic feasibility studies are recommended.

Opsomming

Alternatiewe energie bronne soos hernubare energie is nodig as gevolg van verminderde natuurlike energie bronne en omgewingsbewustheid rakende aardverwarming. ’n Voorbeeld van ’n hernubare energiebron is biomassa. Biomassa sluit onder andere plantmateriaal, landboureste en industriële afval in. Die pulp en papier industrie genereer groot hoeveelhede papierafvalslik, wat ryk is aan organiese materiaal en vog, en dus die potensiaal het om as ’n hernubare energie bron aangewend te word. Hierdie energiebron is die fokus van hierdie studie. Weens die hoë kostes en omgewingsbekommernisse wat gepaard gaan met die storting van papierafvalslik, moet daar gekyk word na ander metodes van waarde-toevoeging, onder andere termochemiese en/of biochemiese omsetting. Die termochemiese prosesse van pirolise ontbind biomassa termies in die afwesigheid van suurstof, wat dan bio-olies, houtskool en nie-kondenseerbare (permanente) gasse produseer, wat almal voordelig aangewend kan word as energie, chemikalieë of bio-materiale. Alternatiewelik kan die biochemiese omskakeling van papierafvalslik na bioëtanol, deur ’n fermentasie proses, gebruik word as ’n aanvanklike stap, gevolg deur die pirolitiese omskakeling van die fermentasiereste.

Die primêre oogmerk van hierdie PhD studie was assessering van die volle potensiaal van alternatiewe pirolise tegnieke as deel van ’n bio-raffinadery, teen verskillende toestande, om die omskakeling van papierafvalslik en sy fermentasiereste, in energie, chemikalieë en bio-materiale besit. Statistiese analise van produkopbrengs en kwaliteit was ook gedoen om nuwe meganistiese kennis te ontsluit.

Die eerste gedeelte van die studie het gekyk na die optimering van die bio-olie opbrengs van lae-as en hoë-as papierafvalslik (8.5 en 46.7 massa %) deur gebruik te maak van die vinnige pirolise proses. Beide reaktor temperatuur en partikel grootte was geoptimeer deur gebruik te maak van ’n 2-wyse lineêre en kwadratiese model. Teen ’n gemiddelde partikel grootte van ~5mm en optimale

reaktor temperatuur, is ’n maksimum bio-olie opbrengs van 45 en 50 massa % (droë as-vrye basis) verkry vir lae-as en hoë-as papierafvalslik. ’n Termogravimetriese studie is ook gedoen om insig in die termodinamiese meganisme te verkry, nadat ’n verhoging in bio-olie opbrengs met die groter partikels opgemerk is. Resultate wys ook dat minder sekondêre teer-krakingsreaksies gebeur as gevolg van laer massa oordrag, wat lei tot ’n groter bio-olie opbrengs.

Vakuum, stadige en vinnige pirolise prosesse is geëvalueer en vergelyk teen verskillende reaktor temperature en partikel groottes in terme van hulle die bruto energie opbrengste (EO) van die rou papierafvalslik na die soliede en vloeistof produkte. Weereens is ’n 2-wyse lineêre en kwadratiese model gebruik vir die statistiese evaluering. ’n Vergelyking van die totale EO, as ’n kombinasie van die soliede en vloeistof produkte, wys dat vinnige pirolise tussen 18.5 en 20.1 % hoër opbrengste vir lae-as papierafvalslik, en 18.4 tot 36.5 % hoër vir hoë-as papierafvalslik, in vergelyking met stadige en vakuum pirolise kon lewer. Hierdie bevinding word verklaar deur die hoër produksie van die organiese kondenseerbare komponente gedurende vinnige pirolise vir alle tipes slyke. Die verhittingswaardes van die teer-fase vanaf vakuum pirolise en vinnige pirolise bio-olie vir beide papierafvalslik, en ook lae-as papierafvalslik houtskool, was hoog (~18 tot 23 $MJ.kg^{-1}$) wat die potensiaal vir industriële energie toepassings, beklemtoon.

Die vermoë van vakuum, stadige en vinnige pirolise om die selektiewe omskakeling van rou papierafvalslik tot chemikalieë (veral glikolaldehied en levoglukosaan) en houtskool-biomateriale (absorberende stof of biohoutskool) was geëvalueer. Produkopbrengs was geoptimeer volgens reaktor temperatuur en partikel grootte (2-wyse lineêre en kwadratiese model) en die wisselvalligheid gekwantifiseer deur gebruik te maak van basiese komponent analise. Resultate wys dat die hoë verhittingstempo gebruik gedurende die vinnige pirolise proses die de-polimerisasie en/of fragmentasie reaksies bevoordeel het, wat lei tot hoë opbrengste van meeste organiese komponente, spesifiek levoglukosaan vir lae-as papierafvalslik (1.5 droë asvrye basis, massa %) en

hoë-as papierafvalslik (3.7 droë asvrye basis, massa %). Die koolstof bio-materiaal verkry met beide papierafvalslyke was ultra-mikroporieus en die gebruik van vakuum pirolise het die absorberende eienskappe van die lae-as papierafvalslik koolstof betekenisvol verbeter.

Om die herwinning van energie te maksimeer is opeenvolgende papierafvalslik fermentasie (bioëtanol produksie – aparte studie), gevolg deur pirolise omskakeling van fermentasiereste teen verskillende reaktor temperature, vergelyking met die uitsette van pirolise alleen. Die herwinning van energie was gemaksimeer deur die kombinasie van papierafvalslik fermentasie en fermentasiereste vinnige-pirolise. Die resultaat was ’n bruto EO van ~75 tot 88% vir lae-as papierafvalslik, en ~41 tot 48% vir hoë-as papierafvalslik. Hierdie bruto EOs was tot ~10% hoër in vergelyking met pirolise van papierafvalslik alleen. Die groter beskikbaarheid van lignien in fermentasiereste na fermentasie het gelei tot bio-olie produkte wat ryk was in fenole.

Ter opsomming, die huidige studie wys na die hoë potensiaal van prosessering van papierafvalslik en fermentasiereste deur pirolise as deel van ’n bio-raffinadery vir produkte van brandstof, chemikalieë en bio-materiale. Vinnige pirolise maksimeer die organiese vloeistof en levoglukosaan opbrengs asook die bruto EV vanaf papierafvalslik. Opeenvolgende fermentasie van papierafvalslik in kombinasie met vinnige pirolise van fermentasiereste maksimeer die bruto EOs. Dit resultate was hoër in vergelyking met papierafvalslik pirolise alleen. Addisionele modellering en ekonomiese uitvoerbaarheidstudies word aanbeveel om te bevestig watter proses is die beste in terme van energie doeltreffendheid en ekonomiese uitvoerbaarheid.

Dedication

This work is dedicated to my late father Jeffrey, my mother Lesley, as well as my lovely wife Romien who has been by myside supporting me every step of the way.

Acknowledgements

I would like to thank my supervisor Prof. Johann Görgens for the guidance as well as the opportunity given to me by him. I am especially indebted to my co-supervisor Dr. Marion Carrier as well as Dr. François-Xavier Collard for their guidance, comments, encouragement and support throughout the course of this degree. I would like to thank Kimberly-Clark SA, the Paper Manufacturers Association of South Africa (PAMSA) and FP&M Seta for their financial support. For the numerous analysis performed I would like to thank the following technicians; Hanlie Botha, Levine Simmers, Cynthia Sanchez-Garrido and Hendricks Solomon. Finally, I thank God for guiding me throughout the project.

Table of contents

List of Figures

Chapter 2

Chapter 4

Chapter 5

Chapter 6

Chapter 7

List of Tables

Chapter 2

Chapter 4

Chapter 5

Chapter 6

Chapter 7

Chapter 9

List of acronyms and abbreviations

AC	Ash content
BET	Brunauer, Emmet and Teller
BFBR	Bubbling fluidised bed reactor
DFT	Density function theory
EC	Energy conversion
FB	Fixed bed
FP	Fast pyrolysis
FR	Fermentation residue
GC-MS	Gas chromatography-mass spectrometery
HAFR	High ash fermentation residue
HAPWS	High ash paper waste sludge
LAFR	Low ash fermentation residue
LAPWS	Low ash paper waste sludge
PA	Peak area percentage
PWS	Paper waste sludge
SP	Slow pyrolysis
TGA	Thermogravimetric analysis
VP	Vacuum pyrolysis

CHAPTER 1: INTRODUCTION

1.1 BACKGROUND AND CONTEXT

The worlds current annual energy demand is estimated at approximately 0.55 quadrillion MJ, and is expected to grow by ~56% by 2040 [1]. Currently fossil fuels such as petroleum liquids, coal, and natural gas dominate the supply of energy accounting for up to 86% [1]. Due to depleting fossil fuel reserves as well as environmental concerns over global warming [2], alternatives sources of renewable energy are required. One such renewable energy source is biomass, which is abundant in the quantity produced in nature [3], and is high in organic content [4]. Plant biomass is not only available through cultivation of so-called "energy crops", but also as agricultural residues and industrial wastes [5,6].

The pulp and paper industry produces large quantities of paper waste sludge (PWS), which is high in organic and moisture content, and has the potential for use as a renewable energy source [4]. PWS is unsuitable for use in pulp and/or paper production due to short fibre length and poor fibre quality being inadequate for the finished product. Typical quantities produced by a mill are in the range of 100 to 500 kg's per ton of paper produced, and these residues are usually disposed of by land filling [7]. However due to increasing costs and negative environmental impacts of land filling, new alternative valorisation methods such as biochemical and/or thermochemical conversion are required.

Low energy density biomass and its processing residues can be converted into high-quality energy products through biochemical and/or thermochemical conversion routes [5,8]. Biochemical conversion, such as fermentation, utilizes a biological catalyst (enzymes) to convert sugars, which are obtained from the fractionation of carbohydrates (cellulose and hemicelluloses), into value-

added bioethanol or biogas leaving behind waste fermentation residues (FR), and in particular most of the initial lignin which is hardly converted [5,8]. The conversion of PWS via fermentation has been shown to be a promising option for bioethanol production as it is easily hydrolysed, due to its high water content (> 60 wt.%), thus reducing process cost, and is mainly comprised of cellulose [8-11]. However, PWS fermentation generates large quantities FR, which contains significant amounts of organic material. Moreover, despite some of the FR being combusted to supplement heat energy requirements (e.g., ethanol distillation), a large fraction remains unused (~60 %) [12]. The thermochemical conversion routes, which include combustion, pyrolysis, gasification and liquefaction, present the advantage of complete conversion all the organic components of the biomass. The main subject of this work will be the process of pyrolysis, whereby biomass is thermally decomposed, in the absence of oxygen, into products of bio-oil, gas and char that have various possible applications (energy, chemicals, materials) [13]. Depending on the type of pyrolysis reactor and operating conditions (e.g., temperature, particle size, pressure, heating rate etc) employed, the production of either bio-oil, char or gas is promoted [13]. The range of pyrolysis processes includes fast, intermediate and slow pyrolysis, whereby major differences lie with the applied heating rate and product residence time [13]. Fast pyrolysis (FP) utilises high heating rates with short vapour residence times, resulting in the promotion of bio-oil production and has not been considered for PWS [13-15]. On the other hand, slow pyrolysis (SP) utilises low heating rates with long vapour residence times, resulting in the maximisation of the char yield [13]. The conditions of intermediate pyrolysis (IP) lie between those of fast and slow pyrolysis, whereby moderate heating rates and vapour residence times lead to a good compromise for bio-oil, char and non-condensable gas production [13]. Recent studies have shown that conversion of PWS via slow and intermediate pyrolysis was promising [16-19]. Slow pyrolysis was a technically feasible approach to PWS

valorisation, while intermediate pyrolysis significantly increased the energy content of its bio-oils (~36 $MJ.kg^{-1}$). Bio-oils with such high calorific values could have promising potential for use in bio-energy applications such as transportation fuels [13], thermal and electrical energy [13-15]. When considering the performance of pyrolysis based on gross energy conversion from raw biomass to the pyrolysis products, studies have highlighted the importance of both the operating conditions and the biomass type [20-22]. However, no studies have compared the ability of different pyrolysis techniques to convert biomass or PWS in terms of gross energy conversion (EC). Alternatively, bio-oil could find use as a feedstock for high-value marketable green chemicals production, which has recently gained interest with the aim of replacing existing petroleum based chemicals [13,23,24]. The literature on the use of PWS bio-oil for high-value chemicals production is limited, and due to the presence of degraded fibres, PWS is likely to give a unique bio-oil composition, compared to products from derived from virgin lignocellulose [25]. Furthermore, studies investigating the chemical selectivity of various pyrolysis processes (FP, SP, IP) are few [26,27], and have only considered the differences between SP and FP. Char can be used as fuel for heat energy production via combustion [28], or as an adsorbent in applications such as soil remediation (biochar) or water treatment (pollutant removal) [29-33]. A number of studies have pointed out the potential of char biomaterials prepared from SP of PWS [29-33], while the potential performance improvement using an intermediate process such vacuum pyrolysis (VP) [34], has not been considered.

When considering the integration of both biochemical and thermochemical processes [35], fermentation can be used as an initial step to convert PWS into bioethanol, followed by pyrolytic conversion of its FR into additional value-added products. Such an option will also be considered and compared with stand-alone pyrolysis. FR is also known to have better dewaterability through

mechanical processing (lower water holding capacity), compared to PWS, thus further reducing the energy demands of drying before pyrolysis [36]. The valorisation of PWS-derived FR via pyrolysis is scarcely reported. The conversion of PWS using either stand-alone pyrolysis or the integrated fermentation and pyrolysis for co-production of materials, chemicals and fuel products, offers a great opportunity to illustrate the biorefinery concept [5,37].

1.2 THESIS OUTLINE

This dissertation is organised in 9 chapters. **Chapter 2** discusses the state of the art of on the origin and composition of paper waste sludge and fermentation residue, as well as pyrolysis processes for their conversion. C**hapter 3** details the objectives synthesised from the gaps in the literature. **Chapter 4** presents the results from the fast pyrolysis of raw PWS, as well as a thermodynamic mechanistic study using thermogravimetric analysis. **Chapter 5** presents an energy conversion assessment on the performance of slow, vacuum and fast pyrolysis processes to convert energy from raw PWS to the solid and liquid products. An assessment on the capability of various pyrolysis processes to drive the conversion of raw PWS into targeted chemicals and biomaterials are detailed in **Chapter 6**. **Chapter 7** presents an exploratory study on the conversion of raw FR using various pyrolysis processes for production of energy, chemicals and biomaterials. **Chapter 8** details a summary of the main findings and **Chapter 9** provides the main conclusions and recommendations.

1.3 REFERENCES

[1] Energy Information Administration (EIA), International Energy Outlook 2013, Department of Energy (DOE), U.S. Government: Washington D.C., 2013.

[2] N. Scarlat, J. Dallemand, F. Monforti-Ferrario, V. Nita, The role of biomass and bioenergy in a future bioeconomy: Policies and facts, Environmental Developments (45) (2015) 3-34.

[3] A. Demirbas, Biomass resource facilities and biomass conversion processing for fuels and chemicals, Energy Conversion and Management (42) (2001) 1357-1378.

[4] S. Yilmaz, H. Selim, A review on the methods for biomass to energy conversion, Renewable and Sustainable Energy Reviews (25) (2013) 420-430.

[5] S.N. Naik, V.V. Goud, P.K. Rout, A.K. Dalai, Production of first and second generation biofuels: A comprehensive review, Renewable and Sustainable Energy Reviews (14) (2010) 578-597.

[6] F. Cherubini, The biorefinery concept: Using biomass instead of oil for producing energy and chemicals, Energy Conversion and Management (51) (2010) 1412-1432.

[7] M.C. Monte, E. Fuente, A. Blanco, C. Negro, Waste management from pulp and paper production in the European Union, Waste Management (29) (2009) 293-308.

[8] P. McKendry, Energy production from biomass (part 2): conversion technologies, Bioresource Technology (83) (2002) 47-54.

[9] H. Chen, R. Venditti, R. Gonzalez, R. Phillips, H. Jameel, S. Park, Economic evaluation of the conversion of industrial paper sludge to ethanol, Energy Economic, (44) (2014) 281-290.

[10] Y. Yamashita, A. Kurosumi, C. Sasaki, Y. Nakamura, Ethanol production from paper sludge by immobilized Zymomonas mobilis, Biochemical Enginnering Journal, (42) (2008) 314-319.

[11] L. Peng, Y. Chen, Conversion of paper sludge to ethanol by separate hydrolysis and fermentation (SHF) using Saccharomyces cerevisiae, Biomass and Bioenergy (35) (2011) 1600-1606.

[12] P. Saasner, M. Galbe, G. Zacchi, Techno-economic evaluation of bioethanol production from three different lignocellulosic materials, Biomass and Bioenergy (32) (2008) 422-430.

[13] A.V. Bridgwater, Review of fast pyrolysis of biomass and product upgrading, Biomass and Bioenergy (38) (2012) 68-94.

[14] D. Mohan C.U, Pittman, P.H. Steele, Pyrolysis of Wood/Biomass for Bio-oil: A critical review, Energy and Fuels, (20) (2006) 848-889.

[15] A.V. Bridgwater, G.V. C. Peacock, Fast pyrolysis processes for biomass, Renewable and Sustainable Energy Reviews (2000) (4) 1-73.

[16] R. Lou, S. Wu, G. Lv, Q. Yang, Energy and resource utilization of deinking sludge, Applied Energy (90) (2012) 46-50.

[17] M. Ouadi, J.G. Brammer, Y. Yang, A. Hornung, M. Kay, The intermediate pyrolysis of deinking sludge to produce a sustainable liquid fuel, Journal of Analytical and Applied Pyrolysis (105) (2013) 135-142.

[18] Y. Yang, J.G. Brammer, M. Ouadi, J. Samanya, A. Hornung, H.M. Xu, Y. Li, Characterisation of waste derived intermediate pyrolysis oils for use as diesel engine fuels, Fuel (103) (2013) 247-257.

[19] V. Strezov, T.J. Evans, Thermal processing of paper sludge and characterisation of its pyrolysis products, Waste Management (2009) (29) 1644-1648.

[20] X. Li, V. Strezov, T. Kan, Energy recovery potential analysis of spent grounds pyrolysis products, Journal of Analytical and Applied Pyrolysis (110) (2014) 79-87.

[21] N. Troger, D. Richter, R. Stahl, Effect of feedstock composition on product yields and energy recovery rates of fast pyrolysis products from different straw types, Journal of Analytical and Applied Pyrolysis (100) (2013) 158-165.

[22] A.L.M.T. Pighinelli, A.A. Boateng, C.A. Mullen, Y. Elkasabi, Evaluation of Brazillian biomasses as feedstocks for fuel production via fast pyrolysis, Energy for Sustainable Development (21) (2014) 42-50.

[23] X. Zhang, G. Yang, H. Jiang, W. Liu, H. Ding, Mass production of chemicals from biomass-derived oil by directly atmospheric distillation coupled with co-pyrolysis, Scientific Reports (3) 1120-1127.

[24] Y. Elkasabi, C.A. Mullen, A.A. Boateng, Distillation and isolation of commodity chemicals from bio-oil made by tail-gas reactive pyrolysis, Sustainable Chemistry and Engineering (2) (2014) 2042-2052.

[25] A. Mendez, J.M. Fidalgo, F. Guerrero, G. Gasco, Characterization and pyrolysis behaviour of different paper mill waste materials, Journal of Analytical and Applied Pyrolysis (86) (2009) 66-73.

[26] C.E. Greenhalf, D.J. Nowakowski, A.B. Harms, J.O. Titiloye, A.V. Bridgwater, Sequential pyrolysis of willow SRC at low and high heating rates – Implications for selective pyrolysis, Fuel (93) (2012) 692-702.

[27] H. Ben, A.J. Ragauskas, Comparison for the compositions of fast and slow pyrolysis oils by NMR characterization, Bioresource Technology (147) (2013) 577-584.

[28] C. Di Blasi, Combustion and gasification rates of lignocellosic chars, Progress in Energy and Combustion Science (35) (2009) 121-140.

[29] V. Calisto, C.I.A. Ferreira, S.M. Santos, M.V. Gil, M. Otera, V.I. Esteves, Production of adsorbents by pyrolysis of paper mill sludge and application on the removal of citalopram from water, Bioresource Technology (166) (2014) 335-344.

[30] A. Mendez, J. Paz-Ferreiro, F. Araujo, G. Gasco, Biochar from pyrolysis of deinking paper sludge and its use in the treatment of a nickel polluted soil, Journal of Analytical and Applied Pyrolysis (107) (2014) 46-52.

[31] S.M. Martin, R.S. Kookana, L. van Zwieten, E. Krull, Marked changes in herbicide sorption-desorption upon ageing of biochars in soil, Journal of Hazardous Materials (231-232) (2012) 70-78.

[32] S. Rajkovich, A. Enders, K. Hanley, C. Hyland, A.R. Zimmerman, J. Lehmann, Corn growth and nitrogen nutrition after additions of biochars with varying properties to a temperate soil, Biology and Fertility of Soils (48) (2012) 271-284.

[33] A. Mendez, S. Barriga, J.M. Fidalgo, G. Gasco, Adsorbent materials from paper industry waste materials and their use in Cu(II) removal from water, Journal of Hazadous Materials (165) (2009) 736-743.

[34] M. Carrier, T. Hugo, J. Gorgens, H. Knoetze, Comparison of slow and vacuum pyrolysis of sugar cane bagasse, Journal of Analytical and Applied Pyrolysis (90) (2011) 18-26.

[35] Y. Shen, L. Jarboe, R. Brown, Z. Wen, A thermochemical-biochemical hybrid processing of lignocellulosic biomass for producing fuels and chemicals, Biotechnology Advances, doi:10.1016/j.biotechadv.2015.10.006.

[36] S. Boshoff, Characterization and fermentation of waste paper sludge for bioethanol production, Masters Dissertation, Department of Process Engineering, Stellenbosch University, Cape Town, 2015.

[37] S. Fernando, S. Adhikari, C. Chandrapal, N. Murali, Biorefineries: Current status, challenges, and future direction, Energy &Fuels (20) (2006) 1727-1737.

CHAPTER 2: LITERATURE REVIEW

This chapter presents an overview of the literature on paper waste sludge and its fermentation residues, as well as the pyrolysis processes for their conversion. Firstly, it introduces the origin and physico-chemical characterisation of paper waste sludge and its fermentation residue, which will have an impact on the pyrolytic pathways. Secondly, the applicability and likely performance of pyrolysis conversion of paper waste sludge and its fermentation residues will be reviewed.

2.1 ORIGIN OF PULP AND PAPER SLUDGE

The pulp and paper industry utilises a cellulose-based feedstock to manufacture pulp, paper, tissue, board and other cellulose type products. It contributes up to 0.6 % to the South African gross domestic product (R 18.2 billion), according to a 2013 report by the Paper Manufacturing Association of South Africa (PAMSA) [1].

Pulp mills use mechanical and/or chemical processes to separate cellulose fibres from woody and/or non-woody (bamboo, sugarcane bagasse) lignocellulosic feedstock for the manufacturing of virgin pulp [2]. Mechanical processing involves physical methods, such as refining-refiner to release the fibres, followed by thermal treatment using steam, and then bleaching to brighten the pulp. This process is costly, although a pulp yield of ~95% of the feedstock can be achieved [2]. One commonly used chemical process is the Kraft process, which uses both NaOH and NaS solution to dissolve the lignin (binder) and release the fibres, which is followed by a bleaching stage to brighten the pulp [2]. When compared to mechanical processes, chemical processing is less costly, although pulp yields of approximately ~45% on feedstock utilisation are achieved [2]. Subsequently, the fraction of unused feedstock forms the waste which includes inorganics (green liquor), short fibres (primary/secondary clarifier), fines and bark (rejects), etc. [2,3].

Paper mills use virgin pulp and/or recycle fibre (newsprint, paper, corrugated boxes etc) as feedstock for the manufacturing of paper, tissue, board and other cellulose type products. Virgin pulp gets directly re-pulped and fed to the paper machines, while recycle fibre must be processed beforehand to remove inks (deinking), fillers, fines, short fibres, chemical additives and contaminants generating large amounts of wastes [2,3]. Depending on the required quality of the paper product, different blends of virgin pulp and/or recycle fibre are used [2].

One of the wastes generated during the pulp or papermaking process is termed paper waste sludge (PWS), and is typically obtained from the wastewater clarification dams. It is rejected for use, ending up in the wastewater circuit, as the fibre length and quality are inadequate for a finished product. Typical quantities produced by pulp and paper mills are in the range of 60-100 kg and 50-600 kg per ton of final product, respectively, and is usually disposed of by landfilling [3]. Depending on the mill type and production rate, typically quantities of PWS generated can vary between ~3000 to 22000 dry tons of PWS per year. Due to increasing costs and negative environmental impact of land filling, a more environmentally alternative is required for the valorisation of PWS.

2.2 ORIGIN OF FERMENTATION RESIDUE

Fermentation residues are a waste by-product generated during fermentation of lignocellulosic material, and are primarily comprised of lignin, unconverted sugars and ash [4,5]. Although some of the fermentation residues are combusted to supplement heat requirements (e.g., ethanol distillation), a large fractions remains unutilized (~60 %) [6]. Considering the techno-economic feasibility of PWS fermentation [7-10], as well as the drive to find alternative valorisation methods, industrial commercialisation could be expected, resulting in large production of PWS-derived FR.

2.3 BIOREFINERY CONCEPT

The biorefinery concept can be defined as the optimised conversion of biomass, utilizing various technologies that are fully integrated, for the co-production of value-added materials, energy, fuels and chemicals [11,12]. The performance parameters of a biorefinery are based holistically on the product yields, costs, economics and environmental impact [12]. The biorefinery concept is not new, although studies on its economic potential are recent [12], and have not yet been considered for PWS. When considering the potential of pyrolysis or integrated fermentation and pyrolysis as a section in a biorefinery, several potential value-added chemicals, energy and biomaterial resources are generated [12-21]. A number of studies investigating the valorisation of PWS via pyrolysis have highlighted the practical feasibility, as well as the potential of the products [17-20,22-28]. Furthermore, fermentation appears to be a promising option for bioethanol production from PWS [7-10], and some studies have pointed out the feasibility of FR pyrolysis [29-31]. Thus, as PWS is generated in large readily available quantities [3], an approach to its valorisation using pyrolysis or the integrated fermentation and pyrolysis in a biorefinery setting would be interesting.

2.4 BIOMASS FEEDSTOCK

2.4.1 First and second-generation feedstock

In the biorefinery concept, the feedstock is considered as either first- or second-generation [32]. First generation feedstocks originate from food crops, such as corn, sugarcane and seed oil, etc. [11,32]. The main disadvantage of using first generation feedstocks for fuel production is that it is in competition for fertile land with food production [32]. On the other hand, second-generation feedstocks, which originates from non-food lignocellulosic sources such as agricultural residues

(tops and trash), industry wastes (paper waste sludge), and forest residues (sawdust), are abundant and do not compete with food production [11,32]. In addition, it is recognized that the conversion of a second-generation feedstock may help to reduce greenhouse gas emissions [11], and has been shown be economically viable (lignocellulose to ethanol biorefinery) [33]. Thus, as paper waste sludge and fermentation residue are readily available wastes, they can be considered a second-generation feedstock [3,10].

2.4.2 Lignocellulosic Biomass composition

Lignocellulosic biomass and its industrial residues are comprised of a composite mixture of materials constructed from oxygen-containing organic polymers, such as cellulose, hemicelluloses and lignin, as well as extractives and inorganic minerals [13].

2.4.2.1 Cellulose

Cellulose forms the main structural component of the plant cell wall [34], and is typically found in quantities of between ~40 to 50 wt.% (dry, ash and extractives free weight basis) (Table 2-1). An illustration of a cellulose polymer, which is typically comprised of between 5000 to 10000 linear interconnecting (C1 conformation) β-(1-4) glucopyranose units [13], is presented by Figure 2-1. Micro-fibril like sheets consists of groups of these cellulose polymers, which twist and bond together, with the help of hydrogen bonding, to form complex fibres [13]. These micro-fibril sheets form composite tubular structures that run along the tree giving structural strength.

Table 2-1. Compositional analysis composition of various biomass types

Biomass	Cellulose	Hemicelluloses	Lignin	Ash	Reference
		(wt.%)[a]		(wt.%, df)	
Woody biomass					
Eucalyptus *grandis*	46.8	20.8	29.3	0.3	[35]
Poplar	50.2	25.2	18.2	0.5	[36]
Bamboo	51.2	24.6	23.8	1.5	[35]
Grassy biomass					
Switchgrass	40.6	32.0	23.0	5.8	[37]
Rice straw	52.0	37.1	18.0	16.1	[36]
Agricultural residues					
Sugarcane bagasse	44.2	31.8	23.8	2.5	[35]
Corn stover	43.6	25.9	17.8	6.3	[36]
Rice husks	41.5	35.3	23.2	17.1	[38]

[a]dry, ash and extractives free weight basis (normalised); df: dry free basis.

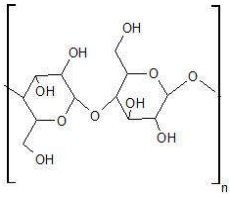

Figure 2-1. Cellulose polymer

2.4.2.2 Hemicelluloses

The hemicellulosic fraction is found between the cellulose cell walls with the function of binding the microfibrils together, and is typically found in quantities of between ~20 to 30 wt.% (dry, ash and extractives free weight basis) (Table 2-1). Unlike cellulose, hemicelluloses are substantially shorter with up to 150 interconnecting linear and/or branched monosaccharide units [13]. The most common monosaccharide units include D-glucose, D-xylose, D-galactose, D-mannose, L-arabinose and D-glucuronic acid (Figure 2-2a) [13], which can form α(1-2), α(1-3), α(1-3), β(1-3), β(1-4), and β(1-6) type bonds between them. An example of a commonly found

branched polymer, xylan, is illustrated by Figure 2-2b. Other typical polymers include mannan, glucan, galactan and pectin.

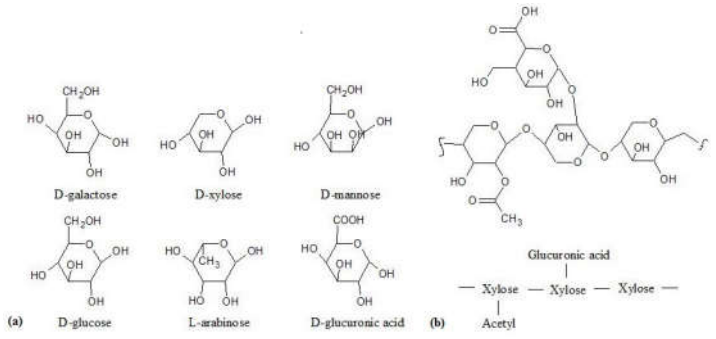

Figure 2-2. a) Examples of hemicellulose monomers; b) Partial structure of xylan

2.4.2.3 Lignin

Lignin is found in the cell walls and acts as a resin (glue) binding the fibre together. It is typically found in quantities of between ~18 to 30 wt.% (dry, ash and extractives free weight basis) (Table 2-1), and is comprised of three monomeric phenylpropane units (Figure 2-3). The monomeric phenylpropane units, which include p-coumaryl, coniferyl, and sinapyl alcohols, randomly interconnect to form three-dimensional lignin polymers with no exact repetitive structure [13]. The specific structure of lignin varies greatly between different biomass species, and can be altered during isolation [39,40]. The types of bonds that exist between the monomeric phenylpropane units include β-alky aryl ether (A), α-alkyl aryl ether (B), phenylcoumaran (C), biphenyl (D), aryl-alkyl-aryl linkage (E), β-β alky linkage (F), and glyceraldehyde-2-aryl ether (G) [41]. From Figure 2-4 it can be seen that bond types A, B, C and G are between carbon and oxygen atoms (C-O), while bonds D, E and F are between two carbon atoms (C-C). The β-alky aryl ether

and α-alkyl aryl ether bonds are often the most prevalent, consisting of up to 60% of the linkages in soft and hardwood lignins [41].

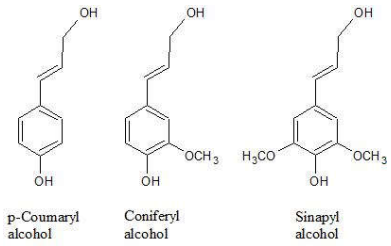

Figure 2-3. Monomeric phenylpropane units found in lignin

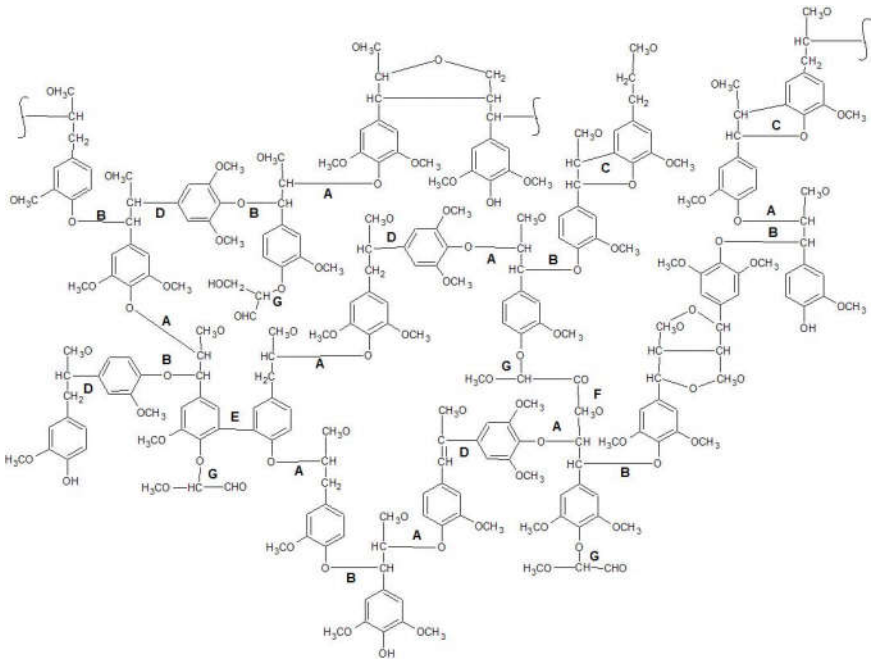

Figure 2-4. Proposed structure of beech lignin with various bonds types (A to G) (redrawn from Nimz [42]). Bond types: β-alky aryl ether (A), α-alkyl aryl ether (B), phenylcoumaran (C), biphenyl (D), aryl-alkyl-aryl linkage (E), β-β alky linkage (F), and glyceraldehyde-2-aryl ether (G)

2.4.2.4 Extractives

Extractives, which are located between the fibres, help the plant defend against microbes, store energy as well as facilitate in the metabolic reactions [13]. It consists mainly of fats, waxes, proteins, alkaloids, phenolics, simple sugars, pectins, mucilages, gums, resins, terpenes, starches, glycosides, saponins, and essential oils [13].

2.4.2.5 Inorganic material

Plant biomass contains various inorganic materials present in the forms of crystalline, semi-crystalline and amorphous solids, which are absorbed from the soil during growth [43]. These inorganic materials include silicates (e.g. SiO_2, $Ca_2SiO_3Cl_2$), oxyhydroxides (CuO, $Al(OH)_3$), sulphates ($CaSO_4$), phosphates ($AlPO_4$), carbonates ($Na_2Mg(CO_3)_2$), chlorides ($CaCl_2$), nitrates (KNO_3) and glasses (Al, Cu, Pb), to name a few [44]. The total inorganic material mass is termed as ash content, which is the solid residue that remains after combustion. The ash content varies between different biomass types [45]. Generally woody (~2.7 wt.%) and grassy (~4.3 wt.%) species have a low ash content when compared to agricultural wastes (~7.8 wt.%) [45]. The inorganic content of PWS requires particular consideration, as is elaborated in Section 2.4.3 below.

2.4.3 Paper waste sludge

Table 2-2 presents previously reported lignocellulosic composition of PWSs obtained from different pulp and paper mills. Large variations are observed in the PWS ash content between the different mills, ~10 and ~50 wt.% for pulp and paper mills, respectively (Table 2-2). The ash content for PWS from paper mills utilising recycle fibres is particularly large when compared to woody biomass (~2.7 wt.%), and agricultural wastes (~7.8 wt.%) [45]. The large ash content for

recycling mills can be attributed to the removal of inorganic fillers from recycled paper during processing [23], and is mainly comprised of $CaCO_3$ [8,22,23]. The organic fraction of PWS is mainly comprised of cellulose at ~53 to 73 % (dry, ash and extractives free weight basis) (Table 2-2), which is higher in comparison to other biomass such as woody, grass and agricultural wastes, and varies between ~40 to 52 wt.% (Table 2-1). The overall total carbohydrate content (~74 to 94 %) is substantially higher than that of lignin (~6 to 24 %) (Table 2-2).

Table 2-2. Composition analysis of various paper waste sludge types

Cellulose	Hemicelluloses	Lignin	Ash	Reference
	(wt.%)[a]		(wt.%, df)	
Pulp mill PWS (feedstock: wood)				
72.9	17.0	10.1	11.2	[8]
62.6	16.3	21.5	8.5	[22]
56.5	37.5	6.0	14.4	[46]
Paper mill PWS (feedstock: recycle fibre and/or virgin pulp)				
52.5	22.3	24.2	35.0	[9]
55.3	21.2	22.9	46.7	[22]
63.8	17.2	16.8	54.5	[7]
61.8	14.8	17.3	56.1	[7]

[a]dry, ash and extractives free weight basis (normalised); df: dry free basis.

2.4.4 Fermentation residues derived from PWS

The cellulose content of PWS is reduced by fermentation due to the conversion of sugars into ethanol, as illustrated by Table 2-3. Consequently, this results in substantial increase in both the FR inert ash and lignin content. Not surprisingly, the organic fraction of FR is mainly comprised of lignin at between ~45 to 60 wt.% (dry, ash and extractives free weight basis), while when that of cellulose (~20 to 38 wt.%) and hemicellulose (~17 to 19 wt.%) were lower (Table 2-3).

Furthermore, the FR lignin content is significantly higher in comparison to other biomass such as woody, grass and agricultural wastes, which varies between ~18 to 29 wt.% (Table 2-1). Lignin is attractive as a feedstock for pyrolysis due to its high-energy content, relative to the other components of lignocellulose [47].

Table 2-3. Composition analysis of various paper waste sludge types (before) and its fermentation residues (after)

Cellulose		Hemicelluloses (wt.%) [a]		Lignin		Ash (wt.%, df)		Reference
Before	**After**	**Before**	**After**	**Before**	**After**	**Before**	**After**	
Pulp mill PWS (feedstock: wood)								
59.6	37.7	18.0	17.6	22.4	44.6	2.7	4.1	[4]
Paper mill PWS (feedstock: recycle fibre and/or virgin pulp)								
63.3	36.9	21.2	18.2	15.5	45.9	26.2	34.6	[4]
71.4	20.2	10.7	18.8	17.8	61.1	14.9	41.2	[5]

[a]dry, ash and extractives free weight basis (normalised); df: dry free basis.

The various treatments during the pulp and/or paper making processing, as well as the pre-treatment stages during fermentation, can lead to modifications in the structure of the fibres [2,10,23]. Consequently, PWS and FR are likely to show some differences in thermal behaviour and give different pyrolysis product yields, when comparing samples from different mills/processes. When these variations in PWS and FR feedstock properties and their impact on pyrolysis conversion have not been considered in literature, analogous information obtained with untreated biomass, cellulose (main PWS constituent) or lignin (main FR constituent) have thus been considered to address the shortcomings.

2.5 PYROLYSIS

Pyrolysis is the thermal decomposition of biomass at elevated temperatures (300 to 600 ^{o}C), in the absence of oxygen, into the products of bio-oil, char and non-condensable gas. The pyrolytic mechanisms are intricate in nature, involving the cracking of the complex lignocellulosic components into radicals, which can further react to form secondary products [48]. The pyrolysis operating conditions of temperature, vapour residence time, particle size, heating rate and pressure, to name a few, have a significant effect on the extent of the primary and secondary reactions, ultimately affecting the product yields and composition, and will be discussed in detail below (Section 2.5.1). In order to optimise the pyrolysis conversion of PWS and its FR, these mechanisms and their influence on the yields and product qualities, need to be examined.

2.5.1 Pyrolytic mechanisms

At the start of pyrolysis, lignocellulosic components are thermally broken down resulting in the formation of volatiles and re-arrangements in the solid residue [21,48]. These reactions are generally termed primary reactions, which includes char formation, depolymerisation and fragmentation [48]. Volatiles can undergo further conversion during secondary reactions.

2.5.1.1 Primary reactions

Char formation

The production of char results from the formation and re-arrangement of benzene rings into stable polycyclic structures (temperatures > 300 ^{o}C) [49], and is mainly exothermic [50]. The release of water and/or non-condensable gas is often observed during these re-arrangements [48,51,52].

Depolymerisation

Depolymerisation involves the scission of bonds between the monomers units of the lignocellulosic polymers [48]. During thermal degradation, the degree of polymerisation of the lignocellulosic polymers is decreased to such an extent that volatiles are produced [48,53]. These volatiles are often found in the liquid product.

Fragmentation

Fragmentation involves the scission of rings/bonds within the monomers units into linear compounds and non-condensable gas [54], and is promoted at temperatures above 600 ^{o}C [21]. As energy is required to vaporize the produced volatiles, both fragmentation and depolymerisation mechanisms are usually endothermic [50].

2.5.1.2 Secondary reactions

The volatiles formed during depolymerisation/fragmentation can undergo further conversion by secondary reactions in the vapour phase and/or between the vapour and solid (char) phase. The types of secondary reactions are specific to cracking [21] and recombination reactions [55], and reportedly these are mainly exothermic [56]. The cracking reactions involve the scission of bonds within the volatiles resulting in the formation of lighter molecular weight components. These reactions often promote the formation of non-condensable gas [57]. Recombination reactions involve the combination of volatiles to form higher molecular weight components (e.g. polycyclic hydrocarbons) [48,57], which sometimes leads to the formation of additional solid called 'secondary' char [55,57].

2.5.2 Pyrolytic conversion of lignocellulosic constituents

Under pyrolysis conditions, the various lignocellulosic constituents show different thermal behaviour which results in different product distribution.

2.5.2.1 Cellulose

Endothermic thermal degradation of the cellulose polymer takes places between the temperatures of 300 to 390 ^{o}C with a maximum rate of degradation (typically measured as weight loss) at ~350 ^{o}C [52,58-61]. Cellulose pyrolysis has been reported to become exothermic at low heating rates and increased mass transfer limitations, due to the promotion of simultaneous char formation over bond scission [50]. At lower temperatures of between 210 to 300 ^{o}C some re-arrangement reactions enhancing char formation are favoured [62], by either intermolecular (< 250 ^{o}C) or intramolecular (> 250 ^{o}C) dehydration reactions [51]. A small loss of weight is observed during thermal degradation, partly due to the release of water [51]. As PWS is mainly comprised of cellulose (Table 2-2), its thermal behaviour would present some similarities [23]. Mendez *et al.* [23] used thermogravimetric analysis (TGA) to investigate the pyrolytic behaviour of different PWS types. In the cases of the low ash PWSs, maximum peak temperatures were observed between 349 to 356 ^{o}C [23], which corresponds to the degradation of the remaining cellulose [23]. On the other hand, the high ash PWSs displayed lower maximum peak temperatures at between 345 to 348 ^{o}C. It was suggested that the lower maximum peak temperatures could be due to degraded fibres and/or the catalytic action of inorganics on primary reactions [63,64]. In another study, the pyrolytic thermal characteristics of a low ash PWS (7.8 wt.%) was investigated by Strezov *et al.* [27]. As expected, the thermal degradation was endothermic up to 330 ^{o}C, although between 330 ^{o}C and 390 ^{o}C a sharp exothermic peak was observed. The authors suggested that exothermicity was due to the

promotion of primary exothermic char formation by hindered heat transfer [27]. This hypothesis has been shown to occur for cellulose [50,60], although due to the large presence of inorganics, some exothermic secondary reactions could have also been promoted. A study to test this alternative hypothesis, whereby potential links could be drawn between the thermal behaviour and pyrolysis products yields, would be interesting.

Depolymerisation of cellulose takes place between 300 to 390 ^{o}C, resulting in the formation of volatiles [65,66]. Many chemical mechanisms have been proposed for cellulose pyrolysis [54,57,67,68]. The generally accepted chemical mechanism involves the scission of the β-(1-4) glycosidic bond to form intermediates, of either an 1,6-anhydride or 1,4-anhydride, which subsequently stabilizes to form levoglucosan [68]. Levoglucosan is one of the main products, and in one case the yield was reported to be as high as 58.8 wt.% from pure cellulose [65]. The large quantity of cellulose present in PWS (Table 2-2), could lead to a high yield of levoglucosan. However, a low degree of crystallinity, particularly in PWS generated from fibre recycling processes [23], could result in lower than expected yields of levoglucosan, while on the other hand it could promote the formation of furans by ring contractions [69]. Levoglucosan can undergo further secondary reactions resulting in the formation of furan derivatives such as furfural and 5-hydroxymethyl-furfural (HMF) [48,57]. Typical chemical components and/or derivatives formed during cellulose pyrolysis include (i) light volatiles such as gasses (i.e., CO, CO_2), methanol, acetaldehyde, and acetic acid, (ii) furans and (iii) pyrans [66].

2.5.2.2 Hemicelluloses

Thermal decomposition of hemicelluloses is globally exothermic [59,60], and takes place between the temperatures of 200 to 320 ^{o}C with a maximum rate of weight loss at ~290 ^{o}C

[52,59,61]. Depending on the constituent polysaccharide/s (i.e., glucomannan, xylan, etc) present in hemicelluloses, slight variations of 20 to 30 ºC can occur in the temperature range of thermal degradation [48]. The typical polysaccharides present in the PWS are mainly xylan and glucomannan [7]. Dehydration reactions during xylan pyrolysis takes place between temperatures of 150 to 240 ºC, while for glucomannan it lies between 150 to 270 ºC [48,52,70]. The char yield from polysaccharides of hemicelluloses can be up to three times larger than that of cellulose [71], although as it is present in low quantities in the PWS (Table 2-2) and FR (Table 2-3), it should not contribute considerably.

The depolymerisation of the hemicelluloses is likely occurring via a similar mechanism previously described [48,72], and results in the formation of numerous anhydrosugars such as levoglucosan, levogalactosan, levomannosan, levoglucosenone to name a few [66,70,72]. Indeed, the hemicelluloses polysaccharide composition (i.e., xylan, glucan, etc) would affect the type and quantity of anhydrosugars evolved [70]. Other typical chemical components and/or derivatives formed during hemicelluloses pyrolysis include (i) light volatiles such as gases (i.e., CO, CO_2), formic acid, acetic acid, and 1-hydroxy-2-propanone, (ii) furans (i.e., HMF, furfural), (iii) lactones and (iv) others [66,70].

2.5.2.3 Lignin

Thermal decomposition of lignin is globally exothermic [59,60], and takes place between the temperatures of 200 to 900 ºC with a maximum rate of weight loss at between 360 to 410 ºC [44,52,59]. Char formation from lignin is somewhat different from that of carbohydrates, due to the presence of benzene rings in the original polymer [73]. This indeed results in lignin char yields (w/w) that can be up to four times higher than those obtained for cellulose [48,52]. Differences in

the lignin structure can slightly affect the thermal decomposition profile [44], as it would be the case in PWS due to the mechanical and/or chemical pulping processes [2], as well as during feedstock pre-treatment for fermentation [2]. Due to the low quantity of lignin present in PWS (Table 2-2), its effect on thermal degradation would not be as substantial as cellulose. However, as FR is mainly comprised of lignin (Table 2-3) its thermal behaviour is expected to show some similarities. Indeed, a TGA study performed by Wang *et al.* [29] showed that wheat-derived FR displayed a similar thermal profile to lignin.

Studies have shown that most of the ether bond linkages (C-O) in lignin undergo depolymerisation between the temperatures of 200 to 300 ^{o}C, while condensed bond linkages (C-C) remain mostly stable [74,75]. The breaking of these ether bond linkages can result in the formation of phenolic compounds (monomers or oligomers) from lignin, which are similar to the original monomeric phenylpropane units (Figure2- 3), and are accompanied by the release of H_2O, CO_2 and CO [74-76]. Above temperatures of ~300 ^{o}C condensed bond linkages (C-C) become unstable [48,73], resulting in the formation of compounds that are similar to the monomeric phenylpropane units (Figure 2-3), although they are mainly characterized by methyl groups (creosol) or by the absence of an alkyl chain (guaiacol) on the initial propyl position [48]. As FR is mainly comprised of lignin (Table 2-3), its conversion could lead to large yields of phenols [29]. The typical chemical components and/or derivatives formed during lignin pyrolysis include (i) light volatiles such as gases (i.e., CO, CO_2), and acetic acid, (ii) catechols (i.e., catechol, 4-methylcatechol), (iii) vanillins (i.e., vanillin, homovanillin), (iv) guaiacols (i.e., guaiacol, 3-methylguaiacol), (vi) phenols (i.e., phenol, o-cresol, 2-methylphenol), (v) aromatic hydrocarbons (i.e., benzene, toluene, styrene) and (vi) others [66].

2.5.3 Pyrolytic products

The thermal decomposition of the lignocellulosic constituents results in the formation of bio-oil, char and non-condensable gas products.

2.5.3.1 Bio-oil

Bio-oil is an organic liquid, which contains numerous amounts highly oxygenated compounds, as well as water [13,77]. Maximisation of the bio-oil yield (> 75 wt.%) typically lies in the temperature range between 450 and 550 ^{o}C, especially with high heating rates (> ~600 ^{o}C.min^{-1}) [12,78-82]. Bio-oil can be used as an bio-energy product [12-14], and/or as a feedstock for high-value chemicals production [13,15,16,83]. It is often mentioned that the production of bio-oil is favoured as it is easily handled, stored and is energy dense [12].

Both slow and intermediate pyrolysis technologies have been considered for PWS conversion [24-26], while pyrolysis of PWS-derived FR has not yet been considered. In a study performed by Lou *et al.* [24], a high ash (41.5 wt.%) PWS was slowly pyrolyzed (fixed bed) to 800 ^{o}C, resulting in a low bio-oil yield of 24.4 wt.% (41.7 daf, wt.%), and high char yield of 45.8 wt.%. A low ash (7.8 wt.%) PWS was slowly pyrolysed at 10 ^{o}C.min^{-1} until 500 ^{o}C, using a packed bed thermal apparatus, by Strezov *et al.* [27], resulting in bio-oil, char and gas yields of 40 wt.% (47.8 daf, wt.%), 36 wt.%, and 24 wt.%, respectively [27]. Yang *et al*. [26] and Ouadi *et al.* [25] subjected two high ash (62.9 and 74.5 wt.%, respectively) deinking sludges to intermediate pyrolysis to investigate the characteristics of bio-oil. The conversion of these materials took place using an Auger reactor at 450 ^{o}C under atmospheric conditions, with short vapour residence times and long feedstock residence times of between 7 to 10 minutes [26]. The product yields reported by Yang *et*

al. [26], for bio-oil, char and non-condensable gas were 10 (27.9 daf, wt.%), 79 and 11 wt.%, respectively.

Bio-oil has been demonstrated to be a promising bio-energy product for transportation fuels [12], thermal and electrical energy [13,14] although upgrading is often recommended to improve its fuel properties. Wood derived bio-oil energy content (~17 $MJ.kg^{-1}$) is typically about 40-50% of that of conventional fossil fuels (~40 $MJ.kg^{-1}$), and has a higher density (~1200 $kg.m^{-3}$) due to the large presence of water (25 wt.%) and oxygenates (O/C: ~0.51) [12]. Full deoxygenation of bio-oil (O/C: >0.06) would be required before it can substitute conventional transport fuels [84], which can be achieved through processes such as hydrotreating or catalytic vapour cracking, to name a few [12,13,85]. However, these processes require additional energy and hydrogen supply, thus limiting the efficiency of the overall process [12]. The higher heating values (HHV) of the bio-oils obtained during intermediate pyrolysis of the two PWSs, 36-37 $MJ.kg^{-1}$ [25,26], were significantly higher in comparison to the typical values for biomass derived products (~17 $MJ.kg^{-1}$) [12]. These high HHVs could be due to the catalytic effect of the high ash content, particularly calcium [23], promoting deoxygenation (O/C: ~0.10) [63,86]. Yang *et al.* [26] showed that the bio-oil had sufficient energy to power a diesel engine, although poor combustion and carbon deposition could be encountered.

High-value marketable chemical production from bio-oil has gained interest, with the aim to partially replace existing petroleum based chemicals [12,15,16,83]. Some of these high-value marketable chemicals include anhydrosugars, furans, aldehydes and phenols, to name a few [87-89]. The chemicals can be recovered by means of physical and/or chemical processing of the bio-oil, and can be further subjected to catalytic upgrading to derive higher quality/value chemicals [15,83,86]. The potential of PWS bio-oil as a feedstock for chemicals productions has not been explored

comprehensively. The studies on PWS pyrolysis mentioned above [24-26], presented only qualitative bio-oil GC-MS results in terms of peak area percentage distribution (PD) pointing out the formation of potential marketable chemicals. The study performed by Lou *et al.* [24], whereby a high ash PWS was slowly pyrolzed (800 ^{o}C), found large PDs for benzene ring type chemicals such as styrene (11.5 %), benzene (6.8 %), toluene (8.8 %), ethylbenzene (13.5 %) and p-xylene (35.0 %). Similarly to Yang *et al.* [26] and Ouadi *et al.* [25], large PDs were obtained for benzene ring type chemicals such as ethylbenzene (~13-23%), toluene (~4-12%) and 1,3,5,7 cyclooctatetraene styrene (~23-28%). Although the organic fraction of PWS is mainly comprised of carbohydrates (Table 2-3), only benzene ring type chemicals have been observed in the bio-oil. This could be attributed to extensive lignocellulosic conversion through severe pyrolysis processes supported by further catalytic conversion [24,26]. Thus, the potential for milder conditions to produce more primary products with a higher value has not been explored. The large quantity of cellulose (Table 2-3) present in PWS could result in large production of high-value marketable primary chemicals such as anhydrosugars, furans and aldehydes to name a few [87-89]. The main anhydrosugar, levoglucosan, has potential use in the production of surfactants, pharmaceuticals and biodegradable polymers for example [90]. Glycolaldehyde, one frequently produced aldehyde, can be used in the food industry [16,90]. Furans such as furfural and 5-hydroxymethyl-furfural have extensive market use in the food industry, pulp and paper industry, as well as the use of an additive for resin and solvent production [91]. In addition, as environmental pressure increases new markets are expected to develop using furans as building blocks for sustainable chemicals production [89]. The large quantity of lignin in FR could result in a high yield of phenols [29,31], which have promising potential in applications such as adhesives, resins, wood preservatives and food flavouring [90].

Taking into account the above, production of high-value marketable chemicals and/or energy could offer a lucrative option for bio-oil generated from PWS and/or FR. Furthermore, fast pyrolysis of these feedstocks, which is known to enhance the mass yields, energy content and quality of bio-oils when compared to slow pyrolysis [12,78,92-94], has not been considered. Thus, it would be interesting to compare different pyrolysis processes, such as fast, vacuum and slow pyrolysis, for their ability to produce chemicals and energy products from PWS and FR bio-oil.

2.5.3.2 Char

Char is a solid product that consists of stable aromatic polycyclic structures [95]. In most cases, char is mainly comprised of fixed carbon, some volatile matter and the remaining inorganic material [46,96]. The production of high char yields are favoured at low temperature (~300 ^{o}C), under slow heating rates, and long vapour residence time [78,92-99]. Char finds application as a bio-energy product for fuel [100], as a reductant for metallurgical applications or as a biomaterial (i.e. sorbent, biochar) [17-20,28,46].

The energy content of char typically varies between 20 to 32 MJ.kg^{-1} [78,80,97], and has the potential to be used as coal substitute for heat generation [100]. The energy content of chars produced from intermediate pyrolysis of the two high ash PWSs [25,26] was poor, at 3.3-4.9 MJ.kg^{-1}, due to their inherently large ash content (54-60 wt.% determined at 900 ^{o}C) [25]. Combustion of this char product would not be feasible as the high AC could cause slagging and fouling [101,102]. On the other hand, the low ash PWS char HHV, generated during slow pyrolysis [27], was significantly higher at 13.3 MJ.kg^{-1}.

Alternatively, char can be used as biomaterial for applications such as sorbents and biochars. Some of the applications of char as a sorbent were done in the field of wastewater treatment for

removal of inorganic and organic pollutants [17,28], while others used biochar in soil amendment experiments to improve the uptake of fertilizers/nutrients, removal of pollutants, and plant growth [18-20]. The char biomaterial can be classified as microporous, mesoporous or macroporous with respective pores sizes of less than 2 nm, between 2 to 50 nm, or larger than 50 nm [103]. Mendez *et al.* [28] tested the ability of two chars, prepared from a high and low ash PWS by slow pyrolysis (3 or 10 $^{o}C.min^{-1}$) conversion at 650 ^{o}C, for its adsorption capability of Cu^{2+} from water. It was found that the high ash PWS char (BET: ~75 to 88 $m^2.g^{-1}$), which was mainly mesoporous, had the highest removal of Cu^{2+}, probably due to the high average pore density, high oxygenated surface groups (high $CaCO_3$ content) and elevated superficial charge density [28]. The adsorption of citalopram from wastewater using char derived from high ash PWS was also shown to be successful by Calisto *et al.* [17]. Few studies have demonstrated the potential of biochar to stabilize and reduce the mobility and bioavailability of inorganic contaminants in soils [18,19]. In a study performed by Mendez *et al.* [18], biochar prepared at 500 ^{o}C during slow pyrolysis of high ash PWS (63.7 wt.%) could limit the detrimental consequences on soils due to the mobility, bioavailabilty and leaching of Ni^{2+}. The biochar prepared at 300 ^{o}C had little effect, emphasizing the importance of the pyrolysis conditions on product quality for specific applications [18]. Martin *et al.* [19] investigated the adsorption-desorption of herbicides (diuron and artrazine) in soil amended with biochar, prepared from high ash PWS. Results indicated that fresh biochar significantly enhanced the uptake of the herbicides, while aged char (32 months) displayed no significant improvement in uptake [19]. All of the above studies [17-20,28] indicated that the alternative use of char as a biomaterial, particularly for those produced from high ash PWS, is a promising and more realistic option than energy application. In particular, vacuum pyrolysis, which is known to significantly enhance the adsorptive

properties of char [78,104], has not yet been considered for PWS. Furthermore, an exploratory study on the potential of FR char biomaterials would be interesting.

2.5.3.3 Non-condensable gas

The non-condensable gas produced from biomass pyrolysis is generally comprised of hydrogen, carbon monoxide, carbon dioxide, methane, ethane and propane [77]. Temperatures above 600 °C enter the gasification region where the non-condensable gas yield and its energy content are increased [12,14]. The non-condensable gas energy content (~5.5-7 $MJ.m^{-3}$) is about 15-18% of that of natural gas (~37 $MJ.m^{-3}$) [77], and is often combusted to supply heat for the pyrolysis process itself [14,14,21,49,77].

The non-condensable gasses generated during the slow (500 °C) [27] and intermediate (450 °C) [25,26] pyrolytic conversion of high ash PWS were mainly comprised of CO_2 (~54 to 71 wt.%; relative conc.), followed by CO (~22 to 41 wt.%), with HHVs of between ~5 to 6 $MJ.m^{-3}$. Strezov *et al.* [27] performed an energy balance on the heat required for pyrolysis, compared to the energy content of the gas product obtained between 20 to 700 °C. They concluded that above 500 °C the energy balance became net positive, with the energy supply from the non-condensable gas product being larger than the pyrolysis process energy requirements, due to the high calorific values of the gasses from the enhanced production of hydrogen, methane, ethane and propane [27]. Although non-condensable gas combustion is useful, it is not a high value product, and thus production of high value-added liquid and char products will be the focus of this study.

2.5.4 Effect of pyrolysis conditions

The following sections describe the effect of various operating conditions on the pyrolysis mechanisms and their influence on the product yields. Moreover, the inorganic compounds present in paper waste sludge and its fermentation residues can have a significant effect on both the pyrolysis mechanisms and product yield. A section about such impacts of inorganics has thus been included.

2.5.4.1 Reactor temperature

The pyrolysis product yields, their energy contents and chemical compositions from biomass are significantly affected by the reactor temperature [12,22,78-81,97,105]. A rise in the reactor temperature from 300 to 600 ^{o}C lowers the char yield [78,80,105], and increases its calorific value by driving off more oxygen and hydrogen [78,81,97]. In addition, a higher temperature also promotes pore development resulting in an increase in the surface area and porosity of chars [78], as observed previously for high ash PWS char generated from slow pyrolysis [17]. Temperatures between 450 to 550 ^{o}C typically lead to the maximisation of the bio-oil yield [13,54,86,92]. The effect of temperature (and other factors) on the bio-oil energy content is not yet well understood. It would make an interesting study to find potential correlations between the bio-oil energy content and chemical composition. Pyrolysis of biomass at temperatures above 600 ^{o}C approaches the gasification region, where the non-condensable gas yield and its energy contents are promoted [12,14]. Only one study performed by Strezov *et al*. [27], has investigated the effect of temperature (up to 700 ^{o}C) during slow pyrolysis (10 ^{o}C.min^{-1}) conversion of a low ash PWS (7.8 wt.%) on the product yields. It was found that the bio-oil yield increased from 4 to 40 wt.% between 100 to 400

^{o}C, after which it remained relatively constant. The gas yield however increased continuously with an increase in temperature, which corresponded to a decrease in the char yield [27].

The evolution of chemicals during pyrolysis is significantly affected by temperature [54,57,105-107]. Lu *et al.* [54] found that an increase in temperature, during fast pyrolysis conversion of cellulose, significantly enhanced the production of anhydrosugars, similar to other findings [57,106]. This indicated that depolymerisation reactions were promoted [54,57,106]. The study performed with high ash PWS by Lou *et al.* [24], using a Py-GC-MS instrument, found that products generated at 400 ^{o}C were similar to the monomeric phenylpropane units (i.e. 4-methoxy-4-vinylphenol). An increase in Py-GC-MS temperature to 800 ^{o}C led to the promotion of phenols characterised by the absence of alkyl groups in the propyl position (i.e. benzene, toluene) [24], indicating the critical influence of temperature on bio-oil composition. Similar observations were made for wheat-derived FR slow pyrolysis bio-oils generated between 480 to 650 ^{o}C [29]. An increase in temperature has also been shown to promote the depolymerisation and/or fragmentation reactions during lignin thermal degradation, resulting in the increased formation of phenols, catechols and cresols, to name a few [72,73,75]. Higher temperatures promote volatiles production, which in turn can also enhance secondary reactions [107] and ultimately lead to changes in the chemical composition of the products [57,108]. For instance, Shen *et al.* [57] suggested that secondary cracking of levoglucosan leads to glycolaldehyde, HMF, and formaldehyde.

2.5.4.2 Particle size

The particle size influences both heat and mass transport phenomena [21], and has been shown to significantly affect the pyrolysis product yields and composition [12,22,79,94,109,110]. During fast pyrolysis of oil mallee wood [109], the char yield increased by 5 wt.%, in response to an

increase in particle size from 0.3 to 1.5 mm, after which it was constant up to 5.2 mm. Similarly, the char yield from slow pyrolysis of agricultural waste increased by ~15 wt.% due to an increase in particle size from 0.5 to 2.3 mm [110]. In general, the use of a smaller particle size promotes the production of bio-oil during fast pyrolysis, by allowing for a regime in which the kinetics are predominantly controlled by chemical reactions, rather than heat and mass transfer limitations [12,14,109].

Shen *et al.* [109] found that a decrease in particle size, from 5.6 to 0.18 mm, resulted in significant increases in the anhydrosugars, phenols, furans and oligomers yields. Indeed, a smaller particle size would enhance heat transfer [21,109], resulting in a promotion of simultaneous bond scission over char formation during primary pyrolysis reactions [54,57,105,107,109]. In addition, the smaller particle size would also enhance mass transfer [107,111], thus limiting the occurrence of secondary reactions [108].

All of the above authors considered a "single particle" during their study. However, due to the physical nature (fluffy and light) of PWS, this material would need to be pelletized thus forming an "agglomerate of particles", which can be assumed having similar pyrolytic behaviour as a "single particle" [107,112]. The effect of the pellet size on the pyrolytic thermal behaviour, products yields and characterisation has not been explored.

2.5.4.3 Heating rate

The mode of heat transfer from the reactor bed to the biomass particle surface determines the extent of the heating rate [93]. For instance, the use of a bubbling fluidised bed reactor (600 to 12000 $^{o}C.min^{-1}$) offers significantly higher heating rates when compared to a fixed bed reactor (1 to 60 $^{o}C.min^{-1}$) (see Section 2.5.4.7) [78,113]. High heating rates enhance the transfer of heat to

biomass, resulting in the promotion of primary reactions, particularly depolymerisation [96,106], as well as the production of bio-oil [12,94,98], while char production is decreased [12]. On the other hand, low heating rates have been observed to promote the sorbent properties of chars generated from high ash PWS [28].

Comparison of the bio-oil obtained from slow pyrolysis of bamboo at low heating rates, of 5 to 30 $^{o}C.min^{-1}$, showed insignificant differences in chemical composition of bio-oil, except for a slight increase in phenol components [96]. Greenhalf *et al.* [106] investigated the effect of low (25 $^{o}C.min^{-1}$) and high (1500 $^{o}C.min^{-1}$) heating rates on the evolution of volatiles components during pyrolysis (Py-GC-MS) of willow short rotational coppice. The high heating rate significantly promoted the formation of anhydrosugars, phenols and furans, indicating that depolymerisation and/or fragmentation reactions were enhanced [106].

2.5.4.4 Vapour residence time

It is generally accepted that long vapour residence times favour secondary reactions [21,48,111], resulting in an increase of char (recombination) and/or gas (cracking) yields, often with an associated decrease in the bio-oil yield [79,94]. Furthermore, the promotion of secondary reactions could significantly affect chemical speciation during pyrolysis [114]. The associated vapour residence time is one of the major differences that lie between the various pyrolysis techniques [98,99]. For instance, fast (< 2 s) and vacuum (1 to 20 s) pyrolysis have significantly shorter vapour residence times when compared to slow pyrolysis (1 min to hours) (see Section 2.5.4.7) [12,78,113].

2.5.4.5 Pressure

A low operating pressure may increase the driving force for mass transfer, thereby enhancing the separation of volatile and solid products, and limiting the occurrence of secondary reactions. However, little is known about its effect on the primary pyrolysis reactions. For the char product, decreased yields [78,104,115,116], lower calorific values [78,99], and enhanced surface area and porosity [78,99,117] are often observed at low operating pressures, while for bio-oil increases in yield, and HHV have been observed [78,104].

The effect of pressure on the mass transfer can significantly alter the bio-oil chemical composition [104,118]. Venkatakrishnan *et al.* [118] studied the effect of temperature on cellulose fast pyrolysis at two elevated pressures (2700 and 5400 kPa). A rise in pressure caused an increase in water yield, with an associated decrease in the levoglucosan yield [118]. In a study performed by Amutio *et al.* [104], the effect of a vacuum (25 kPa) on flash pyrolysis of pinewood was studied. At both 400 and 500 ^{o}C, the presence of a vacuum significantly promoted phenols production, possibly due to the quick removal of volatiles limiting secondary cracking reactions [104]. This limitation in secondary reactions can also lessen the conversion of levoglucosan resulting in higher yields [53].

2.5.4.6 Catalytic pyrolysis

Catalytic pyrolysis has received increasing attention during the last decade, with the aim of reducing the oxygen content in bio-oils (deoxygenation) [114], as well as to drive the selectivity for production of targeted high value chemicals [119,120]. The presence of alkali catalysts can affect the primary pyrolysis reactions [52,63,64,114], and enhance the secondary reactions [52,64,86].

Paper waste sludge, particularly those generated from recycle paper mills, contains a large quantity of ash (~10 to 56 wt.%, Table 3), often in the form of $CaCO_3$ (inorganic filler) [23].

Mendez *et al.* [23] investigated the pyrolytic behaviour of different PWS types using TGA, and demonstrated that the combination of high ash content ($CaCO_3$: ~44 wt.%) and degraded cellulose fibres resulted in a lower starting temperature for thermal degradation. Calcium components have been shown to significantly promote primary pyrolysis reactions [63,64]. Patwardhan *et al.* [63] studied the effect of inorganic salts (NaCl, KCl, $MgCl_2$, $Ca(OH)_2$, $Ca(NO_3)_2$, $CaCO_3$, $CaHPO_4$) on the primary pyrolysis products from cellulose using Py-GC-MS. Promotion of simultaneous competing reactions were observed, which led to a decrease in the levoglucosan yields. In addition, both an increase in the inorganic content (0 to 5 wt.%) and temperature (350 to 650 ^oC) significantly enhanced the formation of low molecular weight species (formic acid, glycoladehyde, acetol), which corresponded to a decrease in levoglucosan yield [63].

The presence of inorganic compounds such calcium in PWS can significantly promote secondary reactions [86]. Gray *et al.* [64] demonstrated that wood doped with calcium acetate catalysed the conversion of pyrolysis tar into smaller oxygenated compounds, with no change in char yield, indicating that secondary tar cracking reactions were enhanced. Lu *et al.* [86] investigated the effect of various catalysts (MgO, CaO, TiO_2, Fe_2O_3, NiO, ZnO) on the secondary reactions during fast pyrolysis using Py-GC-MS (500 ^oC). The presence of CaO had the greatest effect on these reactions, reducing the production levels of anhydrosugars (levoglucosan), acids and phenols significantly, while promoting hydrocarbon formation [86]. The use of ZnO as a catalyst had a marginal effect on the pyrolysis product distribution, while MgO, TiO_2, Fe_2O_3 inorganic species decreased the level of aldehydes and anhydrosugars (not NiO), and increased formation of ketones and cyclopentanones [86].

To alter the composition of the inorganic components and enhance the organic composition of the bio-oil, pre-treatment of biomass via torrefaction and/or acid hydrolysis can be considered.

Reckamp *et al.* [46] subjected a high ash PWS, mainly comprised of calcium components, to both these pre-treatments, followed by pyrolysis using a high heating rate (> 1000 $^{o}C.s^{-1}$) in a Py-GC-MS instrument. They concluded that the combination of both torrefaction and acid-hydrolysis, significantly enhanced the formation of chemicals such as levoglucosenone and furfural, along with a reduction in levoglucosan, acids, aldehydes and ketones [46]. When considering the selectivity of chemicals, studies have shown that a catalyst can have a significant effect [119,120]. For example, the presence of $ZnCl_2$ can enhance the production of furfural by up to 16 times [119,120].

2.5.4.7 Pyrolysis process options

The differences in operating conditions between fast, intermediate and slow pyrolysis processes affect the product yields and energy content thereof [92-94,98,99]. Major differences between these processes lie with the applied heating rate and associated product residence time [98,99]. The application of significantly higher heating rates during fast pyrolysis (FP) (600 to 12000 $^{o}C.min^{-1}$) [113], when compared to slow pyrolysis (1 to 60 $^{o}C.min^{-1}$) [78,113], reduces heat transfer limitations [87]. In addition, slow pyrolysis (SP) employs long vapour residence times (1 min to hours) [12,78,113], when those of fast pyrolysis are shorter (< 2s) [12]. Longer vapour residence times limit mass transfer resulting in the promotion of secondary tar cracking and/or recombination reactions [98]. Typically the production of char is favoured during SP [92,94,97-99], while bio-oil production is maximised during FP [12,92,94,98,99]. However, valorisation of PWS via FP has not been considered previously. With moderate heating rates (10 to 300 $^{o}C.min^{-1}$) [98,121], and vapour residence times (10 to 30s) [12], intermediate pyrolysis (IP) offers a good compromise for bio-oil, char and non-condensable gas [12,121,122]. An additional technique that can be considered an intermediate process is vacuum pyrolysis, which has low heating rates (1 to 60 $^{o}C.min^{-1}$), and short

vapour residence times (1 to 20 s), and results in a good compromise between the yields of pyrolysis products [78,123]. Usually the quality and energy content of bio-oils obtained from FP and VP, are significantly higher than SP [92,94,124], and offers higher quality fuel for heat and power generation, and transport fuel production [14,125,126]. Regarding the char product, the energy content of SP chars is often higher than those of FP [92,98], and has the potential to be used as a coal substitute. The quality and adsorbent capabilities of chars generated from VP is often better than that obtained during SP [78], but these have not been described for PWS valorisation.

The operating conditions employed by the various pyrolysis techniques, as well as the reactor configurations, can affect the bio-oil chemical composition [106,127]. Bio-oils obtained from slow (fixed bed) and fast (continuous stirred bed) pyrolysis of loblolly pine wood were compared by Ben *et al.* [127]. The higher heating rates employed during fast pyrolysis significantly enhanced depolymerisation, promoting the production of both phenols and sugars [127]. Greenhalf *et al.* [106] compared bio-oils produced from slow (fixed bed) and fast (fluidised bed) pyrolysis of willow short rotation coppice. Fast pyrolysis promoted the formation of acetic acid, methyl acetate, phenol and 2,6-dimethoxyphenol, while slow pyrolysis enhanced methyl acetate, 3-hyroxy-2-butane, furfural and cyclopentenes formation [106]. Considering the differences between slow and fast pyrolysis of biomass, too few studies [78,104,115,116] have attempted to describe mechanisms under VP as a means to control selectivity for particular chemical products pyrolysis. In addition, no studies have yet considered the valorisation of PWS-derived FR via pyrolysis. As a result, a comparison of each pyrolysis technique ability to convert PWS and FR into high-value added chemicals would be interesting.

2.5.5 Energy conversion

The ability of pyrolysis to valorise biomass is often based on product mass yields and the physico-chemical characteristics thereof [12,22,79,81,82], as it is critical for the process to be competitive. Some research has considered gross energy conversion (EC) based on the evaluation of changing one form into another, considering biomass as a chemical energy input and the pyrolysis products as an energy output [97,128,129,130]. When considering the net energy conversion, the external inputs such as the heat required for pyrolysis are subtracted from the gross EC, and thus require a complete energy balance of the pyrolysis process. Gross EC can be calculated without a complete energy balance, based either on a target product or all products if suitable for energy applications. Such a criteria could be useful for driving the product distribution to finally maximize the overall energetic output [131].

Phan *et al*. [97] applied slow pyrolysis (10 ^{o}C.min^{-1}; fixed bed) to municipal solid wastes (wood, cardboard, textiles) from 350 to 700 ^{o}C, and determined the gross EC for both the bio-oil and char product. For all three municipal wastes, maximum char ECs (~51 to 56 %) and yields were attained at the lowest temperature (350 ^{o}C), regardless of the lower HHVs. Similarly for bio-oil the maximum ECs corresponded (~25 to 36 %) to the maximum yields, as there was little difference between the HHVs. Regarding the conversion to both char and bio-oil, it was concluded that a temperature of ~500 ^{o}C offered the highest EC of ~85%. The effect of feedstock composition on energy recovery rates from char and bio-oil generated during FP (Lurgi-Ruhrgas) conversion (500 ^{o}C) of different biomass types of straw was studied by Troger *et al*. [129]. The lowest gross EC (bio-oil and char) was obtained from corn stover (69.0 %), and the highest from softwood (79.6 %), which highlights the significance of biomass type. Pighinelli *et al.* [130] subjected *Eucalyptus benthamii* to FP (fluidised bed) conversion at 500 ^{o}C to investigate the effect of different fluidizing

agents (pure N_2 and mixture of N_2 and pyrolysis gas) on the liquid and solid mass, and energy distribution. Fluidisation using the mixed fluidising agent (N_2 and pyrolysis gas) resulted in lower char and bio-oil yield, subsequently decreasing the gross EC (char and bio-oil) from ~96 %, when under N_2, to ~60 % [130]. In a study performed by Li *et al.* [128], spent coffee grounds were pyrolysed at two different heating rates (10 and 60 $^{o}C.min^{-1}$) to 500 ^{o}C to ascertain the energy generating potential of each product. The increase in heating rate resulted in a slight increase in the gross EC (sum of all products) from 86.5 % to 88.2 %. Theoretical efficiencies were also calculated, whereby both the energy required for biomass drying and pyrolysis were deducted from the gross EC, resulting in net ECs that were slightly lower for the two heating rates at 83.4 and 84.8 %, respectively [128]. In summary, the above studies point out the importance of the operating conditions and biomass type on products yields, energy content and EC. However, to our knowledge no studies have yet compared the ability of different pyrolysis process options, or the combination of both fermentation and pyrolysis, to convert biomass in terms of gross energy conversion. In order to confirm the efficiency of the whole pyrolysis and/or fermentation process, the energy input (heat energy for biomass drying, pyrolysis and ethanol distillation) needs to be taken into consideration in a modelling study. This work will recommend the preferred conditions, but will not include the modelling study.

2.6 SHORTCOMINGS FROM LITERATURE

The pulp and paper industry produces large quantities of paper waste sludge, which primarily contains organics, inorganics and water. The PWS is often disposed of by landfilling, however due to increasing costs and negative environmental impact new alternatives are required. Two alternatives are considered in this study: 1) stand-alone pyrolysis, or 2) the sequential application of fermentation followed by pyrolysis. Research on pyrolysis of PWS pyrolysis is limited, whereas

there is none on PWS-derived FR, and thus their conversion into energy, chemicals (bio-oil) and biomaterials (char) will be investigated, in the context of a biorefinery.

Recent studies have shown that conversion of PWS via slow and intermediate pyrolysis were promising. Slow pyrolysis was shown to be a practically feasible approach to PWS valorisation, while intermediate pyrolysis significantly promoted the energy content of its bio-oils. Furthermore, the large quantity of inorganics present in PWS, particularly those generated by recycling mill, was shown to have a significant catalytic effect during pyrolysis. Subsequently, this could result in lower conversion temperatures (less energy required), and likely lead to an original bio-oil composition. Valorisation of PWS via fast and vacuum pyrolysis, both which are known to enhance bio-oil yields and energy content, appears to be an efficient way to drive the selectivity of the reactions, and have not been considered. Not only does vacuum pyrolysis enhance bio-oil yields, but it also promotes the adsorptive properties of chars and production of some phenols. As research on the utilization of PWS bio-oil as a feedstock for high-value marketable chemical production is limited, this will also be investigated. The valorisation of PWS-derived FR via pyrolysis is scarcely documented, while similar potential can be expected. Furthermore, a study on the effect of fermentation on the pyrolysis product yields and properties would be interesting. No studies have yet compared the ability of different pyrolysis techniques or the combination of both fermentation and pyrolysis to convert PWS in terms of gross energy conversion. The current literature available on the degradation pathways and mechanisms for pyrolysis of PWS and its FR are also open for improvement in understanding.

2.7 REFERENCES

[1] Paper manufacturing association of South Africa (2014, June). *Summary of findings from 2013 production, import and export statistics* [pdf]. Available: www.thepaperstory.co.za.

[2] C.J. Biermann, Handbook of pulping and papermaking, Academia Press, U.S.A., 1996, pp 13-282.

[3] M.C. Monte, E. Fuente, A. Blanco, C. Negro, Waste management from pulp and paper production in the European Union, Waste Management (29) (2009) 293-308.

[4] S. Boshoff, Characterization and fermentation of waste paper sludge for bioethanol production, Masters Dissertation, Department of Process Engineering, Stellenbosch University, Cape Town, 2015.

[5] C.L.L. Robus, Production of bioethanol from paper sludge using simultaneous saccharification and fermentation, Masters Dissertation, Department of Process Engineering, Stellenbosch University, Cape Town, 2013.

[6] P. Saasner, M. Galbe, G. Zacchi, Techno-economic evaluation of bioethanol production from three different lignocellulosic materials, Biomass and bionenergy (32) (2008) 422-430.

[7] H. Chen, R. Venditti, R. Gonzalez, R. Phillips, H. Jameel, S. Park, Economic evaluation of the conversion of industrial paper sludge to ethanol, Energy Economic, (44) (2014) 281-290.

[8] Y. Yamashita, A. Kurosumi, C. Sasaki, Y. Nakamura, Ethanol production from paper sludge by immobilized Zymomonas mobilis, Biochemical Enginnering Journal, (42) (2008) 314-319.

[9] L. Peng, Y. Chen, Conversion of paper sludge to ethanol by separate hydrolysis and fermentation (SHF) using Saccharomyces cerevisiae, Biomass and Bioenergy (35) (2011) 1600-1606.

[10] K. Kemppainen, L. Ranta, E. Sipila, A. Ostman, J. Vehmaanpera, T. Puranen, K. Langfelder, J. Hannula, A. Kallionen, M. Siika-aho, K. Sipila, N. von Weymarn, Ethanol

and biogas production from waste fibre and fibre sludge – The FibreEtOH concept, Biomass and Bioenergy (46) (2012) 60-69.

[11] F. Cherubini, The biorefinery concept: Using biomass instead of oil for producing energy and chemicals, Energy Conversion and Management (51) (2010) 1412-1432.

[12] A.V. Bridgwater, Review of fast pyrolysis of biomass and product upgrading, Biomass and Bioenergy (38) (2012) 68-94.

[13] D. Mohan C.U, Pittman, P.H. Steele, Pyrolysis of Wood/Biomass for Bio-oil: A critical review, Energy and Fuels, (20) (2006) 848-889.

[14] A.V. Bridgwater, G.V. C. Peacock, Fast pyrolysis processes for biomass, Renewable and Sustainable Energy Reviews (2000) (4) 1-73.

[15] X. Zhang, G. Yang, H. Jiang, W. Liu, H. Ding, Mass production of chemicals from biomass-derived oil by directly atmospheric distillation coupled with co-pyrolysis, Scientific Reports (3) 1120-1127.

[16] A.V. Bridgwater, Production of high grade fuels and chemicals from catalytic pyrolysis of biomass, Catalysis Today (29) (1996) 285-295.

[17] V. Calisto, C.I.A. Ferreira, S.M. Santos, M.V. Gil, M. Otera, V.I. Esteves, Production of adsorbents by pyrolysis of paper mill sludge and application on the removal of citalopram from water, Bioresource Technology (166) (2014) 335-344.

[18] A. Mendez, J. Paz-Ferreiro, F. Araujo, G. Gasco, Biochar from pyrolysis of deinking paper sludge and its use in the treatment of a nickel polluted soil, Journal of Analytical and Applied Pyrolysis (107) (2014) 46-52.

[19] S.M. Martin, R.S. Kookana, L. van Zwieten, E. Krull, Marked changes in herbicide sorption-desorption upon ageing of biochars in soil, Journal of Hazardous Materials (231-232) (2012) 70-78.

[20] S. Rajkovich, A. Enders, K. Hanley, C. Hyland, A.R. Zimmerman, J. Lehmann, Corn growth and nitrogen nutrition after additions of biochars with varying properties to a temperate soil, Biology and Fertility of Soils (48) (2012) 271-284.

[21] M. Van de Velden, J. Baeyens, A. Brems, B. Janssens, R. Dewil, Fundamentals, kinetics and endothermicity of the biomass pyrolysis reactions, Renwable Energy (35) (2010) 232-242.

[22] A.J. Ridout, M. Carrier, J. Gorgens, Fast pyrolysis of low and high ash paper waste sludge: Influence of reactor temperature and pellet size, Journal of Analytical and Applied Pyrolysis (111) (2015) 64-75.

[23] A. Mendez, J.M. Fidalgo, F. Guerrero, G. Gasco, Characterization and pyrolysis behaviour of different paper mill waste materials, Journal of Analytical and Applied Pyrolysis (86) (2009) 66-73.

[24] R. Lou, S. Wu, G. Lv, Q. Yang, Energy and resource utilization of deinking sludge, Applied Energy (90) (2012) 46-50.

[25] M. Ouadi, J.G. Brammer, Y. Yang, A. Hornung, M. Kay, The intermediate pyrolysis of deinking sludge to produce a sustainable liquid fuel, Journal of Analytical and Applied Pyrolysis (105) (2013) 135-142.

[26] Y. Yang, J.G. Brammer, M. Ouadi, J. Samanya, A. Hornung, H.M. Xu, Y. Li, Characterisation of waste derived intermediate pyrolysis oils for use as diesel engine fuels, Fuel (103) (2013) 247-257.

[27] V. Strezov, T.J. Evans, Thermal processing of paper sludge and characterisation of its pyrolysis products, Waste Management (2009) (29) 1644-1648.

[28] A. Mendez, S. Barriga, J.M. Fidalgo, G. Gasco, Adsorbent materials from paper industry waste materials and their use in Cu(II) removal from water, Journal of Hazadous Materials (165) (2009) 736-743.

[29] Z. Wang, W. Lin, W. Song, X. Wu, Pyrolysis of the lignocellulose fermentation residue by fixed-bed micro reactor, Energy (43) (2012) 301-305.

[30] S. Kern, M. Halwachs, G. Kampichler, C. Pfeifer, T. Proll, H. Hofbauer, Rotary kiln pyrolysis of straw and fermentation residues in a 3 MW pilot plant – Influence of pyrolysis temperature on pyrolysis product performance, Journal of Analytical and Applied Pyrolysis (97) (2012) 1-10.

[31] Z. Yang, B. Zhang, X. Chen, Z. Bai, H. Zhang, Studies on pyrolysis of wheat straw residues from ethanol production by solid-state fermentation, Journal of Analytical and Applied Pyrolysis (81) (2008) 234-246.

[32] S.N. Naik, V.V. Goud, P.K. Rout, A.K. Dalai, Production of first and second generation biofuels: A comprehensive review, Renewable and Sustainable Energy Reviews (14) (2010) 578-597.

[33] H. Huang, S. Ramaswamy, W. Al-Dajani, U. Tschirner, R.A. Cairncross, Effect of biomass species and plant size on cellulosic ethanol: A comparative process and economic analysis, Biomass and Bioenergy (33) (2009) 234-246.

[34] Rowell, R (1984) The chemistry of solid wood, American chemical society, U.S.A.

[35] E.F. Alves, S.K. Bose, R.C. Francis, J.L. Colodette, M. Iakovlev, A. Van Heiningen, Carbohydrate composition of eucalyptus, bagasse and bamboo by a combination of methods, Carbohydrate Polymers (82) (2010) 1097-1101.

[36] X. Zhao, L. Zhang, D. Liu, Biomass recalcitrance. Part 1: the chemical compositions and physical structures affecting the enzymatic hydrolysis of lignocellulose, Biofuels, Bioproducts & Biorefining (6) (2012) 465-482.

[37] A.E. Wiselogel, F.A. Agblevor, D.K. Johnson, S. Deutch, J.A. Fennel, M.A. Sanderson, Compositional changes during storage of large round switchgrass bales, Bioresource Technology (56) (1996) 103-109.

[38] P.T. Williams, N. Nugranad, Comparison of products from the pyrolysis and catalytic pyrolysis of rice husks, Energy (25) (2000) 493-513.

[39] J.A. Caballero, R. Font, A. Marcilla, Study of the primary pyrolysis of Kraft lignin at high heating rate: yields and kinetics, Journal of Analytical and Applied Pyrolysis (36) (1996) 159-178.

[40] J.A. Caballero, R. Font, A. Marcilla, Kinetic study of the secondary thermal decomposition of Kraft lignin, Journal of Analytical and Applied Pyrolysis (38) (1996) 131-152.

[41] E. Adler, The lignin chemistry – past, present, future, Wood Science and Technology (11) (1977) 169-218.

[42] H. Nimz, Beech lignin—Proposal of a constitutional scheme, Angewandte Chemie International Edition in English (13) (1974) 313-321.

[43] S.V. Vassilev, D. Baxter, C.G. Vassileva, An overview of the behaviour of biomass during combustion Part 1. Phase-mineral transformations of organic and inorganic matter, Fuel (112) (2013) 391-449.

[44] E. Jakab, O. Faix, F. Till, T. Szekely, Thermogravimertry mass spectromertry study of six lignins within the scope of an internation round robin test, Journal of Analytical and Applied Pyrolysis (35) (1995) 167-179.

[45] S.V. Vassilev, D. Baxter, L.K. Anderson, C.G. Vassileva, An overview of the chemical composition of biomass, Fuel (89) (2010) 913-933.

[46] J.M. Reckamp, R.A. Garrido, J.A. Satrio, Selective pyrolysis of paper mill sludge by using pretreatment processes to enhance the quality of bio-oil and biochar products, Biomass and Bioenergy (71) (2014) 235-244.

[47] E. Novaes, M. Kirst, V. Chiang, H. Winter-Sederoff, R. Sederoff, Lignin and biomass: A negative correlation for wood formation and lignin content in trees, Plant Physiology (154) (2010) 555-561.

[48] F. Collard, J. Blin, A review on pyrolysis of biomass constituents: Mechanisms and composition of the products obtained from the conversion of cellulose, hemicelluloses and lignin, Renewable and Sustainable Reviews (38) (2014) 594-608.

[49] I. Pastorova, R.E. Botto, P.W. Arisz, J.J. Boon, Cellulose char structure: a combined analytical Py-GC-MS, FTIR, and NMR study, Carbohydrate Research (262) (1994) 27-47.

[50] I. Milosavljevic, V. Oja, M. Suuberg, Thermal effects in cellulose pyrolysis: Relationship to char formation processes, Industrial and Engineering Chemistry Research (35) (1996) 653-662.

[51] J. Scheirs, G. Camino, W. Tumiatti, Overview of water evolution during the thermal degradation of cellulose, European Polymer Journal (37) (2001) 933-942.

[52] M. Widaywati, T.L. Church, N.H. Florin, A.T. Harris, Hydrogen synthesis from biomass pyrolysis with in situ carbon dioxide capture using calcium oxide, International Journal of Hydrogen Energy (36) (2011) 4800-4813.

[53] V. Mamleev, S. Bourbigot, M. Le Bras, J. Yvon, The facts and hypothesis to the phenomenon model of cellulose pyrolysis Interdependance of the steps, Journal of Analytical and Applied Pyrolysis (84) (2009) 1-17.

[54] Q. Lu, X. Yang, C. Dong, Z. Zhang, X. Zhang, X. Zhu, Influence of pyrolysis temperature and time on the cellulose fast pyrolysis products: Analytical Py-GC/MS study, Journal of Analytical and Applied Pyrolysis (92) (2011) 430-438.

[55] C.A. Zaror, I.S. Hutchings, D.L. Pyle, H.N. Stiles, R. Kandiyoti, Secondary char formation in the catalytic pyrolysis of biomass, Fuel (64) (1985) 990-994.

[56] M.G. Gronli, Mathematical model for wood pyrolysis-comparison of experimental measurements with model predictions, Energy Fuels (14) (2000) 791-800.

[57] D.K. Shen, S. Gu, The mechanisms for thermal decomposition of cellulose and its main products, Bioresource Technology (100) (2009) 6496-6504.

[58] S. Soares, G. Camino, S. Levchik, Comparative study of the thermal decomposition of pure cellulose and pulp paper, Polymer Degradation and Stability (49) (1995) 275-283.

[59] H. Yang, R. Yan, H. Chen, D.H. Lee, C. Zheng, Characteristics of hemicellulose, cellulose and lignin pyrolysis, Fuel (86) (2007) 1781-1788.

[60] V. Strezov, B. Moghtaderi, J.A. Lucas, Thermal study of decomposition of selected biomass samples, Journal of Thermal Analysis and Calorimetry (72) (2003) 1041-1048.

[61] W. Yi-min, Z. Zeng-li, L. Hai-bin, H. Fang, Low temperature pyrolysis characteristics of major components of biomass, Journal of Fuel Chemistry and Technology (37) (2009) 427-432.

[62] S. Julien, E. Chornet, P.K. Tiwari, R.P. Overend, Vacuum pyrolysis of cellulose: Fourier transform infrared characterisation of solid residues, products distribution and correlations, Journal of Analytical and Applied Pyrolysis (19) (1991) 81-104.

[63] P.R. Patwardhan, J.A. Satrio, R.C. Brown, B.H. Shanks, Influence of inorganic salts on the primary pyrolysis products of cellulose, Bioresource Technology (101) (2010) 4646-3655.

[64] M.R. Gray, W.H. Corcora, G.R Gavalas, Pyrolysis of wood-derived material. Effect of moisture content and ash content, Industrial and Engineering Chemistry Process Design and Development (24) (1985) 646-651.

[65] P.R. Patwardhan, D.L. Dalluge, B.H. Shanks, R.C. Brown, Distinguishing primary and secondary reactions of cellulose pyrolysis, Bioresource Technology (102) (2011) 5265-5269.

[66] R. Alen, E. Kuoppala, P. Oesch, Formation of the main degradation compound groups from wood and its components during pyrolysis. Journal of Analytical and Applied Pyrolysis (36) (1996) 137-148.

[67] Y. Lin, J. Cho, G.A. Tompsett, P.R. Westmoreland, G.W. Huber, Kinetics and mechanisms of cellulose pyrolysis, Journal of Physical Chemistry (113) (2009) 20097-20107.

[68] G.R. Ponder, G.N. Richards, T.T. Stevenson, Influence of linkage position and orientation in pyrolysis of polysaccharides: a study of several glucans, Journal of Analytical and Applied Pyrolysis (22) (1992) 217-229.

[69] Z. Wang, A.G. McDonald, R.J.M Westerhof, S.R.A Kersten, C.M. Cuba-Torres, S. Ha, B. Pecha, M. Garcia-Perez, Effect of cellulose crystallinity on the formation of a liquid intermediate and on product distribution during pyrolysis, Journal of Analytical and Applied Pyrolysis (2013) (100) 56-66.

[70] K. Werner, L. Pommer, M. Brostom, Thermal decomposition of hemicellulose, Journal of Analytical and Applied Pyrolysis (110) (2014) 130-137.

[71] T. Hosoya, H. Kawamoto, S. Saka, Pyrolysis behaviours of wood and its constituent polymers at gasification temperature, Journal of Analytical and Applied Pyrolysis (78) (2007) 328-336.

[72] D.K. Shen, A.V. Bridgwater, Study on the pyrolytic behaviour of xylan-based hemicellulose using TG-FTIR and Py-GC-FTIR, Journal of Analytical and Applied Pyrolysis (87) (2010) 199-206.

[73] R.K. Sharma, J.B. Wooten, V.L. Baliga, X. Lin, W.G. Chan, M.R. Hajaligol, Characterization of chars from pyrolysis of lignin, Fuel (83) (2004) 1469-1482.

[74] H. Kawamoto, S. Horigoshi, S. Saka, Pyrolysis reactions of various lignin model dimers, Journal of Wood Science (53) (2007) 168-174/

[75] T. Nakamura, H. Kawamoto, S. Saka, Pyrolysis behaviour of Japanese cedar wood lignin studied with various model dimers, Journal of Analytical and Applied Pyrolysis (81) (2008) 173-182.

[76] D.K. Shen, S. Gu, K.H. Luo, S.R. Wang, M.X. Fang, The pyrolytic degradation of wood-derived lignin from pulping process, Bioresource Technology (101) (2010) 6136-6146.

[77] A.K. Hossain, P.A. Davies, Pyrolysis liquids and gases as alternative fuels in internal combustion engines – A review, Renewable and Sustainable Energy Reviews (21) (2013) 165-189.

[78] M. Carrier, T. Hugo, J. Gorgens, H. Knoetze, Comparison of slow and vacuum pyrolysis of sugar cane bagasse, Journal of Analytical and Applied Pyrolysis (90) (2011) 18-26.

[79] H.J. Park, J. Dong, J. Jeon, Y. Park, K. Yoo, S. Kim, J. Kim, S. Kim, Effects of the operating parameters on the production of bio-oil in the fast pyrolysis of Japanese larch, Chemical Engineering Journal (143) (2008) 124-132.

[80] E. Apaydin-Varol, E. Putun, A.E. Putun, Slow pyrolysis of pistachio shell, Fuel (86) (2007) 1892-1899.

[81] M. Garcia-Pereze, X.S. Wang, J. Shen, M.J. Rhodes, F. Tian, W. Lee, H. Wu, C. Li, Fast pyrolysis of oil mallee woody biomass: Effects of temperature on the yield and quality of pyrolysis products, Industrial and Engineering Chemistry Research (47) (2008) 1846-1854

[82] H.B. Goyal, D. Seal, R.C. Saxena, Bio-fuels from thermochemical conversion of renewable resources: A review, Renewable and Sustainable Energy Reviews (12) (2008) 504-517.

[83] Y. Elkasabi, C.A. Mullen, A.A. Boateng, Distillation and isolation of commodity chemicals from bio-oil made by tail-gas reactive pyrolysis, Sustainable Chemistry and Engineering (2) (2014) 2042-2052.

[84] C. Wang, Z. Du, J. Pan, J. Li, Z. Yang, Direct conversion of biomass to bio-petroleum at low temperatures, Journal of Analytical and Applied Pyrolysis (78) (2007) 438-444.

[85] J.D. Adjaye, N.N. Bakhshi, Production of hydrocarbons by catalytic upgrading of a fast pyrolysis bio-oil. Part I: Conversion over various catalysts, Fuel Processing Technology (45) (1995) 161-183.

[86] Q. Lu, Z. Zhang, C. Dong, X. Zhu, Catalytic upgrading of biomass fast pyrolysis vapors with nano metal oxides: An analytical Py-GC/MS study, Energies (3) (2010) 1805-1820.

[87] P. de Wild, H.J. Heeres, Biomass pyrolysis for chemicals, PhD Thesis, University of Groningen, Netherlands, 2011.

[88] T. Werpy, G. Petersen, Top value added chemicals from biomass: Volume 1 – Results of screening for potential candidates from sugars and synthesis gas, U.S. Department of Energy, Oak Ridge, 2004.

[89] R.A. Sheldon, Green and sustainable manufacture of chemicals from biomass: state of the art, Green Chemistry (16) (2014) 950-963.

[90] S. Czernik, A.V. Bridgwater, Overview of applications of biomass fast pyrolysis oil. Energy & Fuels (18) (2004) 590-598.

[91] F.N. Peters, Industrial uses of furans, Industrial and Engineering Chemistry (31) (1939) 178-180.

[92] G. Duman, C. Okutucu, S. Ucar, R. Stahl, J. Yanik, The slow and fast pyrolysis of cherry seed, Bioresource Technology (102) (2011) 1869-1878.

[93] A.V. Bridgwater, Principles and practices of biomass fast pyrolysis processes for liquids, Journal of Analytical and Applied Pyrolysis (51) (1999) 3-22.

[94] O. Onay, O.M. Kockar, Fixed-bed pyrolysis of rapeseed (Brassica napus L.), Biomass and Bioenergy (26) (2004) 289-299.

[95] T.E. McGrath, W.G. Chan, M.R. Hajaligol, Low temperature mechanisms for the formation of polycyclic aromatic hydrocarbons from the pyrolysis of cellulose, Journal of Analytical and Applied Pyrolysis (66) (2003) 51-70.

[96] D. Chen, J. Zhou, Q. Zhang, Effects of heating rate on slow pyrolysis behaviour, kinetic parameters and product properties of moso bamboo, Bioresource Technology (169) (2014) 313-319.

[97] A.N. Phan, C. Ryu, V.N. Sharifi, J. Swithenbank, Characterisation of slow pyrolysis products from segregated waste for energy production, Journal of Analytical and Applied Pyrolysis (81) (2008) 65-71.

[98] A.E. Putun, E. Onal, B.B. Uzun, N. Ozbay, Comparison between the "slow" and "fast" pyrolysis of tobacco residue, Industrial Crops and Products (26) (2007) 307-314.

[99] O. Onay, O.M. Kockar, Slow, fast and flash pyrolysis of rapeseed, Renewable Energy (28) (2003) 2417-2422.

[100] C. Di Blasi, Combustion and gasification rates of lignocellosic chars, Progress in Energy and Combustion Science (35) (2009) 121-140.

[101] R. Kurose, M. Ikeda, H. Makino, Combustion characteristics of high ash coal in a pulverized coal combustion, Fuel (80) (2001) 1447-1455.

[102] S. Jayanti, K. Maheswaran, V. Saravanan, Assessment of the effect of high ash content in pulverized coal combustion, Applied Mathematical Modelling (31) (2007) 934-953.

[103] K.S.W Sing, D.H. Everett, R.A.W. Haul, L. Moscou, R.A. Pierottis, J. Rouquerol, T. Siemieniewska, Reporting physisorption data for Gas/Solid systems, International union of pure and applied chemistry (57) (1985) 603-619.

[104] M. Amutio, G. Lopez, R. Aguado, M. Artetxe, J. Bilbao, M. Olazar, Effect of vaccum on lignocellulosic biomass flash pyrolysis in a conical spouted bed reactor, Energy and Fuels (25) (2011) 3950-3960.

[105] A. Demirbas, The influence of temperature on the yields of compounds existing in bio-oils obtained from biomass samples via pyrolysis, Fuel Processing Technology (88) (2007) 591-597.

[106] C.E. Greenhalf, D.J. Nowakowski, A.B. Harms, J.O. Titiloye, A.V. Bridgwater, Sequential pyrolysis of willow SRC at low and high heating rates – Implications for selective pyrolysis, Fuel (93) (2012) 692-702.

[107] R. Reschmeier, D. Roveda, D. Muller, J. Karl, Pyrolysis kinetics of wood pellets in fluidized beds, Journal of Analytical and Applied Pyrolysis (108) (2014) 117-129.

[108] P. Morf, P. Hasler, T. Nussbaumer, Mechanisms and kinetics of homogenous secondary reactions of tar from continuous pyrolysis of wood chips, Fuel (81) (2002) 843-853.

[109] J. Shen, X. Wang, M. Garcia-Perez, D. Mourant, M.J. Rhodes, C. Li, Effects of particle size on the fast pyrolysis of oil mallee woody biomass, Fuel (88) (2009) 1810-1817.

[110] A. Demirbas, Effects of temperature and particle size on bio-char yield from pyrolysis of agricultural residues, Journal of Analytical and Applied Pyrolysis (2004) (72) 243-248.

[111] W.C. Park, AQ. Atreya, H.R. Baum, Experimental and theoretical investigation of heat and mass transfer processes during wood pyrolysis, Combustion and Flame (157) (2010) 481-494.

[112] M. Jeguirim, L. Limousy, P. Dutournie, Pyrolysis kinetics and physicochemical properties of agropellets produced from spent ground coffee blended with conventional biomass, Chemical Engineering Research and Design (92) (2014) 1876-1882.

[113] M .Basat, M. Balat, E. Kirtay, H. Balat, Main routes for the thermos-conversion of biomass into fuels and chemicals. Part 1: Pyrolysis systems, Energy conversion and Management (50) (2009) 3147-3157.

[114] Y. Lin, C. Zhang, M. Zhang, Jian Zhang, Deoxygenation of bio-oil during pyrolysis of biomass in the presence of CaO in a fluidized-bed reactor, Energy Fuels (24) (2010) 5686-5695.

[115] W.S.L. Mok, M.J. Antal, Effects of pressure on biomass pyrolysis. 1. Cellulose pyrolysis products, Thermochimica (68) (1983) 155-164.

[116] L. Basile, A. Tugnoli, C. Stramigioli, V. Cozzani, Influnce of pressure on the heat of biomass pyrolysis, Fuel (137) (2014) 277-284.

[117] G. Newalkar, K. Iisa, A.D. D'Amico, C. Sievers, P. Agrawal, Effect of temperature, pressure, and residence time on pyrolysis of pine in an entrained flow reactor, Energy and Fuels (28) (2014) 5144-5157.

[118] V. K. Venatakrishnan, J.C. Degenstein, A.D. Smeltz, W.N. Delgass, R. Agrawal, F.H. Ribeiro, High-pressure fast pyrolysis, fast-hydropyrolysis and catalytic hydrodeoxygenation of cellulose: production of liquid fuel from biomass, Green

[119] S. Leng, X. Wang, Q. Cai, F. Ma, Y. Liu, Jianguo, Selective production of chemicals from biomass pyrolysis over metal chlorides supported by zeolite, Bioresource technology (149) (2013) 341-345.

[120] Q. Lu, Z. Wang, C. Dong, Z. Zhang, Y. Zhang, Y. Yang, X. Zhu, Selective fast pyrolysis of biomass impregnated with $ZnCl_2$: Furfural production together with acetic acid and activated carbon as by-products, Journal of Analytical and Applied Pyroylsis (91) (2011) 273-279.

[121] F. Tinwala, P. Mohanty, S. PArmar, A. Patel, K.K. Pant, Intermediate pyrolysis of agro-industrial biomasses in bench-scale pyrolyser: Product yields and its characterization, Bioresource Technology (188) (2015) 258-264.

[122] Y. Yang, J.G. Brammer, A.S.N. Mahmood, A. Hornung, Intermediate pyrolysis of biomass energy pellets for producing sustainable liquid, gaseous and solid fuels, Bioresource Technology (169) (2014) 794-799.

[123] W.A. de Jongh, M. Carrier, J.H. Knoetze, Vacuum pyrolysis of intruder plant biomasses, Journal of Analytical and Applied Pyrolysis (2011) (92) 184-193.

[124] A.V. Bridgwater, Review of fast pyrolysis of biomass and product upgrading, Biomass and Bioenergy (38) (2012) 68-94.

[125] D. Chiaramonti, A. Oasmaa, Y. Solantausta, Power generation using fast pyrolysis liquids from biomass, Renewable and Sustainable Energy Reviews (11) (2007) 1056-1086.

[126] A.V. Bridgwater, Renewable fuels and chemicals by thermal processing of biomass, Chemical Engineering Journal (91) (2003) 87-102.

[127] H. Ben, A.J. Ragauskas, Comparison for the compositions of fast and slow pyrolysis oils by NMR characterization, Bioresource Technology (147) (2013) 577-584.

[128] X. Li, V. Strezov, T. Kan, Energy recovery potential analysis of spent grounds pyrolysis products, Journal of Analytical and Applied Pyrolysis (110) (2014) 79-87.

[129] N. Troger, D. Richter, R. Stahl, Effect of feedstock composition on product yields and energy recovery rates of fast pyrolysis products from different straw types, Journal of Analytical and Applied Pyrolysis (100) (2013) 158-165.

[130] A.L.M.T. Pighinelli, A.A. Boateng, C.A. Mullen, Y. Elkasabi, Evaluation of Brazillian biomasses as feedstocks for fuel production via fast pyrolysis, Energy for Sustainable Development (21) (2014) 42-50.

[131] J. Han, A. Elgowainy, J.B. Dunn, M.Q. Wang, Life cycle analysis of fuel production from fast pyrolysis of biomass, Bioresource Technology (133) (2013) 421-428.

CHAPTER 3: RESEARCH OBJECTIVES

The overall research goal of this PhD project is to assess the full potential of conventional pyrolysis techniques as a part of a biorefinery by converting various paper waste sludges and its fermentation residues (FR) containing variable amounts of organic material into energy, chemical (bio-oil), and/or biomaterial (char) resources. Optimisation and statistical analysis of the yields will provide a better understanding of the degradation pathways and mechanisms involved in pyrolysis to draw the maximal benefit from the conversion of PWS and its FR More specifically, the objectives are:

1) To assess the technical feasibility of pyrolytic conversion of PWS (low and high ash PWS), obtained from the full range of types and properties available in South Africa, and its FRs.

From the full range of available mills in South Africa (separate study), the extremes in PWS ash content was used as a criterion for sample selection: the pulp mill Sappi Ngodwana was selected to supply a low ash PWS, and the tissue paper mill Kimberly-Clark was selected to supply the high ash PWS. In a separate study, the low and high PWSs were subjected to fermentation generating both bioethanol and waste fermentation residues, of which the latter was used for the pyrolysis experiments. The technical difficulties associated with fast pyrolysis, such as feeding, fluidisation and char separation, needed to be overcome in order for it to be a technically feasible approach for PWS/FR valorisation. These technical difficulties were overcome by pelletizing the PWS/FR (**Chapter 4 and 7**).

2) To maximize the production of bio-oil or char by optimising key operating conditions during fast, slow and vacuum pyrolysis conversion of low and high ash PWS/FR.

To accomplish this objective, fast (**Chapter 4**), vacuum and slow (**Chapter 5**) pyrolysis were optimised for reactor temperature and pellet size, using a 2-way linear and quadratic model, to either maximise the bio-oil or char yield from PWS. Slow pyrolysis was used as the benchmark and was compared to other published works, as vacuum and fast pyrolysis were not yet considered. A similar approach was taken for the pyrolytic conversion of FR, except only the most influential variable, reactor temperature, was selected as this was an exploratory study (**Chapter 7**).

3) To describe the fate and role of the inorganic components during PWS/FR pyrolysis by adapting analytical methods.

Due to the inherently large ash content, particularly in high ash PWS, some analytical methods (e.g., proximate and ultimate analysis) were adapted to account for thermal decomposition as well as changes in the composition of the inorganics compounds during pyrolysis (**Chapters 4, 5, 7 and 8**). Furthermore, the role of the inorganics (primarily calcium) on the thermodynamic and chemical pyrolytic mechanisms was of interest (**Chapters 4 to 8**).

4) To evaluate the capability of each conversion process in an energy context, at various key operating conditions, by comparing the gross energy conversion.

The strategy for accomplishing this objective was to assess and compare the performance of vacuum, slow and fast pyrolysis, at varying reactor temperatures and pellet sizes, to maximise the transfer of energy from raw PWS to the liquid and solid products (**Chapter 5**). In a similar way, the conversion of energy from PWS to bioethanol, during fermentation, as well as from its FR to the

pyrolytic solid and liquid products was assessed, and then compared to the stand-alone pyrolysis performance (**Chapter 7**).

5) To evaluate the capability of each pyrolysis process in a chemical and biomaterial resource production context, at various key operating conditions, by comparing yields of some valuable chemicals and physico-chemicals characteristics of the char.

In order to achieve this objective, the capability of vacuum, slow and fast pyrolysis, at varying key operating conditions, to selectively drive the conversion of raw PWS/FR into target chemicals (liquid) and biomaterials (char) was evaluated by comparing the chemical yields and char physico-chemical characteristics (**Chapters 6 and 7**).

6) To compare the product distribution and physico-chemical characteristics between each pyrolysis process, as well as at various key operating conditions, to reveal new thermodynamic and chemical mechanistic insights.

The effect of specific operating conditions, nature and content of inorganics, as well as the pyrolysis technique, on the product yields and physico-chemical characteristics were investigated (**Chapters 4 to 7**). This study provided new thermodynamic (**Chapter 4**) and chemical (**Chapters 5, 6 and 7**) mechanistic insights into pyrolysis and improved conversion of PWS/FR.

7) To assess for each type of PWS/FR the potential of the pyrolysis products as value-added marketable energy, chemical (bio-oil) and biomaterial (char) resources, considering pyrolysis as a process converting the PWS/FR generated in a biorefinery context.

The quality of the bio-oil and char products generated from low and high ash PWS/FR were evaluated for their potential as sources of energy, chemicals (bio-oil) and biomaterials (char)

(**Chapters 5, 6 and 7**). Char was recommended for energy and/or adsorbent production, while bio-oil was recommended for energy and/or chemicals production.

8) To evaluate the consequence of fermentation pre-treatment on the pyrolysis product distribution and physico-chemical characteristics.

The effect of fermentation pre-treatment on the vacuum, slow and fast pyrolysis product yields and physico-chemical characteristics was evaluated by comparing the FR results to those obtained during stand-alone pyrolysis of PWS (**Chapter 7**).

CHAPTER 4: FAST PYROLYSIS OF LOW AND HIGH ASH PAPER WASTE SLUDGE: INFLUENCE OF REACTOR TEMPERATURE AND PELLET SIZE

Published in Journal of Analytical and Applied Pyrolysis (111) (2013) 64-75 (ISI impact factor 3.898).

Title: "Fast pyrolysis of low and high ash paper waste sludge: Influence of reactor temperature and pellet size"

Authors: Angelo J. Ridout, Marion Carrier, Johann Görgens.

OBJECTIVE OF DISSERTATION AND SUMMARY OF FINDINGS IN PRESENT CHAPTER

This chapter addresses **objectives 1 to 3 and 6** which focusses on the technical feasibility of FP conversion of low and high PWS (8.5 and 46.7 wt.%) (**objective 1**), bio-oil yield maximisation (**objective 2**), and the role and fate of inorganics during PWS pyrolysis (**objective 3**). Furthermore, a thermogravimetric analysis was performed to gain insight on thermodynamic pyrolysis mechanisms (**objective 4**).

The optimal reactor temperatures for maximisation of the bio-oil yields were 400 ^{o}C and 340 ^{o}C for LAPWS and HAPWS, respectively, and were significantly lower than optima reported for other lignocellulosic biomass (450 to 550 ^{o}C), probably due to the catalytic effect of calcium on primary pyrolysis reactions. Furthermore, the highest bio-oil yields were attained using an intermediate pellet size (~5-6 mm), which is contrary to trends typically reported in literature, whereby smaller particle sizes enhance bio-oil production. The thermogravimetric analysis indicated that the decrease in the bio-oil yield at smaller particle sizes was due to an increase in non-condensable gas yield. This increase in non-condensable gas yield was associated with an increase in exothermic secondary reactions for high heating rates using smaller pellet sizes, and was apparently catalysed by the presence of inorganics in PWS.

Candidate declaration

With regards to chapter 4, page numbers 78-120 of this dissertation, the nature and scope of my contribution were as follows:

Name of contribution	Extent of contribution (%)
Experimental planning	70
Executing experiments	90
Interpretation of results	70
Writing the chapter	100

The following co-authors have contributed to chapter 4 page 78-120 of this dissertation:

Name	e-mail address	Nature of contribution	Extent of contribution (%)
1. Marion Carrier	m.carrier@aston.ac.uk	• Experimental planning • Executing experiments • Reviewing the chapter • Interpretation of results	20 10 80 30
2. Johann Görgens	jgorgens@sun.ac.za	• Reviewing the chapter • Experimental planning	20 10

Signature of candidate…….

Date…….

Declaration by co-authors

The undersigned hereby confirm that:

1. The declaration above accurately reflects the nature and extent of the contributions of the candidates and co-authors to chapter 4 page numbers 78-120 in the dissertation,
2. no other authors contributed to chapter 4 page numbers 78-120 in the dissertation beside those specified above, and
3. potential conflicts of interest have been revealed to all interested parties and that are necessary arrangements have been made to use the material in chapter 4 page numbers 78-120 of the dissertation

Signature	Institutional affiliation	Date
	Universidad de Concepcion	
	Stellenbosch Univeristy	

FAST PYROLYSIS OF LOW AND HIGH ASH PAPER WASTE SLUDGE: INFLUENCE OF REACTOR TEMPERATURE AND PELET SIZE

Angelo J. Ridout*, Marion Carrier[x], Johann Görgens

Department of Process Engineering, University of Stellenbosch, Private Bag X1, Matieland 7602, South Africa

ABSTRACT

Paper waste sludge (PWS) is a waste produced in large quantities by the pulp and paper industry, and is usually disposed by landfilling. This study investigates the pyrolytic conversion of PWS as an alternative to its valorisation. Low and high ash PWSs (8.5 and 46.7 wt.%) were subjected to fast pyrolysis conversion to maximise the bio-oil yield by optimising the reactor temperature and pellet size. Maximum bio-oil yields of 44.5 ± 1.7 daf, wt.% at 400 ºC, and 59.9 ± 4.1 daf, wt.% at 340 ºC, for an intermediate pellet size of 4.84 ± 0.15 mm, were attained from the conversion of the low and high PWS, respectively. The low optimal reactor temperatures, as well as the high bio-oil yields, make valorisation via fast pyrolysis conversion promising. A significant reduction in the O/C molar ratio of up to 35%, from the high ash PWS to its bio-oil product, led to a 65% increase of the higher heating value. A thermogravimetric study was implemented to investigate the pyrolytic mechanisms behind the increase in bio-oil yield with intermediate pellets sizes. It revealed that the observed increase in non-condensable gas yield, which corresponded to a decrease in the bio-oil yield, was due to the promotion of exothermic reactions for high heating rates using smaller pellet sizes.

Keywords: Paper waste sludge, Fast pyrolysis, Optimisation, Bio-oil, Energy

[x] *Present address: Technological Development Unit (UDT) Universidad de Concepcion, Av. Cordillera Nº 2634 – Parque Industrial Coronel. 4191996. Casilla 4051, Conception, Chile*

4.1 INTRODUCTION

The pulp and paper industry produces large quantities of paper waste sludge (PWS), which is composed of organic matter and has the potential to be used as a renewable energy source [1]. It is rejected for use in pulp and/or paper production due to the fibre length and quality being inadequate for the finished product. Typical quantities produced by pulp and paper mills are in the range of 60 to 100 kg's and 50 to 600 kg's per ton of final product, respectively, and is usually disposed of by landfilling [2]. Due to increasing costs and negative environmental impact of land filling, a more environmentally friendly alternative such as thermochemical conversion of PWS is required [3-6]. In this study, the process of pyrolysis, whereby the feedstock is thermally decomposed in the absence of oxygen, into the products of bio-oil, non-condensable gas and char, is used.

PWS varies in ash content (AC) depending on the type of mill (pulp or paper), and feedstock used. Paper mills that use recycled paper as a feedstock, typically produce PWS (deinking sludge) that is high in AC (~40 wt.%) due to the removal of fillers such as calcium carbonate [3]. While pulp mills that use wood species as a feedstock, typically produce PWS that is low in AC (~6 wt.%) [3]. The presence of ash is generally seen as a disadvantage in pyrolysis conversion as bio-oil yields are decreased. Thermogravimetric studies were performed on a range of different PWS types by Mendez *et al.* [3] to characterize their pyrolytic behaviour. Results indicated that the presence of high AC and degraded fibres, particularly in PWS from paper mills using recycled paper as a feedstock, lowered the starting temperature for weight loss [3]. This result pointed out the critical role of the ash content on the whole pyrolysis process. Recent studies by Strevoz *et al.* [6] investigated the thermal characteristics and energy required for pyrolysis of recycle PWS with a low AC of 7.8 wt.%. The samples were slowly pyrolyzed (10 $^{o}C.min^{-1}$), in a packed bed thermal apparatus, to 700 ^{o}C offering a good compromise for the production of bio-oil (36 wt.% or 43 daf,

wt.%), gas (31 wt.%) and char (32 wt.%). Lou *et al.* [4] subjected deinking sludge, with a high AC of 41.5 wt.%, to thermogravimetry, Py-GC/MS and slow pyrolysis (fixed bed) to investigate its thermal characteristics. The slow pyrolysis experiment, performed at 800 ^{o}C, resulted in bio-oil, gas and char yields of 24.4 (41.7 daf, wt.%), 28.8 and 45.8 wt.%, respectively. In another study, Yang *et al.* [7] and Ouadi *et al.* [5] investigated the characteristics of bio-oil produced from intermediate pyrolysis of two different pelletized deinking sludges which were high in AC (62.9 and 74.5 wt.%, respectively). Intermediate pyrolysis was performed on the deinking sludges using an Auger reactor at 450 ^{o}C under atmospheric pressure. The conditions of intermediate pyrolysis lie between those of fast and slow pyrolysis whereby feedstock residence times are long (7 to 10 minutes; slow pyrolysis), but vapour residence times are short (few seconds; fast pyrolysis) [7]. It was suggested by Yang *et al.* [8] that the heating rate is significantly lower than in fast pyrolysis. The product yields, reported by Yang *et al.* [7], for the bio-oil, char and gas yield were 10 (27.9 daf, wt.%), 79 and 11 wt. %, respectively. The bio-oil, with a higher heating value (HHV) of 36.5 MJ.kg^{-1} and low oxygen content, was shown to supply sufficient heat to power a diesel engine [7]. Ouadi *et al.* [5] concluded that intermediate pyrolysis of PWS is a feasible method for its valorisation. This brief retrospect on pyrolysis of PWSs indicates that bio-oil yields vary in large extent depending on their origin and that the products offer a good potential energy source.

While fast pyrolysis technologies are known to enhance bio-oil yields [9], only slow and intermediate pyrolysis has been considered in all cases mentioned above. Typically the conversion of biomass via fast pyrolysis (FP), when compared to other techniques, offers the highest quantity, quality and energy content of bio-oil [10-13]. In this study, the FP of PWS is investigated in order to determine the potential of bio-oil as a high-energy feedstock. Indeed it is often mentioned that the production of bio-oil is favoured as it is easily handled, stored and is energy dense [10]. The FP

conversion of biomass has been demonstrated to be a promising process for bio-energy production such as transportation fuels [10], thermal and electrical energy [10,13,14].

Therefore, the aim of this work focussed on the maximisation of the bio-oil from the FP conversion of low and high ash PWS, by optimising the reactor temperature and pellet size. This is performed using a 2-way linear and quadratic statistical model. In addition to that a thermogravimetric study was performed on different PWS pellet sizes at different heating rates to gain insight on the pyrolysis mechanisms.

4.2 MATERIALS AND METHODS

4.2.1 Raw materials and preparation

Two different PWS types were sourced based on the type of mill. The first type of PWS, which was particularly low in AC (8.5 wt.% at 525 ^{o}C, Table 4-1), and was termed as low ash paper waste sludge (LAPWS), was supplied by the Kraft pulp mill, Sappi Ngodwana. The second type, which had a high AC (46.7 wt.% at 525 ^{o}C, Table 4-1), and was termed as high ash paper waste sludge (HAPWS), was supplied by the recycle tissue paper mill, Kimberly-Clark Enstra. The as-received wet LAPWS and HAPWS were dried in an oven for 12 hours at 105 ± 2 ^{o}C. The dried sludge was then milled to separate the clumped fibres, using a 2 mm sieve on a Retsch hammer mill. The PWS was subsequently pelletized to improve feeding (screw fed) and fluidisation in the bubbling fluidised bed reactor. Initially the milled PWS was rehydrated (PWS:Water 1:1), and then pelletized using a Trespade No.12 electric meat mincer, after which the pellets were dried for 12 hours at 105 ± 2 ^{o}C. The pellets were produced in sizes varying between 3, 4, 5 and 6 mm. All the pellet sizes were found to fluidise well in the bed.

4.2.2 Feedstock characterisation

4.2.2.1 Physico-chemical characterisation

The cone and quartering sub-sampling method (DD CEN/TS 14780:2005) was used on the LAPWS and HAPWS batches to select samples for physico-chemical characterization. The moisture content for the as-received PWS was determined in accordance with the TAPPI T264 om-88 standard procedure. Ash content (AC_{525}) was determined in accordance with the ISO 1762 standard procedure using a muffle furnace to combust the samples at 525 ± 5 ^{o}C. The mineral composition (oxides) of the PWS was determined via X-ray fluorescence (XRF) analysis using an AXIOS PANalytical. Fused glass discs were used for the major elemental analysis. Trace elemental ICP analysis was performed on the HAPWS to determine the calcium content. Samples (0.25 g) were initially digested by microwave using nitric acid (7 mL) after which 43 mL of deionised water was added. The digested samples where then subjected to ICP analysis using a Thermo Scientific iCap 6200 series spectrometer. The HAPWS was further subjected to Fourier transform infrared (FT-IR) spectroscopy to determine the form of the calcium components. This was performed using a Perkin Elmer Paragon 1000PC FTIR spectrometer with a MTEC Photoacoustic Model 300 attachment. The resulting FT-IR spectra of the HAPWS feedstock was compared to those of pure compounds such as calcium carbonate, calcium hydroxide and calcium oxide (Edu Trade). Proximate analysis was determined for the LAPWS in accordance with the ASTM E1131 standard procedure using a TGA/DSC 1-LF1100 Mettler Toledo. In Section 4.3.1, the inorganic composition of the HAPWS was shown to be comprised mainly of calcium carbonate which thermally decomposes at temperatures above 650 ^{o}C [3] according to Equation 1.

$$CaCO_3 \longrightarrow CaO + CO_2 \quad (1)$$

Thus the ASTM E1131 method was altered for HAPWS, by including a step holding the temperature at 650 ^{o}C for 5 minutes to drive off the organic volatiles, after which it was heated to 900 ^{o}C and held for an additional 5 minutes to insure full calcium carbonate decomposition occurred before combustion of the fixed carbon. The remaining ash, after combustion of the fixed carbon, was termed AC_{900}. Ultimate analysis was performed using a TruSpec Micro from LECO. During ultimate analysis samples are combusted in a fluidised bed at 1080 ^{o}C, thus making calcium carbonate decomposition into CO_2 (Equation 1) for HAPWS inevitable. To determine the organic carbon content the weight percentage of CO_2, produced by calcium carbonate decomposition (difference in AC_{525} and AC_{900}), was used to correct the mass balance. The higher heating values of the dried PWSs were determined using a Cal2K ECO bomb calorimeter that was calibrated using benzoic acid. For purposes of comparison the HHVs were calculated and expressed on a dry basis.

Lignocellulosic composition analysis of the PWSs was determined in accordance with the NREL laboratory analytical procedure. The extractives contained in the PWS were determined in accordance with NREL/TP-510-42619 standard method, using distilled water followed by 95 % ethanol (Science World SA). Structural carbohydrates and lignin were determined in accordance with the revised NREL/TP-510-42618 standard method, whereby the extracted samples were hydrolysed using 72 wt.% sulphuric acid (Fluka Analytical, Sigma Aldrich) and then autoclaved for 1 hour at 121 ^{o}C. The acid soluble lignin content in the resulting hydrolysis liquor was determined using a Varian Cary 50 Bio UV-Visible spectrophotometer. Structural carbohydrates were determined by subjecting the hydrolysis liquor to HPLC (Thermo Separation Products). Initially the hydrolysis liquor was neutralized to a pH of 7, using a potassium hydroxide solution which was prepared by dissolving 115.52 g of pellets (Merck) in 250 mL of deionised water. The neutralised hydrolysis liquor was then subsequently filtered using a 20 µL filter (Kimix). Thirty micro-litres of

the prepared hydrolysis liquor was injected into the HPLC and the product was separated using an Aminex HPX-87H ion exclusion column (300mm x 7.8mm, Bio-Rad). The column heating program was set constant at 65 ^{o}C with no heating rate. Helium was used as the carrier gas and was set at a flow rate of 0.6 mL.min^{-1}.

4.2.2.2 Thermogravimetric analysis

Thermogravimetric analysis using a TGA/DSC 1-LF1100 system (Mettler-Toledo) was performed on LAPWS and HAPWS to illustrate the potential mass and heat transfer limitations using different pellet sizes and heating rates. Experiments were carried out at atmospheric pressure in a 900 µL alumina crucible at TGA heating rates of 20 ^{o}C.min^{-1} and 150 ^{o}C.min^{-1} using pellets sizes (diameter) of 3, 4, 5 and 6 mm. The temperature ranged from 40 ^{o}C to 900 ^{o}C. Nitrogen was used as an inert purge gas at a flow rate of 70 mL min^{-1}. Heat flux curves were calculated from simultaneous differential thermal analysis (SDTA) curves. The SDTA measured the difference between the sample temperature and the reference temperature. The SDTA signal was calibrated using three different substances namely indium, aluminium and gold (Mettler-Toledo).

4.2.3 Characterisation of pyrolysis products

4.2.3.1 Bio-oil product

The water content in the bio-oil product was determined in accordance with the ASTM E203 standard using a Metrohm 701 Titrino Karl-Fischer titrator. A hydranal composite 5 titrant (Sigma Aldrich) was used. The ash content of the bio-oil was determined in accordance with the ISO 1762 standard procedure using a muffle furnace to combust the samples at 525 ± 5 ^{o}C. Ultimate analysis was performed using a TruSpec Micro from LECO in accordance with ASTM D5291-10. The

calibration of C, H, N and S content was made using the residual oil standard (AR100, LECO) and the calibration was checked using the standard Sulfamethazine (QC, LECO) for bio-oil. The HHV of the bio-oil was determined using Equation 2 from Channiwala *et al.* [15].

$$HHV\ (MJ\ kg^{-1}) = 0.3491*C + 1.1783*H + 0.1005*S - 0.1034*O - 0.0151*N - 0.0211*AC \quad (2)$$

where C, H, S, O, N and AC represent respectively carbon, sulphur, oxygen, nitrogen and ash content in wt.% with the ranges as, $0 < C < 92.25$, $0.43 < H < 25.14$, $0 < O < 50.00$, $0 < N < 5.60$, $0 < S < 94.08$, $0 < AC < 71.4$ and $4.745 < HHV < 55.245$. The calcium content in the HAPWS FP 4 mm bio-oil products obtained at 300, 340 and 390 °C was measured using ICP spectroscopy. The sample preparation and method were performed as previously described (Section 4.2.2.1).

The conversion of energy (CE) from the PWS to the bio-oil product is determined by Equation 3 below:

$$CE\,(\%) = \frac{M_{bio-oil} * HHV_{bio-oil}}{M_{PWS} * HHV_{PWS}} * 100 \quad (3)$$

where $M_{bio\text{-}oil}$ and $HHV_{bio\text{-}oil}$, are respectively the mass and higher heating value (HHV) of the bio-oil product, while M_{PWS} and HHV_{PWS} apply to PWS.

4.2.3.2 Char product

The ash content of the char was determined in accordance with the ISO 1762 standard procedure using a muffle furnace to combust the samples at 525 ± 5 °C. The calcium content in the HAPWS FP 4 mm char products obtained at 300, 340 and 390 °C was measured using ICP spectroscopy. The sample preparation and method were performed as previously described (Section 4.2.2.1). FT-IR spectroscopy was also performed on these char samples to determine whether the calcium components underwent changes during FP.

The ash loss (AL) during fast pyrolysis conversion was determined by Equation 4 below:

$$AL\,(\%) = \frac{M_{PWS} * X_{ash} - X_{char\text{-}ash} * Y_{char} * M_{PWS}}{M_{PWS} * X_{ash\text{-}pws}} * 100 = (1 - \frac{X_{char\text{-}ash} * Y_{char}}{X_{ash\text{-}pws}}) * 100 \qquad (4)$$

where M_{PWS}, is the initial mass of PWS, $X_{ash\text{-}pws}$, is the mass fraction of ash in the PWS (525 ^{o}C, ISO 1762), $X_{char\text{-}ash}$, is the mass fraction of ash in the char (525 ^{o}C, ISO 1762), and Y_{char} is the yield of char in weight percentage.

4.2.4 Fast pyrolysis experiments

The experiments were carried out using the fast pyrolysis unit with a feed capacity of 1kg.hr^{-1}, which was described in detail by Carrier *et al.* [16] and in Appendix A-1 to A-2. In summary, the set-up can be divided in four main sections namely feeding, bubbling fluidised bed reactor (BFBR), char separation system and the liquid condensation chain. The feeding system consists of a hopper and motorised screw feeder, which has a slight nitrogen overpressure to prevent hot vapours pushing back from the BFBR. The PWS pellets were screw-fed at a rate 0.5 kg.h^{-1} into the BFBR where it got fluidised with silica sand (AFS 45 fused silica sand, CONSOL minerals) that acts as the heat transfer medium. The heat supplied to the BFBR is from a 6.6 kW cylindrical furnace, which encases the BFBR and char separation sections. Nitrogen (Technical grade, AFROX) was used as a fluidising a medium, using a fixed flow rate of 2.4 m^3.hr^{-1}. The nitrogen was pre-heated by a stainless steel heat exchanger before it entered the BFBR. The formed pyrolysis vapours and some of the char particles exited the BFBR and were separated by ways of a cyclone. The majority of the formed char remained in the BFBR. From the char separation section, the pyrolysis vapours entered the liquid condensation chain whereby an iso-paraffinic hydrocarbon (Isopar, Engen Petroleum limited) was sprayed in direct contact to condense the bio-oil by quenching. Isopar was used as it was immiscible with the bio-oil. The heat gained by the Isopar was removed by a water bath, which

was cooled by a 13 kW Daikin chiller. The uncondensed vapours then entered two electrostatic precipitators set to 14 kV and 12 kV to remove any condensable compounds. The remaining non-condensable gases were purged to the atmosphere.

The fast pyrolysis product yields were calculated on a dry ash free basis and are specific to bio-oil yield, $Y_{bio\text{-}oil}$, char yield, Y_{char}, non-condensable gas yield, Y_{gas}, and organic liquid yield, $Y_{organics}$.

$$Y_{char}\,(\text{daf wt.\%}) = \frac{M_{char\text{-}pots} + (M_{reactor\text{-}content} - M_{sand}) - M_{ash\text{-}char}}{M_{PWS} - M_{ash-pws} - M_{moisture}} * 100 \quad (5)$$

$$Y_{bio\,-\,oil}\,(\text{daf wt.\%}) = \frac{M_{bulk\text{-}liquid} + M_{tarry\text{-}phase} - M_{ash-oil}}{M_{PWS} - M_{ash-pws} - M_{moisture}} * 100 \quad (6)$$

$$Y_{organics}\,(\text{daf wt.\%}) = \frac{M_{bulk-liquid} + M_{tarry-phase} - M_{KFwater} - M_{ash-oil}}{M_{PWS} - M_{ash-pws} - M_{moisture}} * 100 \quad (7)$$

$$Y_{gas}\,(\text{daf wt.\%}) = 100\% - Y_{bio-oil} - Y_{char} \quad (8)$$

where M is the mass of products in grams, KF_{water} stands for the water content determined by the Karl-Fisher method, and $M_{moisture}$ is the moisture contained in the PWS. The difference in weight of the liquid condensation train equipment (bio-oil residue), before and after each pyrolysis run, as well as the bio-oil recovered from the reservoir formed the bulk liquid ($M_{bulk\text{-}liquid}$). The bulk liquid along with tarry phase, $M_{tarry\text{-}phase}$, recovered from acetone washing of the internal reservoir walls, forms the total bio-oil mass. The tarry phase was not mixed back into the bulk liquid and no further analysis was performed on it.

4.2.5 Design of experiments

A three level two factor full factorial statistical design was implemented to optimise the reactor temperature and pellet size for maximization of the bio-oil yield from fast pyrolysis of the PWS. The reactor temperature was selected as it has a large influence on the pyrolysis reactions [17,18].

From pre-screening fast pyrolysis runs, the appropriate reactor temperature levels of 300, 425 and 550 ^{o}C for LAPWS, and 290, 340 and 390^{o}C for HAPWS were selected. Particle size is known to influence the heat and mass transfer effects during pyrolysis [18-20]. Although this phenomenon is typically stated for "single particle models", it is plausible to assume that a pellet, in the form of an "agglomerate of particles", has similar pyrolytic behaviour [21,22]. Therefore pellet size will be considered as a single particle as a preliminary approach. Pellet sizes in the range of 2.92 ± 0.12, 4.04 ± 0.18 and 4.84 ± 0.15 mm were used. An ANOVA analysis was performed using the parametric data analysis function 'regression' in Microsoft Excel (2010, ver. 14.0.7128.5000, SP2) whereby a 2-way linear and quadratic model was fitted (Equation 9). The model was adapted such that the best fit was acquired. The coefficient of determination (R^2) was used to determine how well the model fitted to the data, and the adjusted coefficient of determination (R^2_{adj}) was used to ensure that the model was not over fitted [23]. The hierarchy and heredity principles were also taken into consideration during the model fitting. The model was checked for consistency by insuring no heteroscedasticity in the normality, constant variance and independence assumptions [23]. A 95% confidence interval was used whereby a p-value of less than 0.05 indicated a significant effect of the factors on the responses. Equation 9 below represents the 2-way linear and quadratic model used:

$$Y_{product}\ (\text{wt.}\%) = \text{intercept} + \beta_1 * RT + \beta_2 * PS + \beta_3 * RT^2 + \beta_4 * PS^2 + \beta_5 * RT * PS + \beta_6 * RT^2 * PS + \beta_7 * PS^2 * RT + \beta_8 * RT^2 * PS^2 \quad (9)$$

where $Y_{product}$ is the pyrolysis product yield, β_{n+1} is the model coefficients, RT is the reactor temperature (^{o}C) and PS is the pellet size (mm).

During the fast pyrolysis runs the reactor temperature varied around the set point with a standard deviation of up ±10 ^{o}C. The pellet size also varied having a standard deviation of up ± 0.18

mm. The average reactor temperature and pellet size, for each run, was used to account for the deviations when doing the ANOVA analysis and modelling. Three repeated runs were performed to determine the experimental error. To confirm an optimal pellet size range, an additional FP run for both PWSs was performed using ~6 mm pellets at their respective optimal reactor temperatures.

4.3 RESULTS AND DISCUSSION

4.3.1 Physico-chemical characterisation of PWSs

The physico-chemical characteristics reveal large variations in the ash content (AC_{525}) between the PWSs, 46.7 and 8.5 wt.% for HAPWS and LAPWS, respectively (Table 4-1). HAPWS is substantially larger in comparison to other biomass, such as woody species (~2.7 wt.%) and agricultural wastes (~7.8 wt.%) [24]. Concerning the organic fraction, the presence of high oxygen content in both PWSs can be attributed to the large carbohydrate proportions, varying between 68.5 to 74.0 daf, wt.% (Table 4-1). After drying the PWSs, the HHV (dry basis) of the LAPWS, 17.82 MJ/kg, was found to be substantially larger than this of HAPWS, 12.12 MJ/kg, which is explained by the greater availability of organic matter (Table 4-1), and is also comparable to other HHVs obtained for biomass such as birch wood, sugar cane bagasse etc [11,16]. The XRF inorganic composition of HAPWS showed the occurrence of one main form of calcium, CaO (21.5 wt.%) (Table 4-2). However, from FT-IR analysis, the absence of the peak at 3640 cm^{-1} ($Ca(OH)_2$ and CaO), and presence of the broad band at 1400 cm^{-1}, with a peak at 870 cm^{-1}, indicated that calcium was mainly in the form of $CaCO_3$ (Figure 4-1). By using Equation 1 an estimate of 38.4 wt.% was attained for $CaCO_3$. This large presence of $CaCO_3$ would be due to the removal of inorganic fillers from recycled paper during processing [3].

4.3.2 Influence of operating conditions: reactor temperature and pellet size

4.3.2.1 On FP bio-oil yield

Well fitted models and surface plots for the yield of bio-oil from the fast pyrolysis of LAPWS and HAPWS are respectively shown in Table 4-3 and Figure 4-2. The optimal reactor temperatures for maximisation of the bio-oil yields were 400 ^{o}C and 340 ^{o}C for LAPWS and HAPWS, respectively, and are significantly lower than reported optima for other lignocellulosic biomass (450 to 550 ^{o}C) [10,17,18,26]. These low temperatures could be the due to the catalytic effect of the inorganics (Table 4-2) promoting the reaction rate. Indeed calcium has been shown to significantly promote the primary pyrolysis reactions [27-29]. Trends in the bio-oil and char yield at the optimal reactor temperatures, for LAPWS and HAPWS, for different pellets sizes (3 to 6 mm) are illustrated in Figure 4-3. At elevated pellet sizes of ~6 mm, a decrease in bio-oil yield was observed for both PWSs, which could be attributed to increased heat and mass transfer limitations that would promote char formation (Figure 4-3). This confirms that there is an optimal pellet size ranging between 4.84 ± 0.15 and ~6 mm (Figure 4-3).

Both factors, the reactor temperature and pellet size, had a significant effect on the bio-oil yield obtained from the FP conversion of the LAPWS (Table 4-3). However, only the pellet size had a significant effect on the bio-oil yield of the HAPWS, although it is often reported in literature that the reactor temperature (dry basis) has a significant effect [9,17,18,30]. The significant linear interactions (β_5) between the reactor temperature and pellet size indicated that both parameters are interdependent, and thus temperature still plays a significant role during FP conversion of HAPWS (Table 4-3). Other high order non-linear higher order functions (β_3-β_4, β_6-β_8) were found to have a significant effect, however according to the hierarchy principle these are assumed to be less important than the lower order functions [31].

At the pellet size of 4.84 ± 0.15 mm and optimal reactor temperatures, maximum bio-oil yields of 44.5 ± 1.7 and 59.9 ± 4.1 daf, wt.% were attained for LAPWS and HAPWS, respectively. The maximum HAPWS bio-oil yield are up to ~40% higher than those reported by other authors using alternate pyrolysis techniques for PWS conversion [4,6,7]. In general, the use of small particle size promotes the production of bio-oil during fast pyrolysis by allowing for a more predominant chemical kinetic regime [10,19,32]. If this latter statement can be applied to the influence of the pellet size on the bio-oil yield, the above mentioned results contradict those of literature, as higher bio-oil yields were attained with an intermediate pellet size. A possible explanation of this is discussed in further detail by the thermogravimetric study in Section 4.3.3.

4.3.2.2 On organic liquid yield

Only the organic fraction of the fast pyrolysis bio-oil from LAPWS was found to be significantly affected by the reactor temperature (Table 4-3 and Figure 4-4). On the other hand, the pellet size significantly affected both LAPWS and HAPWS organic yield. It is interesting to note that the statistical results, shape of the surface plots and optimal conditions of the organic yields (Figure 4-4 and Table 4-3) were in qualitative agreement to those of the bio-oil yields (Figure 4-2 and Table 4-3).

4.3.2.3 On the energy content of bio-oil

The conversion of energy from PWS to the liquid form is illustrated by Figure 4-5. The maximum conversion of energy for LAPWS and HAPWS was found to be 39.6 ± 2.3% at 400 ^{o}C, and 45.6 ± 2.9% at 340 ^{o}C for a pellet size of 4.84 ± 0.15 mm, respectively. It is observed that the

maximum conversion of energy lies at the optimal bio-oil yields conditions (Figure 4-2). In both cases, no statistical significance could be found for either of the factors.

The calculated bio-oil higher heating values (HHV) varied between 17.4 to 22 $MJ.kg^{-1}$ for LAPWS, and 17.0 to 20.0 $MJ.kg^{-1}$ for HAPWS. A substantial increase of up to 65% in the HHV is noted between the HAPWS and its bio-oil product. These HHVs were in agreement with bio-oils produced from fast pyrolysis of other biomass such as wood species [10,17,18] and rice husks [33]. These HHVs are however lower than those reported for bio-oils produced by intermediate pyrolysis of deinking sludge by Ouadi *et al.* [5] confirming the detrimental effect of oxygen content (Figure 4-6).

The van Krevelen diagram (Figure 4-6) revealed a decrease of between 18 to 35% in the O/C molar ratios amongst the HAPWS and its FP bio-oil products, which is similar to findings (21% reduction) reported by Lin *et al.* [29] using calcium as catalyst during FP. Only four FP bio-oil products obtained from the LAPWS (pellets sizes above 4 mm) displayed a decreased O/C molar ratio (Figure 4-6). The average O/C molar ratio for the HAPWS FP bio-oil products (0.55 ± 0.01) were found to be lower than that of LAPWS FP bio-oil products (0.64 ± 0.01), indicating that the presence of calcium intensified the deoxygenation process. Indeed, calcium components have been shown to play a significant role in the catalysis of pyrolytic reactions [27-29,34], particularly secondary reactions such as the cracking of tars [28,35,36]. The deoxygenation could be explained by the presence of water-gas shift reactions occurring at low temperatures such as 300 ^{o}C [35]. This is the likely route as the water yield in the bio-oil was found to be lower than the moisture contained in the PWS indicating that water could have been consumed. As large standard deviations of ± 0.12 for LAPWS and ± 0.07 for HAPWS were obtained for the H/C molar ratios of the FP bio-oil

products, no conclusions could be drawn. In order to use the bio-oil as a petroleum derivative, further processing would be required to lower the high O/C molar ratios down to 0.06 [37].

4.3.2.4 On the char yield

Given the high inorganic content found in the HAPWS (Table 4-2), precise char yield determination required the confirmation that the $CaCO_3$ remained unchanged after FP conversion. Qualitative comparison between FT-IR spectra (Figure 4-1) of the HAPWS 4 mm char products obtained at 300, 340 and 390 ^oC and $CaCO_3$, confirmed that the $CaCO_3$ amount remained unchanged after FP conversion of HAPWS.

Trends in the char yield models indicated that reactor temperature (Figure 4-7 and Table 4-3) had a significant effect on the production of char for both LAPWS and HAPWS. The thermogravimetric study clearly illustrated that char formation was promoted under low heating conditions (Table 4-4) as reported previously [17,18,33,38,39]. No significant trend in the char yield was observed for increasing pellet sizes for either of the PWSs, which in agreement with findings by Shen *et al.* [19] for particles larger than 2 mm. The higher char yield observed at 300 ^oC, for HAPWS when compared to LAPWS, could be attributed to the presence of calcium components (Table 4-2) promoting char formation [40].

4.3.2.5 On ash loss

The effect of the reactor temperature and pellet size was shown to significantly affect the loss of ash during pyrolysis of HAPWS (Table 4-3 and Figure 4-8). As the inorganic composition in HAPWS mainly consist of calcium species (Table 4-2), a calcium mass balance (MB_{Ca}) was performed for the 4 mm FP bio-oil and char products at the reactor temperatures of 300, 340 and

390 °C (Table 4-5). The MB_{Ca} could not be closed (deficit of 23.7 %) at 300 °C suggesting that a portion of the Ca, remaining in the char product, was retained in the reactor. No substantial loss of ash was found for LAPWS during fast pyrolysis, and thus it is not discussed.

4.3.2.6 On the non-condensable gas yield

The calculated non-condensable gas yield from the fast pyrolysis conversion of LAPWS and HAPWS (Figure 4-9) was significantly affected by pellet size (Table 4-3). Reactor temperature, however, was shown only to significantly affect the LAPWS non-condensable gas yield (Table 4-3). In both cases, a temperature increase was observed to greatly promote the non-condensable gas yield as reported previously [17,18,39]. For both PWSs, the char yield plateaus out at higher temperatures (above 450 °C) (Figure 4-7), while non-condensable gas continues to increase (Figure 4-9) and bio-oil continues to decrease (Figure 4-2). This observation suggests that the increase in non-condensable yield is due to the cracking of tars that could be promoted by the presence of calcium, silicon and/or aluminium components (Table 4-2) [28,35,41-43]. An increase in the non-condensable gas yield was observed for smaller pellet sizes for both PWSs (Figure 4-9). A possible explanation of this is discussed in further detail by the thermogravimetric study in Section 4.3.3.

4.3.3 Thermal behaviour of pelletized PWS

To gain insight on the mechanisms involved during conversion of pelletized PWS, a thermogravimetric study was implemented to illustrate the potential mass and heat transfer mechanisms on pyrolysis. Heat flux curves during the pyrolysis of LAPWS and HAPWS were recorded using TGA under low (20 $^{o}C.min^{-1}$) and high (150 $^{o}C.min^{-1}$) heating rates (Figure 4-10). The heat flux curves showed an initial endotherm, followed by an increasingly exothermic

behaviour at higher temperatures. The initial endothermicity can be attributed to the volatilization of water present in PWS, followed by the initiation of the volatile formation during the primary pyrolysis reactions at around 180 ^{o}C (20 ^{o}C.min^{-1}) and 240 ^{o}C (150 ^{o}C.min^{-1}). The exothermicity could be attributed to a number of different potential reactions, including hemicellulose and lignin decomposition [44], char forming reactions [45] and secondary reactions [46].

Under the low heating rate and from ~300 ^{o}C onwards, pyrolysis reactions were mostly exothermic (Figure 4-10a,b). Similar exothermic pyrolytic behaviour has been reported by Strezov *et al.* [6] for PWS and Park *et al.* [47] for maple wood. This can be attributed to the promotion of exothermic charring reactions by lowered heat and mass transfer during cellulose pyrolysis (Table 4-1). Typically the pyrolysis of cellulose is endothermic [44,48] (between 300 ^{o}C to 380 ^{o}C), however it has been shown to become exothermic [44,45,48] under char favoured conditions of lowered heat and mass rates [45]. The exothermic pyrolysis of the hemicellulose (between 220 ^{o}C to 500 ^{o}C) and lignin (between 160 ^{o}C to 500 ^{o}C) fraction could also contribute to the exothermic behaviour (Table 4-1) [44]. A third stage of decomposition (650 ^{o}C to 850 ^{o}C) was observed for the HAPWS (Figure 4-10b), which could be attributed to the full endothermic decomposition of $CaCO_3$ [3].

In addition, it can be seen that the use of large pellet sizes promotes exothermic reactions for both PWSs (Figure 4-10a,b). Furthermore, char formation from HAPWS was also increased by larger pellet sizes at low heating rates (Table 4-4). The larger pellet size would decrease the heat transfer rate, which could favour simultaneous exothermic charring reactions over bond scission (vapour formation).

The use of the high heating rate resulted in a late thermal decomposition (240 ^{o}C) and maximization in the devolatization rates (Figure 4-10c,d and Table 4-4). The promotion of heat

transfer by the increased heating rate would favour simultaneous bond scission (vapour formation) over charring reactions. The larger vapour formation, from favoured bond scission, would increase the mass transfer limitations [22], and result in a promotion of the exothermic secondary tar cracking reactions [46,49]. The large presence of inorganics (Table 4-2), particularly the calcium components, could significantly promote the exothermic secondary tar cracking reactions [28,35,36]. Once more a third stage third stage of decomposition (700 ^{o}C to 900 ^{o}C) was observed for the HAPWS (Figure 4-10d), which could be attributed to the partial and delayed endothermic decomposition of $CaCO_3$ [3], due to a greater thermal lag at the high heating rate.

Unlike the low heating rate, the high heating rate was observed to promote the exothermicity of smaller pellet sizes, especially for LAPWS (Figure 4-10c). The smaller pellets size would increase the heat transfer rate, which would favour vapour formation and increase mass transfer limitations [22], which could promote exothermic secondary tar cracking reactions [46,49]. A similar promotion of the exothermicity by smaller pellet size was observed for the HAPWS (Figure 4-10d). However, the 6 mm pellet has the largest exothermicity. This could be attributed to the promotion of char forming reactions (Table 4-4) over bond scission due to decreased heat transfer rates.

Taking the above into the mind, the trends observed during FP conversion of both PWSs can be explained. As the FP char yield did not vary with pellet size (Figure 4-7), the decreasing bio-oil yield (Figure 4-2), for smaller pellet sizes (~3 mm), was attributed to the production of non-condensable gases (Figure 4-9). Therefore the smaller pellet size would increase the heat transfer rate, which would favour vapour formation and increase mass transfer limitations [22], thus promoting the secondary exothermic tar cracking reactions [46], resulting in the increase of the non-condensable gas yield observed.

4.4 CONCLUSION

Valorization of PWS into energy dense bio-oil products via fast pyrolysis offers a promising alternative, giving high maximum bio-oil yields of up to 44.5 ± 1.7 (400 ^{o}C at 4.84 ± 0.15 mm) and 59.9 ± 4.1 daf, wt.% (340 ^{o}C at 4.84 ± 0.15 mm), at low temperatures, for LAPWS and HAPWS, respectively. Energy conversion, between the PWS and its FP bio-oil products, was shown to be highest at the maximum bio-oil yields. A reduction in the O/C molar ratio, between both PWSs and it FP bio-oil products, led to an increase in the HHV. Of particular significance was the decrease of up to 35% in the O/C molar ratio, between the HAPWS and its FP bio-oil product, which led a 65% increase in its HHV. The large calcium content found in the HAPWS, mainly in the form $CaCO_3$, could have promoted the catalytic deoxygenation of its FP bio-oil product.

The thermogravimetric study revealed that both parameters, heating rate and pellet size, significantly affected the pyrolytic behaviour of the PWSs. It was suggested that the promotion of exothermic secondary tar cracking reactions, during fast pyrolysis, by smaller pellet sizes could have led to the observed increase in the non-condensable gas yield, which corresponded to a decrease in bio-oil yield.

Acknowledgments

This work was financially supported by Kimberley Clark SA, the Paper Manufacturers Association of South Africa (PAMSA) and FP&M Seta. The authors would like to thank these organisations for their support.

4.5 REFERENCES

[1] S. Yilmaz, H. Selim, A review on the methods for biomass to energy conversion, Renewable and Sustainable Energy Reviews (25) (2013) 420-430.

[2] M.C. Monte, E. Fuente, A. Blanco, C. Negro, Waste management from pulp and paper production in the European Union, Waste Management (29) (2009) 293-308.

[3] A. Mendez, J.M. Fidalgo, F. Guerrero, G. Gasco, Characterization and pyrolysis behaviour of different paper mill waste materials, Journal of Analytical and Applied Pyrolysis (86) (2009) 66-73.

[4] R. Lou, S. Wu, G. Lv, Q. Yang, Energy and resource utilization of deinking sludge, Applied Energy (90) (2012) 46-50.

[5] M. Ouadi, J.G. Brammer, Y. Yang, A. Hornung, M. Kay, The intermediate pyrolysis of deinking sludge to produce a sustainable liquid fuel, Journal of Analytical and Applied Pyrolysis (105) (2013) 135-142.

[6] V. Strezov, T.J. Evans, Thermal processing of paper sludge and characterisation of its pyrolysis products, Waste Management (29) (2009) 1644-1648.

[7] Y. Yang, J.G. Brammer, M. Ouadi, J. Samanya, A. Hornung, H.M. Xu, Y. Li, Characterisation of waste derived intermediate pyrolysis oils for use as diesel engine fuels, Fuel (103) (2013) 247-257.

[8] Y.Yang, J.G. Brammer, A.S.N. Mahmood, A. Hornung, Intermediate pyrolysis of biomass energy pellets for producing sustainable liquid, gaseous and solid fuels, Bioresource (169) (2014) 794-799.

[9] A.V. Bridgwater, Principles and practices of biomass fast pyrolysis processes for liquids, Journal of Analytical and Applied Pyrolysis (51) (1999) 3-22.

[10] A.V. Bridgwater, Review of fast pyrolysis of biomass and product upgrading, Biomass and Bioenergy (38) (2012) 68-94.

[11] W.N.R.W. Isahak, M.W.M. Hisham, M.A. Yarmo, T.Y. Hin, A review on bio-oil production from biomass by using pyrolysis method, Renewable and Sustainable Energy Reviews (16) (2012) 5910-5923.

[12] G. Duman, C. Okutucu, S. Ucar, R. Stahl, J. Yanik, The slow and fast pyrolysis of cherry seed, Bioresource Technology (2011) (102) 1869-1878.

[13] A.V. Bridgwater, G.V. C. Peacock, Fast pyrolysis processes for biomass, Renewable and Sustainable Energy Reviews (2000) (4) 1-73.

[14] D. Mohan, C.U. Pittman, P.H. Steele, Pyrolysis of wood/biomass for bio-oil: A critical review, Energy and Fuels (20) (2006) 846-889.

[15] S.A. Channiwala, P.P. Parikh, A unified correlation for estimating HHV of solid, liquid and gaseous fuels, Fuel (81) (2002) 1051-1063.

[16] M. Carrier, J. Joubert, S. Danje, T. Hugo, J. Görgens, J.H. Knoetze, Impact of the lignocellulosic material on fast pyrolysis yields and product quality, Bioresource Technology (150) (2013) 129-138.

[17] M. Garcia-Perez, X.S. Wang, J. Shen, M.J. Rhodes, F. Tian, W.J. Lee, H. Wu, C. Li, Fast pyrolysis of oil mallee woody biomass: Effect of temperature on the yield and quality of pyrolysis products, Industrial and Engineering Chemistry Research (47) (2008) 1846-1854.

[18] H.J. Park, J. Dong, J. Jeon, Y. Park, K. Yoo, S. Kim, J. Kim, S. Kim, Effects of the operating parameters on the production of bio-oil in the fast pyrolysis of Japanese larch, Chemical Engineering Journal (143) (2008) 124-132.

[19] J. Shen, X. Wang, M. Garcia-Perez, D. Mourant, Effects of particle size on the fast pyrolysis of oil mallee woody biomass, Fuel (88) (2009) 1810-1817.

[20] K. Papadikis, S. Gu, A.V. Bridgwater, CFD modelling of the fast pyrolysis of biomass in fluidised bed reactors: Modelling the impact of biomass shrinkage, Chemical Engineering Journal (149) (2009) 417-427.

[21] M. Jeguirim, L. Limousy, P. Dutournie, Pyrolysis kinetics and physicochemical properties of agropellets produced from spent ground coffee blended with conventional biomass, Chemical Engineering Research and Design, http://dx.doi.org/10.1016/j.cherd.2014.04.08.

[22] R. Reschmeier, D. Roveda, D. Muller, J. Karl, Pyrolysis kinetics of wood pellets in fluidized beds, Journal of Analytical and Applied Pyrolysis (2014) (108) 117-129.

[23] D.C. Montgomery, Design and analysis of experiments, U.S.A: John Wiley & Sons (2001) 363-422.

[24] S.V. Vassilev, D. Baxter, L.K. Anderson, C.G. Vassileva, An overview of the chemical composition of biomass, Fuel (2010) 913-933.

[25] J. Scheirs, G. Camino, W. Tumiatti, Overview of water evolution during the thermal degradation of cellulose, European Polymer Journal (2001) (37) 933-942.

[26] H.B. Goyal, D. Seal, R.C. Saxena, Bio-fuels from thermochemical conversion of renewable resources: A review, Renewable and Sustainable Energy Reviews (2008) (12) 504-517.

[27] P.R. Patwardhan, J.A. Satrio, R.C. Brown, B.H. Shanks, Influence of inorganic salts on the primary pyrolysis products of cellulose, Bioresource Technology (101) (2010) 4646-4655.

[28] M.R. Gray, W.H. Corcora, G.R. Gavalas, Pyrolysis of wood-derived material. Effects of moisture and ash content, Industrial and Engineering Chemistry Process Design and Development (24) (1985) 646-651.

[29] Y. Lin, C. Zhang, M. Zhang, Jian Zhang, Deoxygenation of bio-oil during pyrolysis of biomass in the presence of CaO in a fluidized-bed reactor, Energy Fuels (2010) (24) 5686-5695.

[30] Z. Lou, S. Wang, K. Cen, A model of wood flash pyrolysis in fluidized bed reactor, Renewable Energy (30) (2005) 377-392.

[31] C.F. Wu, M.S. Hamada, Experiments: Planning, analysis, and optimization, U.S.A: John Wiley & Sons (2009) 172-173.

[32] B. Kang, K.H. Lee, H. Park, Y. Park, J. Kim, Fast pyrolysis of radiate pine in a bench scale plant with a fluidized bed: Influence of a char separation system and reaction conditions on the production of bio-oil, Journal of Analytical and Applied Pyrolysis (2006) (76) 32-37.

[33] J. Zheng, X. Zhu, Q. Guo, Q. Zhu, Thermal conversion of rice husks and sawdust to liquid fuels, Waste Management (26) (2006) 1430-1435.

[34] J. Shao, R. Yan, H. Chen, H. Yang, D.H. Lee, Catalytic effect of metal oxides on pyrolysis of sewage sludge, Fuel Processing Technology (2010) (91) 1113-1118.

[35] M. Widyawati, T.L. Church, N.H. Florin, A.T. Harris, Hydrogen synthesis from biomass pyrolysis with in situ carbon dioxide capturing using calcium oxide, Journal of Hydrogen Energy (36) (2011) 4800-4813.

[36] Q. Lu, Z. Zhang, C. Dong, X. Zhu, Catalytic upgrading of biomass fast pyrolysis vapors with nano metals oxides: An analytical Py-GC/MS study, Energies (2010) (3) 1805-1820.

[37] C. Wang, Z. Du, J. Pan, J. Li, Z. Yang, Direct conversion of biomass to bio-petroleum at low temperatures, Journal of Analytical and Applied Pyrolysis (78) (2007) 438-444.

[38] A. Demirbas, Effects of temperature and particle size on bio-char yield from pyrolysis of agricultural residues, Journal of Analytical and Applied Pyrolysis (2004) (72) 243-248.

[39] C. Di Blasi, G. Signorelli, C. Di Russo, G. Rea, Product distribution from pyrolysis of wood and agricultural resides, Industrial & Engineering and Chemistry Research (1999) (38) 2216-2224.

[40] A. Hlavsova. A. Corsaro, H. Raclavska, D. Juchelkova, The effects of varying CaO content and rehydration treatments on the composition, yield, and evolution of gaseous products from the pyrolysis of sewage sludge, Journal of Analytical and Applied Pyrolysis (2014) (108) 160-169.

[41] F. Ates, M.A. Isikday, Influence of temperature and alumina catalyst on pyrolysis of corncob, Journal of Analytical and Applied Pyrolysis (88) (2009) 1991-1997.

[42] K. Chiang, C. Lu, L. Chien, The aluminium silicate catalyst effect on efficiency of energy yield in gasification of paper-reject sludge, International Journal of Hydrogen Energy (38) (2013) 15787-15793.

[43] C. Myrén, C. Hörnell, E. Björnbom, K. Sjöstrom, Catalytic tar decomposition of biomass pyrolysis gas with a combination of dolomite and silica, Biomass and Bioenergy (2002) (23) 217-227.

[44] H. Yang, R. Yan, H. Chen, D.H. Lee, C. Zheng, Characterisitcs of hemicellulose, cellulose and lignin pyrolysis, Fuel (86) (2007) 1781-1788.

[45] I. Milosavljevic, V. Oja, E.M. Suuberg, Thermal effects in cellulose pyrolysis: Relationship to char formation processes, Industrial & Engineering Chemistry Research (35) (1996) 653-662.

[46] M.G. Gronli, Mathematical model for wood pyrolysis – Comparison of experimental measurements with model predictions, Energy and Fuels (14) (2000) 791-800.

[47] W.C. Park, A. Atreya, H.R. Baum, Experimental and theoretical investigation of heat and mass transfer processes during wood pyrolysis, Combustion and Flame (157) (2010) 481-494.

[48] S. Soares, G. Camino, S. Levchi, Comparative study of the thermal decomposition of pure cellulose and pulp paper, Polymer Degradation and Stability (1995) (49) 275-283

[49] V. Strezov, B. Moghtaderi, J.A. Lucas, Thermal study of decomposition of selected biomass samples, Journal of Thermal Analysis and Calorimetry (72) (2003) 1041-1048.

Table 4-1. Physico-chemical characterisation of the LAPWS and HAPWS

	LAPWS	HAPWS
Moisture content after drying (wt. %)	80.9	54.6
Proximate Analysis (wt.%,db)		
Volatile Matter	78.7	50.3
Fixed Carbon	15.5	2.9
Ash (900 °C)	5.8	24.6
Ash (525 °C)	8.5	46.7
HHV (MJ/kg)	17.8	12.1
Lignocellulosic Composition (daf, wt.%)		
Extractives	6.3	10.5
Cellulose	58.7	49.5
Hemicelluloses	15.3	19.0
Lignin	20.1	20.5
Ultimate Analysis (daf, wt.%)		
C	49.2	47.2
H	5.9	6.7
O (by difference)	44.8	45.7
N	0.08	0.41
S	0.00	0.00

Table 4-2. Inorganic composition of LAPWS and HAPWS from XRF analysis

	Inorganic content (wt.%)										
	Al_2O_3	CaO	Cr_2O_3	Fe_2O_3	K_2O	MgO	MnO	Na_2O	P_2O_5	SiO_2	TiO_2
LAPWS	1.28	0.88	0.02	0.42	0.08	0.22	0.02	0.46	0.03	2.96	0.07
HAPWS	2.08	21.5	0	0.13	0.03	0.52	0.01	0.06	0.04	3.25	0.08

Table 4-3. Statistical models fitted for the different product yields obtained from fast pyrolysis conversion of LAPWS and HAPWS

	Yield	Model									Statistics				
		Int.	β_1	β_2	β_3	β_4	β_5	β_6	β_7	β_8	R^2 (%)	R^2_{adj} (%)	P_{RT}	P_{PS}	Exp. Error
LAPWS	$Y_{Bio\text{-}oil}$	123.0	-0.07	-56.8	-	5.04	0.10	$1.04*10^{-4}$	-	-	95.7	92.2	0.05	0.00	1.70
	Y_{char}	75.47	-0.22	-	$2.2*10^{-4}$	-	-	-	-	-	87.0	84.1	0.01	-	1.89
	Y_{gas}	-77.80	0.08	50.7	-	-6.90	-	-	-	-	94.2	92.0	0.00	0.00	1.08
	$Y_{organics}$	55.53	-0.09	-16.6	-	-	0.08	$-8.0*10^{-5}$	-	-	89.6	83.7	0.05	0.03	1.44
	EC	65.53	-0.10	-18.8	-	-	0.09	$-8.7*10^{-5}$	-	-	81.6	71.2	0.11	0.08	2.31
HAPWS	$Y_{Bio\text{-}oil}$	-105.5	0.34	-146	-	-	1.14	$-1.8*10^{-3}$	-	-	82.9	71.4	0.29	0.04	4.08
	Y_{char}	113.3	-0.24	101	-	-	-0.58	$8.3*10^{-4}$	-	-	95.9	93.2	0.05	0.01	3.62
	Y_{gas}	59.78	-	-20.6	-	-	-	$9.9*10^{-5}$	-	-	84.2	80.3	-	0.00	2.10
	$Y_{organics}$	-106.2	0.36	-129	-	-	0.88	$-1.4*10^{-3}$	-	-	84.3	73.9	0.17	0.03	3.68
	EC	-116.0	0.38	-86.7	-	-	0.64	$-1.1*10^{-3}$	-	-	78.5	64.2	0.17	0.12	2.86
	AL	-1467	4.13	1223	-	-175	-4.73	$3.7*10^{-3}$	0.72	$-6.4*10^{-4}$	92.6	75.3	0.03	0.02	2.93

Int: intercept; βn+1: model coefficients; R2: coefficient of determination; R^2_{adj}: adjusted coefficient of determination; P_{RT}: p-value for reactor temperature; P_{PS}:p-value for pellet size; Exp. Error: experimental error.

Table 4-4. Thermal decomposition characteristics from thermogravimetric analysis of LAPWS and HAPWS with PS: Pellet Size; DRmax: Maximal devolatization rate; and Tmax: Maximal devolatization temperature

	PS (mm)	Density ($g.cm^{-3}$)	DRmax ($\%.min^{-1}$)	Tmax (^oC)	Enthalpy of reaction ($J.g^{-1}$)	Char (wt.%) 525 ^oC	Char (wt.%) 900 ^oC
LAPWS 20 $^oC.min^{-1}$	2.9	0.325	-15.23	359.4	229.4	29.0	24.5
	4.0	0.265	-17.69	366.6	239.3	27.9	23.4
	4.5	0.426	-17.15	362.3	293.1	29.0	24.6
	5.5	0.354	-17.68	359.7	287.2	29.3	24.5
LAPWS 150 $^oC.min^{-1}$	2.8	0.347	-101.21	388.8	155.5	26.7	22.4
	4.2	0.244	-100.36	395.6	173.0	25.9	21.9
	4.8	0.309	-99.13	385.0	158.0	27.1	23.0
	5.4	0.316	-98.13	379.2	154.1	26.5	22.3
HAPWS 20 $^oC.min^{-1}$	2.9	0.550	-13.96	373.6	19.5	53.2	32.7
	3.7	0.620	-11.97	372.5	1.70	53.9	33.0
	4.4	0.570	-11.79	371.9	13.0	54.1	33.2
	4.9	0.680	-11.25	370.6	14.6	54.0	33.2
HAPWS 150 $^oC.min^{-1}$	3.0	0.520	-61.96	411.3	146.5	53.4	41.2
	3.7	0.610	-57.39	412.4	138.9	54.2	42.3
	4.8	0.520	-58.77	425.2	146.9	53.8	42.5
	5.2	0.660	-60.34	426.9	110.0	54.6	43.0

Table 4-5. Calcium mass balance of the 4 mm fast pyrolysis runsfor reactor temperatures of 300, 340and 390°C

Temperature (°C)	Sample	Calcium (wt.%)	*MB_{Ca} Closure (%)
-	HAPWS	16.9	-
300	Bio-oil	2.96	76.3
	Char	22.5	
340	Bio-oil	5.45	91.5
	Char	25.5	
390	Bio-oil	5.15	89.6
	Char	29.0	

*MB_{Ca}:Calcium mass balance.

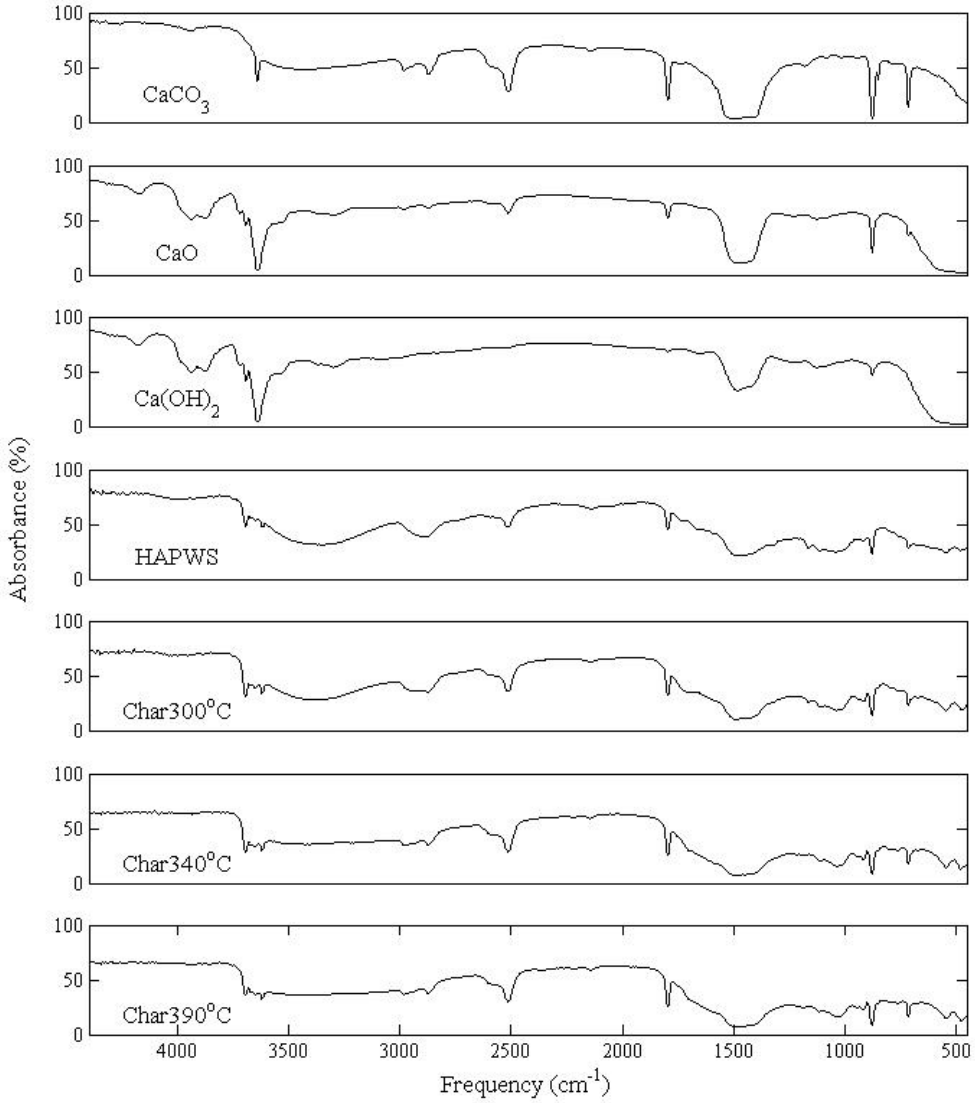

Figure 4-1. IR spectra of $CaCO_3$, CaO, $Ca(OH)_2$, HAPWS and its fast pyrolysis char (4 mm) produced at various reactor temperatures.

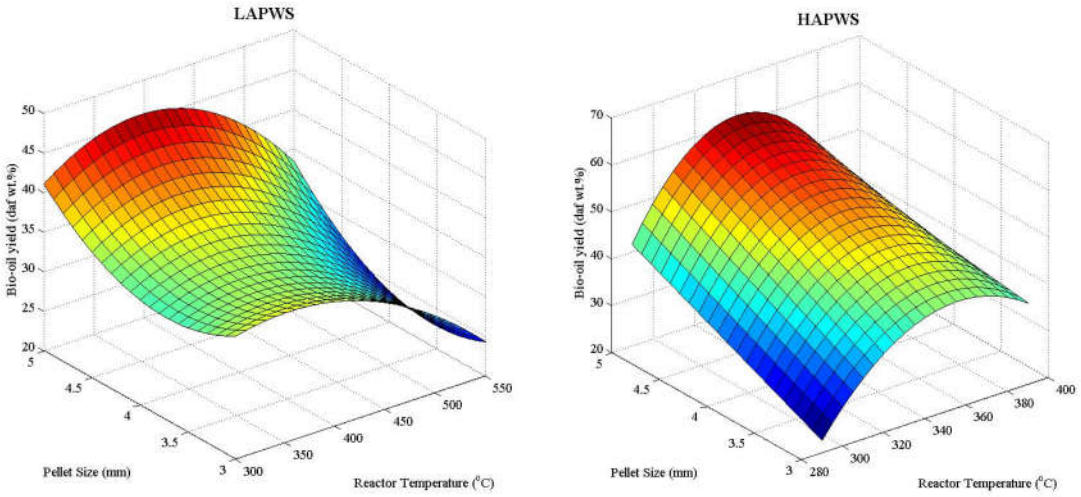

Figure 4-2. Evolution of bio-oil product yields (daf, wt.%) from fast pyrolysis conversion of LAPWS and HAPWS for different reactor temperatures and pellet sizes.

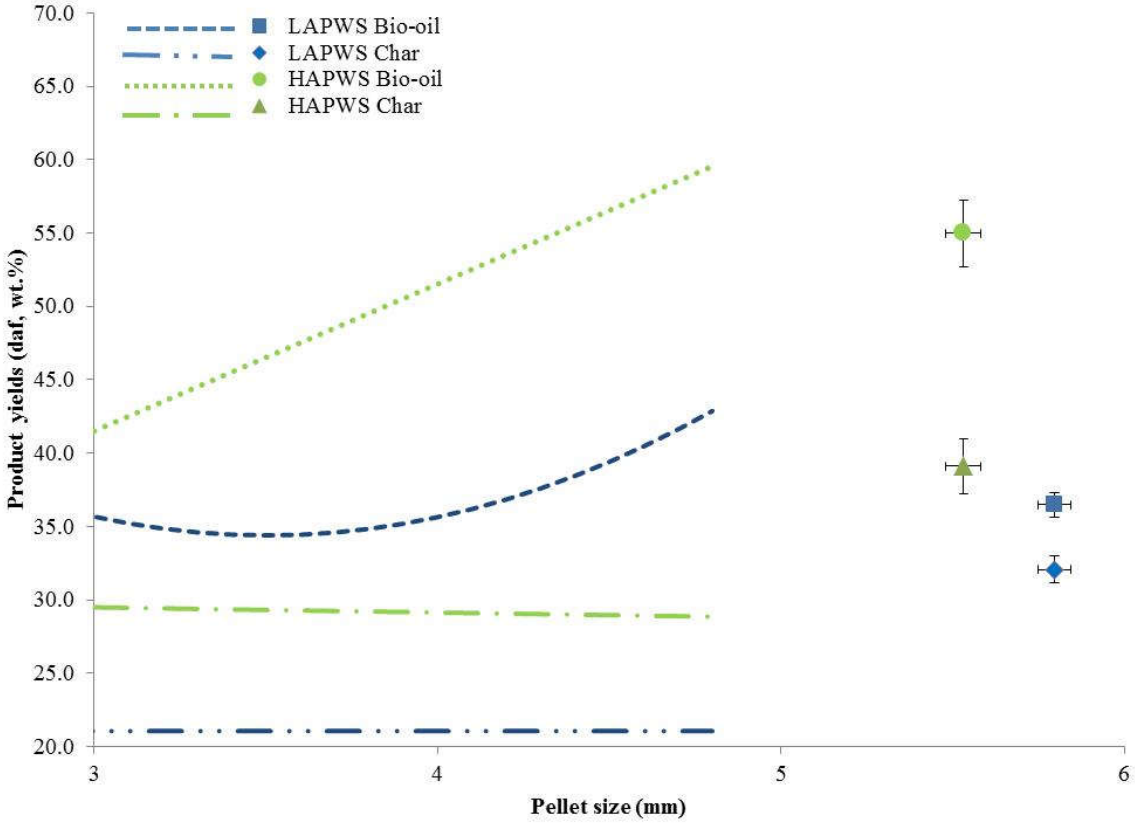

Figure 4-3. Experimental product yields (daf, wt.%) (dots) and model data points (curves) at optimal reactor temperatures for LAPWS (400 °C) and HAPWS (340 °C) for different pellet sizes.

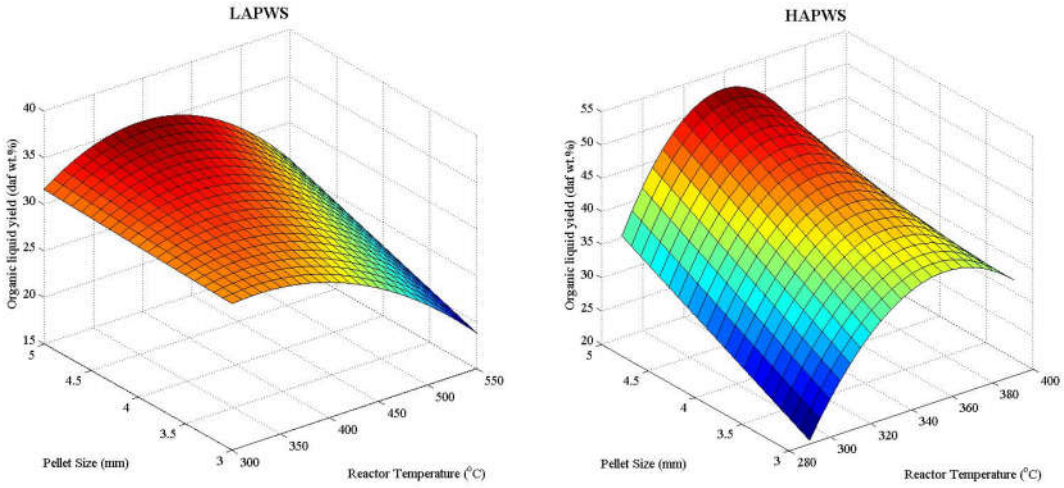

Figure 4-4. Evolution of organic liquid yields (daf, wt.%) from fast pyrolysis conversion of LAPWS and HAPWS for different reactor temperatures and pellet sizes.

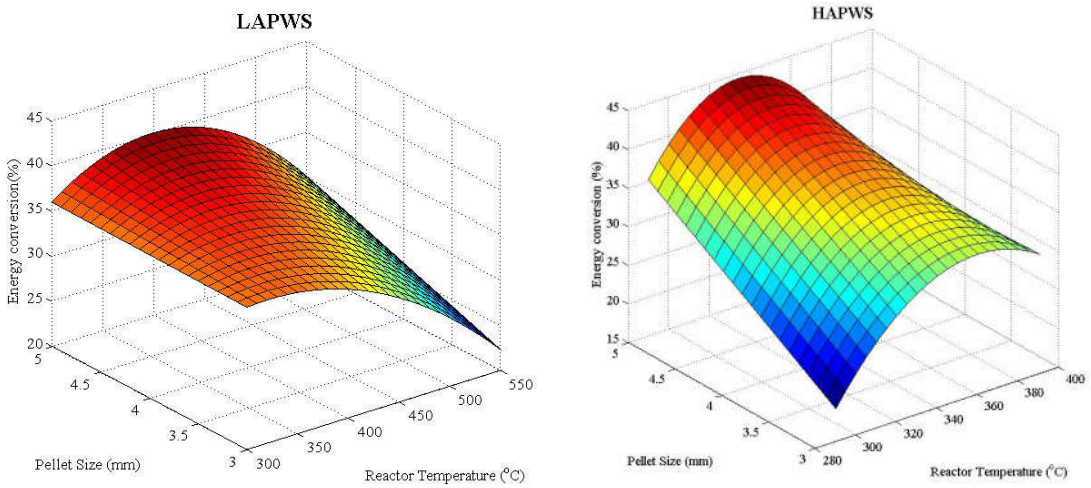

Figure 4-5. Evolution of energy conversion between PWS to fast pyrolysis bio-oil for different reactor temperatures and pellet sizes.

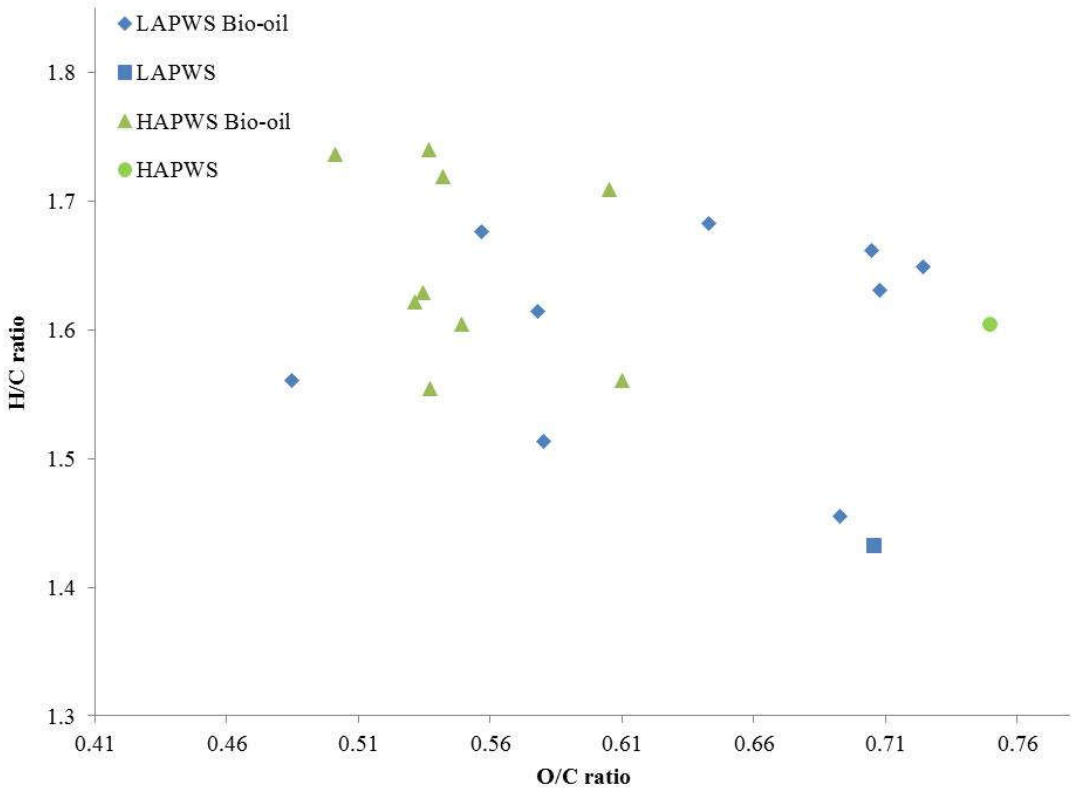

Figure 4-6. van Krevelen diagram for PWSs and their respective FP bio-oil products.

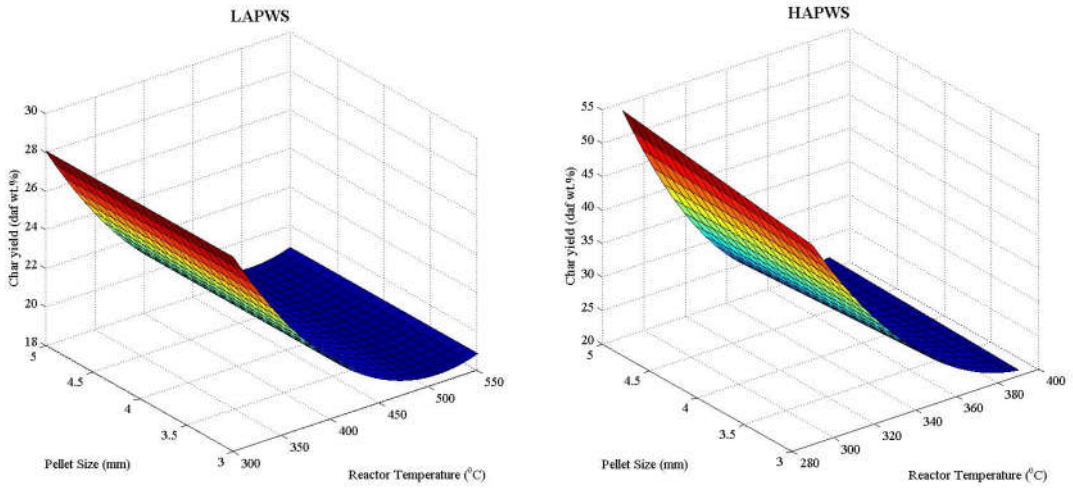

Figure 4-7. Evolution of char product yields (daf, wt.%) from fast pyrolysis conversion of LAPWS and HAPWS for different reactor temperatures and pellet sizes.

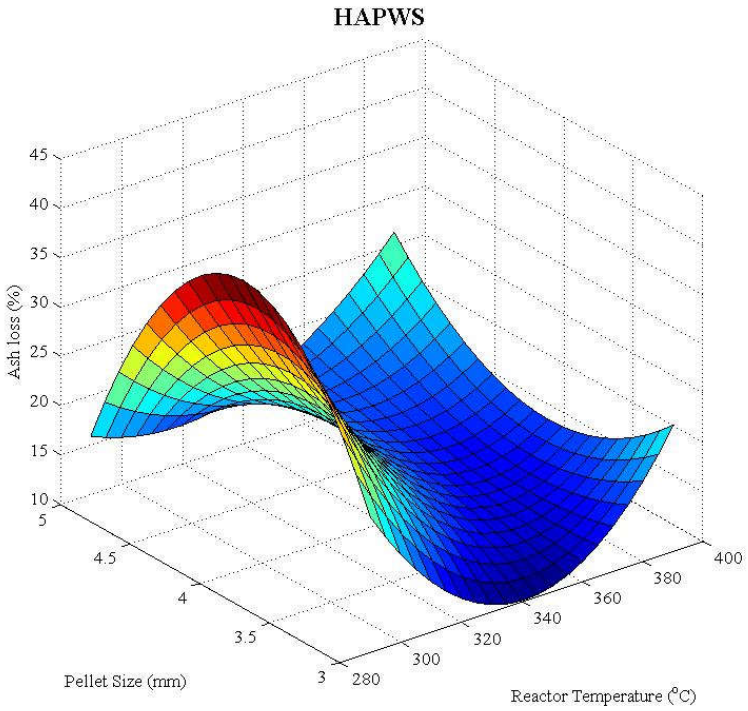

Figure 4-8. Evolution of loss of ash during fast pyrolysis conversion of HAPWS for different reactor temperatures and pellet sizes.

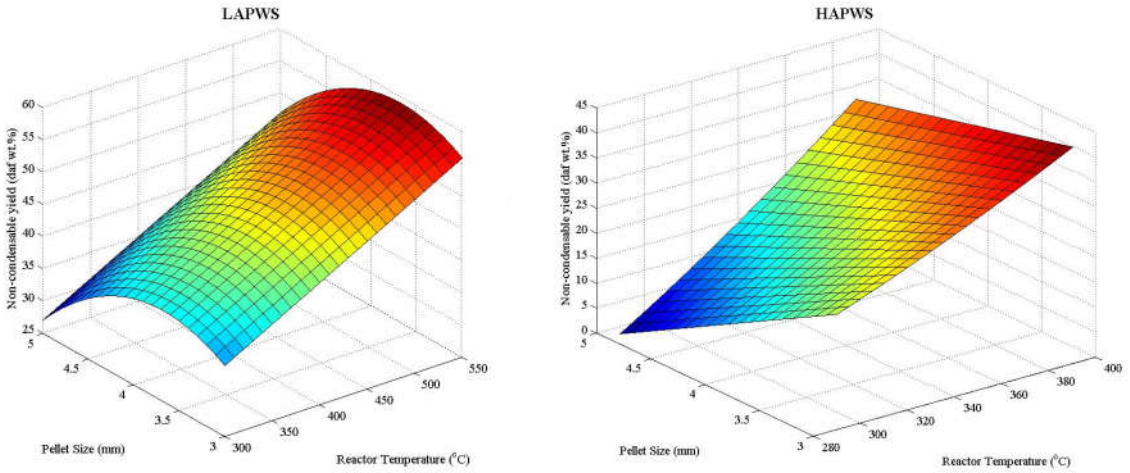

Figure 4-9. Evolution of non-condensable gas product yields (daf, wt.%) from fast pyrolysis conversion of LAPWS and HAPWS for different reactor temperatures and pellet sizes.

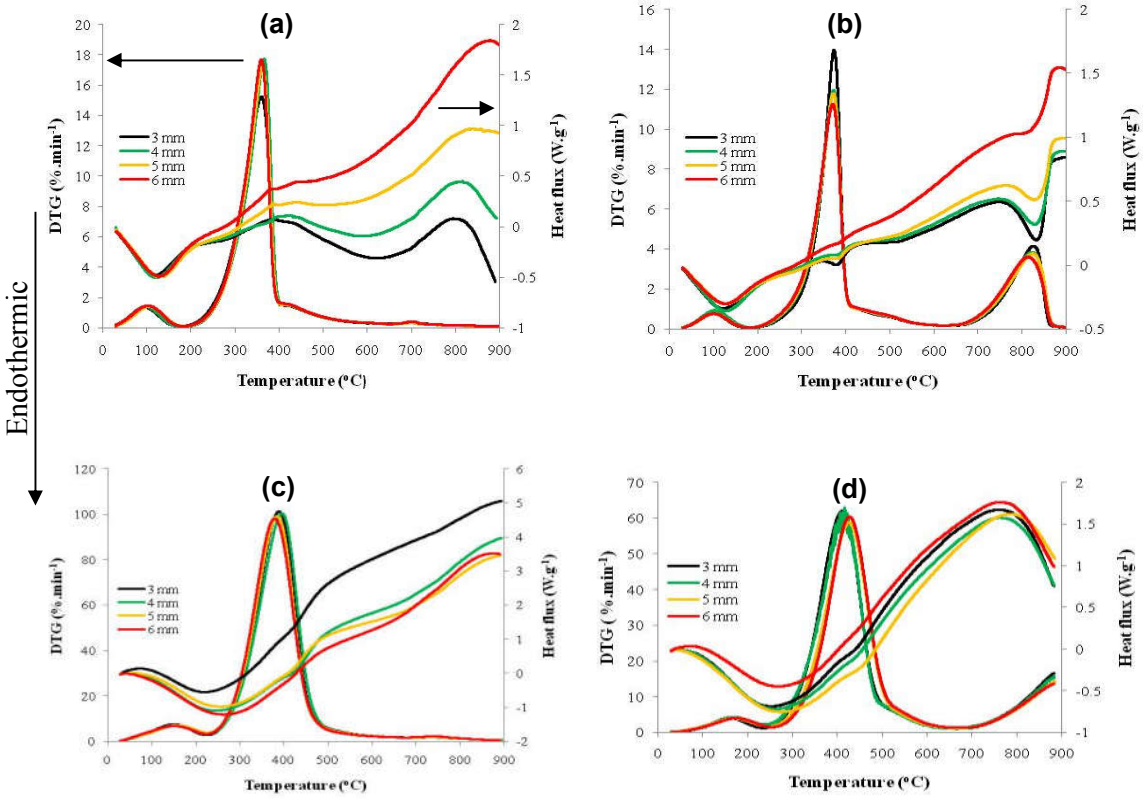

Figure 4-10. DTG and heat flux curves for LAPWS (a-c) and HAPWS (b-d) obtained at heating rates of 20 $^{o}C.min^{-1}$ (a-b) and 150 $^{o}C.min^{-1}$ (c-d) for different pellet sizes.

CHAPTER 5: ENERGY CONVERSION ASSESMENT OF VACUUM, SLOW AND FAST PYROLYSIS PROCESSES FOR LOW AND HIGH ASH PAPER WASTE SLUDGE

Published in journal of Energy Conversion and Management (111) (2016) 103-114 (ISI impact factor 4.512).

Title: "Energy conversion assessment of vacuum, slow and fast pyrolysis processes for low and high ash paper waste sludge"

Authors: Angelo J. Ridout, Marion Carrier, François-Xavier Collard, Johann Görgens.

OBJECTIVE OF DISSERTATION AND SUMMARY OF FINDINGS IN PRESENT CHAPTER

This chapter addresses **objectives 2 to 4 and 6 to 7** which focusses on the maximisation of the solid and/or liquid yield and calorific value (**objective 2**), as well as the gross energy conversion using various pyrolysis techniques (**objective 6**). The role and fate of inorganics during PWS pyrolysis are also investigated (**objective 3**), and the suitability of solid/liquid products as sources for industrial energy are assessed (**objective 7**). Furthermore, differences in product distribution and properties are used to reveal insights into the pyrolytic mechanisms (**objective 6**).

The higher production of organic liquid during FP resulted in gross energy conversions, a sum of the char and bio-oil/tarry phase (EC_{sum}), which were between 18.5 to 20.1 % higher for LAPWS, and 18.4 to 36.5 % higher for HAPWS, when compared to SP and FP. Both PWSs FP and VP bio-oil/tarry phase, as well as the LAPWS char, had high calorific values making them promising for energy applications. Considering the low calorific values of the chars from alternative pyrolysis processes (~4 to 7 $MJ.kg^{-1}$), the high ash PWS should rather be converted to fast pyrolysis bio-oil to maximise the recovery of usable energy products.

Candidate declaration

With regards to chapter 5, page numbers 121-164 of this dissertation, the nature and scope of my contribution were as follows:

Name of contribution	Extent of contribution (%)
Experimental planning	70
Executing experiments	100
Interpretation of results	60
Writing the chapter	100

The following co-authors have contributed to chapter 5 page 121-164 of this dissertation:

Name	e-mail address	Nature of contribution	Extent of contribution (%)
1. Marion Carrier	m.carrier@aston.ac.uk	• Experimental planning • Reviewing the chapter • Interpretation of results	20 50 25
2. François-Xavier Collard	fcollard@sun.ac.za	• Reviewing the chapter • Interpretation of results	40 15
3. Johann Görgens	jgorgens@sun.ac.za	• Reviewing the chapter • Experimental planning	10 10

Signature of candidate…….

Date…….

Declaration by co-authors

The undersigned hereby confirm that:

1. The declaration above accurately reflects the nature and extent of the contributions of the candidates and co-authors to chapter 5 page numbers 121-164 in the dissertation,
2. no other authors contributed to chapter 5 page numbers 121-164 in the dissertation beside those specified above, and
3. potential conflicts of interest have been revealed to all interested parties and that are necessary arrangements have been made to use the material in chapter 5 page numbers 121-164 of the dissertation

Signature	Institutional affiliation	Date
	Universidad de Concepcion	
	Stellenbosch University	
	Stellenbosch University	

ENERGY CONVERSION ASSESSMENT OF VACUUM, SLOW AND FAST PYROLYSIS PROCESSES FOR LOW AND HIGH ASH PAPER WASTE SLUDGE

Angelo J. Ridout[1,*], Marion Carrier[2], François-Xavier Collard[1], Johann Görgens[1]

[1]*Department of Process Engineering, University of Stellenbosch, Private Bag X1, Matieland 7602, South Africa*

[2]*Technological Development Unit (UDT) Universidad de Concepción, Av. Cordillera Nº 2634 – Parque Industrial Coronel. 4191996. Casilla 4051, Concepción, Chile*

ABSTRACT

The performance of vacuum, slow and fast pyrolysis processes to transfer energy from the paper waste sludge (PWS) to liquid and solid products was compared. Paper waste sludges with low and high ash content (8.5 and 46.7 wt.%) were converted under optimised conditions for temperature and pellet size to maximise both product yields and energy content. Comparison of the gross energy conversions, as a combination of the bio-oil/tarry phase and char (EC_{sum}), revealed that the fast pyrolysis performance was between 18.5 and 20.1% higher for the low ash PWS, and 18.4 and 36.5 % higher for high ash PWS, when compared to the slow and vacuum pyrolysis processes respectively. For both PWSs, this finding was mainly attributed to higher production of condensable organic compounds and lower water yields during FP. The low ash PWS chars, fast pyrolysis bio-oils and vacuum pyrolysis tarry phase products had a high calorific values (~18 to 23 $MJ.kg^{-1}$) making them promising for energy applications. Considering the low calorific values of the chars from alternative pyrolysis processes (~4 to 7 $MJ.kg^{-1}$), the high ash PWS should rather be converted to fast pyrolysis bio-oil to maximise the recovery of usable energy products.

Keywords: Paper waste sludge, pyrolysis, energy conversion

5.1 INTRODUCTION

In recent years, thermochemical technologies have been considered for the recovery of energy contained in paper waste sludge (PWS) [1-8], one of the main waste streams from the pulp and paper industry [9]. In particular pyrolysis appears as a promising technology to convert any type of lignocellulosic mixture into solid, liquid and gas products that can be used for various applications (energy, chemicals, materials) [10], which could offer a more environmentally friendly alternative to landfilling.

The performance of biomass valorisation via pyrolysis for energy production depends on product mass yields and the energy contents thereof [6,10,11]. Some research has considered gross energy conversion (EC) based on the evaluation of changing one form into another, considering biomass as a chemical energy input and the pyrolysis products as an energy output [12-15]. When considering the net EC of the whole pyrolysis process, the external energy inputs (e.g., heat energy for pyrolysis) are subtracted from the gross EC. Gross energy conversion can be calculated either based on one targeted product (for instance $EC_{bio\text{-}oil}$) or based on all the products if suitable for energy applications. Such an approach is then useful for controlling the product distribution to maximise the overall energetic output [16]. Previous studies have pointed out the importance of operating conditions and biomass type on the gross EC [12-15]. However, while PWS can be considered as an original lignocellulosic material (partially degraded fibres with high ash content), no studies have yet compared the ability of different pyrolysis techniques to convert it in terms of EC.

In the case of untreated lignocellulosic biomass conversion, it has clearly been shown that process and reactional differences existing between fast, intermediate and slow pyrolysis, affect the outcome of the product yields and their energy contents [10,17-21]. When considering the process,

the applied heating rate and vapour residence time vary in large extent [10,22]. In the case of fast pyrolysis (FP), the use of higher heating rates (300 to 12000 $^{o}C.min^{-1}$) [22] is known to maximise the volatiles yield by enhancing heat transfer [21]. Whereas, slow pyrolysis (SP) occurs under slow heating rates usually in the range of 1 to 60 $^{o}C.min^{-1}$ with long vapour residences times (1 min to hours) [10,22,23], when those of FP are shorter (< 2 s) [10]. Longer vapour residence times limit mass transfer resulting in the promotion of secondary tar cracking and/or recombination reactions [24,25]. For conversion at common temperatures (< 600 ^{o}C) typically the production of char is favoured during SP [13,17-20], while bio-oil production is maximised during FP [10,18-19]. With moderate heating rates (10 to 300 $^{o}C.min^{-1}$) [26,27] and vapour residence times (10 to 30 s) [10], intermediate pyrolysis (IP) offers a good compromise for the production of bio-oil, char and non-condensable gas [10,27]. It is well established that when the reactor temperature is raised the efficiency of the conversion to gas is increased, while the overall energy balance of the pyrolysis process can be negatively affected due to the energy required for higher temperatures [10]. On the other hand, low temperature treatments promote the production of liquid and solid products for which quality and energy content vary. In general, FP bio-oils produced in large amounts offers better potential as a liquid fuel source for heat, power generation and transport fuel production, when compared to SP [28-30]. With respect to the char product, the energy conversion into char products (EC_{char}) during SP is often higher than that during FP [19,20], and is often considered as a coal substitute.

Pyrolysis of PWS at various scales has been investigated in the last decade [1-8]. Mendez *et al.* [1] used thermogravimetric analysis (TGA) to study the pyrolytic behaviour of different PWS types. They showed that PWS from recycled processes containing high ash content (mostly $CaCO_3$; ~44 wt.%) and degraded fibres had a lower starting temperature for degradation. The slow pyrolysis (10

$^{o}C.min^{-1}$) of low ash PWS (7.8 wt.%) at 500 ^{o}C, using a packed bed thermal apparatus, led to bio-oil, char and gas yield of 40 wt.% (47.8 daf, wt.%), 36 wt.%, and 24 wt.%, respectively [4]. Given only the char's calorific value (13.3 $MJ.kg^{-1}$), an EC_{char} of 33.8% was determined. Lou *et al.* [2] subjected a high ash PWS (41.5 wt.%) to slow pyrolysis using a fixed bed reactor at 800 ^{o}C, resulting in a bio-oil yield of 24.4 wt.% (41.7 daf, wt.%), and high gas yields of 28.8 wt.%. In a recent study, low and high ash PWSs were subjected to FP to maximize the bio-oil yield by optimising reactor temperature (300, 425 and 550 ^{o}C) and pellet size (3, 4 and 5 mm) (Chapter 4) [6]. Maximum bio-oil yields of 44.5 daf, wt.% for low ash PWS and above 50 daf, wt.% for high ash PWS were attained; thus allowing in both cases for an energy transfer of ~40 % from the PWS into liquid products [6]. Intermediate pyrolysis was used by Yang *et al.* [5] and Ouadi *et al.* [3] to valorise two different deinking sludges, which were high in ash content (62.9 and 74.5 wt.%, respectively). The conversion of these materials took place in an Auger reactor at 450 ^{o}C under atmospheric conditions applying short vapour residence times and long feedstock residence times [5]. The product yields, reported by Yang *et al.* [5], for bio-oil, char and gas were 10 (28 and 41 daf, wt.%, respectively), 79 and 11 wt. %, respectively. High calorific values of 36 and 37 $MJ.kg^{-1}$ were obtained for the PWS bio-oils [3], while those of char, 4.9 and 3.3 $MJ.kg^{-1}$, were dramatically affected by the large amount of ash (54-60 wt.% at 900 ^{o}C) [3]. The resulting $EC_{bio\text{-}oil}$ were 46.3 and 52.0 % (higher in comparison to FP [6]), while EC_{char} were 52.5 and 38.7 %,respectively [3]. Although reasonable bio-oil yields of high-energy content were produced at low reactor temperatures using FP, the brief overview above confirms the potential of intermediate pyrolysis in producing high energy density products. For example, vacuum pyrolysis (VP) with low heating rates (1 to 60 $^{o}C.min^{-1}$) and short vapour residence times (2 to 30 s) is classified as an intermediate process, and offers a good compromise for pyrolysis product yields [23,29], but has not been

applied to PWS. In addition, the application of VP often enhances bio-oil calorific values, which could improve the $EC_{bio\text{-}oil}$ [23,31].

Therefore, the purpose of this research is to assess and compare the performance of vacuum, slow and fast pyrolysis, at various key operating conditions, to maximize the gross energetic transfer from raw PWS to the liquid and solid pyrolysis products. The energy contents of the solid and liquid products were also compared, to determine suitability as industrial energy sources. The same statistical approach used in our previous study on the fast pyrolysis of PWS was applied (Chapter 4) [6].

5.2 MATERIALS AND METHODS

5.2.1 Raw materials and preparation

Two different PWSs types were sourced based on the type of mill. The first PWS type, which originated from the Kraft pulp mill, Sappi Ngodwana, had a low ash content (AC) of 8.5 wt.% determined at 525 ºC (Table 5-1) and was termed low ash paper waste sludge (LAPWS). The second type, which originated from a tissue paper mill utilizing recycle processes, Kimberly Clark Enstra, had a high AC of 46.7 wt.% determined at 525 ºC (Table 5-1), and was termed high ash paper waste sludge (HAPWS). The as-received wet PWSs were dried in an oven for 12 hours at 105 ± 2 ºC, after which it was milled using a 2 mm sieve on a Retsch hammer mill. The milled PWS was subsequently pelletized to improve the packing density in the fixed bed reactor. For this the milled PWS was rehydrated (PWS:Water 1:1), mechanically agitated until a homogenous mixture was obtained, and then pelletized using a Trespade No.12 meat mincer, after which the pellets were dried for 12 hours at 105 ± 2 ºC. The pellets were produced in sizes varying between 3, 4, 5 and 6 mm.

5.2.2 Pyrolysis experiments

5.2.2.1 Vacuum and slow pyrolysis

Slow and vacuum pyrolysis experiments were performed with a unit that has been described earlier by Carrier *et al.* [23] and in Appendix A-3 to A-4. In summary, the unit is comprised of a fixed bed (FB) reactor and a liquid condensation train. The FB reactor consists of a 1 m long, 60 mm outer diameter quartz glass tube, which is externally heated by six well insulated and computer controlled heating elements. The stainless steel pipe between the reactor and first condenser was kept at 160 ^{o}C to limit condensation of the pyrolysis vapours.

A 20 g mass of paper waste sludge was used for each experimental pyrolysis run. During vacuum pyrolysis, the pyrolytic vapours were removed from the FB by a vacuum pump (~8 kPa_{ab}), resulting in a residence time of around ~2 s. Under slow pyrolysis, the pyrolytic vapours were swept from the reactive zone by a N_2 (Technical grade, Afrox) at a flow rate of 1 $L.min^{-1}$ resulting in an average residence time of 54 s. The volatiles were condensed in a series of five traps varying in temperature. For slow pyrolysis, the first was held at room temperature, and all remaining condensers (2 to 5) were held at 0 ^{o}C (crushed ice), whereas for vacuum pyrolysis, the last two were held at -78 ^{o}C (dry ice temperature) to ensure condensation. For both vacuum and slow pyrolysis a slow heating rate of 30 $^{o}C.min^{-1}$ was applied. Once the desired temperature was reached, the reactor was held there for an additional 30 min to ensure the complete devolatilization of the organic material. Once the experiment was completed, the pyrolysis unit was allowed to cool down to 120 ^{o}C before it was dismantled.

The vacuum and slow pyrolysis product yields were calculated on a dry ash free basis with Y_{char} standing for char yield, Y_{tarry} for tarry phase yield, $Y_{aqueous}$ for aqueous phase yield, $Y_{bio\text{-}oil}$ for bio-oil yield, $Y_{pyro\text{-}water}$ for pyrolytic water yield, and $Y_{organics}$ for organic liquid yield in the tarry phase.

$$Y_{char}\,(\text{daf wt.\%}) = \frac{m_{\text{fixed-bed}} - m_{\text{ash-char}}}{m_{PWS} - m_{\text{ash-pws}} - m_{\text{moisture}}} * 100 \quad (1)$$

$$Y_{tarry}\,(\text{daf wt.\%}) = \frac{m_{C1} + m_{\text{steel-pipe}}}{m_{PWS} - m_{\text{ash-pws}} - m_{\text{moisture}}} * 100 \quad (2)$$

$$Y_{aqueous}\,(\text{daf wt.\%}) = \frac{m_{C2-5} + m_{\text{rubber-pipes}}}{m_{PWS} - m_{\text{ash-pws}} - m_{\text{moisture}}} * 100 \quad (3)$$

$$Y_{\text{bio-oil}}\,(\text{daf wt.\%}) = Y_{tarry} + Y_{aqueous} \quad (4)$$

$$Y_{\text{pyro-water}}\,(\text{daf wt.\%}) = \frac{m_{KFwater} - m_{\text{moisture}}}{m_{PWS} - m_{\text{ash-pws}} - m_{\text{moisture}}} * 100 \quad (5)$$

$$Y_{organic}\,(\text{daf wt.\%}) = \frac{m_{C1} + m_{\text{steel-pipe}} - m_{KFwater}}{m_{PWS} - m_{\text{ash-pws}} - m_{\text{moisture}}} * 100 \quad (6)$$

where m_i is the mass of products in grams collected in a specific piece of the setup, KF_{water} (wt.%) stands for the water content determined by the Karl-Fisher method, and $m_{moisture}$ (wt.%) is the moisture contained in the PWS. The difference in weight of the steel pipe leading to the first condenser (bio-oil residue), $m_{steel-pipe}$, as well as the liquid product recovered in condenser 1, m_{C1}, makes up the total tarry phase (Equation 2), which was dark brown in colour. The mass difference of the rubber pipes connecting the last four condensers (bio-oil residue), $m_{rubber-pipes}$, as well as the liquid product recovered in the condensers 2 to 5, m_{C2-5}, makes up the total aqueous phase (Equation 3), which was light brown/yellow in colour. The total bio-oil yield is the sum of both tarry and aqueous phases (Equation 4).

In some cases there was a limited amount of aqueous phase in condensers 3 to 5, which made the determination of KFwater content impossible. When KFwater determination was possible, water content (WC) ratios were determined between condensers 3 to 5 (C_{3-5}) and condenser 2 (C_2). Based on the available experimental values it appeared that the WC ratios remained constant (SP: C_{3-5}: 1.47 ± 0.02; VP: C_3: 1.06 ± 0.09; C_4: 1.38 ± 0.10; C_5: 1.34 ± 0.03). As a consequence when WC

determination was not possible, assuming that the condensation efficiency was constant between experiments, it was estimated using the WC ratios.

5.2.2.2 Fast pyrolysis

Fast pyrolysis experiments were carried out with a unit as previously described in detail by Ridout *et al.* [6] and in Appendix A-1 to A-2. The FP unit consists of four interconnected sections namely a feeding system (max. 1 $kg.hr^{-1}$), bubbling fluidised bed reactor (BFBR), char separation and liquid condensation train. A 500 g mass of paper waste sludge was used for each experimental run, of which it was screw fed from the hopper, at 0.5 $kg.hr^{-1}$, to the BFBR where it got fluidised with silica sand (AFS 35 fused silica sand, CONSOL minerals) which acted as the heat transfer medium. Once PWS screw feeding was complete, the reactor temperature was held at the set point for an additional 10 min to ensure complete devolatilization of the organic material. The bed was fluidised with N_2 (Technical grade, Afrox) using a fixed flow rate of 2.4 $m^3.hr^{-1}$. The char was separated from the formed vapours by ways of a cyclone, located at the exit of the BFBR. The vapours then entered the liquid condensation system whereby they were quenched in direct contact with an immiscible iso-paraffinic hydrocarbon (Isopar, Engen Petroleum limited) to condense the liquid fraction. Any remaining condensable compounds entered two electrostatic precipitators set at 14 kV and 12 kV to complete the condensation stage. The non-condensable gas was purged to the atmosphere.

The fast pyrolysis product yields were calculated on a dry ash free basis with Y_{char} standing for char yield, $Y_{bio\text{-}oil}$ for bio-oil yield, $Y_{pyro\text{-}water}$ for pyrolytic water yield (Equation 5), and $Y_{organics}$ for organic liquid yield.

$$Y_{char}\,(\text{daf wt.\%}) = \frac{m_{char\text{-}pots} + (m_{reactor-content} - m_{sand}) - m_{ash\text{-}char}}{m_{PWS} - m_{ash-pws} - m_{moisture}} * 100 \quad (7)$$

$$Y_{bio\text{-}oil}\,(\text{daf wt.\%}) = \frac{m_{bulk\text{-}liquid} + m_{residue} - m_{ash\text{-}oil}}{m_{PWS} - m_{ash-pws} - m_{moisture}} * 100 \quad (8)$$

$$Y_{organics}\,(\text{daf wt.\%}) = \frac{m_{bulk\text{-}liquid} + m_{residue} - m_{KFwater} - m_{ash\text{-}oil}}{m_{PWS} - m_{ash-pws} - m_{moisture}} * 100 \quad (9)$$

The bio-oil recovered in the reservoir as well as bio-oil residue, determined by the difference in weight between condensation train equipment before and after each run, forms the bulk liquid ($m_{bulk\text{-}liquid}$). The residue ($m_{residue}$), recovered during acetone washing of the reservoir internal walls, along with the bulk liquid forms the total bio-oil mass. The residue was not mixed back into that bulk liquid and no further analysis was performed on it.

5.2.3 Physico-chemical characterisation

5.2.3.1 Raw materials and char products

While standardized methods were used to determine the composition of LAPWS and its solid products, some of these methods had to be adapted to take into account the eventual conversion of the inorganic material of HAPWS and its solid products. The moisture content for the as-received PWS was determined in accordance with the TAPPI T264 om-88 standard procedure. The ash content (AC_{525}) of the PWSs and the LAPWS char products were determined in accordance with the ISO 1762 standard procedure whereby samples were combusted in a muffle furnace at 525 ± 5 ^{o}C. The proximate analysis of LAPWS and its char was determined in accordance with the ASTM E1131 standard procedure using a TGA/DSC 1-LF1100 Mettler Toledo. The calorific value of the

dried PWS were experimentally determined using a Cal2K ECO bomb calorimeter, which was calibrated using benzoic acid (Cal2K).

The inorganic fraction of the HAPWS was mainly comprised of $CaCO_3$ (38.4 wt.%) [6], which thermally decomposes (forward reaction) above 650 ^oC according to Eq. 10.

$$CaCO_3 \longleftrightarrow CaO + CO_2 \quad (10)$$

In order to distinguish CO_2 produced by this reaction and the volatiles released from the biomass/char (mostly generated at T < 650 ^oC) the ASTM E1131 method was altered for HAPWS and its char products, by including a step holding the temperature at 650 ^oC for 5 minutes to drive off volatiles, after which it was heated to 900 ^oC and held for an additional 5 minutes to ensure full calcium carbonate decomposition occurred before combustion of the fixed carbon (FC), as implemented previously [6].

Given the large presence of $CaCO_3$ in the HAPWS [6], Fourier transform infrared (FT-IR) spectroscopy was performed on the HAPWS and on its chars obtained from SP at 580 ^oC (SP_{580}), VP at 425 and 550 ^oC (VP_{425} and VP_{550}), and FP at 290, 340 and 390 ^oC (FP_{290}, FP_{340} and FP_{390}), to determine extent of $CaCO_3$ conversion. An alternative method was used for analyzing the SP and VP char products, due to the adsorption properties of black carbon interfering with the analysis [32]. This analysis was then performed using a Thermo Scientific Nicolet iS10 with an ATR attachment using a ZnSe crystal, whereas the analysis of HAPWS was performed using a Perkin Elmer Paragon 1000 PC utilising a MTEC Photoacoustic Model 300 attachment [6]. The resulting FT-IR spectra of HAPWS char products were compared to those obtained for pure compounds (i.e. $CaCO_3$, $Ca(OH)_2$ and CaO) (Appendix D-1).

Qualitative comparison of FT-IR spectra bands (broad band at 1400 cm^{-1} and peak at 870 cm^{-1}) confirmed that large amounts of $CaCO_3$ remained in the SP_{580}, VP_{425} and FP_{390} chars (Appendix D-

1). The net decrease of FT-IR bands for VP_{550}, FP_{290} and FP_{340}, combined with the appearance of a in the region of 3640-3645 cm^{-1}, confirmed the partial transformation of $CaCO_3$ into CaO and/or $Ca(OH)_2$. Thus, to determine the extent of the $CaCO_3$'s changes, DTG curves for the proximate analysis (altered ASTM E1131 method) of the chars, as well as $Ca(OH)_2$ and $CaCO_3$ were studied. An illustration in the case of VP_{425} and VP_{550} is given in Figure 5-1. Peaks 1 and 2 respectively correspond to the driving off of moisture and volatiles, peak 4 is the thermal decomposition of $CaCO_3$ (Eq. 10), and peak 5 is the combustion of the fixed carbon (Figure 5-1). The presence of peak 3 for VP_{550} was attributed to the thermal decomposition of $Ca(OH)_2$ (Eq. 11). The formation of $Ca(OH)_2$ could be explained by the successive transformation of carbonate compounds in the presence of water during pyrolysis [33] (Eq. 12).

$$Ca(OH)_2 \longleftrightarrow CaO + H_2O \quad (11)$$

$$CaCO_3 + H_2O \longleftrightarrow Ca(OH)_2 + CO_2 \quad (12)$$

$$VM\,(wt.\%,df) = 100 - FC - CO_2 - H_2O - AC_{900} \quad (13)$$

Volatile matter (VM) produced from the organic fraction was thus calculated according to Equation 13, which includes the deduction of CO_2 and H_2O contributions during the conversion of $CaCO_3$ and $Ca(OH)_2$, respectively. The total ash content (AC_{525}) for all the HAPWS VP, SP and FP char products were determined by summing the CO_2 and H_2O, produced from inorganic conversion, and the ash content at 900 ^oC (AC_{900}). While Ca was only present in the form of $CaCO_3$ in the raw HAPWS, the VM was calculated in a similar manner as described by Equation 13. Both PWSs AC_{525} and AC_{900} were displayed in Table 5-1 to highlight the significant differences before and after (> 650 ^oC) thermal decomposition of the $CaCO_3$, particularly for HAPWS.

Ultimate analysis was performed on the PWSs and its char products using a TruSpec Micro from LECO in accordance with ASTM D5373. A coal (AR2781, LECO), Atropine (QC, LECO),

and Cytine (QC, LECO) were used as standards to calibrate the content of C, H, N and S. Samples are usually combusted at 1080 ^{o}C, making thermal decomposition of $CaCO_3$ (CO_2 release, Eq. 10) and $Ca(OH)_2$ (H_2O release, Eq. 11) inevitable for the HAPWS and its char products. Based on this observation, both C and H contents were corrected by deducting the CO_2 and H_2O contribution from the $CaCO_3$ and $Ca(OH)_2$ thermal decomposition. The HHV of the char was calculated using the correlation from Mott *et al.*[34] (Eq. 14).

$$HHV(KJ.kg^{-1}) = 0.336X_C + 1.418X_H - 0.145X_O + 0.0941X_S \quad (14)$$

where X_i is the mass fraction of each element with the ranges the range $X_O < 15$ wt.%.

5.2.3.2 Bio-oil product

The bio-oil product generated from vacuum and slow pyrolysis consists of two tarry and aqueous phases collected separately. The water content of both phases, as well as the fast pyrolysis bio-oil, was determined in accordance with the ASTM E203 standard using a Metrohm 701 Titrino Karl-Fischer titration. A hydranal composite 5 titrant (Sigma Aldrich) was used. As the water content of the aqueous phase was very high (see Section 5.3.2.1) this phase was not considered for energy applications. Ultimate analysis was performed on the tarry phase and FP bio-oil using a TruSpec Micro from LECO in accordance with ASTM D5291-10. A residual oil standard (AR100, LECO) and Sulfamethazine (QC, LECO) were used for the calibration of C, H, N and S content. The higher heating value (HHV) for the tarry phase and FP bio-oil was calculated using Channiwala's correlation as shown in Eq. (15) [35] and was corrected for water content:

$$HHV(MJ.kg^{-1}) = 0.3491X_C + 1.1783X_H + 0.1005X_S - 0.1034X_O - 0.0151X_N - 0.0211X_{AC} \quad (15)$$

where X_i is the mass fraction of each element with the ranges as, $0 < X_C < 92.25$, $0.43 < X_H < 25.14$, $0 < X_O < 50.00$, $0 < X_N < 5.60$, $0 < X_S < 94.08$, $0 < X_{AC} < 71.4$ and $4.745 < HHV < 55.245$.

Due to a particularly low density, fast pyrolysis bio-oil obtained from HAPWS was found to be slightly miscible with the iso-paraffinic hydrocarbon (Isopar, Engen Petroleum limited, 100%), which was used to condense the hot vapours (Section 5.2.2.2). Thus the amount of iso-paraffinic hydrocarbons in the bio-oil was determined by GC-MS. Initially, the bio-oil (0.06 g) was dissolved in 2 mL of methanol (Riedel-de Haen, 99.9%) and 0.4 mL of internal standard (0.2 g in 50 mL MeOH) methyl behenate (Fluka P/N 11940, 99.0%). The sample was filtered using a 22 µL nylon micro filter (Anatech) before injection. The GC-MS analysis was carried out using an Agilent GC/MSD 7890A/5975C (single quadrupole) with a multi-mode injector on a Zebron ZB-1701 column (60 m x 250 µm x 0.25 µm). The helium (carrier gas) was set to a flow rate of 1.3 $mL.min^{-1}$. The column-heating program was as follows: the column was initially held constant at 45 ^{o}C for 8 min, then ramped to 100 ^{o}C at 2 $^{o}C.min^{-1}$, after which it was again ramped to 260 ^{o}C at 7 $^{o}C.min^{-1}$. The iso-paraffinic hydrocarbon was used as a standard for quantification.

After GC-MS analysis, the iso-paraffinic hydrocarbon content in the FP HAPWS bio-oil was found to be between ~0 wt.% at 290 ^{o}C to 14 wt.% at 390 ^{o}C. As a result, yield, ultimate analysis and calorific value of bio-oil were corrected for comparison purposes. The ultimate analysis of the bio-oil was corrected by subtracting the mineral oil's C and H content, which is comprised of C_9 to C_{12} alkanes (C: 84.5 ± 0.14 wt.%, H: 15.5 ± 0.14 wt.%) [36].

5.2.4 Energy conversion

The partial biomass gross energy conversion (EC) from the PWS to the bio-oil/tarry phase and char is determined by Equation 16 below:

$$EC(\%) = \frac{m_i * HHV_i}{m_{PWS} * HHV_{PWS}} * 100 \qquad (16)$$

where m_i and HHV_i, are respectively the mass and higher heating value of the bio-oil/tarry phase or char, while m_{PWS} and HHV_{PWS} apply to PWS. The resulting gross EC compares the energy output in products only to the process energy input in the form of the PWS feedstock; external energy inputs for heating and vacuum were not considered. The sum of gross energy conversion (EC_{sum}) was determined by summing the char and bio-oil/tarry phase ECs. No analysis was performed on the non-condensable gas making determination of the experimental HHV impossible.

5.2.5 Design of experiments

A three level two factor full factorial statistical design was implemented to optimize the reactor temperature and pellet size to maximise both the higher heating values and pyrolysis product yields, and subsequently enhance energy conversion. The reactor temperature was selected as it has a large influence on the pyrolysis reactions [11,23,37-41]. From pre-screening pyrolysis runs that allow for location of optima, the appropriate reactor temperature levels of 340, 460 and 580 ^oC for slow pyrolysis, and 300, 425 and 550^oC for vacuum pyrolysis were selected. The fast pyrolysis temperature levels were 300, 425 and 550 ^oC for LAPWS and 290, 340 and 390 ^oC for HAPWS. Particle size is known to influence heat and mass transport effects during pyrolysis [17,41-43]. Although this phenomenon is typically stated for "single particle models", it is plausible to assume that a pellet, in the form of an "agglomerate of particles", has similar pyrolytic behaviour [44,45]. Therefore pellet size will be considered as a single particle as a preliminary approach. Pellet sizes in the range of 2.92 ± 0.12, 4.04 ± 0.18 and 4.84 ± 0.15 mm were used.

An ANOVA analysis was performed using the parametric data analysis function 'regression' in Microsoft Excel (2010, ver. 14.0.7128.5000, SP2) whereby a 2-way linear and quadratic model was fitted (Equation 17). The model was adapted such that the best fit was acquired. The coefficient of

determination (R^2) was used to determine how well the model fitted to the data, and the adjusted coefficient of determination (R^2_{adj}) was used to ensure that the model was not over fitted [46]. The hierarchy and heredity principles were also taken into consideration during the model fitting. The model was checked for consistency by insuring no heteroscedasticity in the normality, constant variance and independence assumptions [46]. A 90% confidence interval was used whereby a p-value of less than 0.1 indicated a significant effect of the factors on the responses. Equation 17 below represents the 2-way linear and quadratic model used:

$$Y_{product}\ (wt.\%) = intercept + \beta_1 * RT + \beta_2 * PS + \beta_3 * RT^2 + \beta_4 * PS^2 + \beta_5 * RT * PS + \beta_6 * RT^2 * PS + \beta_7 * PS^2 * RT + \beta_8 * RT^2 * PS^2 \quad (17)$$

where $Y_{product}$ is the pyrolysis product yield, β_{n+1} is the model coefficient, RT is the reactor temperature (°C) and PS is the pellet size (mm).

As the pellet size varied up to ± 0.18 mm, the average pellet size for each run was used to account for the deviations during ANOVA analysis and modelling. Three repeated runs were performed to determine the experimental error.

5.3 RESULTS AND DISCUSSION

5.3.1 Char product

5.3.1.1 Yields

Reactor temperature was shown to significantly (p-value < 0.1) affect the VP, SP and FP char yields for both PWSs, as it is confirmed by the well-fitted models (Appendix D-2 to D-4) and surface plots (Figure 5-2). Char formation was maximised at low temperatures (~300 °C) (Figure 5-2), which is in accordance with previous findings [4]. However, no significant trends were observed in the char yield for an increase in pellet size during VP, SP or FP for either of the PWSs.

On a common temperature range from 340 °C and upwards for both PWSs, SP had the highest char yields, followed by FP then VP (Figure 5-2), due to the promotion of secondary char formation reactions by longer vapour residence times [24], which is similar to findings often reported in literature [10,23,31]. These reactions are limited during FP due to the short vapour residence times of the volatiles, and during VP due to the vacuum that enhances mass transfer within in the particle [10,23,31].

5.3.1.2 Energy content

Models and surface plots for the calorific values of the char and bio-oil/tarry phase products generated during vacuum, slow and fast conversion of LAPWS and HAPWS are respectively presented in Appendix D-5 and Figure 5-3. Reactor temperature was shown to have a significant effect on all the char calorific values (Appendix D-5). While for pellet size, all but the LAPWS VP and FP, and HAPWS FP char calorific values were affected (Appendix D-5).

For LAPWS, an increase in temperature resulted in the promotion of VP, SP and FP char calorific values (Figure 5-3a,c,e) due to the conversion of oxygenated groups into volatiles and the formation of more benzene polycyclic structures [47]. This observation is also corroborated by the Van Krevelen diagram (Figure 5-4), whereby an increase in temperature resulted in significant decreases in the char O/C and H/C molar ratios. Although similar trends were observed for the HAPWS char with increasing temperature, O/C values (~0.01) were found significantly lower than those of LAPWS chars (~0.08) (Figure 5-4). This extensive deoxygenation stage is most probably due to the catalytic effect of the calcium components [33,48,49]. Despite the increase in C content, a decrease was observed in VP, SP and FP HAPWS char calorific values with an increase in temperature

(Figure 5-3b,d,f), due to the large and increasing ash content (> 80 wt.%) as illustrated by the proximate analysis in Figure 5-5.

As explained above, for each technology, a higher degree of pyrolytic conversion is usually associated with a calorific value increase in the char. When comparing the different technologies it can be observed that VP enhanced devolatilization and gave lower char yields (Figure 5-2a), although the calorific values of its LAPWS char (20.5 to 22.0 $MJ.kg^{-1}$) were in close correspondence to those of SP (21.5 to 22.8 $MJ.kg^{-1}$) and FP (21.2 to 22.3 $MJ.kg^{-1}$) (Figure 5-3a,c,e). This result can be explained by the difference in pyrolysis mechanisms (lower deoxygenation efficiency under vacuum conditions [50]) and the higher ash content in VP chars (Figure 5-5). For HAPWS, the FP char calorific values (4.0 to 7.2 $MJ.kg^{-1}$) were highest, followed by SP (4.8 to 5.2 $MJ.kg^{-1}$), then by VP (2.9 to 4.0 $MJ.kg^{-1}$) (Figure 5-3b,d,f). The FP char had a lower ash content in comparison to VP and SP (Figure 5-5), possibly due to the loss of ash during fluidisation [6], explaining the higher calorific value. Due to the large ash content (~81 to 92 wt.%), combustion of this low caloric value char is not recommended as it could cause slagging and fouling [51,52]. In addition, combustion temperatures above 400/650 ºC could lead to endothermic decomposition of $Ca(OH)_2/CaCO_3$ [1,6]. While it is clear that the HAPWS char cannot be used for industrial energy applications, it was considered in the energy conversion study for comparison purposes (Section 5.3.1.3).

5.3.1.3 Energy conversion

The surface plots and statistical models for the energy conversion from the PWS to its pyrolysis char (EC_{char}) and bio-oil/tarry phase ($EC_{bio\text{-}oil}/EC_{tarry}$) products are respectively presented by Figure

5-6 and Appendix D-6. In all instances reactor temperature significantly affected the EC_{char}, while this was not always the case for pellet size (Appendix D-6).

Although the calorific values of the LAPWS char were promoted at higher reactor temperatures (Figure 5-3a,c,e), the decrease in char yield (Figure 5-2a,c,e) resulted in lower EC_{char} for VP, SP and FP (Figure 5-6a,c,e), which is similar to previous findings for SP of segregated wastes by Phan *et al.* [13]. Lower EC_{char} were obtained during VP (~28 to 34 %) when compared to SP (~32 to 43 %) and FP (~29 to 41 %), which can be attributed to a lower char yield. Not surprisingly, higher EC_{char} were obtained for HAPWS at lower reactor temperatures for all three pyrolysis processes (Figure 5-6b,e,f), where both the char yields (Figure 5-2b,e,f) and calorific values (Figure 5-3b,e,f) were promoted. Similarly to the char calorific values, FP offered the highest EC_{char} (~16 to 37 %), followed by SP (~20 to 25 %), then by VP (~8 to 18 %).

5.3.2 Liquid product

5.3.2.1 Yields

Results from statistical models indicated that both the pellet size and reactor temperature have a significant effect on the bio-oil produced during SP and FP of LAPWS, as well as during VP of HAPWS (Appendix D-2 to D-4). However, only the pellet size affected the HAPWS SP and FP bio-oil yield, although reactor temperature is often reported to have a significant affect [11,21,23]. The significance of the linear interaction term (β_5) between the reactor temperature and pellet size indicated that both parameters are interdependent, and thus temperature still plays a significant role during SP and FP of HAPWS (Appendix D-3 to D-4). During VP of LAPWS, only the reactor temperature had a significant effect on its bio-oil yield (Appendix D-2).

The vacuum, slow and fast pyrolysis bio-oil yields are presented by Figure 5-7. An increase in reactor temperature led to an initial promotion in the SP and FP bio-oil yields for both PWSs, followed afterwards by a decrease due to the increased conversion of condensable organic compounds into gas by cracking reactions, which is similar to trends often observed in literature (Figure 5-7) [10,11]. During SP and FP of HAPWS, as well as during FP of LAPWS, an increase in pellet size led to a promotion in the bio-oil yield. This observation could be attributed to promotion of secondary exothermic reactions [6,53], by mass transfer limitations [45], subsequently resulting in higher heating rates and in turn greater bio-oil production [9]. The maximum bio-oil yields of VP were low in comparison to those of FP and SP for both PWSs (Figure 5-7). Unlike most studies that always report highest yields for FP [10,18,20], FP and SP led to similar bio-oil yields for both PWSs (Figure 5-7). These results can be explained in terms of the levels of pyrolytic water, whereby SP had the highest and FP the lowest yields (Figure 5-8). Indeed, the large production of pyrolytic water during SP can be attributed to a greater occurrence of dehydration reactions associated to the char formation mechanisms [54]. In addition, the HAPWS SP pyrolytic water yields were higher than those of LAPWS, indicating that the dehydration reactions where catalysed in the presence of inorganics (Figure 5-8) [48,49].

In an energy context, a large amount of water in a pyrolysis product is not favourable as it plays a critical role in the fuel quality and significantly lowers the calorific value [10]. As the aqueous phase obtained by SP and VP conversion is mainly comprised of water (~75 wt.%), its energy content is significantly lower than that of the tarry phase. As a consequence thereafter only the tarry phase (Figure 5-9) was considered for the energy conversion study (Section 5.3.2.3); the influence of this choice is discussed later (Section 5.3.3).

5.3.2.2 Energy content

The bio-oil/tarry phase calorific models indicated that both reactor temperature and pellet size had a significant effect for all cases, except the LAPWS SP tarry phase, which was only affected by the pellet size (Appendix D-5).

Trends in the organic liquid (Figure 5-10) and pyrolytic water (Figure 5-8) yields can help explain the observations in the bio-oil/tarry phase calorific value surface plots (Figure 5-3). For all cases of LAPWS, and SP of HAPWS, similar trends are observed between the organic liquid yields (Figure 5-10), bio-oil/tarry phase yields (Figures 5-7 and 5-9), and their respective calorific values (Figure 5-3a,c,d,e). These findings suggest that at conditions where the bio-oil/tarry phase yields are promoted, a higher yield of organic liquid with a high calorific value is produced, explaining the observed promotion in the calorific values. On the other hand, an opposite trend was observed for the HAPWS FP bio-oil, whereby smaller pellet sizes resulted in higher calorific values (Figure 5-3f) but lower yields (Figure 5-7b). This trend is explained by the difference in water content (Figure 5-8b). It is noted that below a pellet size of 3.8 mm the FP HAPWS pyrolytic water yield became negative suggesting that pyrolytic water as well as a fraction of the initial PWS moisture, could have been converted by secondary reactions [33] (Figure 5-3f). No conclusion could be drawn for the HAPWS VP tarry phase calorific values due to the large standard deviation (± 2.7 $MJ.kg^{-1}$).

The Van Krevelen diagram of the FP, VP and SP bio-oil/tarry phase is presented by Figure 5-11. For both PWSs, lower VP tarry phase O/C and H/C molar ratios led to slightly higher calorific values (19.9 to 22.3 $MJ.kg^{-1}$ for LAPWS; 22.5 to 24.4 $MJ.kg^{-1}$ for HAPWS), when compared to the FP bio-oils (17.6 to 22.2 $MJ.kg^{-1}$ for LAPWS; 14.4 to 19.7 $MJ.kg^{-1}$ for HAPWS) (Figures 5-3a,b,e,f and 11). This is most likely due to the lower water content displayed in the VP tarry phase (~3 to 7 wt.%) when compared to the FP bio-oil (~7 to 22 wt.%). On the other hand, due to the large

water content (~40 to 58 wt.%), slow pyrolysis tarry phase displayed significantly higher O/C and H/C molar ratios (Figure 5-11) as well as lower calorific values (7.5 to 9.5 $MJ.kg^{-1}$ for LAPWS; 8.2 to 13.0 $MJ.kg^{-1}$ for HAPWS) (Figure 5-3c,d). A substantial increase in the calorific value is noted between the raw HAPWS and its VP tarry phase of between 86 and 100 %, which is higher than that obtained for FP bio-oil (19 to 63 %).

5.3.2.3 Energy conversion

The statistical models indicated that reactor temperature significantly affected all the FP $EC_{bio-oil}$, and SP/VP EC_{tarry}, except for the HAPWS VP EC_{tarry} (Appendix D-6). Pellet size affected all the FP $EC_{bio-oil}$, and SP/VP EC_{tarry}, except for the LAPWS SP EC_{tarry} (Appendix D-6).

Higher $EC_{bio-oil}$ and EC_{tarry} were obtained at similar conditions to that where both the bio-oil/tarry phase calorific values (Figure 5-3a,c,d,e) and yields (Figures 5-7 and 5-9) were maximised during VP, SP and FP conversion of LAPWS (Figure 5-6a,c,e), as well as during SP conversion HAPWS (Figure 5-6d). This observation can be explained by a greater availability of organic liquid (Figure 5-10). On the other hand, higher HAPWS $EC_{bio-oil}$ (Figure 5-6f) was obtained at similar conditions to that where only the bio-oil yields were maximised (Figure 5-7b), regardless of the decreasing calorific values (Figure 5-3f). The VP EC_{tarry} (Figure 5-6b) trends are similar to those of the tarry phase yields (Figure 5-9b) but not necessarily with its calorific values. For both PWSs, FP displayed substantially higher $EC_{bio-oil}$ ranging from 22.2 to 45.1 % for LAPWS, and 19.1 to 45.4 % for HAPWS when compared to the VP and SP EC_{tarry} (Vacuum: 16.8 to 27.0 % for LAPWS and 11.7 to 17.9 % for HAPWS; Slow: 10.9 to 17.4 % for LAPWS and 12.2 to 17.9 % for HAPWS) (Figure 5-6), due to higher production of condensable organic compounds and lower water yields (Figures 5-8 and 5-10).

5.3.3 Energy conversion assessment

Amongst the various scenarios, the sum of char and bio-oil/tarry phase ECs (EC_{sum}) were compared to reveal which key operating conditions result in the maximisation of the EC_{sum} ($EC_{sum-max}$) (Figure 5-6). During VP of LAPWS, a $EC_{sum-max}$ of ~58.7 ± 3.1 % was obtained in the reactor temperature range of 300 and 500 ^{o}C, and for pellet sizes of 3 to 4.4 mm (Figure 5-6a). These conditions are in the region where both the yield (Figure 5-7a) and calorific value (Figure 5-3a) of the tarry phase are maximised. A LAPWS slow pyrolysis $EC_{sum-max}$ of 57.1 ± 1.0 % was obtained at the reactor temperature and pellet size ranging between 390 to 500 ^{o}C and 3.3 to 4.4 mm, respectively (Figure 5-6c). These conditions correspond to the ranges where both the tarry phase yields (Figure 5-7c) and calorific values (Figure 5-3c) are promoted. During FP conversion of LAPWS, a reactor temperature of 300 ^{o}C and pellet size range 3 to 5 mm, corresponded to conditions where the char yield (Figure 5-2a) and bio-oil calorific value (Figure 5-3e) were maximised, resulting in a $EC_{sum-max}$ of 77.2 ± 0.8 % (Figure 5-6e). For HAPWS, the conditions ranging between 300 to 350 ^{o}C and 3 to 4.2 mm correspond to areas where both the VP char and tarry phase yields (Figure 5-2b,5-7b), as well as the char calorific values (Figure 5-3b), are promoted resulting in a $EC_{sum-max}$ of 32.2 ± 2.6 % (Figure 5-6b). Maximisation of both the HAPWS SP char and tarry phase yields (Figure 5-2b,5-7d) and calorific values (Figure 5-3d) (340 ^{o}C and 5 mm) led to a $EC_{sum-max}$ of 50.3 ± 2.5 % (Figure 5-6d). During FP conversion of HAPWS, the operating conditions of 290 ^{o}C and 5 mm resulted in the maximisation of both the char and bio-oil calorific values (Figure 5-3f), as well as the char yield (Figure 5-2b), which led to a $EC_{sum-max}$ of 68.7± 2.0 % (Figure 5-6f).

Significant differences are observed in the $EC_{sum-max}$ between the pyrolysis processes. Fast pyrolysis displayed a $EC_{sum-max}$ that was between 18.5 to 20.1% higher for LAPWS, and 18.4 to 36.5 % higher for HAPWS, when compared to vacuum and slow pyrolysis (Figure 5-6). Assuming that the organic composition of the aqueous phase is similar to that of the tarry phase, a $EC_{aqueous}$ of between ~5.0 to 11.3 % for VP, and ~0.7 to 3.0 % for SP was calculated. Thus, given the difference in the $EC_{sum-max}$, it is clear that having considered the aqueous phase would not have changed the conclusion of this work. While the EC_{char} are relatively comparable between the pyrolysis processes for LAPWS, the higher $EC_{sum-max}$ obtained under FP conditions can mainly be attributed to a higher $EC_{bio-oil}$ (Figure 5-6). However, for HAPWS both the $EC_{bio-oil}$ and EC_{char} where high in comparison to VP and SP explaining the significant difference in the $EC_{sum-max}$ (Figure 5-6b,d,f).

5.4 CONCLUSION

An energy assessment based on gross energy conversion of three pyrolysis technologies at varying key operating parameters, reactor temperature and pellet size, was performed to compare performances. Comparison between the pyrolysis techniques revealed that the $EC_{sum-max}$ for fast pyrolysis was between 18.5 to 20.1% higher for LAPWS, and 18.4 to 36.5 % higher for HAPWS, when compared to the vacuum and slow pyrolysis processes. For both PWSs, this finding was mainly attributed to higher production of condensable organic compounds and lower water yields during FP. The substantial differences that lie within $EC_{sum-max}$ between the pyrolysis processes, especially for HAPWS, highlight the detrimental effect of ash on the SP and VP processes. When considering the low calorific values of the HAPWS chars and SP tarry phase, which cannot be used for industrial energy applications, it should rather be converted to bio-oil via FP conversion to maximise the recovery of usable energy products. Alternative uses for the HAPWS char product

should be investigated such as in biomaterials (i.e., biochar, adsorbents). The LAPWS high calorific value chars, FP bio-oil and VP tarry phase can be considered for industrial energy applications.

While this work has recommended the preferred conditions to maximise the gross ECs, additional modelling studies would be required, taking into account energy input (heat energy for biomass drying and pyrolysis), in order to confirm the efficiency of the whole pyrolysis process.

Acknowledgments

This work was financially supported by Kimberley Clark SA, the Paper Manufacturers Association of South Africa (PAMSA) and FP&M Seta. The authors would like to thank these organisations for their support.

5.5 REFERENCES

[1] A. Mendez, J.M. Fidalgo, F. Guerrero, G. Gasco, Characterization and pyrolysis behaviour of different paper mill waste materials, Journal of Analytical and Applied Pyrolysis (86) (2009) 66-73.

[2] R. Lou, S. Wu, G. Lv, Q. Yang, Energy and resource utilization of deinking sludge, Applied Energy (90) (2012) 46-50.

[3] M. Ouadi, J.G. Brammer, Y. Yang, A. Hornung, M. Kay, The intermediate pyrolysis of deinking sludge to produce a sustainable liquid fuel, Journal of Analytical and Applied Pyrolysis (105) (2013) 135-142.

[4] V. Strezov, T.J. Evans, Thermal processing of paper sludge and characterisation of its pyrolysis products, Waste Management (2009) (29) 1644-1648.

[5] Y. Yang, J.G. Brammer, M. Ouadi, J. Samanya, A. Hornung, H.M. Xu, Y. Li, Characterisation of waste derived intermediate pyrolysis oils for use as diesel engine fuels, Fuel (103) (2013) 247-257.

[6] A.J. Ridout, M. Carrier, J. Gorgens, Fast pyrolysis of low and high ash paper waste sludge: Influence of reactor temperature and pellets size, Journal of Analytical and Applied Pyrolysis (111) (2015) 64-75.

[7] J.M. Reckamp, R.A. Garrido, J.A. Satrio, Selective pyrolysis of paper mill sludge by using pretreatment processes to enhance the quality of bio-oil and biochar products, Biomass and Bioenergy (71) (2014) 235-244.

[8] S. Fang, Z. Yu, Y. Lin, S. Hu, Y. Liao, X. Ma, Thermogravimetric analysis of the co-pyrolysis of paper waste sludge and municipal solid waste, Energy Conversion and Management (101) (2015) 626-631.

[9] M.C. Monte, E. Fuente, A. Blanco, C. Negro, Waste management from pulp and paper production in the European Union, Waste Management (29) (2009) 293-308.

[10] A.V. Bridgwater, Review of fast pyrolysis of biomass and product upgrading, Biomass and Bioenergy (38) (2012) 68-94.

[11] M. Garcia-Perez, X.S. Wang, J. Shen, M.J. Rhodes, F. Tian, W. Lee, H. Wu, C. Li, Fast pyrolysis of oil mallee woody biomass: Effect of temperature on the yield and quality of pyrolysis products, Industrial & Engineering Chemistry Research (47) (2008) 1846-1854.

[12] X. Li, V. Strezov, T. Kan, Energy recovery potential of spent coffee grounds pyrolysis products, Journal of Analytical and Applied Pyrolysis (110) (2014) 79-87.

[13] A.N. Phan, C. Ryu, V.N. Sharifi, J. Swithenbank, Characterisation of slow pyrolysis products from segregated wastes for energy production, Journal of Analytical and Applied Pyrolysis (81) (2008) 65-71.

[14] N. Troger, D. Richter, R. Stahl, Effect of feedstock composition on product yields and energy recovery rates of fast pyrolysis products from different straw types, Journal of Analytical and Applied Pyrolysis (100) (2013) 158-165.

[15] A.L.M.T. Pighinelli, A.A. Boateng, C.A. Mullen, Y. Elkasabi, Evaluation of Brazillian biomasses as feedstocks for fuel production via fast pyrolysis, Energy for Sustainable Development (21) (2014) 42-50.

[16] J. Han, A. Elgowainy, J.B. Dunn, M.Q. Wang, Life cycle analysis of fuel production from fast pyrolysis of biomass, Bioresource Technology (133) (2013) 421-428.

[17] O. Onay, O.M. Kockar, Fixed-bed pyrolysis of rapeseed (Brassica napus L.), Biomass and Bioenergy (26) (2004) 289-299.

[18] O. Onay, O.M. Kockar, Slow, fast and flash pyrolysis of rapeseed, Renewable Energy (28) (2003) 2417-2422.

[19] A.E. Putun, E. Onal, B.B. Uzun, N. Ozbay, Comparison between the “slow” and “fast” pyrolysis of tobacco residue, Industrial Crops and Products (26) (2007) 307-314.

[20] G. Duman, C. Okutucu, S. Ucar, R. Stahl, J. Yanik, The slow and fast pyrolysis of cherry seed, Bioresource Technology (102) (2011) 1869-1878.

[21] A.V. Bridgwater, Principles and practices of biomass fast pyrolysis processes for liquids, Journal of Analytical and Applied Pyrolysis (51) (1999) 3-22.

[22] M. Balat, M. Balat, E. Kirtay, H. Balat, Main routes for the thermo-conversion of biomass into fuels and chemicals. Part 1: Pyrolysis systems, Energy conversion and Management (50) (2009) 3147-3157.

[23] M. Carrier, T. Hugo, J. Gorgens, H. Knoetze, Comparison of slow and vacuum pyrolysis of sugar cane bagasse, Journal of Analytical and Applied Pyrolysis (90) (2011) 18-26.

[24] C.A. Zaror, I.S. Hutchings, D.L. Pyle, H.N. Stiles, R. Kandiyoti, Secondary char formation in the catalytic pyrolysis of biomass, Fuel (64) (1985) 990-994.

[25] A. Anca-Couce, R. Mehrabian, R. Scharler, I. Obernberger, Kinetic scheme of biomass pyrolysis considering secondary charring reactions, Energy Conversion and Management (87) (2014) 687-696.

[26] L. Rossendahl, Biomass combustion science, technology and engineering, Elsevier Denmark, (2013) 172-173.

[27] F. Tinwala, P. Mohanty, S. Parmar, A. Patel, K.K. Pant, Intermediate pyrolysis of agro-industrial biomasses in bench-scale pyrolyser: Product yields and its characterization, Bioresource Technology (188) (2015) 258-264.

[28] D. Chiaramonti, A. Oasmaa, Y. Solantausta, Power generation using fast pyrolysis liquids from biomass, Renewable and Sustainable Energy Reviews (11) (2007) 1056-1086.

[29] D. Mohan, C.U. Pittman, P.H Steel, Pyrolysis of wood/biomass for bio-oil: A critical review, Energy and Fuels (20) (2006) 848-889.

[30] A.V. Bridgwater, Renewable fuels and chemicals by thermal processing of biomass, Chemical Engineering Journal (91) (2003) 87-102.

[31] M. Amutio, G. Lopez, R. Aguado, M. Artetxe, J. Bilbao, M. Olazar, Effect of vacuum on lignocellulosic biomass flash pyrolysis in a conical spouted bed reactor, Energy & Fuels (25) (2011) 3950-3960.

[32] J. Scheirs, A guide to polymeric geomembranes, Great Britain: John Wiley & Sons (2009) 304.

[33] M. Widyawati, T.L. Church, N.H. Florin, A.T. Harris, Hydrogen synthesis from biomass pyrolysis with in situ carbon dioxide capturing using calcium oxide, Journal of Hydrogen Energy (36) (2011) 4800-4813.

[34] R.A Mott, C.E. Spooner, The calorific value of carbon in coal: the Dulong relationship, Fuel (19) (1940) 242-251.

[35] S.A. Channiwala, P.P. Parikh, A unified correlation for estimating HHV of solid, liquid and gaseous fuels, Fuel (81) (2002) 1051-1063.

[36] Exxon Mobil (2014, January), Product safety summary: Isopar G fluid [pdf], Available: www.exxonmobilchemical.com

[37] S. Ucar, S. Karagoz, The slow pyrolysis of pomegranate seeds: The effect of temperature on the product yields and bio-oil properties, Journal of Analytical and Applied Pyrolysis (84) (2009) 151-156.

[38] E. Apaydin-Varol, E. Putun, A. Putun, Slow pyrolysis of pistachio shell, Fuel (2007) (86) 1892-1899.

[39] P. Das, A. Ganesh, Bio-oil from pyrolysis of cashew nut shell-a near future, Biomass and Bioenergy (25) (2003) 113-117.

[40] S. Julien, E. Chornet, P.K. Tiwari, R.P. Overend, Vacuum pyrolysis of cellulose: Fourier transform infrared characterisation of solid residues, product distribution and correlations, Journal of Analytical and Applied Pyrolysis (1991) (19) 81-104.

[41] A. Demirbas, Effects of temperature and particle size on bio-char yield from pyrolysis of agricultural residues, Journal of Analytical and Applied Pyrolysis (2004) (72) 243-248.

[42] M. Van de Velden, J. Baeyens, A. Brems, B. Janssens, R. Dewil, Fundamentals, kinetics and endothermicity of the biomass pyrolysis reactions, Renewable Energy (25) (2010) 232-242.

[43] J. Shen, X. Wang, M. Garcia-Perez, D. Mourant, M.J. Rhodes, C. Li, Effects of particle size on the fast pyrolysis of oil mallee woody biomass, Fuel (88) (2009) 1810-1817.

[44] M. Jeguirim, L. Limousy, P. Dutournie, Pyrolysis kinetics and physicochemical properties of agropellets produced from spent ground coffee blended with conventional biomass, Chemical Engineering Research and Design (92) (2014) 1876-1882.

[45] R. Reschmeier, D. Roveda, D. Muller, J. Karl, Pyrolysis kinetics of wood pellets in fluidized beds, Journal of Analytical and Applied Pyrolysis (2014) (108) 117-129.

[46] D.C. Montgomery, Design and analysis of experiments, U.S.A: John Wiley & Sons (2001) 363-422.

[47] F. Collard, J. Blin, A review on pyrolysis of biomass constituents: Mechanisms and composition of the products obtained from the conversion of cellulose, hemicellulose and lignin, Renewable and Sustainable Energy Reviews (38) (2014) 594-608.

[48] M.R. Gray, W.H. Corcora, G.R. Gavalas, Pyrolysis of wood-derived material. Effects of moisture and ash content, Industrial and Engineering Chemistry Process Design and Development (24) (1985) 646-651.

[49] A. Hlavsova, A. Corsaro, H. Raclavska, D. Juchelkovam The effects of varying CaO content on rehydration treatments on the composition, yield, and evolution of gaseous products from pyrolysis of sewage sludge, Journal of Analytical and Applied Pyrolysis (108) (2014) 160-169.

[50] P. Ahuja, S. Kumar, P.C. Singh, A model for primary and heterogeneous secondary reactions of wood pyrolysis, Chemical Engineering & Technology (19) (1996) 272-282.

[51] R. Kurose, M. Ikeda, H. Makino, Combustion characteristics of high ash coal in a pulverized coal combustion, Fuel (80) (2001) 1447-1455.

[52] S. Jayanti, K. Maheswaran, V. Saravanan, Assessment of the effect of high ash content in pulverized coal combustion, Applied Mathematical Modelling (31) (2007) 934-953.

[53] M.G. Gronli, Mathematical model for wood pyrolysis - comparison of experimental measurements with model predictions, Energy Fuels (14) (2000) 791-800.

[54] J. Scheirs, G. Camino, W. Tumiatti, Overview of water evolution during the thermal degradation of cellulose, European Polymer Journal (37) (2001) 933-942.

Table 5-1. Physico-chemical characterisation of the LAPWS and HAPWS (modified from Ridout *et al.* [6])

	LAPWS	HAPWS
As-received moisture content (wt. %)	80.9	54.6
Ash (525 °C, df wt.%)	8.5	46.7
Proximate Analysis (df, wt.%)		
Volatile Matter	78.7	50.3
Fixed Carbon	15.5	2.9
Ash (900 °C)	5.8	24.6
Ultimate Analysis (daf, wt.%)		
C	49.2	47.2
H	5.9	6.7
O (by difference)	44.8	45.7
N	0.08	0.41
S	0.00	0.00
HHV (MJ/kg)	17.8	12.1

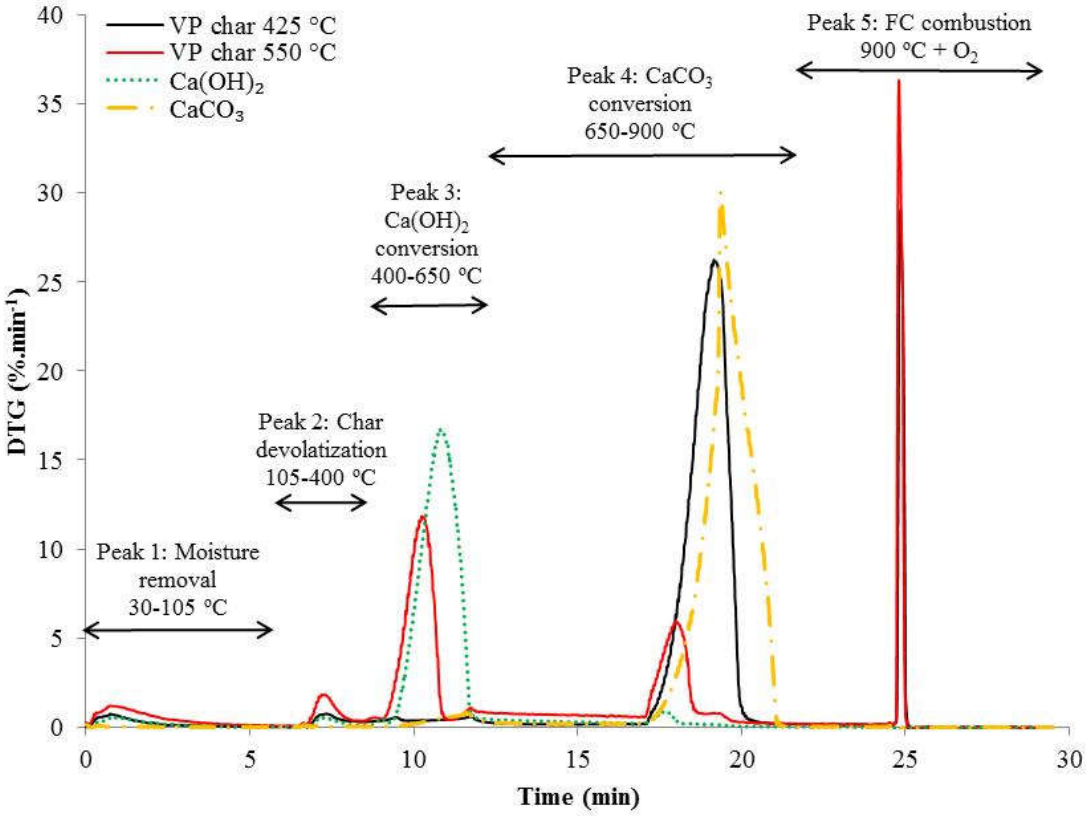

Figure 5-1. Altered proximate analysis of chars obtained from vacuum pyrolysis of HAPWS, as well as $Ca(OH)_2$ and $CaCO_3$.

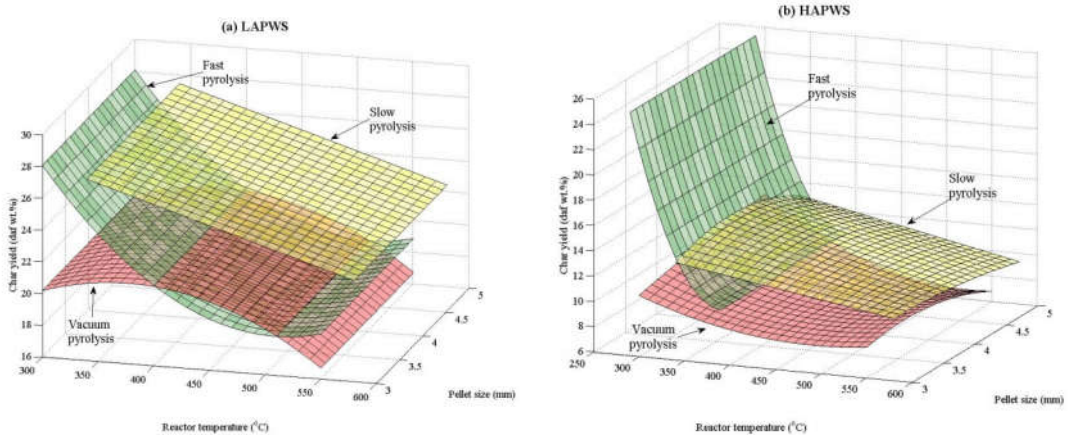

Figure 5-2. Dependence of char yield on reactor temperature and pellet size during vacuum, slow and fast pyrolysis conversion of LAPWS (a) and HAPWS (b).

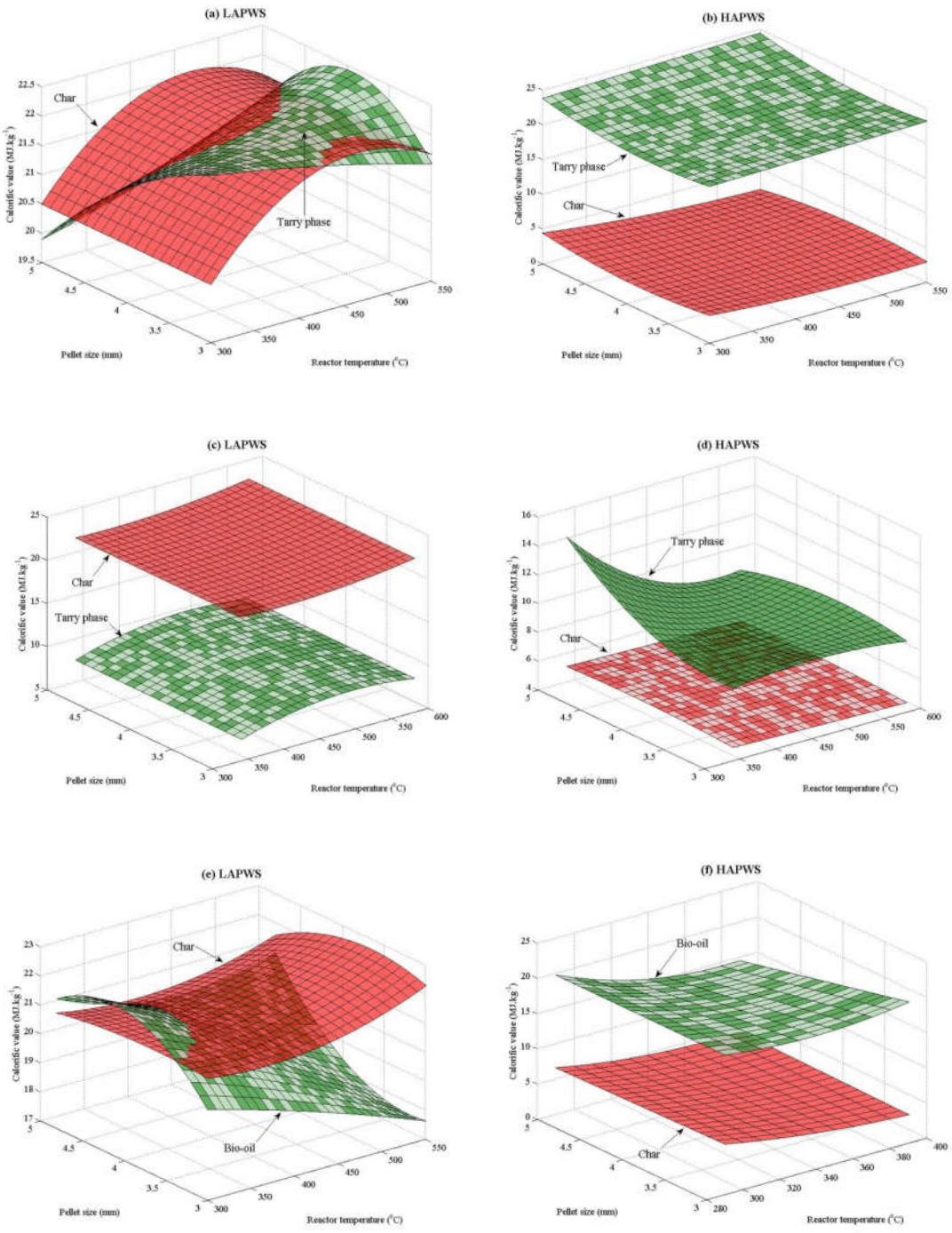

Figure 5-3. Calorific values of chars and bio-oil/tarry products obtained from the vacuum (a-b), slow (c-d) and fast (e-f) pyrolysis of LAPWS (a,c,f) and HAPWS (b,d,f) according to reactor temperature and pellet size.

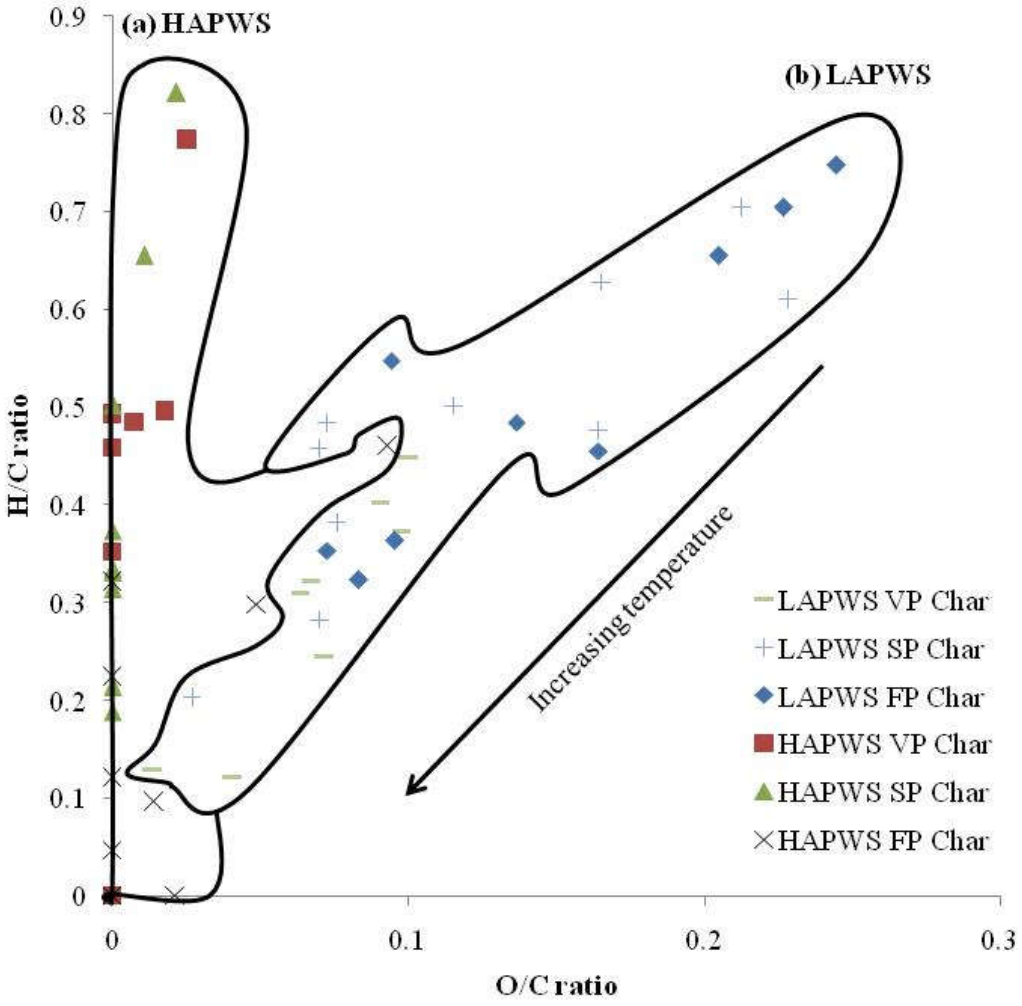

Figure 5-4. van Krevelen diagram of the HAPWS (a) and LAPWS (b) vacuum, slow and fast pyrolysis char products.

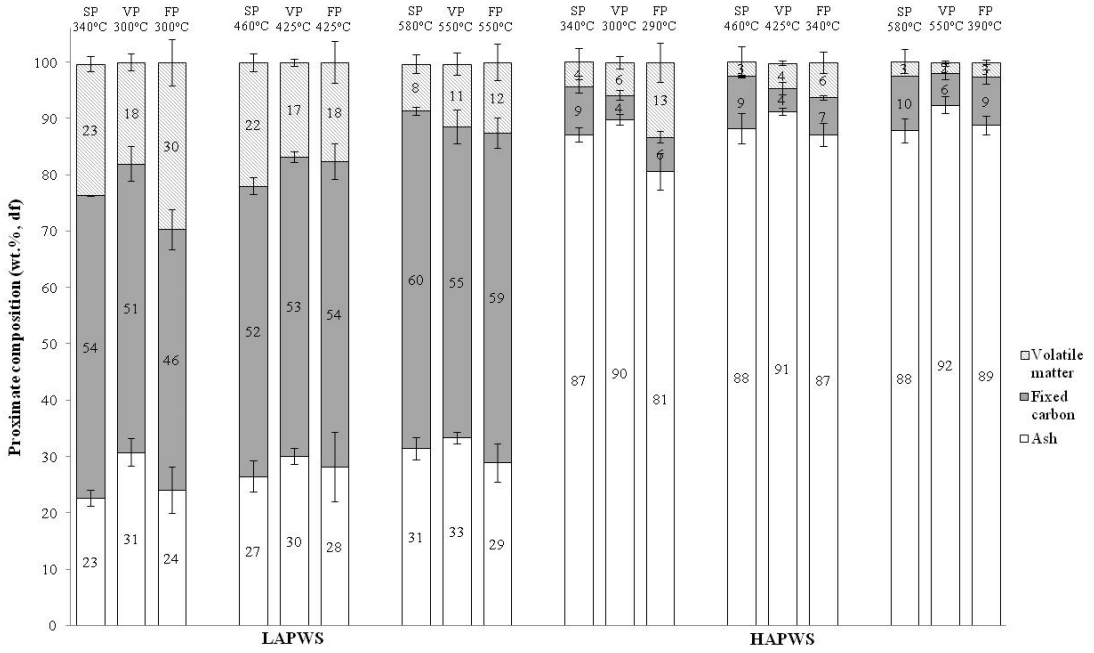

Figure 5-5. Proximate composition of LAPWS and HAPWS char produced via slow, vacuum and fast pyrolysis at different reactor temperatures.

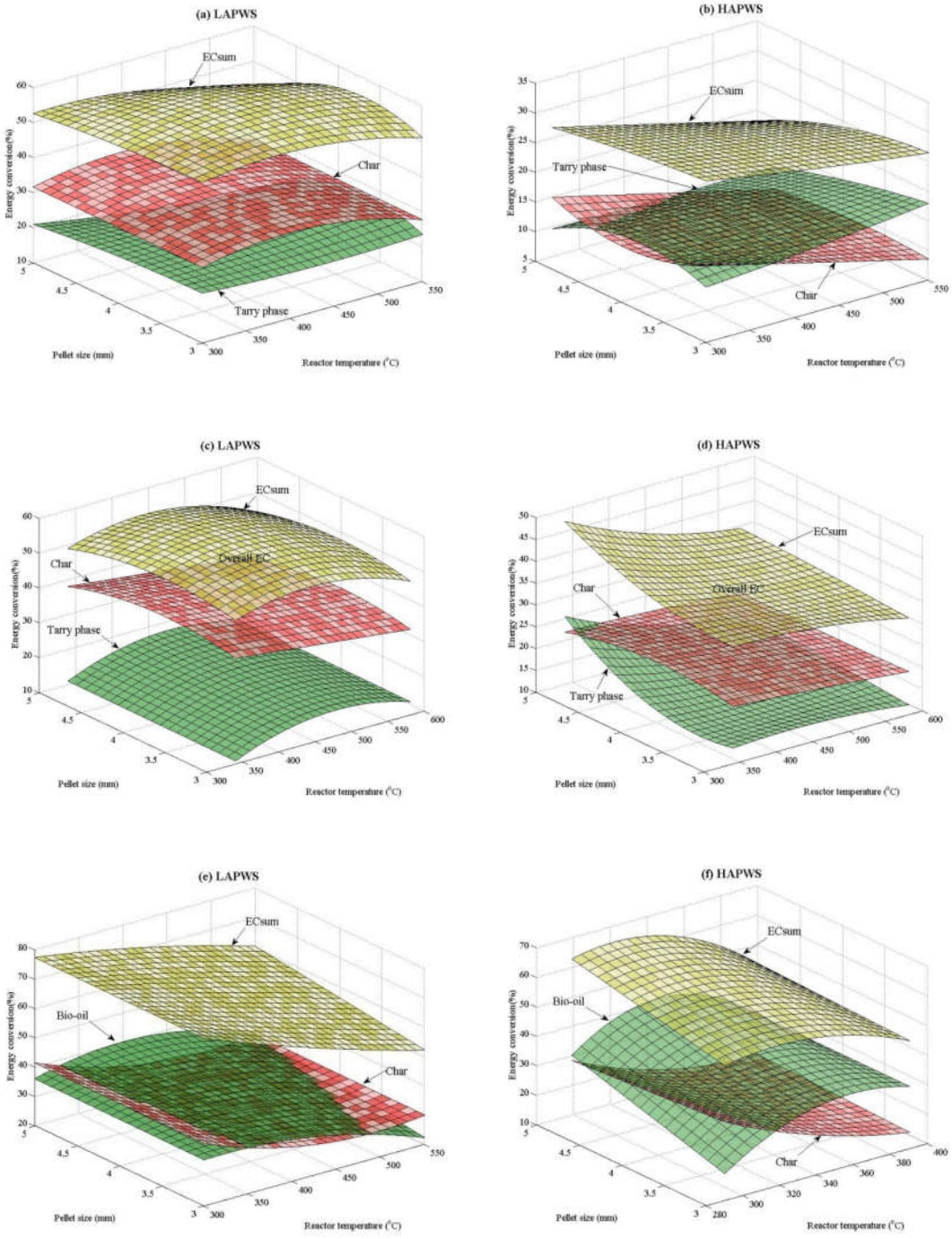

Figure 5-6. Dependence of energy conversion from PWS to its vacuum (a-b), slow (c-d) and fast (e-f) pyrolysis bio-oil/tarry and char products on reactor temperature and pellet size. (EC_{sum}: Sum of char and bio-oil/tarry EC)

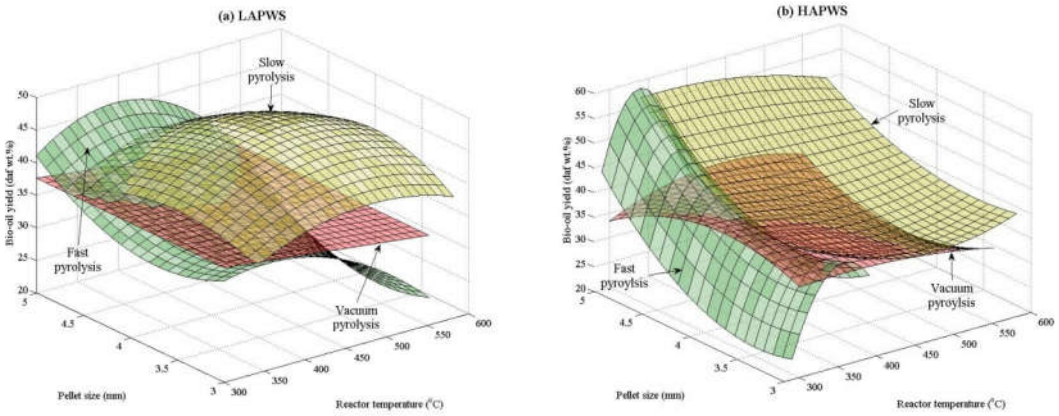

Figure 5-7. Dependence of bio-oil yield on reactor temperature and pellet size during vacuum (a-b), slow (c-d) and fast (e-f) pyrolysis of LAPWS (a,c,e) and HAPWS (b,d,f).

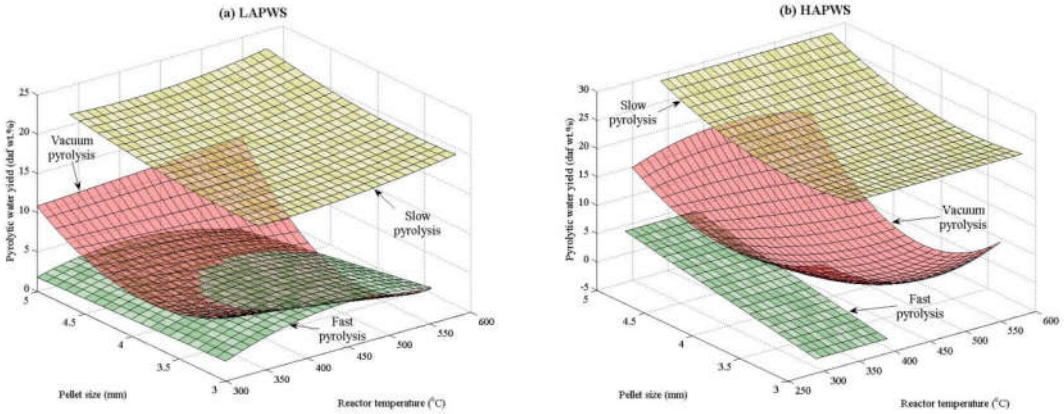

Figure 5-8. Evolution of pyrolytic water from vacuum, slow and fast pyrolysis of LAPWS (a) and HAPWS (b) for different reactor temperatures and pellet sizes.

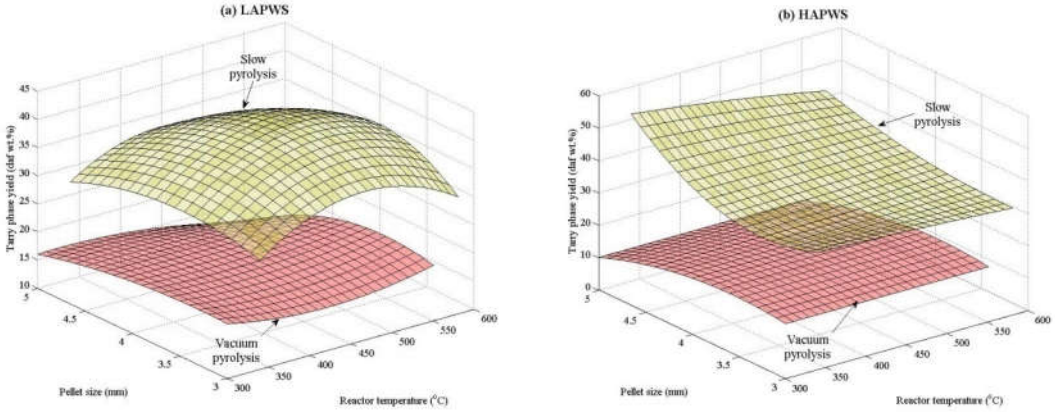

Figure 5-9. Evolution of tarry phase products from vacuum and slow pyrolysis of LAPWS (a) and HAPWS (b) for different reactor temperatures and pellet sizes.

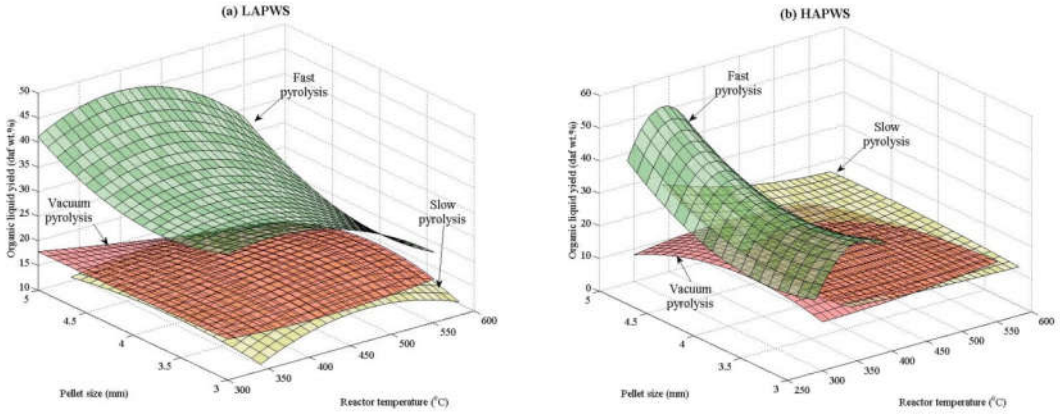

Figure 5-10. Organic liquid yield in bio-oil for fast pyroylsis, and in the tarry phase for vacuum and slow pyrolysis, of LAPWS (a) and HAPWS (b) at different reactor temperatures and pellet sizes.

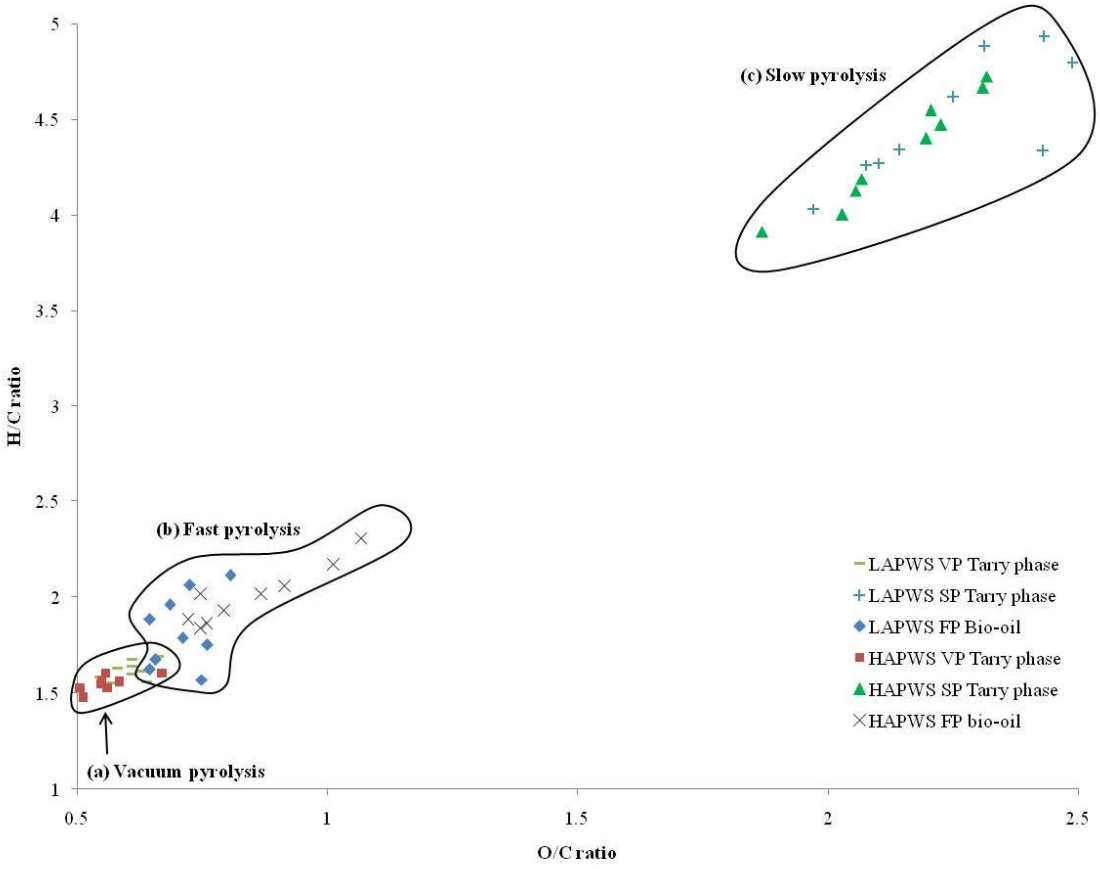

Figure 5-11. van Krevelen diagram of the LAPWS and HAPWS vacuum (a), fast (b) and slow (c) pyrolysis bio-oil/tarry phase products.

CHAPTER 6: CHEMICALS AND BIOMATERIALS PRODUCTION FROM VACUUM, SLOW AND FAST PYROLYSIS PROCESSES FOR LOW AND HIGH ASH PAPER WASTE SLUDGE

A paper in preparation for submission to Bioresource Technology (ISI impact factor 5.330).

Title: "Chemicals and biomaterials production from vacuum, slow and fast pyrolysis processes for low and high ash paper waste sludge"

Authors: Angelo J. Ridout, Marion Carrier, François-Xavier Collard, Johann Görgens.

OBJECTIVE OF DISSERTATION AND SUMMARY OF FINDINGS IN PRESENT CHAPTER

This chapter addresses **objectives 3 and 5 to 7** which focusses on targeted production of value-added marketable chemical and biomaterial resources (**objective 7**) from PWS using various pyrolysis techniques (**objective 5**). To draw maximal benefit from this latter, the effect of key operating conditions, the role and fate of ash (**objective 3**) and the pyrolytic mechanisms (**objective 6**) are addressed.

The pyrolysis technology selection was shown to have a greater influence on chemical yields than reactor temperature and pellet size. More specifically the higher heating rates employed during FP enhanced glycosidic bond cleavage resulting in the promotion the levoglucosan yields for both PWSs. Furthermore, the large quantity of inorganics present in HAPWS catalysed glycosidic bond cleavage resulting in a lower optimum reactor temperature for which higher levoglucosan yields (3.7 daf, wt.%, 340 ^{o}C) were obtained when compared to LAPWS (1.5 daf, wt.% 430 ^{o}C). Production of char biomaterials (sorption medium or biochar) during VP of LAPWS offered the highest sorption capacity as well as DFT surface areas (281 to 344 $m^2.g^{-1}$) when compared to SP and FP due to enhanced devolalitilization. However, for HAPWS no particular pyrolysis process offered improvement in the sorptive properties of the biomaterial char.

Candidate declaration

With regards to chapter 6, page numbers 165-204 of this dissertation, the nature and scope of my contribution were as follows:

Name of contribution	Extent of contribution (%)
Planning and experiments	70
Executing experiments	100
Interpretation of results	70
Writing the chapter	100

The following co-authors have contributed to chapter 6 page 165-204 of this dissertation:

Name	e-mail address	Nature of contribution	Extent of contribution (%)
1. Marion Carrier	m.carrier@aston.ac.uk	• Experimental planning • Reviewing the chapter • Interpretation of results	20 45 15
2. François-Xavier Collard	fcollard@sun.ac.za	• Reviewing the chapter • Interpretation of results	45 15
3. Johann Görgens	jgorgens@sun.ac.za	• Reviewing the chapter • Experimental planning	10 10

Signature of candidate…….

Date…….

Declaration by co-authors

The undersigned hereby confirm that:

4. The declaration above accurately reflects the nature and extent of the contributions of the candidates and co-authors to chapter 6 page numbers 165-204 in the dissertation,
5. no other authors contributed to chapter 6 page numbers 165-204 in the dissertation beside those specified above, and
6. potential conflicts of interest have been revealed to all interested parties and that are necessary arrangements have been made to use the material in chapter 6 page numbers 165-204 of the dissertation

Signature	Institutional affiliation	Date

CHEMICALS AND BIOMATERIALS PRODUCTION FROM VACUUM, SLOW AND FAST PYROLYSIS PROCESSES FOR LOW AND HIGH ASH PAPER WASTE SLUDGE

Angelo J. Ridout[1], Marion Carrier[2], François-Xavier Collard[1], Johann Görgens[1]

[1]*Department of Process Engineering, University of Stellenbosch, Private Bag X1, Matieland 7602, South Africa*

[2]*Bioenergy Research Group, European Bioenergy Research Institute (EBRI), Aston University, Birmingham B47ET, United Kingdom*

ABSTRACT

Differences in the design of pyrolysis processes, as well as varying reactor temperature and pellet size, were explored in this study to evaluate the capability of vacuum, slow and fast pyrolysis to convert of low and high ash paper waste sludge (PWS) into renewable chemicals (primarily glycolaldehyde and levoglucosan) and biomaterials (sorption medium or biochar). The pyrolysis technology selection was shown to have a greater influence on chemical yields than reactor temperature and pellet size. In particular, the high heating rates employed during fast pyrolysis (FP) had the most significant impact on product formation, whereby glycosidic bond cleavage was enhanced, leading to the highest yields of levoglucosan for both PWSs. In addition to heating rate, the catalytic effect of inorganics during FP of high ash PWS also had a prevalent effect, by increasing the levoglucosan yield (3.7 daf, wt.%, 340 ^{o}C) at lower temperatures, compared to low ash PWS (1.5 daf, wt.%, 430 ^{o}C). Moreover, the production of phenols, furans and glycolaldehyde was also promoted significantly by higher ash content. The application of vacuum pyrolysis (VP) significantly enhanced the biomaterial sorption capacity (CO_2 volume adsorbed) and micropore development, leading to the highest DFT surface areas (281 to 344 $m^2.g^{-1}$) for low ash PWS. For high ash PWS, no significant differences were observed in the DFT surface areas (28 to 66 $m^2.g^{-1}$)

between pyrolysis processes possibly due to the filling of pores by inorganics and/or lower organic content.

Keywords: Paper waste sludge, pyrolysis, chemicals, biomaterial

6.1 INTRODUCTION

The large quantities of paper waste sludge (PWS) generated by the pulp and paper industry are usually disposed of by landfill, which poses a threat to the environment [1]. An alternative valorisation method, such as pyrolysis, is useful for converting any lignocellulosic material into solid, liquid and gaseous products, which have various beneficial applications (chemicals, energy, biomaterials) [1-9].

Production of green value-added marketable chemicals from pyrolysis bio-oil has gained interest with the aim to replace existing petroleum based chemicals [10,11]. These chemicals are generated during the depolymerisation and/or fragmentation of the lignocellulosic components, and are comprised of numerous oxygenated compounds such as acids, ketones, aldehydes, sugars, alcohols, phenols and furans [12]. While many of these chemicals are valuable, their concentrations in bio-oils are usually low, making their recovery technically difficult and expensive.

Thus, selective pyrolysis can be used to drive the yield and/or concentration of a target chemical product, by manipulating the pyrolysis mechanisms by applying different operating conditions (i.e., temperature, vapour residence time, heating rate) [13,14], and/or by using a catalyst [15]. The various pyrolysis processes, such as fast, slow and intermediate pyrolysis, have different operating conditions (heating rate and vapour residence time), which could be used to drive selectivity of pyrolysis reactions [10,13,14]. Fast pyrolysis (FP) utilises significantly higher heating rates (300 to 12000 $^{o}C.min^{-1}$) [16], when compared to slow pyrolysis (1 to 60 $^{o}C.min^{-1}$) [10,16,17], resulting in enhanced heat transfer and a promotion of devolatilization reactions by depolymerisation and

fragmentation [18-20], as well as limitation of char formation [10,13]. On the other hand, slow pyrolysis (SP) vapour residence times (1 min to hours) are long in comparison to FP (< 2 s) [10,16,17], resulting in greater mass transfer limitation and the promotion of secondary tar cracking reactions, catalysed by char, and/or secondary recombination reactions [12,21]. Intermediate pyrolysis (IP) operating conditions lie between those of SP and FP with moderate heating rates (10 to 300 $^{o}C.min^{-1}$) [22,23] and vapour residence times (10 to 30 s) [10]. Amongst the intermediate process, vacuum pyrolysis (VP) presents the advantage of reducing the vapour residence times (1 to 20 s) and the extent of secondary reactions [20,24].

Few studies have compared the evolution of chemicals in bio-oils between different pyrolysis processes [13,14]. Ben *et al.* [14] compared SP and FP bio-oils produced from loblolly pine woods, and found that the higher heating rate employed by FP significantly enhanced depolymerisation, prompting the production of both phenols and sugars. In another study, Greenhalf *et al.* [13] compared the chemical composition of bio-oils produced during SP and FP of willow short rotation coppice, and found a significant promotion in the production of anhydrosugars, phenols and furans under fast heating conditions. Considering the differences between SP and FP of biomass, few studies have attempted to describe pyrolysis mechanisms under an intermediate process, such as VP [24], as a means to control the chemical selectivity. Studies have shown that the addition of a catalyst can improve the selectivity of specific compounds [15]. For instance, the presence of $ZnCl_2$ has been shown to multiple the furfural yield by up to 16 times [15].

Although PWS contains large amount of inorganics (mainly $CaCO_3$) likely to influence the pyrolysis mechanisms and product distribution, studies on the potential of its bio-oil as a feedstock for chemicals productions are limited [2-4]. The study performed by Lou *et al.* [2], whereby a high ash PWS (41.5 wt.%) was slowly pyrolyzed to a temperature of 800 ^{o}C, showed a large percentage

distribution (PD) on the GC-MS chromatogram for benzene ring type chemicals such as styrene (13.5 %), benzene (6.8 %), toluene (8.8 %), ethylbenzene (13.5 %), p-xylene (35.0 %) and o-xylene (10.4 %). Yang *et al.* [4] and Ouadi *et al.* [3] subjected two high ash PWSs (62.9 and 74.5 wt.%, respectively) to intermediate pyrolysis at 450 ^{o}C. Similarly to the findings by Lou *et al.* [2], the GC-MS chromatogram had large PDs for benzene ring type chemicals such as ethylbenzene (~13-23%), toluene (~4-12%) and 1,3,5,7 cyclooctatetraene styrene (~23-28%) [3,4]. It is worthwhile to note that despite the large amount of holocellulose, between ~68.0 and 74 daf, wt.%, within the PWS reported earlier [1], mainly benzene ring type chemicals have been observed in the bio-oil. This could be attributed to extensive lignocellulosic conversion through more severe pyrolysis conditions supported by further catalytic conversion [2-4]. Thus the potential for milder conditions to produce higher value primary products from cellulose (e.g., anhydrosugars, furans, aldehydes, etc), should be considered [25,26]. The combination of both torrefaction and chemical pre-treatment of PWS have also been presented as alternatives to improve the performance of fast pyrolysis in producing anhydrosugars and furans, while reducing the formation of phenols, aldehydes and ketones [5].

In addition to chemicals production from bio-oil, the use of char as a biomaterial for application as a sorption medium or biochar, rather than a fuel, is also of interest as it has greater economic potential [27]. Moreover, given the high ash content (~50 wt.%) of the char derived from PWS pyrolysis, its application as fuel is not recommended. The elementary adsorptive characteristics of char are often defined by its surface area, pore size distribution and surface chemistry [28,29], which are affected by the type of feedstock and operating conditions employed [7,17]. Carrier *et al.* [17] showed that char produced from sugar cane bagasse during VP displayed a significantly higher BET surface area (~410 $m^2.g^{-1}$) in comparison to those of SP (~330 $m^2.g^{-1}$), due to greater devolatilization under vacuum conditions. Despite the well-known fact that high heating rates

promote volatiles production during FP [10,13], which could result in differences in pore development [30], no studies have compared the adsorptive characteristics of char generated from FP, VP and SP.

A number of studies have already pointed out the promising potential of char from SP of PWS as a biomaterial for sorption or biochar applications [6-9]. Mendez *et al.* [7] tested the adsorption capability of two chars, prepared from a low and high ash PWS under slow conditions at 650 ^{o}C, to remove Cu^{2+} from water. It was found that the high ash PWS char with a BET surface area of ~75 to 88 $m^2.g^{-1}$ was mainly mesoporous, and had the highest removal aptitude for Cu^{2+}. The authors attributed this result to the presence of highly oxygenated surface groups (high $CaCO_3$ content), elevated superficial charge density and large average pore density [7]. In another study, the removal of organics such as citalopram from wastewater using char prepared from high ash PWS (55.3 wt.%) under SP was demonstrated by Calisto *et al.* [6]. The highest citalopram adsorption capacities were achieved using chars prepared at high temperature of 800 ^{o}C [6]. Few researchers have demonstrated the potential of biochar to stabilize and reduce the mobility and bioavailability of inorganic contaminants in soils [8,9]. Mendez *et al.* [8] could off-set the detrimental consequences on soils due to the mobility, bioavailability and leaching of Ni^{2+} using biochar produced from the slow pyrolysis of high ash PWS (64.7 wt.%) at 500 ^{o}C, while chars prepared at 300 ^{o}C had little effect. Unfortunately, the authors did not provide any explanations, although only the char obtained at 500 ^{o}C displayed a higher BET surface area (22.9 $m^2.g^{-1}$) when compared to the char derived at 300 ^{o}C (7.3 $m^2.g^{-1}$); thus emphasizing the important role of temperature on char's sorption performance [8]. Martin *et al.* [9] investigated the adsorption-desorption of herbicides (diuron and artrazine) in soil amended with char prepared through slow pyrolysis of high ash PWS at 550 ^{o}C. Results indicated that soil amended with fresh char doubled the sorption of the herbicides, while

aged char (32 months) showed no significant improvement in uptake [9]. The few above-mentioned examples confirm the promising potential of PWS char as a sorption medium, whose performance could be enhanced by the application of a vacuum during char processing [17,24], which has not yet been considered.

Therefore, the aim of this work is to evaluate the capability of vacuum, slow and fast pyrolysis at various key operating conditions, to selectively drive the conversion of raw PWS into targeted chemicals (primarily glycolaldehyde and levoglucosan) and biomaterials (sorption medium or biochar) as renewable products. To do this, product yields were optimised according to the reactor temperature and pellet size using a statistical design of experiments and the chemical variability quantified using principal component analysis (PCA).

6.2 MATERIALS AND METHODS

6.2.1 Raw materials and preparation

The PWS sample with the lowest ash content of 8.5 wt.% (Table 6-1) was sourced from Kraft pulp mill (Sappi Ngodwana) and was termed low ash paper waste sludge (LAPWS). The PWS sample with the highest ash content of 46.7 wt.% (Table 6-1) was provided by the tissue paper mill Kimberly-Clark Enstra and was termed high ash paper waste sludge (HAPWS). The as-received wet PWSs were dried in an oven for 12 hours at 105 ± 2 ^{o}C, and subsequently milled using a Retsch hammer mill with a 2 mm sieve. The milled PWS was subsequently pelletized to improve the packing density in the fixed bed reactor, as well as improve fluidisation in the bubbling fluidised bed reactor. For this the milled PWS was rehydrated (PWS:Water 1:1), mechanically agitated until a homogenous mixture was obtained, and then pelletized using a Trespade No.12 meat mincer, after which the pellets were dried for 12 hours at 105 ± 2 ^{o}C. The pellet produced varied in size between 3, 4, 5 and 6 mm.

6.2.2 Physico-chemical characterisation of raw materials

The moisture content for the as-received PWS was determined in accordance with the TAPPI T264 om-88 standard procedure. Ash content (AC_{525}) was determined in accordance with the ISO 1762 standard procedure using a muffle furnace to combust the samples at 525 ± 5 ^{o}C. The lignocellulosic composition analysis of the PWS was determined in accordance with the NREL laboratory analytical method, as previously described in detail [1]. In brief, the extractives and structural carbohydrates/lignin were determined according to the NREL/TP-510-42619 and NREL/TP-510-42618 standard methods, respectively. A Varian Cary 50 Bio UV-Visible spectrophotometer was used to determine the acid soluble lignin content in the resulting hydrolysis liquor. Structural carbohydrates were determined by analysing the hydrolysis liquor via HPLC (Thermo Separation Products).

6.2.3 Pyrolysis experiments

6.2.3.1 Slow and vacuum pyrolysis

The vacuum and slow pyrolysis experiments were carried out in a unit that consists of a fixed bed (FB) reactor and condensation train previously described (Appendix A-3 to A-4) [17]. The FB reactor consists of a 1 m long, 60 mm outer diameter quartz glass tube, which is externally heated by six, well-insulated, computer-controlled elements. Each pyrolysis run used a mass of 20 g (dry weight) of paper waste sludge. During slow pyrolysis, the pyrolytic vapours were swept from the reactive zone by a N_2 (Technical grade, Afrox) at a flow rate of 1 L.min^{-1} resulting in an average residence time of 54 s. During vacuum pyrolysis, the residence time of these vapours was reduced to ~2 s by ways of a ~8 kPa_{ab} vacuum. A series of five traps varying in temperatures were used to condense vapours. For slow pyrolysis, the first was held at room temperature, and all remaining

condensers (2 to 5) were held at 0 ^{o}C (crushed ice). In the case of vacuum pyrolysis, the last two were held at -78 ^{o}C (dry ice temperature) to ensure condensation. Once the desired reactor temperature was reached, after applying a heating rate of 30 ^{o}C.min^{-1}, it was held there for a further 30 min to ensure complete devolatilization of the PWS. The sum of liquid collected in the steel pipe (residue) connecting the outlet of the reactor to the condensation train and the first condenser weight, $m_{steelpipe} + m_{condenser\text{-}1}$, makes up the total tarry phase which, was dark brown in colour. In the remaining condensers, the collected aqueous phase presented a light brown/yellow colour and contained in average ~75 wt.% water [31]. As the chemicals are recovered by means of physical and/or chemical processing of the liquid, a high concentration is beneficial for ease of isolation and is more economical [11]. Thus, for vacuum and slow pyrolysis only the tarry phase was considered, as it has a significantly higher organic content and concentration when compared to the aqueous phase.

The vacuum and slow pyrolysis chemical product yields (Y_i) were calculated after GC-MS analysis of the tarry phase (Section 6.2.4.1) on a dry ash free basis using Eq. 1 below:

$$Y_i\,(\text{daf wt.}\%) = \frac{(m_{condenser\ -1} + m_{steel\text{-}pipe}) * x_i}{m_{PWS} - m_{ash-pws} - m_{moisture}} * 100 \qquad (1)$$

where m is the mass of products in grams, x_i stands for the mass fraction of the chemical component in the tarry phase, and $m_{moisture}$ (wt.%) is the moisture contained in the PWS pellets.

6.2.3.2 Fast pyrolysis

As previously described (Appendix A-1 to A-2) [1], the fast pyrolysis experiments were carried out in a unit that consisted of four sections: feeding system (max. 1 kg.hr^{-1}), bubbling fluidised bed reactor (BFBR), char separation and liquid condensation train. Paper waste sludge pellets were

screw fed from the hopper to the BFBR at a rate of 0.5 $kg.hr^{-1}$, whereafter they were fluidised with silica sand (AFS 35 fused silica sand, CONSOL minerals). The bed was fluidised with N_2 (Technical grade, Afrox) using a fixed flow rate of 2.4 $m^3.hr^{-1}$. Upon entering the cyclone from the BFBR, the char was separated from the vapours. The vapours then entered the liquid condensation system whereby they were quenched in direct contact with an immiscible iso-paraffinic hydrocarbon (Isopar, Engen Petroleum limited) to condense the liquid fraction. Any remaining condensable compounds entered two electrostatic precipitators set at 14 kV and 12 kV to complete the condensation stage. The remaining non-condensable gas was purged to the atmosphere. The fast pyrolysis chemical product yields (Y_i) were calculated after GC-MS analysis of the bio-oil (or bulk-liquid) on a dry ash free basis using Eq. 2 below:

$$Y_i\,(\text{daf wt.}\%) = \frac{(m_{\text{bulk-liquid}} + m_{\text{residue}}) * x_i}{m_{\text{PWS}} - m_{\text{ash–pws}} - m_{\text{moisture}}} * 100 \qquad (2)$$

where $m_{\text{bulk-liquid}}$ is the liquid recovered in the reservoir as well as the bio-oil residue, determined by the difference in weight of the condensation train equipment before and after each pyrolysis run, and x_i stands for the mass fraction of the chemical component in bio-oil. The remaining residue in the reservoir (m_{residue}) as well as the $m_{\text{bulk-liquid}}$ makes up the total bio-oil mass.

6.2.4 Characterisation of pyrolysis products

6.2.4.1 Bio-oil product

The identification and quantification of condensable compounds contained in the VP and SP tarry phase and the FP bio-oil was performed with a gas chromatography-mass spectrometry (GC-MS) system using an internal calibration procedure. The internal standard solution was prepared by dissolving 0.2 g of methyl behenate (Fluka, 99.0 %) in 50 mL MeOH (Riedel-de Haenm 99.9 %).

Liquid samples were initially prepared in a volumetric flask by adding 0.06 g of FP bio-oil, or 0.06 g of VP tarry phase or 0.3 g of SP (due to higher water content) tarry phase with 400 µL of internal standard in 2000 µL of MeOH. The mixture was then filtered using a 22 µL nylon micro filter (Anatech) before injection. The GC-MS analysis was carried out using an Agilent GC/MSD 7890A/5975C (single quadrupole) with a multi-mode injector on a Zebron ZB-1701 column (60 m x 250 µm x 0.25 µm). The helium (carrier gas) was set to a flow rate of 1.3 $mL.min^{-1}$. The column-heating program was as follows: the column was initially held constant at 45 ^{o}C for 8 min, then ramped to 100 ^{o}C at 2 $^{o}C.min^{-1}$, after which it was again ramped to 260 ^{o}C at 7 $^{o}C.min^{-1}$. A number of external standards were selected based on the typical chemical products obtained from main lignocellulosic constituents (i.e. hemicelluloses, cellulose and lignin). The following chemical compounds were chosen to represent the carbohydrate fraction (cellulose and hemicelluloses): levoglucosan (99 %), 2-furanmethanol (98 %), 2(5H)-furanone (98 %), 5-hydroxymethylfurfural (99%), glycolaldehyde (98%) and 2-cyclopenten-1-one (%). The lignin-derived chemicals were classed into 2 groups: (i) primary compounds (1^{st} Lignin) supposedly produced from the monolignol block characterised by an alkyl chain with 2 or 3 carbon atoms, and (ii) the secondary compounds group (2^{nd} lignin) which are produced during degradation of primary compounds and have no alkyl chain in the para position of the hydroxyl group. The 1^{st} lignin derived chemicals included: 4-vinylguaiacol (98 %), eugenol (99 %) and apocynin (98 %). The secondary lignin compounds included: phenol (98 %), guaiacol (98 %), 2,3-dimethyl phenol (99 %) and 2,6-dimethyl phenol (99.5 %). All external standards were supplied by Sigma Aldrich. An example of a GC-MS chromatogram for the LAPWS vacuum and slow pyrolysis tarry phase, as well as the fast pyrolysis bio-oil, as shown in Appendix E-1.

6.2.4.2 Char product

The porous structure of chars was described using surface area and pore characteristics (i.e., pore volume and pore size distribution). Char samples were initially degassed using a VacPrep 061 system at 90 °C for 1 hour, followed by a second overnight degassing step at 250 °C. Once degassed, chars were introduced in a Micrometrics ASAP 2010 system.

The nonselective physical adsorption of appropriate adsorbent is generally determined using N_2 at liquid nitrogen temperature (-196 °C). Despite the pre-degassing stage, the determination of surface area was long and sometimes could not be completed, which was attributed to the highly microporous (pore width < 1 nm) character of the studied chars. An alternative gas, CO_2, was used to run the volumetric adsorption measurement at 0 °C. Indeed, CO_2 is well-known as being better suited to describe highly microporous materials [32,33], as it is has a greater rate of diffusion due to higher adsorption temperature [32].

To display the adsorption profile, the selection of a model is required. In the case of N_2 adsorption measurement, the Brunauer, Emmet and Tellet (BET) equation based on an infinite number of layers model is used (Eq. 3) [34]. A common way to explore the CO_2 data is by using the density function theory method (DFT) (Eq. 4), which offers an algorithm that is better suited for microporous materials [33,35].

$$\frac{p/p_o}{n(1-p/p_o)} = \frac{1}{n_m c} + \frac{c-1}{n_m c}\frac{p}{p_o} \qquad (3)$$

where p_o is the vapour saturation pressure (mmHg), p/p_o is the relative gas pressure, n is the quantity of gas adsorbed ($cm^3.g^{-1}$), n_m is the quantity of monolayer gas adsorbed ($cm^3.g^{-1}$), and c is the BET dimensionless constant.

$$N(P) = \int_{W_{min}}^{W_{max}} f(w)\ \rho(P, w)\ dw \qquad (4)$$

where N(P) is quantity of gas adsorbed (mol) at pressure P (mmHg), w_{min} and w_{max} are the widths (Å) of the smallest and largest pores, ρ(P,w) is the density (mol.cm^{-3}) of the gas at pressure P (mmHg) and pore width w(Å), and f(w) is the distribution of pore volumes (cm^3.Å^{-1}).

6.2.5 Statistical analysis

6.2.5.1 Design of experiments

The optimal conditions (reactor temperature and pellet size) were determined for chemical compounds that displayed the highest yields (> 1 daf, wt.%). To do this, a three level two factor full factorial statistical design was implemented. The reactor temperature was selected as it has a large influence on the pyrolysis reactions [15,36]. The temperature levels were 340, 460 and 580 ^{o}C for SP, and 300, 425 and 550^{o}C for VP. The FP temperature levels were 300, 425 and 550 ^{o}C for LAPWS and 290, 340 and 390 ^{o}C for HAPWS [1,31]. Particle size is known to influence heat and mass transport effects during pyrolysis [21]. Although this phenomenon is typically stated for "single particle models", it is plausible to assume that a pellet, in the form of an "agglomerate of particles", has similar pyrolytic behaviour [37,38]. Therefore pellet size was considered as a single particle as a preliminary approach. Pellet sizes in the range of 2.92 ± 0.12, 4.04 ± 0.18 and 4.84 ± 0.15 mm were used.

The ANOVA analysis was carried using the parametric data analysis function 'regression' in Microsoft Excel (2010, ver. 14.0.7128.5000, SP2) whereby a 2-way linear and quadratic model was fitted (Eq. 5). Both the coefficient of determination (R^2) and the adjusted coefficient of determination (R^2_{adj}) were used to get the best model fit, at the same time ensuring that no heteroscedasticity was observed in the normality, constant variance and independence assumptions [39]. A 90% confidence interval was used, whereby a p-value of less than 0.1 indicated a significant

effect of the factors on the responses. Three repeated runs were performed to determine the experimental error. Equation 5 below represents the 2-way linear and quadratic model used:

$$Y_{product}\ (wt.\%) = intercept + \beta_1 * RT + \beta_2 * PS + \beta_3 * RT^2 + \beta_4 * PS^2 + \beta_5 * RT * PS + \beta_6 * RT^2 * PS + \beta_7 * PS^2 * RT + \beta_8 * RT^2 * PS^2 \quad (5)$$

where $Y_{product}$ is the pyrolysis product yield, β_{n+1} is the model coefficient, RT is the reactor temperature (^oC) and PS is the pellet size (mm).

6.2.5.2 Principal component analysis (PCA)

Principal component analysis (PCA) was used to investigate the variability in chemical yields (active variables) between vacuum, slow and fast pyrolysis of LAPWS and HAPWS using Statistica software (ver. 12.6.255.0). A number of studies have utilised PCA to evaluate large datasets making it possible for variations to be better visualised [40,41]. PCA reduces the dimensionality of larger data sets to new smaller sets, the principal components (PCs), keeping the trends of the original data. The software generates score and correlation loading plots, which are used to chemometrically analyse the similarities and dissimilarities in the data [42].

6.3 RESULTS AND DISCUSSION

In the work prior to this study [31], reactor temperature and pellet size were optimised to maximise the solid and liquid product yields during vacuum, slow and fast pyrolysis of low and high ash PWS. Application of low temperatures during slow pyrolysis were shown to maximise the yield of char, while on the other hand vacuum pyrolysis minimised the char yield. Fast pyrolysis displayed a higher production of condensable organic compounds and lower water yields [31]. While the previous work focussed on the distribution of liquid and solid products as energy sources, the present study focuses on their potential quality for chemical and biomaterial production.

6.3.1 Chemical selectivity during pyrolysis

6.3.1.1 LAPWS

The results of the linear combination of the low ash PWS vacuum, slow and fast pyroylsis chemical yields (Appendix E-2 to E-3) are presented for the first two principal components (PCs) with a description of their score and of the correlation loadings plots (Figure 6-1). It can be observed that the SP, VP and FP scores are grouped into three distinct clusters (Figure 6-1a), indicating that their yields of chemicals are statistically different. The variances explained by PC1 and PC2 were 58.80 and 28.04 %, respectively. On PC1, the FP cluster position was mostly negative while the SP cluster position was positive, highlighting the difference between these two technologies (Figure 6-1a). The VP cluster had an intermediate position on PC1 displaying its intermediate trait, but was distinguished from SP and FP by its positive position on PC2.

The correlation loading plots illustrated the relationships between the yields of chemicals, generated by the various pyrolysis processes, and PC1 and PC2 (Figure 6-1b). For convenience of analysis the lignin-derived compounds were grouped into primary (1st lignin, with an alkyl chain containing 2 or 3 carbon atoms) and secondary (2nd lignin) products. Comparison of the position of FP cluster on the scores plot (Figure 6-1a) to that of the chemicals on the correlation loadings plot (Figure 6-1b), indicated that FP promoted the production of carbohydrate derived compounds such as levoglucosan, 2(5H)-furanone and 5-hydroxymethylfurfural. During primary pyrolysis of cellulose, higher heating rates are known to enhance the cleavage of glycosidic bonds promoting the production of levoglucosan [13,43], which is likely to be further converted to more stable furan compounds by ring contractions [12]. While a vacuum is expected to limit levoglucosan conversion, due to the fast removal of volatiles, VP did not give higher levoglucosan yields than FP due to the slow heating rate that limits the rate of glycosidic bond cleavage [18]. Production of primary lignin

compounds were promoted during VP, whereas secondary lignin compounds were promoted during FP (Figure 6-1). This observation could be due to the fast removal of volatiles during VP before the reactor temperature reaches the specified temperature, thus limiting secondary cracking of side chains (alkyl chain) from primary lignin compounds [20]. Vacuum pyrolysis also promoted the formation of 2-furanmethanol (Figure 6-1), possibly due to the application of lower heating rates as suggested by Greenhalf *et al.* [13] and short residence times. According to the position of the SP cluster only 2-cyclopenten-1-one production was promoted (Figure 6-1). Indeed, low heating rates are known to enhance the production of these types of compounds [13].

In order to visualise their influence on the chemical yields, the pellet size (PS) and reactor temperature (RT) were plotted as supplementary variables (not used in the statistical analysis). The fact that the RT and PS position is close to the centre confirmed that the pyrolysis process selection had greater influence on the chemical yields than these two factors (Figure 6-1b). Reactor temperature and the yields of most chemicals were inversely correlated (Figure 6-1b), certainly due to an increase of thermal cracking reactions of primary and secondary compounds at higher temperatures [13,43].

6.3.1.2 HAPWS

Figure 6-2 presents the high ash PWS PCA score and correlation loadings plots for the slow, vacuum and fast pyrolysis chemical yields. Distinct clusters are observed between the pyrolysis processes for the conversion of HAPWS, indicating that there are statistically significant differences in the yields of chemicals (Figure 6-2a). The variances explained by PC1 and PC2 were 49.80 and 32.00 %, respectively. The FP cluster was distinguished from the VP and SP clusters by its negative position on PC1 (Figure 6-2a). The SP and VP clusters were separated by respectively negative and

positive positions on PC2, while the FP cluster overlapped with both of them. Unlike the closely grouped SP and VP clusters, FP clusters were fairly dispersed suggesting that there are significant differences in the yields of chemicals between the bio-oils produced by FP (Figure 6-2a).

Comparison of the FP cluster to that of the yields of chemicals on the correlation loadings plots (Figure 6-2) indicated that FP promoted the production most of the chemical compounds, except cyclopenten-1-one which was promoted by SP. As previously discussed this significant promotion of chemicals production during FP can be attributed to the application of higher heating rates [13,43], but also the catalytic effect of inorganics enhancing primary and secondary reactions [18,44]. This latter is obvious when comparing the PCA scores and correlation plots between LAPWS and HAPWS (Figures 6-1 and 6-2), whereby the role of ash on the pyrolysis reactions becomes evident. The location of the VP cluster indicated no specific compound was promoted by VP relative to FP and SP (Figure 6-2). The RT and PS positions were close to the centre, again indicating that the pyrolysis process selection had a greater influence on the yields of chemicals (Figure 6-2b). The RT was inversely correlated with levoglucosan, 2-furanmethanol and 1st lignin, certainly due to the extensive cracking of such compounds at high temperatures [13,43].

6.3.2 Chemicals production

6.3.2.1 Levoglucosan

Of the quantified compounds, levoglucosan displayed the highest yield (~0.3 to 3.7 daf, wt.%, Appendix E-2 to E-4) and concentration (~1.2 to 7.8 wt.%, Appendix E-5 to E-7) for both PWSs. Multiple potential markets have been found for levoglucosan such as in production of surfactants, pharmaceuticals and biodegradable polymers [45]. Models and surface plots for the yield of levoglucosan are respectively presented by Table 6-2 and Figure 6-3. Both the reactor temperature

and pellet size were shown to significantly affect the levoglucosan yield for FP and VP, while for SP only the reactor temperature had an effect (Table 6-2). For SP of HAPWS, the significance of the linear interaction term (β_5) indicated that pellet size still plays a significant role.

An initial increase in the reactor temperature promoted the levoglucosan yield, while further RT increases subsequently decreased the yield, due to promotion of secondary reactions, for all pyrolysis conversion of LAPWS and for FP of HAPWS (Figure 6-3), which is similar to previous findings [13]. During FP of HAPWS, an increase in pellet size significantly promoted the levoglucosan yield (Figure 6-3b). This observation could be the result of an increase in the number of exothermic secondary reactions [1], due to limited mass transfer [37], leading to enhanced heating rates and subsequent promotions in depolymerisation reactions [13,14]. When comparing the yield of levoglucosan between the pyrolysis processes (Figure 6-3), it is not surprising that FP offered the highest yields at 1.5 daf, wt.% (430 ^{o}C, 5 mm) for LAPWS, and at 3.7 daf, wt.% (340 ^{o}C, 5 mm) for HAPWS, in accordance with the PCA (Figures 6-1 and 6-2). The optimum temperature to maximise the levoglucosan yields under FP was lowered from 430 ^{o}C to 340 ^{o}C by an increase in the PWS ash content from LAPWS to HAPWS. This confirmed the key catalytic role of inorganics such as $CaCO_3$ on the promotion of primary pyrolysis reactions [18,44]. Furthermore, higher levoglucosan yields were attained for HAPWS when compared to LAPWS, indicating that glycosidic bond cleavage was promoted in the presence of the inorganic catalysts [18]. The opposite trend was observed at temperatures above 400 ^{o}C, due to the cracking of levoglucosan catalysed at the surface of the inorganics.

Compared to the typical levoglucosan yields found in literature, the ones attained during FP of PWS were moderate to high (~1.5 to 3.7 daf, wt.%): 0.7 daf, wt.% during FP (fluidised bed) of willow SRC [13]; 3.5 to 4 wt.% during FP (Py-GC-MS) of switchgrass [46]; 0.5 (unwashed) and

2.0 (washed) daf, wt.% during FP (fixed bed) of beech wood [47], 0.8 wt.% during FP (fixed bed) of beechwood [48]. In addition, the FP levoglucosan concentrations (~2.8 to 7.8 wt.%, Appendix E-7) were also moderate to high in comparison to literature: 0.14 and 6.4 wt.% during FP (fluidised bed) of alfalfa-early bud and switchgrass, respectively [49]; ~2.6 wt.% during FP (fluidised bed) of willow and switchgrass [50]; 8.2 and 21.6 wt.% during FP (auger) of pine and oak wood, respectively [51]. Indeed, these promising levoglucosan yields and concentrations, observed in the present study, could be attributed to the large cellulose content found in the PWSs (~50 to 60 daf, wt.%, Table 6-1). Levoglucosan has potential for use in the production of surfactants, pharmaceuticals and biodegradable polymers [45], and can be isolated at a high purity using liquid-liquid extraction followed by solvent crystallisation (patent) [52].

6.3.2.2 Glycolaldehyde

Glycolaldehyde is a common product of polysaccharides pyrolysis and fragmentation of levoglucosan during secondary reactions [19,43], and is typically utilised in the food industry for meat-browning [45]. This compound displayed the second highest yield (~0.1 to 1.2 daf, wt.%, Appendix E-2 to E-4) as well as concentration (~0.1 to 6.3 wt.%, Appendix E-5 to E-7) for both PWSs. The surface plots and statistical models for the glycolaldehyde yield are respectively presented by Figure 6-4 and Table 6-3. The statistical models indicated that both reactor temperature and pellet size affected the glycolaldehyde yields for all types of pyrolysis, except those of FP and VP of LAPWS, which were only affected by reactor temperature, and SP of HAPWS, which was only affected by pellet size (Table 6-3).

While an increase in temperature is expected to promote the glycolaldehyde yield, due to secondary cracking of levoglucosan [18], decreases were also observed (Figure 6-4). This

observation could be attributed to severe secondary cracking reactions converting the already formed glycolaldehyde into other products, which is similar to previous findings [36]. Larger pellet sizes promoted the glycolaldehyde yield in all cases (Figure 6-4), except SP of LAPWS and VP of HAPWS, likely due enhanced secondary cracking of levoglucosan by mass transfer limitations [18]. Comparison of the LAPWS glycolaldehyde yields among the pyrolysis processes (Figure 6-4) indicated that both FP and VP offered the highest yield at ~1.2 daf, wt.% (300 ^{o}C, 3-5 mm). While for HAPWS, FP displayed the highest yield at 0.7 daf, wt.% (340 ^{o}C, 5 mm). These glycolaldehyde yields were found to be moderate when in comparison to literature: 0.7 (unwashed) and 0.8 (washed) daf, wt.% during FP (fixed bed) of beech wood [47]; 2.30 wt.% during FP (fixed bed) of beechwood [48]. Of the three pyrolysis processes, VP displayed the highest glycolaldehyde concentrations at ~6.3 wt.% for LAPWS, and 3.5 wt.% for HAPWS, which were low in comparison to literature: 2.46 wt.% during FP (fluidised bed) of switchgrass [49]; 16 and 36 wt.% during FP (fluidised bed) of willow and switchgrass, respectively [51]. Glycolaldehyde has potential for use in the food industry as a meat browning agent or in food flavouring [45], and can be isolated to a high purity using distillation followed by liquid-liquid extraction (patent) [53].

6.3.3 Biomaterial production from PWS

The use of char as a biomaterial for sorption or biochar application has been shown to offer greater economic potential than its use in energy applications [27]. Biomaterials have a wide range of applications such as in pollutant removal, soil remediation, gas storage, catalysis and gas separation to name a few [33]. Often the efficacy of their application in such areas is based on criteria such as surface area, pore size distribution and surface chemistry [28,29].

The carbon dioxide adsorption isotherms and pore size distribution plots of the char derived during vacuum, slow and fast pyrolysis of LAPWS and HAPWS are presented in Figure 6-5. Isotherms (Figure 6-5a,c) of type I indicated that PWS-derived chars adsorbed significant volumes of CO_2 in the lower relative pressure regions ($P/P_o < 0.005$), which is characteristic of microporous materials [33]. The pore size distributions shown in Figure 6-5b and 6-5d confirmed the ultra-microporous nature of the produced chars, with pore widths of 0.55 to 0.85 nm, which is similar to previous findings for PWS [6,7]. Microporous biomaterials have promising applications such as in gas separation (carbon molecular sieves) [54] and pollutant removal from water treatment through sorption [6,7]. The effect of reactor temperature on the CO_2 volume adsorbed is important (Figure 6-5): Higher temperatures of pyrolysis conversion resulted in greater CO_2 volume adsorbed and greater micropore development, leading to higher DFT surfaces for both PWSs (Figure 6-6), which is similar to other findings for PWS char [6,8]. No significant differences were observed in the char CO_2 adsorption isotherms, pore size distribution and DFT surface area for varying PWS pellet sizes.

When comparing the trend of DFT isotherms of LAPWS-derived chars obtained between the pyrolysis processes, VP-derived chars exhibit the highest DFT surface areas (281 to 344 $m^2.g^{-1}$), followed by SP (200 to 309 $m^2.g^{-1}$) then FP (157 to 236 $m^2.g^{-1}$) (Figure 6-6a). These results are in accordance with the study performed by Carrier *et al.* [17] whereby VP chars, derived from sugar cane bagasse, were shown to offer higher BET surface areas when compared to SP chars. This result was attributed to a promotion in devolatilization under vacuum conditions. Similarly in our previous work, VP was shown to enhance devolatilization [31]. The higher char DFT surface areas obtained during SP, when compared to FP (Figure 6-6a), could be attributed to the increasing pressure within the pores, due to increasing formation of volatiles when primary volatiles are degraded into secondary volatiles, thereby enhancing the microporosity [30]. On the other hand,

HAPWS-derived chars displayed much lower CO_2 adsorbed volume (Figure 6-5) and consequently lower DFT surface areas (28-66 $m^2.g^{-1}$ independently of process type) (Figure 6-6). This result is in line with the previous works whose authors attributed the decrease in surface areas to the filling of pores with inorganics [55], most likely with calcium carbonate [56], but could also be due to the lower organic content [7]. Contrary to LAPWS-derived chars, the DFT surface are of HAPWS-derived chars (Figure 6-6b) and distribution of pore width (Figure 6-5b,d) were not affected by the selection of pyrolysis type.

6.4 CONCLUSION

Three pyrolysis technologies were assessed for their ability to selectively drive the conversion of low and high PWS into chemicals and biomaterials, by varying the key operating conditions, reactor temperature and pellet sizes. The PCA indicated that the type of pyrolysis categorized by their heating rate, pressure and vapour residence time had a greater influence on the yields of chemicals than reactor temperature and pellet size. In particular, the heating rate had the most significant effect on the chemical yields, whereby FP enhanced glycosidic bond cleavage resulting in the highest levoglucosan yields for both PWSs. Moreover, the large amount of inorganics present in the HAPWS catalysed depolymerisation and/or fragmentation reactions during FP, leading to enhanced production of phenols, glycolaldehyde and furans. Not only did FP of HAPWS display the highest levoglucosan yield (3.7 daf, wt.%, 340 ^oC) when compared to LAPWS (1.5 daf, wt.%, 430 ^oC), its optimum temperature was also lower, highlighting the significant effect of inorganic catalysts on glycosidic bond cleavage reactions. Unlike glycolaldehyde, levoglucosan yields and concentrations were moderate to high when compared to literature, thus making it a promising target when considering chemicals production from PWS.

Higher pyrolysis temperatures resulted in chars with enhanced CO_2 volume adsorbed and micropore development, leading to higher DFT surfaces for both PWSs. For LAPWS, enhanced devolatilization during VP produced biomaterials that displayed the highest DFT surface areas (281 to 344 $m^2.g^{-1}$), when compared to SP (200 to 309 $m^2.g^{-1}$) and FP (157 to 236 $m^2.g^{-1}$). No significant differences were observed in the HAPWS biomaterial DFT surface areas (28 to 66 $m^2.g^{-1}$ independently of process type) among pyrolysis processes, nevertheless values were lower than those obtained by LAPWS due to the filling of pores by inorganics and/or lower organic content.

Acknowledgments

This work was financially supported by Kimberly-Clark SA, the Paper Manufacturers Association of South Africa (PAMSA) and FP&M Seta. The authors would like to thank these organisations for their financial support.

6.5 REFERENCES

[1] A.J. Ridout, M. Carrier, J. Gorgens, Fast pyrolysis of low and high ash paper waste sludge: Influence of reactor temperature and pellets size, Journal of Analytical and Applied Pyrolysis 111 (2015) 64-75.

[2] R. Lou, S. Wu, G. Lv, Q. Yang, Energy and resource utilization of deinking sludge, Applied Energy 90 (2012) 46-50.

[3] M. Ouadi, J.G. Brammer, Y. Yang, A. Hornung, M. Kay, The intermediate pyrolysis of deinking sludge to produce a sustainable liquid fuel, Journal of Analytical and Applied Pyrolysis 105 (2013) 135-142.

[4] Y. Yang, J.G. Brammer, M. Ouadi, J. Samanya, A. Hornung, H.M. Xu, Y. Li, Characterisation of waste derived intermediate pyrolysis oils for use as diesel engine fuels, Fuel 103 (2013) 247-257.

[5] J.M. Reckamp, R.A. Garrido, J.A. Satrio, Selective pyrolysis of paper mill sludge by using pretreatment processes to enhance the quality of bio-oil and biochar products, Biomass and Bioenergy 71 (2014) 235-244.

[6] V. Calisto, C.I.A. Ferreira, S.M. Santos, M.V. Gil, M. Otera, V.I. Esteves, Production of adsorbents by pyrolysis of paper mill sludge and application on the removal of citalopram from water, Bioresource Technology 166 (2014) 335-344.

[7] A. Mendez, S. Barriga, J.M. Fidalgo, G. Gasco, Adsorbent materials from paper industry waste materials and their use in Cu(II) removal from water, Journal of Hazadous Materials 165 (2009) 736-743.

[8] A. Mendez, J. Paz-Ferreiro, F. Araujo, G. Gasco, Biochar from pyrolysis of deinking paper sludge and its use in the treatment of a nickel polluted soil, Journal of Analytical and Applied Pyrolysis 107 (2014) 46-52.

[9] S.M. Martin, R.S. Kookana, L. van Zwieten, E. Krull, Marked changes in herbicide sorption-desorption upon ageing of biochars in soil, Journal of Hazardous Materials 231-232 (2012) 70-78.

[10] A.V. Bridgwater, Review of fast pyrolysis of biomass and product upgrading, Biomass and Bioenergy 38 (2012) 68-94.

[11] A.V. Bridgwater, Production of high grade fuels and chemicals from catalytic pyrolysis of biomass, Catalysis Today 29 (1996) 285-295.

[12] F. Collard, J. Blin, A review on pyrolysis of biomass constituents: Mechanisms and composition of the products obtained from the conversion of cellulose, hemicellulose and lignin, Renewable and Sustainable Energy Reviews 38 (2014) 594-608.

[13] C.E. Greenhalf, D.J. Nowakowski, A.B. Harms, J.O. Titiloye, A.V. Bridgwater, Sequential pyrolysis of willow SRC at low and high heating rates – Implications for selective pyrolysis, Fuel 93 (2012) 692-702.

[14] H. Ben, A.J. Ragauskas, Comparison for the compositions of fast and slow pyrolysis oils by NMR characterization, Bioresource Technology 147 (2013) 577-584.

[15] Q. Lu, Z. Wang, C. Dong, Z. Zhang, Y. Zhang, Y. Yang, X. Zhu, Selective fast pyrolysis of biomass impregnated with $ZnCl_2$: Furfural production together with acetic acid and activated carbon as by-products, Journal of Analytical and Applied Pyroylsis 91 (2011) 273-279.

[16] M .Basat, M. Balat, E. Kirtay, H. Balat, Main routes for the thermo-conversion of biomass into fuels and chemicals. Part 1: Pyrolysis systems, Energy conversion and Management 50 (2009) 3147-3157.

[17] M. Carrier, T. Hugo, J. Gorgens, H. Knoetze, Comparison of slow and vacuum pyrolysis of sugar cane bagasse, Journal of Analytical and Applied Pyrolysis 90 (2011) 18-26.

[18] V. Mamleev, S. Bourbigot, M. Le Bras, J. Yvon, The facts and hypotheses relating to the phenomenological model of cellulose pyrolysis: Interdependence of steps, Journal of Analytical and Applied Pyrolysis 84 (2009) 1-17.

[19] P.R. Patwardhan, R.C. Brown, B.H. Shanks, Product distribution from the fast pyrolysis of hemicellulose, ChemSusChem 4 (2011) 636-643.

[20] M. Asmadi, H. Kawamoto, S. Saka, Gas- and solid/liquid-phase reactions during pyrolysis of softwood and hardwood lignins, Journal of Analytical and Applied Pyrolysis 92 (2011) 417-425.

[21] M. Van de Velden, J. Baeyens, A. Brems, B. Janssens, R. Dewil, Fundamentals, kinetics and endothermicity of the biomass pyrolysis reactions, Renewable Energy 25 (2010) 232-242.

[22] L. Rossendahl, Biomass combustion science, technology and engineering, Elsevier Denmark, (2013) 172-173.

[23] F. Tinwala, P. Mohanty, S. Parmar, A. Patel, K.K. Pant, Intermediate pyrolysis of agro-industrial biomasses in bench-scale pyrolyser: Product yields and its characterization, Bioresource Technology 188 (2015) 258-264.

[24] M. Amutio, G. Lopez, R. Aguado, M. Artetxe, J. Bilbao, M. Olazar, Effect of vaccum on lignocellulosic biomass flash pyrolysis in a conical spouted bed reactor, Energy and Fuels 25 (2011) 3950-3960.

[25] T. Werpy, G. Petersen, Top value added chemicals from biomass: Volume 1 – Results of screening for potential candidates from sugars and synthesis gas, U.S. Department of Energy, Oak Ridge, 2004.

[26] R.A. Sheldon, Green and sustainable manufacture of chemicals from biomass: state of the art, Green Chemistry 16 (2014) 950-963.

[27] W. Liu, F. Zheng, H. Jiang, X. Zhang, Preparation of high adsorption capacity bio-chars from waste biomass, Bioresource Technology 102 (2011) 8247-8252.

[28] X. Xu, J.M. Anderson, C. Song, B.G. Miller, A.W. Scaroni, Novel polyethyleneimine-model mesoporous molecular sieve for MCM-41 type as adsorbent for CO_2 capture, Energy Fuels 16 (2002) 1463-1469.

[29] M.J. Ayotamuno, R.B Kogbara, S.O.T. Ogajib, S.D. Probert, Petroleum contaminated ground-water: Remediation using activated carbon, Applied Energy 83 (2006) 1258-1264.

[30] K. Raveendran, A. Ganesh, Adsorption characteritics and pore-development of biomass-pyrolysis char, Fuel 97 (1998) 769-781.

[31] A.J. Ridout, M. Carrier, F.X. Collard, J. Gorgens, Energy conversion assessment of vacuum, slow and fast pyrolysis processes for low and high ash paper waste sludge, Energy Conversion and Management 111 (2016) 103-114.

[32] D. Lozano-Castello, D. Cazorla-Amoros, A. Linares-Solano, Usefulness of CO_2 adsoprtion at 273 K for the characterization of porous carbons, Carbon 42 (2004) 1231-1236.

[33] J. Landers, G.Y. Gor, A.V. Neimark, Density functional theory methods for characterization of porous materials, Colloids and Surfaces A: Physicochemical and Engineering Aspects 437 (2013) 3-32.

[34] B.C. Lippens, J.H. De Boer, Studies on pore systems in catalysts, Journal of Catalysis 4 (1965) 319-323.

[35] N.A. Seaton, J.P.R.B Walton, N. Quirke, A new analysis method for the determination of the pore size distribution of porous carbons from nitrogen adsorption measurements, Carbon 27 (1989) 853-861.

[36] D. Mourant, C. Lievens, R. Gunawan, Y. Wang, X. Hu, L. Wu, S.S.A. Syed-Hassan, C. Li, Effects of temperature on the yields and properties of bio-oil from fast pyrolysis of mallee bark, Fuel 108 (2013) 400-408.

[37] R. Reschmeier, D. Roveda, D. Muller, J. Karl, Pyrolysis kinetics of wood pellets in fluidized beds, Journal opf Analytical and Applied Pyrolysis 108 (2014) 117-129.

[38] M. Jeguirim, L. Limousy, P. Dutournie, Pyrolysis kinetics and physicochemical properties of agropellets produced from spent ground coffee blended with conventional biomass, Chemical Engineering Research and Design 92 (2014) 1876-1882.

[39] D.C. Montgomery, Design and analysis of experiments, U.S.A: John Wiley & Sons (2001) 363-422.

[40] A.M. Azeez, D. Meier, J. Odermaat, Temperature dependence of fast pyrolysis volatile products from European and African biomasses, Journal of Analytical and Applied Pyrolysis 90 (2011) 81-92.

[41] A. Pattiya, J.O. Titiloye, A.V. Bridgwater, Evaluation of catalytic pyroyiss of cassava rhizome by principal component analysis, Fuel 89 (2010) 244-253.

[42] R. Wehrens, Chemometrics with R: Multivariate data ananlysis in the natural sciences and life sciences, Berlin: Springer Science & Business Media (2011) 43-66.

[43] D.K. Shen, S. Gu, The mechanism for thermal decomposition of cellulose and its main products, Bioresource Technology 100 (2009) 6496-6504.

[44] P.R. Patwardhan, J.A. Satrio, R.C. Brown, B.H. Shanks, Influence of inorganic salts on the primary pyrolysis procuts of cellulose, Bioresource Technology 101 (2010) 4646-4655.

[45] S. Czernik, A.V. Bridgwater, Overview of applications of biomass fast pyrolysis oil. Energy & Fuels 18 (2004) 590-598.

[46] M.J. Serapiglia, C.A. Mullen, A.A. Boateng, L.M. Cortese, S.A. Bonos, L. Hoffman, Evaluation of the impact of compositional differences in switchgrass genotypes on pyrolysis product yield, Industrial Crops and Products 74 (2015) 957-968.

[47] F. Collard, J. Blin, A. Bensakhria, J. Valette, Influence of impreganated metal on the pyrolysis conversion of biomas constituents, Journal of Analytical and Applied Pyrolysis 95 (2012) 213-226.

[48] C. Branca, P. Giudicianni, C. Di Blasi, GC-MS characterization of liquids generated from low temperature pyrolysis of wood, Industrial & Engineering Chemistry Research 42 (2003) 3190-3202.

[49] C.A. Mullen, A. Boateng, Chemical composition of bio-oils produced by fast pyrolysis of two energy crops, Energy and Fuels 22 (2008) 2104-2109.

[50] R. Fahmi, A.V. Bridgwater, I. Donnison, N. Yates, J.M. Jones, The effect of lignin and inorganic species in biomass on pyrolysis oil yields, quality and stability, Fuel 87 (2008) 1230-1240.

[51] L. Ingram, D. Mohan, M. Bricka, P. Steele, D. Strobel, D. Crocker, B. Mitchell, J. Mohammad, K. Cantrell, C.U. Pittman, Pyrolysis of wood and bark in an auger reactor: physical proterties and chemical analysis of produced bio-oils, Energy and Fuels 22 (2008) 614-625.

[52] L. Moens, Isolation of levoglucosan from pyrolysis oil derived from cellulose, U.S patent number W09405704, 1994.

[53] J.A. Stradal, G.L. Udnerwood, Process for producing hydroxyacetaldehyde, U.S patent number US5252188, 1995.

[54] O.N. Baklanova, G.V. Plaksin, V.A. Drozdov, V.K. Duplyakin, N.V. Chesnokov, B.N. Kuznetsov, Preparation of microporous sorbents from cedar nutshells and hydrolytic lignin, Carbon 41 (2003) 1793-1800.

[55] M. Carrier, H.W. Neomagus, J. Gorgens, J.H. Knoetze, Influence of chemical pretreatments on the internal structure and reactivity of pyrolysis char produced from sugar can bagasse, Energy & Fuels 26 (2012) 4497-4506.

[56] P. Girods, A. Dufour, V. Fierro, Y. Rogaume, C. Rogaume, A. Zoulalian, A. Celzard, Activated carbons prepared from wood particleboard wastes: Charactreisation and phenol adsorption capacities, Journal of Hazardous Materials 166 (2009) 491-501.

Table 6-1. Physico-chemical characterisation of the LAPWS and HAPWS (modified from Ridout *et al.* [11])

	LAPWS	HAPWS
Moisture content after drying (wt. %)	80.9	54.6
Ash Content (525 ^{o}C)	8.5	46.7
Lignocellulosic Composition (daf, wt.%)		
Extractives	6.3	10.5
Cellulose	58.7	49.5
Hemicelluloses	15.3	19.0
Lignin	20.1	20.5

Table 6-2. Statistical models fitted for levoglucosan yields obtained from slow, vacuum and fast pyrolysis conversion of LAPWS and HAPWS

		Model									Statistics				
		Int.	**β_1**	**β_2**	**β_3**	**β_4**	**β_5**	**β_6**	**β_7**	**β_8**	**R^2 (%)**	**R^2_{adj} (%)**	**P_{RT}**	**P_{PS}**	**Exp. E**
LA	SP	-1.82	0.010	-	$-1.7*10^{-5}$	-	-	$3.3*10^{-6}$	-	$-4.2*10^{-7}$	88.2	78.6	0.00	-	0.08
	VP	-5.06	0.020	0.96	-	-	-	$-1.3*10^{-5}$	$-6.7*10^{-4}$	$2.4*10^{-6}$	97.8	95.2	0.02	0.03	0.09
	FP	3.09	$-4.4*10^{-3}$	-1.34	-	-	$5.5*10^{-3}$	$-5.4*10^{-6}$	-	-	93.4	88.2	0.02	0.00	0.11
HA	SP	0.49	$5.0*10^{-3}$	0.15	-	-	$-2.7*10^{-3}$	-	$3.3*10^{-4}$	-	85.8	74.4	0.05	0.27	0.65
	VP	-10.1	0.020	5.87	-	-0.76	-0.010	-	$1.3*10^{-3}$	-	94.3	87.2	0.04	0.02	0.22
	FP	139	-0.753	-46.0	$1.1*10^{-3}$	0.84	0.237	$-3.5*10^{-4}$	-	-	99.7	99.0	0.00	0.00	0.36

Int: intercept; βn+1: model coefficients; R^2: coefficient of determination; R^2_{adj}: adjusted coefficient of determination; P_{RT}: p-value for reactor temperature; P_{PS}:p-value for pellet size; Exp. E: experimental error.

Table 6-3. Statistical models fitted for glycolaldehyde yields obtained from slow, vacuum and fast pyrolysis conversion of LAPWS and HAPWS

		Model									Statistics				
		Int.	**β_1**	**β_2**	**β_3**	**β_4**	**β_5**	**β_6**	**β_7**	**β_8**	**R^2 (%)**	**R^2_{adj} (%)**	**P_{RT}**	**P_{PS}**	**Exp. E**
LA	SP	0.57	$-7.4*10^{-3}$	-1.11	-	-	$8.9*10^{-3}$	$-5.1*10^{-6}$	$-5.39*10^{-4}$	-	96.2	91.5	0.01	0.01	0.28
	VP	2.51	$-9.3*10^{-3}$	-	$1.3*10^{-5}$	0.048	-	-	$-1.2*10^{-4}$	-	88.2	76.4	0.03	-	0.16
	FP	3.51	$-7.3*10^{-3}$	-0.43	-	-	$1.3*10^{-3}$	-	-	-	81.5	73.6	0.02	0.15	0.34
HA	SP	0.17	$4.5*10^{-4}$	0.25	-	-	$-8.4*10^{-4}$	$7.7*10^{-7}$	-	-	87.5	75.0	0.30	0.02	0.41
	VP	1.76	$-1.2*10^{-2}$	-1.50	-	0.173	$1.1*10^{-2}$	$-6.2*10^{-6}$	$-1.5*10^{-3}$	$9.0*10^{-7}$	99.9	99.9	0.03	0.05	0.15
	FP	9.08	$-7.8*10^{-3}$	-3.27	-	-	-	-	$2.2*10^{-3}$	$-2.7*10^{-6}$	80.7	65.3	0.09	0.02	0.19

Int: intercept; βn+1: model coefficients; R^2: coefficient of determination; R^2_{adj}: adjusted coefficient of determination; P_{RT}: p-value for reactor temperature; P_{PS}:p-value for pellet size; Exp. E: experimental error.

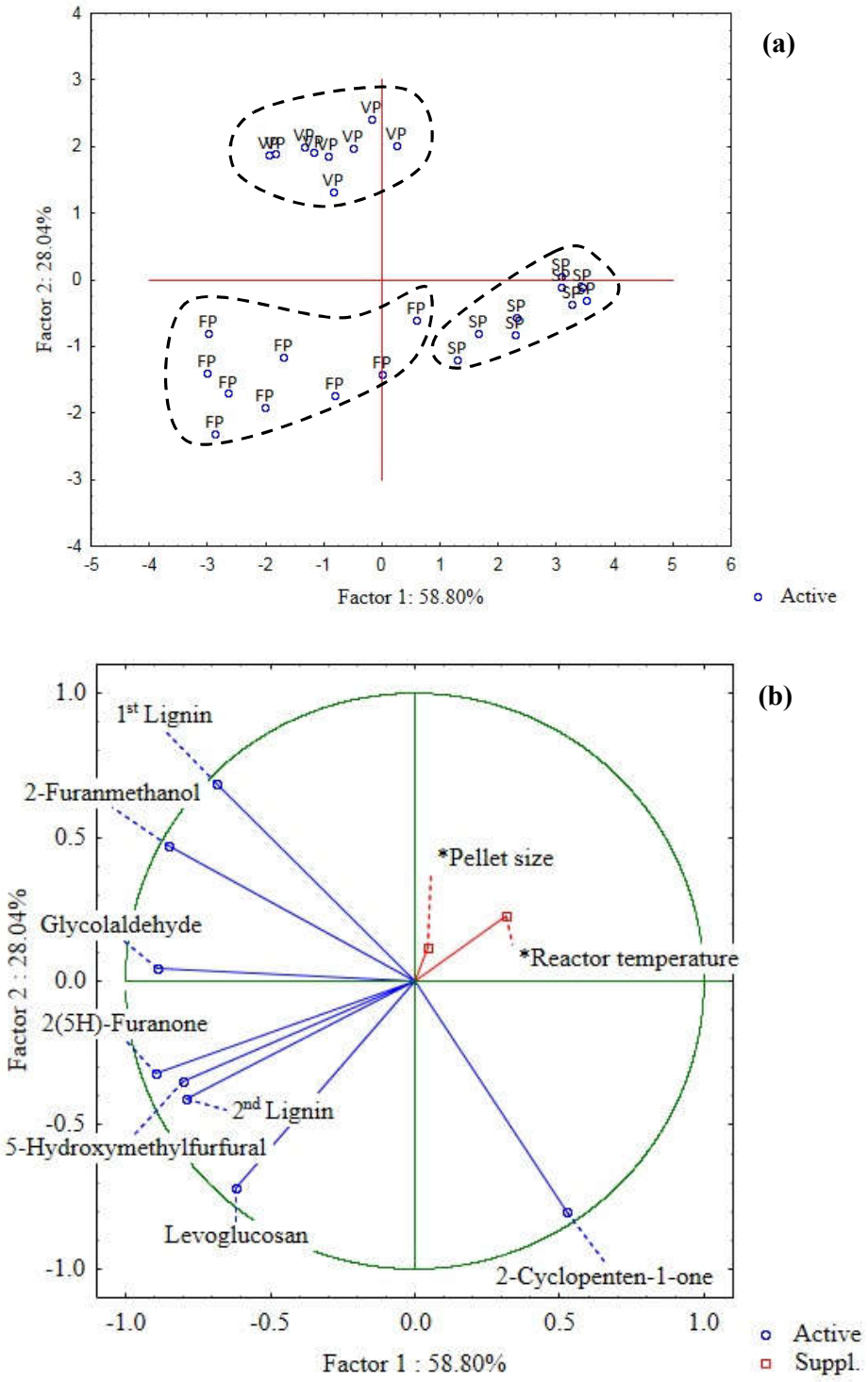

Figure 6-1. PCA scores (a) and correlation loading plots (b) of factor 1 (PC1) versus factor 2 (PC2) based on chemical yields from vacuum, slow and fast pyrolysis of LAPWS.

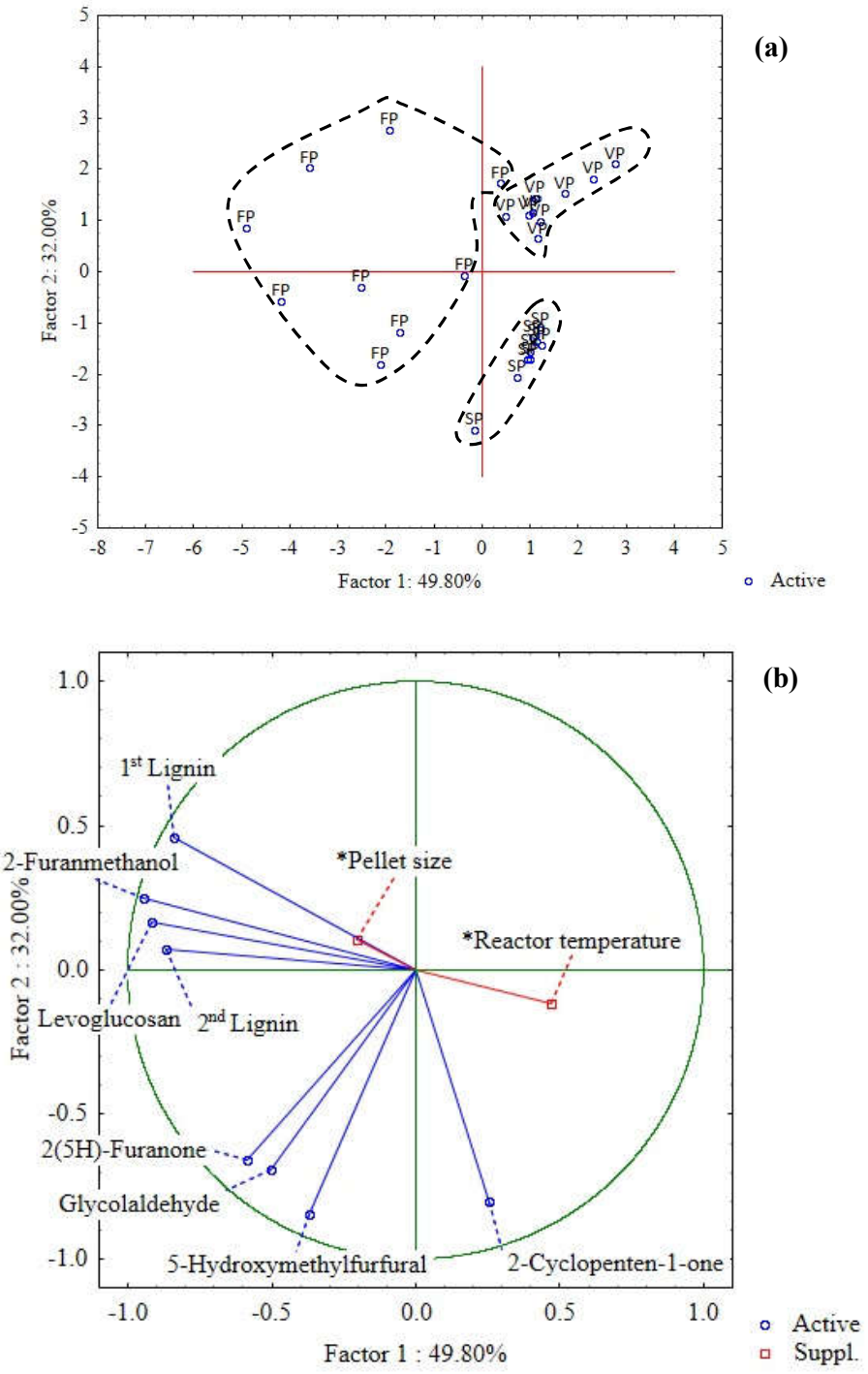

Figure 6-2. PCA scores (a) and correlation loading plots (b) of factor 1 (PC1) versus factor 2 (PC2) based on chemical yields from vacuum, slow and fast pyrolysis of HAPWS (PS: pellet size; RT: reactor temperature).

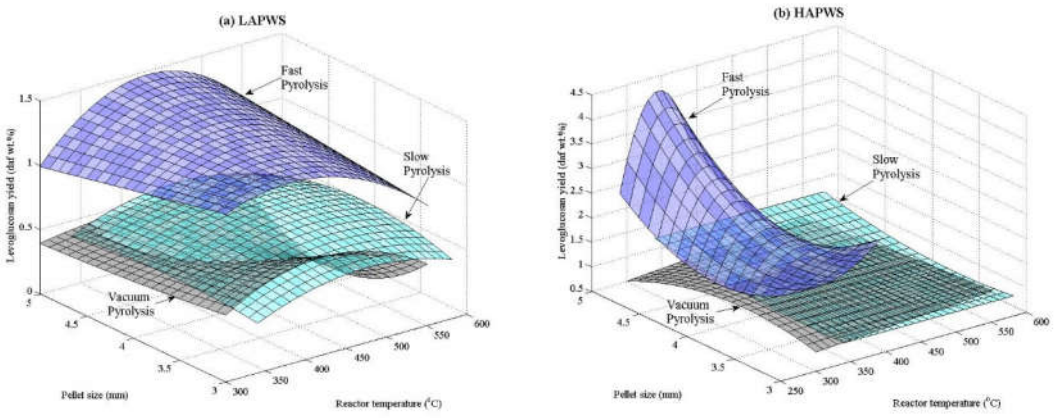

Figure 6-3. Production of levoglucosan from vacuum, slow and fast pyrolysis conversion of LAPWS (a) and HAPWS (b) at different reactor temperatures and pellet sizes.

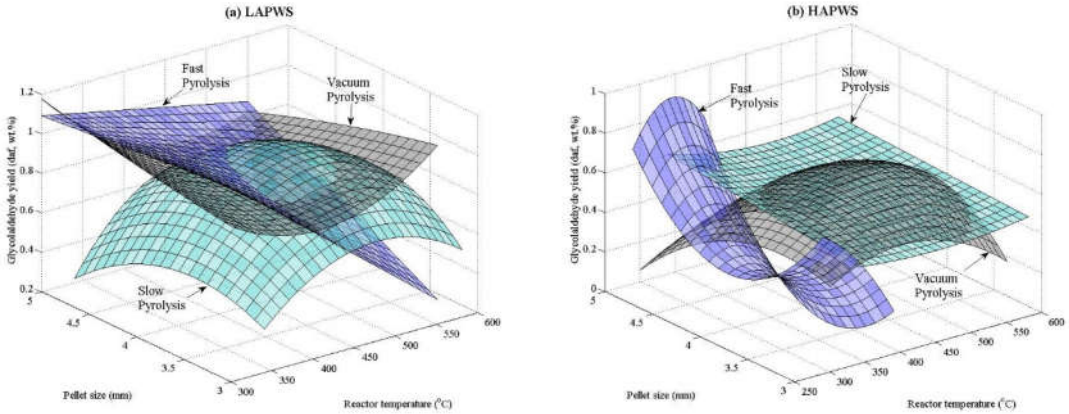

Figure 6-4. Evolution of glycolaldehyde during vacuum, slow and fast pyrolysis conversion of LAPWS (a) and HAPWS (b) at different reactor temperatures and pellet sizes.

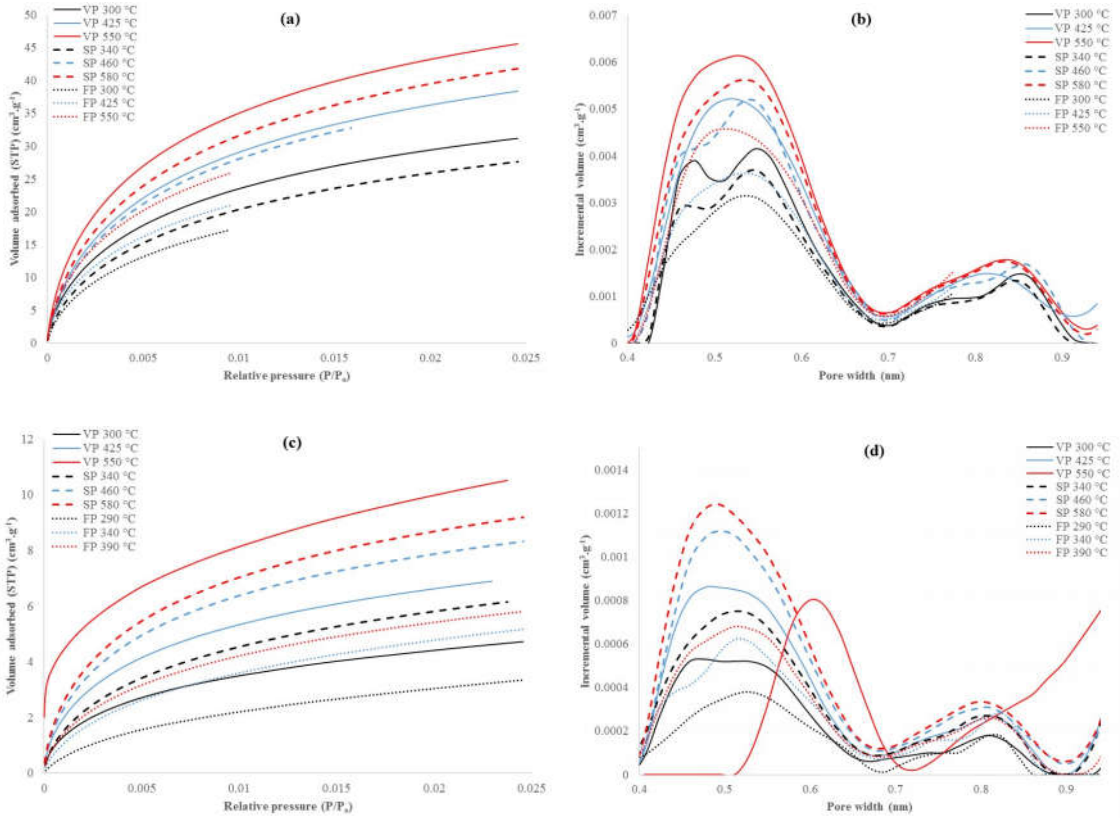

Figure 6-5. CO_2 adsorption isotherms (a,c) and pore size distribution (b,c) for chars derived during vacuum, slow and fast pyrolysis of LAPWS (a,b) and HAPWS (c,d) at different reactor temperatures.

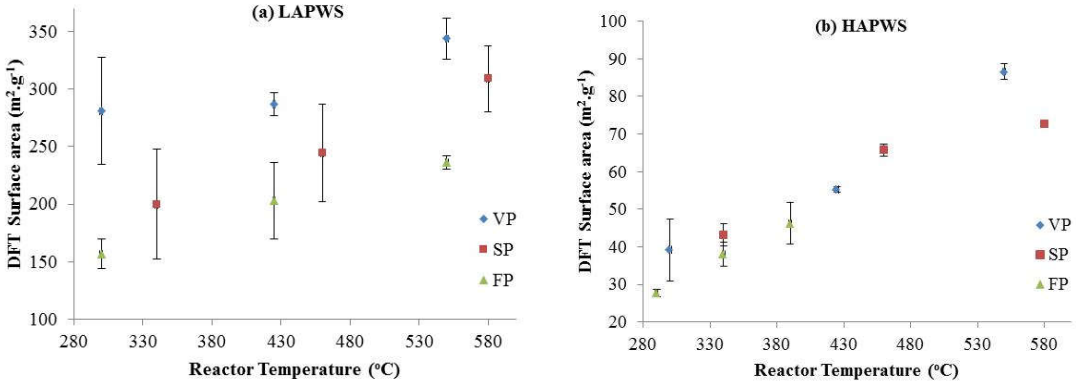

Figure 6-6. DFT pore surface areas of LAPWS (a) and HAPWS (b) vacuum, slow and fast pyrolysis chars at different reactor temperatures.

CHAPTER 7: SEQUENTIAL BIOCHEMICAL-THERMOCHEMICAL PROCESSING OF LOW AND HIGH ASH PAPER WASTE SLUDGE FOR PRODUCTION OF ENERGY, CHEMICALS AND BIOMATERIALS

A paper in preparation for submission to the journal of Bioresourece Technology (ISI impact factor 5.3305).

Title: "Sequential biochemical-thermochemical processing of low and high ash paper waste sludge for production of energy, chemicals and biomaterials"

Authors: Angelo J. Ridout, Marion Carrier, François-Xavier Collard, Johann Görgens.

OBJECTIVE OF DISSERTATION AND SUMMARY OF FINDINGS IN PRESENT CHAPTER

This chapter addresses **objectives 1 to 8** which focuses on the capability (**objective 1**) of vacuum, slow and fast pyrolysis to maximise the conversion of FR into value-added solid and/or liquid products (**objective 2**) for use in energy, chemicals and biomaterial applications (**objective 5 and 7**). The effect of fermentation pre-treatment on the pyrolysis product yields and properties (**objective 8**), as well as on the overall gross energy recovery (**objective 4**) was investigated by comparing the results to those of stand-alone pyrolysis (Chapters 4 to 6). Furthermore, the role and fate of ash is described (**objective 3**), and differences in product distribution and properties are used to reveal insights into new pyrolytic mechanisms (**objective 6**).

The combination of the fermentation conversion of PWS with FR fast pyrolysis offered the highest energy conversions (ECs), at between ~75 and 88% for the low ash PWS, and ~41 and 48 % for the high ash PWS. Moreover, these ECs were up to ~10 % higher than those obtained during stand-alone fast pyrolysis of PWS. Not only did fermentation of PWS promote the bulk energy and yield of pyrolysis char products, it led to the production of phenols-rich bio-oil and slightly improved the sorption properties of char biomaterials.

Candidate declaration

With regards to chapter 7, page numbers 205-243 of this dissertation, the nature and scope of my contribution were as follows:

Name of contribution	Extent of contribution (%)
Planning and experiments	90
Executing experiments	100
Interpretation of results	70
Writing the chapter	100

The following co-authors have contributed to chapter 7 page 205-243 of this dissertation:

Name	e-mail address	Nature of contribution	Extent of contribution (%)
1. Marion Carrier	m.carrier@aston.ac.uk	• Reviewing the chapter • Interpretation of results	50 20
2. François-Xavier Collard	fcollard@sun.ac.za	• Reviewing the chapter • Interpretation of results	40 10
3. Johann Görgens	jgorgens@sun.ac.za	• Reviewing the chapter • Experimental planning	10 10

Signature of candidate…….

Date…….

Declaration by co-authors

The undersigned hereby confirm that:

7. The declaration above accurately reflects the nature and extent of the contributions of the candidates and co-authors to chapter 7 page numbers 205-243 in the dissertation,
8. no other authors contributed to chapter 7 page numbers 205-243 in the dissertation beside those specified above, and
9. potential conflicts of interest have been revealed to all interested parties and that are necessary arrangements have been made to use the material in chapter 6 page numbers 205-243 of the dissertation

Signature	Institutional affiliation	Date

SEQUENTIAL BIOCHEMICAL-THERMOCHEMICAL PROCESSING OF LOW AND HIGH ASH PAPER WASTE SLUDGE FOR PRODUCTION OF ENERGY, CHEMICALS AND BIOMATERIALS

Angelo J. Ridout[1], Marion Carrier[2], François-Xavier Collard[1], Johann Görgens[1]

[1]*Department of Process Engineering, University of Stellenbosch, Private Bag X1, Matieland 7602, South Africa*

[2]*Bioenergy Research Group, European Bioenergy Research Institute (EBRI), Aston University, Birmingham B47ET, United Kingdom*

ABSTRACT

Residues from fermentation (FRs) of low and high ash paper waste sludge (PWS) were converted into usable solid and liquid energy products using vacuum, slow and fast pyrolysis. After studying the influence of pyrolysis types on product yield and fuel properties, the recovery levels of energy by coupling fermentation of PWS and pyrolysis of FR were compared to those obtained in the case of the stand-alone pyrolysis of PWS. Highest gross energy conversions (EC) were attained by combining PWS fermentation and FR fast pyrolysis, between ~75 and 88% for the low ash PWS, and ~41 and 48 % for the high ash PWS. Furthermore, comparison of these latter ECs to the ones obtained during stand-alone fast pyrolysis of PWS revealed an increase of up to ~11 % for low ash PWS and ~10 % for high ash PWS, which was attributed to the enhanced production of both liquid and solids products. The pre-treatment of PWS via fermentation not only increased the bulk energy and yield of the pyrolysis char products, but also led to the production of phenols-rich bio-oil and slightly favoured char pore development.

Keywords: Fermentation residue, pyrolysis, energy, chemicals, biomaterials

7.1 INTRODUCTION

It has been demonstrated that fermentation of paper waste sludge (PWS), an industrial waste generated in large quantities by the pulp and paper industry [1], is a promising process for bioethanol production [2-4]. The use of PWS for fermentation is advantageous as the degraded cellulose fibre content is easily hydrolysed to yield fermentable sugars [2-4]. However, PWS fermentation generates a large amount of fermentation residue (FR), which contains significant amounts of organic material.

A number of researchers have already considered the integration of both thermochemical and biochemical processes as a way to increase the carbon conversion efficiency and therefore to mitigate 'some of the deficiencies of conventional biochemical (pre-treatment–hydrolysis–fermentation) and thermochemical (pyrolysis or gasification) processing' [5]. These new platforms are presented as hybrid thermochemical-biochemical processing of biomass. For example, fast pyrolysis can be used as a pre-treatment step to breakdown the recalcitrant materials, and generate bio-oil whose sugar fraction can be easily fermented to produce drop-in hydrocarbon fuels [5]. Alternatively, fermentation could be used as pre-treatment step to selectively convert the carbohydrate fractions into high energy bioethanol [2-4], followed by pyrolytic conversion of its fermentation residues into char and bio-oil products for energy, chemical and/or biomaterial applications [6-8]. Such an approach could enhance the energetic transfer from biomass to usable energy products and improve the overall process economics [5]. Although this last conversion route has been explored for wheat-derived FRs [6-8], it has not been considered for PWS-derived FR.

Differences in the process operating conditions between fast, slow and vacuum pyrolysis can have a significant effect on the distribution and physico-chemical characteristics of the pyrolysis products [9-14]. The two main differences between the pyrolysis technologies lie in the applied

heating rate and vapour residence times [10,15]. For instance, fast pyrolysis (FP) with its high heating rates (300 to 12000 $^{o}C.min^{-1}$) [15] reduces heat transfer limitations, thus promoting devolatilization reactions by depolymerisation and fragmentation [15-18], which often leads to maximised bio-oil yields [10]. On the other hand, slow pyrolysis (SP) uses slow heating rates (1 to 60 $^{o}C.min^{-1}$) with long vapour residence times (1 min to hours) [10,15,19], compared to the short vapour residence times of FP (< 2 s) [10]. The longer vapour residence time of SP hinder mass transfer, thus promoting secondary recombination reactions [20], which often leads to greater char formation [9,10]. Vacuum pyrolysis (VP) conditions lie between those of FP and SP, whereby low heating rates with short vapour residence times (2 to 20 s) are employed, resulting in a good compromise for the pyrolysis product yields [19,21]. Considering the energy content, FP and VP typically generate liquid products with higher calorific values, which offer better potential as fuel sources for heat, power and transport fuel production, when compared to SP [21-23]. On the other hand, SP typically produces chars with higher calorific values when compared to those of FP and VP [11,12,19], and such char can be utilized as a coal substitute for various energy applications. When considering the performance of pyrolysis based on gross energy conversion, as a measure of the gross energy transfer from biomass to the products, the type of pyrolysis technology can have a significant effect [23]. In a previous study [23], FP was shown to offer the highest gross conversion of energy (~70-78 %) from raw PWSs to the liquid and solid products, when compared to SP (~50-57 %) and VP (~32-58 %). Alternatively to energy applications, the char product can also find application as a biomaterial (i.e. biochar or sorption medium), which may have better economic potential [24]. In particular, the adsorptive properties displayed by VP biomaterials are usually better than those of SP and FP, due to enhanced devolatilization and/or limitation of recondensation reactions by fast removal of volatiles [19]. Furthermore, pyrolytic bio-oil contains numerous

oxygenated compounds such as aldehydes, ketones, sugars, furans and phenols, to name a few [25], which can have higher market values than energy products, if isolated [26,27]. The application of FP has been shown to enhance the production of chemicals such as sugars, phenols, aldehydes and furans due to enhanced depolymerisation and/or fragmentation reactions [13,14]. The fast removal of volatiles at relatively low temperatures during VP limits secondary reactions and is likely to lead to greater yields of some primary phenols [28,29]. The large inorganic content found in PWSs, often in the form of calcium [30], could affect pyrolysis reactions leading to differences in chemical yields [31,32]. For instance, the presence of calcium components has been shown to reduce levels of levoglucosan and enhance the formation of glycolaldehyde [31,32].

Alongside the extensive effect of the operating conditions on the pyrolysis mechanisms and their subsequent products [9-14], the biomass type can significantly influence the product yields and properties. Indeed, the lignocellulosic composition governs the pyrolytic pathways [33], and thus the reduction of cellulose during fermentation pre-treatment could lead to large differences in the distribution and physico-chemical characteristics of products, compared to untreated PWS.

Thus, the aim of this is study was to assess the capability of vacuum, slow and fast pyrolysis, at varying temperatures, to convert raw FR into value-added energy, chemicals and biomaterials. In addition to this, the consequence of fermentation, considered as a pre-treatment stage, on the distribution and physico-chemical characteristics of products, as well as on gross energy conversions, was investigated by comparing results to previous works on PWS pyrolysis (Chapters 5 to 6) [23,29].

7.2 MATERIALS AND METHODS

7.2.1 Raw materials and preparation

The low and high ash fermentation residues utilized in this study were obtained from paper waste sludge fermentation experiments as described elsewhere [34]. In brief, a low ash paper waste sludge (LAPWS) sample was sourced from the Kraft pulp mill Sappi Ngodwana, and a high ash paper waste sludge (HAPWS) was sourced from the paper mill MPact Springs. Both PWSs were subjected to enzymatic hydrolysis and fermentation to maximise the ethanol yield, after which the dried low ash fermentation residue (LAFR) and high ash fermentation residue (HAFR) were milled using a Retsch hammer mill with a 2 mm sieve. The milled FR was subsequently rehydrated (FR:Water 1:1), pelletized into 5 mm pellets using a Trespade N^{o}12 meat mincer, after which they were dried for 12 hours at 105 ± 2 ^{o}C. It must be noted that the PWSs used for the fermentation study [34] were obtained from different batches as the ones in the previous works on PWS (Chapters 4 to 6) [23,29].

7.2.2 Pyrolysis experiments

7.2.2.1 Vacuum and slow pyrolysis

The vacuum and slow pyrolysis experiments were carried out using a unit previously described (Appendix A-3 to A-4) [19]. The unit consists of two consecutively connected sections; fixed bed (FB) reactor and condensation train. The FB reactor consists of a 1 m long, 60 mm OD quartz glass tube, which is externally heated by six well insulated and computer controlled heating elements. A mass of 20 g of FR was used in each run. During the slow pyrolysis runs, pyrolytic vapours were swept from the reactive zone by N_2 (Technical grade, Afrox) at a flow rate of 1 L.min^{-1} resulting in an average residence time of 54 s. During vacuum pyrolysis, the application of a vacuum (~8 kPa$_{ab}$)

reduced the pyrolytic vapour residence times down to ~2 s. The volatiles were condensed in a series of five traps varying in temperature. For slow pyrolysis, the first was held at room temperature, and all remaining condensers (2 to 5) were held at 0 ^{o}C (crushed ice), whereas for vacuum pyrolysis, the last two were held at -78 ^{o}C (dry ice temperature) to ensure condensation. A heating rate of 30 ^{o}C.min^{-1} was applied until the desired temperature was reached (300, 425 or 550 ^{o}C), after which it was held there for 30 min to ensure complete devolatilization of the organic material. As the chemicals are recovered by a physical and/or chemical means, higher concentrations ease isolation and lower costs [35,36]; thus only the tarry phase was considered (Eq. 2), as it had contained most of the condensable organics compounds when compared to the aqueous phase (see Section 7.3.3.1). The vacuum and slow pyrolysis product yields were calculated on a dry ash free basis with Y_{char} standing for char yield, Y_{tarry} for tarry phase yield, $Y_{aqueous}$ for aqueous phase yield, $Y_{bio\text{-}oil}$ for bio-oil yield, $Y_{pyro\text{-}water}$ for pyrolytic water yield, $Y_{organic}$ for organic liquid yield, Y_{gas} for non-condensable gas yield and Y_i for chemical product yield, calculated after quantitate GC-MS analysis of tarry phase (see Section 7.2.3.2).

$$Y_{char}\,(\text{daf wt.\%}) = \frac{M_{\text{fixed-bed}} - M_{\text{ash–char}}}{M_{FR} - M_{\text{ash–}FR} - M_{\text{moisture}}} * 100 \quad (1)$$

$$Y_{tarry}\,(\text{daf wt.\%}) = \frac{M_{C1} + M_{\text{steel-pipe}}}{M_{FR} - M_{\text{ash–}FR} - M_{\text{moisture}}} * 100 \quad (2)$$

$$Y_{aqueous}\,(\text{daf wt.\%}) = \frac{M_{C2\text{-}5} + M_{\text{rubber -pipes}}}{M_{FR} - M_{\text{ash–}FR} - M_{\text{moisture}}} * 100 \quad (3)$$

$$Y_{bio\text{ - }oil}\,(\text{daf wt.\%}) = Y_{tarry} + Y_{aqueous} \quad (4)$$

$$Y_{pyro\text{ - }water}\,(\text{daf wt.\%}) = \frac{M_{KFwater} - M_{moisture}}{M_{FR} - M_{\text{ash–}FR} - M_{\text{moisture}}} * 100 \quad (5)$$

$$Y_{organics}\,(\text{daf wt.\%}) = Y_{bio\text{ - }oil} - Y_{pyro\text{ - }water} \quad (6)$$

$$Y_{gas}\,(\text{daf wt.\%}) = 100\% - Y_{char} - Y_{bio\,-\,oil} \quad (7)$$

$$Y_i\,(\text{daf wt.\%}) = Y_{tarry} * X_i \quad (8)$$

where M_i is the mass of products in grams collected in a specific piece of the setup, KF_{water} (wt.%) stands for the water content determined by Karl-Fischer method, X_i is the mass fraction of the chemical component in the tarry phase, and $m_{moisture}$ (wt.%) is the moisture contained in the FR. The total tarry phase, which was dark brown in colour, consisted of the residue in the steel pipe leading to the first condenser, $m_{steelpipe}$, as well as the liquid product recovered in condenser 1, M_{C1} (Eq. 2). The total aqueous phase, which was light brown/yellow in colour, consists of the residue in the rubber piper connecting the four condensers, $M_{rubber\text{-}pipes}$, as well as the liquid product recovered in the condensers 2 to 5, $M_{C2\text{-}5}$ (Eq. 3). The total bio-oil yield is the sum of both tarry and aqueous phases (Eq. 4).

Determination of KF_{water} content for some aqueous phase (condensers 3 to 5) samples was impossible due to a limited amount available. Thus, when water content (WC) determination was not possible, it was estimated using a WC ratio as described in our previous work [23].

7.2.2.2 Fast pyrolysis

The fast pyrolysis experiments were performed at varying temperatures levels of 300, 425 and 550 ^{o}C using a unit that has been previously described (Appendix A-1 to A-2) [37], and consists of four interconnected section: feeding system (max. 1 $kg.hr^{-1}$), bubbling fluidised bed reactor (BFBR), char separation and liquid condensation train. The fermentation residue pellets were screw fed at 0.5 $kg.hr^{-1}$ from the hopper to the BFBR, whereby they were fluidised with silica sand (AFS 35 fused silica sand, CONSOL minerals). Nitrogen (Technical grade, AFROX) was used as a fluidising medium, with a fixed flow rate of 2.4 $m^3.hr^{-1}$. The char was separated from the pyrolysis

vapours by ways of a cyclone, located at the exit of the BFBR. The pyrolysis vapours then entered the liquid condensation chain whereby an iso-paraffinic hydrocarbon (Isopar, Engen Petroleum limited) was sprayed in direct contact to condense the bio-oil by quenching. Any remaining uncondensed vapours entered two electrostatic precipitators set at 14 kV and 12 kV to remove any condensable compounds. The non-condensable gas was purged to the atmosphere.

The fast pyrolysis product yields were calculated on a dry ash free basis with Y_{char} standing for char yield, $Y_{bio\text{-}oil}$ for bio-oil yield, $Y_{pyro\text{-}water}$ for pyrolytic water yield (Eq. 5), $Y_{organic}$ for organic liquid yield (Eq. 6), Y_{gas} for non-condensable gas yield (Eq. 7) and Y_i for chemical yield, calculated after quantitate GC-MS analysis of bio-oil (see Section 7.2.3.2).

$$Y_{char}\,(\text{daf wt.\%}) = \frac{M_{char\text{-}pots} + (M_{reactor-content} - M_{sand}) - M_{ash\text{-}char}}{M_{FR} - M_{ash-FR} - M_{moisture}} * 100 \quad (9)$$

$$Y_{bio\text{-}oil}\,(\text{daf wt.\%}) = \frac{M_{bulk\text{-}liquid} + M_{residue}}{M_{FR} - M_{ash-FR} - M_{moisture}} * 100 \quad (10)$$

$$Y_i\,(\text{daf wt.\%}) = Y_{bio\text{-}oil} * X_i \quad (11)$$

where X_i is the mass fraction of the chemical component in the bio-oil. The bulk liquid, $M_{bulk\text{-}liquid}$, consisted of the bio-oil recovered in the reservoir as well as the residue in the condensation train equipment. Experimental errors related to fast, vacuum and slow pyrolysis of PWS have already been reported by determining standard deviations of triplicate runs (Chapters 4 and 5) [23,37]. The FR experiments were performed using the same procedure and operating conditions. Considering that the FR has a higher compositional homogeneity than raw PSW, it was decided that the same standard deviation values were to be used in this study.

7.2.3 Physico-chemical characterisation

7.2.3.1 Raw materials and char products

While standardized methods were used to determine the composition of LAPWS, LAFR, and the LAFR solid products, some of these methods had to be adapted to take into account the eventual conversion of the inorganic material of HAPWS, HAFR, and the HAFR solid products. The ash content of the PWSs, FRs and LAFR chars were determined in accordance with the ISO 1762 standard procedure whereby samples were combusted in a muffle furnace at 525 ± 5 ^{o}C. The proximate analysis of the LAFR and its char, as well as LAPWS, was determined in accordance with the ASTM E1131 standard procedure using a TGA/DSC 1-LF1100 Mettler Toledo. The lignocellulosic composition analysis of the PWSs and FRs was determined in the previous study in accordance with NREL laboratory analytical methods [34]. The calorific value of the dried PWSs and FRs were experimentally determined using a Cal2K ECO bomb calorimeter, which was calibrated using benzoic acid (Cal2K). The mineral composition (oxides) of the FR was determined via X-ray fluorescence (XRF) analysis using an AXIOS PANalytical. Fused glass discs were used for the major elemental analysis.

As the inorganic fraction of HAPWS is mainly comprised of CaCO3 [30], HAFR was subjected to fourier transform infrared (FT-IR) spectroscopy (Thermo Scientific Nicolet iS10 with an ATR attachment using ZnSe crystal) to determine whether changes occurred during fermentation, by comparing its spectrum to calcium carbonate, calcium hydroxide and calcium oxide which were analysed elsewhere (Edu Trade) [25]. Qualitative comparison of the FT-IR spectra revealed the absence of the peak at 3640 cm^{-1} ($Ca(OH)_2$ and CaO), and presence of the broad band at 1400 cm^{-1}, confirming that the calcium was mainly in the form of $CaCO_3$ and remained unchanged during

fermentation (Figure 7-1). Due to the thermal decomposition of $CaCO_3$ (Eq. 12) above 650 °C, the ASTM E1131 method had to be adapted.

$$CaCO_3 \rightarrow CaO + CO_2 \quad (12)$$

In order to distinguish CO_2 produced by this reaction and the volatiles released from the biomass/char (mostly generated at T < 650 °C) the ASTM E1131 method was altered, by including a step holding the temperature at 650 °C for 5 minutes to drive off volatiles, after which it was heated to 900 °C and held for an additional 5 minutes to ensure full calcium carbonate decomposition occurred before combustion of the fixed carbon (FC), as implemented previously [37]. As previously shown [23], calcium carbonate can partially transform into CaO and/or $Ca(OH)_2$ during pyrolysis. Thus, to determine the extent of the $CaCO_3$'s changes, DTG curves for the proximate analysis (altered ASTM E1131 method) of the chars, as well as $Ca(OH)_2$ and $CaCO_3$ were studied. Figure 7-2 illustrates the DTG curves for the VP at 425 and 550 °C (VP_{425} and VP_{550}) chars. Peaks 1 and 2 respectively correspond to the driving off of moisture and volatiles, peak 4 is the thermal decomposition of $CaCO_3$ (Eq. 12), and peak 5 is the combustion of the fixed carbon (Figure 7-2). The presence of peak 3 for VP_{550} was attributed to the thermal decomposition of $Ca(OH)_2$ (Eq. 13). The formation of $Ca(OH)_2$ could be explained by the transformation of carbonate compounds in the presence of water during pyrolysis [38] (Eq. 14). This finding was only observed for VP_{550}.

$$Ca(OH)_2 \longleftrightarrow CaO + H_2O \quad (13)$$

$$CaCO_3 + H_2O \longleftrightarrow Ca(OH)_2 + CO_2 \quad (14)$$

$$VM\ (wt.\%, df) = 100 - FC - CO_2 - H_2O - AC_{900} \quad (15)$$

Volatile matter (VM) was calculated using Eq. 15 whereby CO_2 and H_2O, generated during the respective conversion of $CaCO_3$ and $Ca(OH)_2$, were deducted. While Ca was only present in the

form of $CaCO_3$ in the raw HAPWS and HAFR, the VM was calculated in a similar manner as described by Eq. 15. The total ash content of the HAFR chars were determined by summing the CO_2 and H_2O, produced from inorganic conversion, as well as the ash content determined at 900 °C (AC_{900}).

The C, H, N and S content of the PWSs, FRs and chars were determined by ultimate analysis in accordance with the ASTM D5373 standard procedure using a TruSpec Micro from LECO. Coal (AR2781, LECO), Atropine (QC, LECO), and Cytine (QC, LECO) standards were used to calibrate the content of C, H, N and S for chars, while only an Atropine standard (CSG, LECO) was used for the PWSs and FRs. Samples are usually combusted at 1080 °C, making thermal decomposition of $CaCO_3$ (CO_2 release, Eq. 12) and $Ca(OH)_2$ (H_2O release, Eq. 13) inevitable for the HAFR and its char products, as well as for HAPWS. Based on this observation, both C and H contents were corrected by deducting the CO_2 and H_2O contribution from the $CaCO_3$ and $Ca(OH)_2$ thermal decomposition. The HHV of the char was calculated using the correlation from Mott *et al.* [39] (Eq. 16).

$$HHV\,(kJ.kg^{-1}) = 0.336\,W_C + 1.418\,W_H - 0.145\,W_O + 0.0941\,W_S \quad (16)$$

where W_i is the mass fraction of each element with the ranges the range $W_O < 15$ wt.%.

The porous structure of FR chars produced at 425 °C was described using surface area and pore characteristics (i.e., pore volume and pore size distribution). As previously described [29], char samples were initially degassed using a VacPrep 061 system at 90 °C (1 hour), after which they were introduced into a Micrometrics ASAP 2010 system. The nonselective physical adsorption of appropriate adsorbent is generally determined using N_2 at liquid nitrogen temperature (-196 °C). However, due to the highly microporous nature (pore width < 1 nm) of the these chars, CO_2 was used to run the volumetric adsorption measurement at 0 °C, as it has a greater rate of diffusion due

to higher adsorption temperature [40,41]. To display the adsorption profile, the selection of a model is required. One way to explore the CO_2 data is by using the density function theory method (DFT) (Eq. 17) which offers an algorithm that is better suited for microporous materials [42,43].

$$N(P) = \int_{w_{min}}^{w_{max}} f(w)\ \rho(P, w)\, dw \quad (17)$$

where N(P) is quantity of gas adsorbed (mol) at pressure P (mmHg), w_{min} and w_{max} are the widths (Å) of the smallest and largest pores, $\rho(P,w)$ is the density ($mol.cm^{-3}$) of the gas at pressure P (mmHg) and pore width w(Å), and f(w) is the distribution of pore volumes ($cm^3.Å^{-1}$).

7.2.3.2 Liquid product

The bio-oil product produced during vacuum and slow pyrolysis consisted of two phases; tarry and aqueous phase. The water content of both phases, and the FP bio-oil, were determined in accordance with the ASTM E203 standard method using a Metrohm 701 Titrino Karl-Fischer titrator. A hydranal composite 5 titrant (Sigma Aldrich) was used. Due to the high water content in the aqueous phase, it was not considered for energy applications (see Section 7.3.3.1). Ultimate analysis was performed on the VP and SP tarry phase and FP bio-oil in accordance with the ASTM D5291-10 standard method using a TruSpec Micro from LECO. The C, H, N, and S content were calibrated using a residual bio-oil standard (AR100, LECO) and Sulfamethazine (QC, LECO). The higher heating value (HHV) of the tarry phase and FP bio-oil was calculated using Channiwala's correlation (Eq. 18) and was corrected for water [44].

$$HHV(MJ.kg^{-1}) = 0.3491W_C + 1.1783W_H + 0.1005W_S - 0.1034W_O - 0.0151W_N - 0.0211W_{AC} \quad (18)$$

where W_i is the mass fraction of each element with the ranges as, $0 < W_C < 92.25$, $0.43 < W_H < 25.14$, $0 < W_O < 50.00$, $0 < W_N < 5.60$, $0 < W_S < 94.08$, $0 < W_{AC} < 71.4$ and $4.745 < HHV < 55.245$.

A gas chromatography-mass spectrometry (GC-MS) system with an internal calibration procedure was used to identify and quantify the condensable compounds contained in the VP and SP tarry phase and FP bio-oil. The internal standard solution was prepared by dissolving 0.2 g of methyl behenate (Fluka, 99.0 %) in 50 mL MeOH (Riedel-de Haenm 99.9 %). Initially GC samples were prepared by adding 0.06 g of FP bio-oil, or 0.06 g of VP tarry phase or 0.3 g of SP tarry phase (due to higher water content) to a volumetric flask with 400 µL of internal standard and 2000 µL of MeOH. Before injection, the mixture was filtered using a 22 µL nylon micro filter (Anatech). The GC-MS analysis was carried out using an Agilent GC/MSD 7890A/5975C (single quadrupole) with a multi-mode injector on a Zebron ZB-1701 column (60 m x 250 µm x 0.25 µm). The helium (carrier gas) was set to a flow rate of 1.3 $mL.min^{-1}$. The column-heating program was as follows: the column was initially held constant at 45 ^{o}C for 8 min, then ramped to 100 ^{o}C at 2 $^{o}C.min^{-1}$, after which it was again ramped to 260 ^{o}C at 7 $^{o}C.min^{-1}$. The selection of external standards was based on the typical chemical products produced from the main lignocellulosic constituents (i.e. hemicelluloses, cellulose and lignin). For the carbohydrate fraction (cellulose and hemicelluloses), the following chemical compounds were selected: levoglucosan (99 %), 2-furanmethanol (98 %), 2(5H)-furanone (98 %), 5-hydroxymethylfurfural (99%), glycolaldehyde (98%) and 2-cyclopenten-1-one (%). The lignin-derived chemicals were classed into 2 groups: (i) primary compounds (1^{st} lignin) which contain an alkyl chain with 2 to 3 carbons supposedly derived from the monomer units, and (ii) the secondary compounds group (2^{nd} lignin) which are produced during degradation of primary compounds and have no alkyl chain in the para position of the hydroxyl group. The 1^{st} lignin derived chemicals included: 4-vinylguaiacol (98 %), eugenol (99 %) and apocynin (98 %). The secondary lignin compounds included: phenol (98 %), guaiacol (98 %), 2,3-dimethyl phenol (99 %) and 2,6-dimethyl phenol (99.5 %). All external standards were supplied by Sigma Aldrich.

An example of a GC-MS chromatogram for the LAFR vacuum and slow pyrolysis tarry phase, as well as the fast pyrolysis bio-oil, is shown in Appendix F-1.

The iso-paraffinic hydrocarbon used in the FP experiments was found to be slightly miscible with the bio-oil, thus GC-MS analysis was used to determine its concentration using the same procedure described above. Results indicated that the FP bio-oil contained between ~3 to 9 wt.% of the iso-paraffinic hydrocarbon. Subsequently the yield, ultimate analysis and the calorific values of the bio-oil was corrected by subtracting the mineral oil's C and H content, which is comprised of C_9 to C_{12} alkanes (C: 84.5 ± 0.14 wt.%, H: 15.5 ± 0.14 wt.%) [45].

7.2.4 Energy conversion

The partial biomass gross energy conversion (EC) from the PWS to the bio-oil/tarry phase, char and ethanol product is determined by Eq. 19 below:

$$EC\,(\%) = \frac{M_i * HHV_i}{M_{PWS} * HHV_{PWS}} * 100 \qquad (19)$$

where M_i and HHV_i, are respectively the mass and higher heating value of the bio-oil/tarry phase, char or ethanol (29.7 $MJ.kg^{-1}$), while M_{PWS} and HHV_{PWS} apply to PWS. The resulting gross EC compares the energy output in the products only to the process energy input in the form of the PWS feedstock; external energy inputs for heating, vacuum and ethanol distillation were not considered. The sum of gross energy conversion for pyrolysis of PWS/FR (EC_{pyro}) was determined by summing the char (EC_{char}) and bio-oil/tarry phase ($EC_{bio\text{-}oil}$/EC_{tarry}) energy conversions. To determine the sum of gross energy conversion for the integrated fermentation pyrolysis process ($EC_{ferm\text{-}pyro}$), the fermentation gross energy conversion to ethanol (EC_{ferm}) was summed with the EC_{pyro} obtained during pyrolysis of FR. An average ethanol yield of 19.8 ± 1.3 wt.% (dry basis) and 14.5 ± 2.8 wt.% (dry basis) was used when calculating the EC_{ferm} for LAPWS and HAPWS, respectively [34]. All

ECs were normalised to PWS. No analysis was performed on the non-condensable gas making determination of the experimental HHV impossible.

7.3 RESULTS AND DISCUSSION

7.3.1 Physico-chemical characterisation of PWS and its FR

Comparison of the lignocellulosic composition of the PWSs used in the previous works [37] to these PWSs (Table 7-1) reveal similarity, whereby both exhibit large amounts of cellulose (~50 to 58 daf, wt.%), as well as similar lignin (~14 to 20 daf, wt.%) and hemicelluloses (~15 to 19 daf, wt.%) content. However, the ash content of the HAPWS (46.7 wt.%) [37] in the previous works was much higher than the HAPWS in this present study (27.9 wt.%) due to differences in origin (Section 7.2.1). Significant differences were observed in the physico-chemical characteristics between PWS and its FR (Table 7-1). The cellulose content of unprocessed PWSs (~57 daf, wt.%) was reduced by hydrolysis fermentation to ~32 and 28 daf, wt.% for LAFR and HAFR, respectively (Table 7-1), due to the conversion of sugars during fermentation. Consequently, both the lignin and ash contents for both FRs were increased relative to untreated PWS. Although some of the organic matter (cellulose) was converted, only small decreases were observed in the HHVs between the PWSs (18.8 $MJ.kg^{-1}$ for LAPWS; 13.1 $MJ.kg^{-1}$ for HAPWS) and their FRs (18.0 $MJ.kg^{-1}$ for LAFR; 11.3 $MJ.kg^{-1}$ for HAFR) (Table 7-3). The XRF analysis indicated that the inorganic fraction of HAFR was mainly comprised of the Ca component (12.1 wt.%) (Table 7-2), which is mostly in the form of $CaCO_3$ (Figure 7-1).Using Eq. 12, $CaCO_3$ was estimated to be 21.6 wt.%.

7.3.2 Product yields

The pyrolysis product yields obtained at varying reactor temperatures during vacuum, slow and fast pyrolysis of the low and high ash fermentation residues are illustrated by Figure 7-3. Higher temperatures decreased the char yield, and increased the non-condensable gas yield for both FRs (Figure 7-3), similar to previous findings for wheat-derived FR [6-8]. For LAFR at 300 ^{o}C and for HAFR at 300 and 425 ^{o}C (Figure 7-3), higher char yields were observed for FP when compared to SP and VP, which is contrary to typical trends observed in literature for the pyrolysis of PWS and other biomasses whereby the highest char yields are typically obtained for SP, followed by FP then VP [10,23]. However, it was shown that lignin's degradation deviates from typical biomass thermal behaviour, whereby higher heating rates enhance char formation as shown by Nowakowski *et al.* [46]. In general, no specific pyrolysis technique displayed a higher bio-oil yield (Figure 7-3); however, FP did offer the highest organic liquid yield for both FRs particularly at 425 ^{o}C (Figure 7-4).

Comparison of the char and bio-oil yields obtained from PWS and FR highlighted the significant effect of fermentation pre-treatment on pyrolysis reactions. The average char yield (independent of pyrolysis process and temperature) obtained for LAFR and HAFR was 26.3 and 20.4 daf, wt.%, respectively, which was higher than those of LAPWS and HAPWS at 21.7 and 11.7 daf, wt.%, respectively [23]. This observation can be attributed to the higher lignin content in the FRs (Table 7-1), a constituent known to give the highest char yields due to the greater availability of benzene rings, which form the char complex [33,38]. On the other hand, LAPWS and HAWPS displayed higher average bio-oil yields at 37.5 and 44.3 daf, wt.% respectively, when compared to LAFR and HAFR at 31.0 and 27.1 daf, wt.%, respectively [23]; thus confirming the key role of the carbohydrate fraction in the production of condensable volatiles.

7.3.3 Energy conversion assessment

In the sections to follow, the focus will now turn to potential of re-using FR pyrolysis for the production of energy, chemicals and biomaterials, and will be compared to the stand-alone biorefinery concept presented earlier (Chapters 5 and 6) [23,29]. Energy production will be assessed by means of gross energy conversion.

7.3.3.1 Product energy content

Figure 7-5 displays the calorific values of char and liquid products obtained with FR pyrolysis at different reactor temperatures. For all three pyrolysis processes, higher temperatures resulted in slight increases in the LAFR char calorific values, while the calorific values of HAFR chars calorific were decreased (Figure 7-5), which is similar to previous findings on PWS pyrolysis [23]. The char calorific values displayed by LAFR (~21 to 27 $MJ.kg^{-1}$) and HAFR (~6 to 9 $MJ.kg^{-1}$) (Figure 7-5) were slightly higher than those obtained during pyrolysis of LAPWS (~20 to 23 $MJ.kg^{-1}$) and HAPWS (~3 to 7 $MJ.kg^{-1}$) [23]. Due to the large ash content within HAFR chars (> 70 wt.%, Figure 7-6), direct industrial energy applications would not be suitable due to possible slagging and fouling during combustion [47,48], and thus their calorific input was not considered for the energy conversion study (Section 7.3.3.2).

While no particular trends were observed in liquid calorific values for a varying temperature, substantial differences were observed between pyrolysis technologies (Figure 7-5). For both FRs, higher calorific values were obtained for the VP tarry phase (~23 to 24 $MJ.kg^{-1}$) when compared to the FP bio-oil (~11 to 17 $MJ.kg^{-1}$), which is likely due to the lower water content (VP: ~ 2 to 7 wt.%; FP: ~20 to 48 wt.%), and were found to be similar to the liquid calorific values previously

obtained for PWS (VP: ~20 to 24 $MJ.kg^{-1}$; FP: ~18 to 22 $MJ.kg^{-1}$) [23]. Due to the high water content present in the SP tarry phase (~65 wt.%), as well as in the VP and SP aqueous phases (> ~80 wt.%), it is unlikely that these liquids would be used for industrial energy applications; as a result the calorific input of these fractions were not considered for the energy conversion study (Section 7.3.3.2).

7.3.3.2 Energy conversion

The gross energy conversion from the PWS to the products at different temperatures can be found in Table 7-3. Only the solid/liquid products that could be utilised in energy application were considered in the calculation of the gross EC, while external inputs other than the FRs, were neglected. Although the LAFR char calorific values were promoted at higher temperatures (Figure 7-5), the decrease in char yield (Figure 7-3) resulted in lower EC_{char} for all three pyrolysis processes (Table 7-3), which is similar to previous findings on PWS [23]. For both FRs, higher FP $EC_{bio\text{-}oil}$ as well as VP EC_{tarry} (Table 7-3) were obtained at similar conditions to those where their bio-oil yields were maximised (Figure 7-3).

Comparison of the EC_{pyro} obtained during conversion of FR revealed that FP was highest at between ~43 to 57 % for LAFR, and ~8 to 15 % for HAFR when compared to VP (~36 to 46 % for LAFR; ~9 to 10 % for HAFR) and SP (~28 to 34 % for LAFR; ~0 % for HAFR) (Table 7-3). Similarly for stand-alone pyrolysis of PWS, FP offered the highest EC_{pyro} at between ~59 to 77 % for LAPWS, and ~25 to 38 % for HAPWS when compared to VP (~44 to 53 % for LAPWS; ~12 % for HAPWS) and SP (~32 to 38 % for LAPWS; ~0 % for HAPWS), and was higher than the FP EC_{pyro} obtained for FR (Table 7-3). This latter can be attributed to the higher yields of bio-oil obtained during FP of PWS when compared to FR.

The gross energy conversion achieved during fermentation (EC_{ferm}) was 31.3 and 32.8 % for LAPWS and HAPWS, respectively (Table 7-3). Coupling of the EC_{ferm} with the EC_{pyro} for FR gives the $EC_{ferm-pyro}$, of which FP was highest at between ~75 to 88 % for LAPWS, and ~41 to 48 % for HAPWS when compared to VP (~68 to 77 % for LAPWS; ~42 % for HAPWS) and SP (~59 to 66 % for LAPWS; ~32.8 % for HAPWS). Furthermore, comparison between $EC_{ferm-pyro}$ and EC_{pyro} obtained during stand-alone fast pyrolysis of PWS, revealed a ~11 % increase for LAPWS and ~10 % increase for HAPWS (Table 7-3). This observation can be attributed to higher production of both solid and liquid products during fermentation-fast pyrolysis processing of PWS (~65 daf, wt.% average normalised to PWS), when compared to stand-alone fast pyrolysis of PWS (~60 daf, wt.% average normalised to PWS).

7.3.4 Chemicals production from FR

Table 7-4 displays the chemical yields obtained during VP, SP and FP of the FRs at different temperatures. Of the chemicals quantified in the FR liquids, levoglucosan was ranked highest in yield (~0.1 to 1.0 daf, wt.%) and was promoted under FP conditions probably due to the higher heating rate enhancing glycosidic bond cleavage [13,14,29]. Significantly higher FP levoglucosan yields were obtained for stand-alone pyrolysis of PWS (~0.9 to ~1.5 daf, wt.% for LAPWS; ~1.9 to 3.7 daf, wt.%) [29] when compared to those obtained by FR (~0.6 to 1.0 daf, wt.% for LAFR; ~0.4 to 0.6 daf, wt.% for HAFR) (Table 7-4), probably due to the greater availability of cellulose (Table 7-1) [37].

The yields of 1st and 2nd lignin compounds were enhanced during VP conversion of both FR (Table 7-4), which could be attributed to the limitation of secondary reactions by the quick removal of volatiles [29]. Comparison of the total phenol yield (sum of 1st and 2nd lignin) obtained for VP of

FR (~0.29 to 0.33 daf, wt.% for LAFR; ~0.10 to 0.15 daf, wt.% for HAFR) to those obtained during VP of PWS (~0.17 to 0.25 daf, wt.% for LAPWS; ~0.02 to 0.10 daf, wt.% for HAPWS) [29], revealed an increase which is explained by the higher lignin content (Table 7-1) [37].

7.3.5 Biomaterial production from FR

The DFT surfaces areas of the PWS and FR chars generated during vacuum, slow and fast pyrolysis are presented in Table 7-5. The char DFT surface areas were enhanced during VP for LAFR and during SP for HAFR (Table 7-5), which is similar to previous findings on PWS (Table 7-5) [29]. The DFT surfaces areas displayed by the LAFR (~254 to 353 $m^2.g^{-1}$) and HAFR (~70 to 104 $m^2.g^{-1}$) chars were higher than those of LAPWS (~240 to 286 $m^2.g^{-1}$) and HAPWS (~46 to 66 $m^2.g^{-1}$) chars (Table 7-5), independently of pyrolysis process and temperature. This observation could be explained by the lower ash contents within FRs (~10 to 18 wt.% for LAFR; ~70 to 82 wt.% for HAFR) and PWS (~23 to 33 wt.% for LAPWS; ~81 to 92 wt.% for HAPWS) (Figure 7-6) [23].

7.4 CONCLUSION

PWS-derived FRs were subjected to three pyrolysis technologies to explore the potential of the liquid and solid products for energy, chemicals and biomaterials applications, but also to improve the overall energy recovery by performing hybrid fermentation-pyrolysis processing. The pyrolytic conversion of the FRs via fast pyrolysis offered the highest gross energy conversions for LAFR (~43 and 57 %) and HAFR (~8 and 15 %) when compared to SP and VP. The combination of PWS fermentation with FR fast pyrolysis led to the highest overall gross ECs of between ~75 to 88 % for LAPWS, and ~41 to 48 % for HAPWS. Moreover, these latter gross ECs were found to be up ~11 % higher for LAPWS, and ~10 % higher for HAPWS when compared to stand-alone fast pyrolysis of PWS. For both PWSs, this observation was mainly attributed to higher production of both liquid

and solids during fermentation-fast pyrolysis processing of PWS, when compared to stand-alone FP of PWS. The higher levels of lignin in the FR, after fermentation pre-treatment of PWS, led to enhanced yields of char that displayed increased energy content, probably due to the greater availability of benzene rings. Furthermore, the FR pyrolysis liquid products were rich in phenol compounds which could have potential market value if isolated. Fermentation pre-treatment also resulted in slight improvements in the sorptive properties of the char biomaterials.

Acknowledgments

This work was financially supported by Kimberly-Clark SA, the Paper Manufacturers Association of South Africa (PAMSA) and FP&M Seta. The authors would like to thank these organisations for their support.

7.5 REFERENCES

[1] M.C. Monte, E. Fuente, A. Blanco, C. Negro, Waste management from pulp and paper production in the European Union, Waste Management (29) (2009) 293-308.

[2] H. Chen, R. Venditti, R. Gonzalez, R. Phillips, H. Jameel, S. Park, Economic evaluation of the conversion of industrial paper sludge to ethanol, Energy Economic, (44) (2014) 281-290.

[3] Y. Yamashita, A. Kurosumi, C. Sasaki, Y. Nakamura, Ethanol production from paper sludge by immobilized Zymomonas mobilis, Biochemical Enginnering Journal, (42) (2008) 314-319.

[4] L. Peng, Y. Chen, Conversion of paper sludge to ethanol by separate hydrolysis and fermentation (SHF) using Saccharomyces cerevisiae, Biomass and Bioenergy (35) (2011) 1600-1606.

[5] Y. Shen, L. Jarboe, R. Brown, Z. Wen, A thermochemical-biochemical hybrid processing of lignocellulosic biomass for producing fuels and chemicals, Biotechnology Advances, doi:10.1016/j.biotechadv.2015.10.006

[6] Z. Wang, W. Lin, W. Song, X. Wu, Pyrolysis of the lignocellulose fermentation residue by fixed-bed micro reactor, Energy (43) (2012) 301-305.

[7] Z. Yang, B. Zhang, X. Chen, Z. Bai, H. Zhang, Studies on pyrolysis of wheat straw residues from ethanol production by solid-state fermentation, Journal of Analytical and Applied Pyrolysis (81) (2008) 243-246.

[8] S. Kern, M. Halwachs, G. Kampichler, C. Pfeifer, T. Proll, H. Hofbauer, Rotary kiln pyrolysis of straw and fermentation residues in a 3 MW pilot plant – Influence of pyrolysis temperature on pyrolysis product performance, Journal of Analytical and Applied Pyrolysis (97) (2012) 1-10.

[9] A.V. Bridgwater, Principles and practices of biomass fast pyrolysis processes for liquids, Journal of Analytical and Applied Pyrolysis (51) (1999) 3-22.

[10] A.V. Bridgwater, Review of fast pyrolysis of biomass and product upgrading, Biomass and Bioenergy (38) (2012) 68-94.

[11] Putun AE, Onal E, Uzun BB, Ozbay N. Comparison between the “slow” and “fast” pyrolysis of tobacco residue. Industrial Crops and Products 2007; 26: 307-314.

[12] Duman G, Okutucu C, Ucar S, Stahl R, Yanik J. The slow and fast pyrolysis of cherry seed. Bioresource Technology 2011; 102: 1869-1878.

[13] C.E. Greenhalf, D.J. Nowakowski, A.B. Harms, J.O. Titiloye, A.V. Bridgwater, Sequential pyrolysis of willow SRC at low and high heating rates – Implications for selective pyrolysis, Fuel (93) (2012) 692-702.

[14] H. Ben, A.J. Ragauskas, Comparison for the compositions of fast and slow pyrolysis oils by NMR characterization, Bioresource Technology (147) (2013) 577-584.

[15] Basat M, Balat M, Kirtay E, Balat H. Main routes for the thermo-conversion of biomass into fuels and chemicals. Part 1: Pyrolysis systems. Energy conversion and Management 2009; 50: 3147-3157.

[16] V. Mamleev, S. Bourbigot, M. Le Bras, J. Yvon, The facts and hypotheses relating to the phenomenological model of cellulose pyrolysis: Interdependence of steps, Journal of Analytical and Applied Pyrolysis (84) (2009) 1-17.

[17] P.R. Patwardhan, R.C. Brown, B.H. Shanks, Product distribution from the fast pyrolysis of hemicellulose, ChemSusChem (4) (2011) 636-643.

[18] M. Asmadi, H. Kawamoto, S. Saka, Gas- and solid/liquid-phase reactions during pyrolysis of softwood and hardwood lignins, Journal of Analytical and Applied Pyrolysis (92) (2011) 417-425.

[19] Carrier M, Hugo T, Gorgens J, Knoetze H. Comparison of slow and vacuum pyrolysis of sugar cane bagasse. Journal of Analytical and Applied Pyrolysis 2011; 90: 18-26.

[20] Zaror CA, Hutchings IS, Pyle DL, Stiles HN, Kandiyoti R. Secondary char formation in the catalytic pyrolysis of biomass. Fuel 1985; 64: 990-994.

[21] Mohan D, Pittman CU, Steel PH. Pyrolysis of wood/biomass for bio-oil: A critical review. Energy and Fuels 2006; 20: 848-889.

[22] Chiaramonti D, Oasmaa A, Solantausta Y. Power generation using fast pyrolysis liquids from biomass. Renewable and Sustainable Energy Reviews 2007; 11: 1056-1086.

[23] A. Ridout, M. Carrier, F. Collard, J. Gorgens, Energy conversion assessment of vacuum, slow and fast pyrolysis processes for low and high ash paper waste sludge, Energy Conversion and Management (111) (2016) 103-114.

[24] W. Liu, F. Zheng, H. Jiang, X. Zhang, Preparation of high adsorption capacity bio-chars from waste biomass, Bioresource Technology (102) (2011) 8247-8252.

[25] R. Alen, E. Kuoppala, P. Oesch, Formation of the main degradation compound groups from wood and its components during pyrolysis. Journal of Analytical and Applied Pyrolysis (36) (1996) 137-148.

[26] T. Werpy, G. Petersen, Top value added chemicals from biomass: Volume 1 – Results of screening for potential candidates from sugars and synthesis gas, U.S. Department of Energy, Oak Ridge, 2004.

[27] R.A. Sheldon, Green and sustainable manufacture of chemicals from biomass: state of the art, Green Chemistry (16) (2014) 950-963.

[28] M. Amutio, G. Lopez, R. Aguado, M. Artetxe, J. Bilbao, M. Olazar, Effect of vaccum on lignocellulosic biomass flash pyrolysis in a conical spouted bed reactor, Energy and Fuels (25) (2011) 3950-3960.

[29] A. Ridout, M. Carrier, F. Collard, J. Gorgens, Chemicals and biomaterials production from vacuum, slow and fast pyrolysis processes for low and high ash paper waste sludge, a paper that will be submitted to the journal of Bioresource and Technology.

[30] A. Mendez, J.M. Fidalgo, F. Guerrero, G. Gasco, Characterization and pyrolysis behaviour of different paper mill waste materials, Journal of Analytical and Applied Pyrolysis (86) (2009) 66-73.

[31] Q. Lu, Z. Zhang, C. Dong, X. Zhu, Catalytic upgrading of biomass fast pyrolysis vapors with nano metal oxides: An analytical Py-GC/MS study, Energies (3) (2010) 1805-1820.

[32] P.R. Patwardhan, J.A. Satrio, R.C. Brown, B.H. Shanks, Influence of inorganic salts on the primary pyrolysis products of cellulose, Bioresource Technology (101) (2010) 4646-3655.

[33] F. Collard, J. Blin, A review on pyrolysis of biomass constituents: Mechanisms and composition of the products obtained from the conversion of cellulose, hemicellulose and lignin, Renewable and Sustainable Energy Reviews (38) (2014) 594-608.

[34] S. Boshoff, L. Gottumukkala, E. van Rensburg, J. Gorgens, Paper sludge to bioethanol: Evaluation of virgin and recycle mill sludge for low enzyme, high-solids fermentation, Bioresource and Technology (203) (2016) 103-111.

[35] X. Zhang, G. Yang, H. Jiang, W. Liu, H. Ding, Mass production of chemicals from biomass-derived oil by directly atmospheric distillation coupled with co-pyrolysis, Scientific Reports (3) 1120-1127.

[36] Y. Elkasabi, C.A. Mullen, A.A. Boateng, Distillation and isolation of commodity chemicals from bio-oil made by tail-gas reactive pyrolysis, Sustainable Chemistry and Engineering (2) (2014) 2042-2052.

[37] A.J. Ridout, M. Carrier, J. Gorgens, Fast pyrolysis of low and high ash paper waste sludge: Influence of reactor temperature and pellets size, Journal of Analytical and Applied Pyrolysis (111) (2015) 64-75.

[38] M. Widyawati, T.L. Church, N.H. Florin, A.T. Harris, Hydrogen synthesis from biomass pyrolysis with in situ carbon dioxide capturing using calcium oxide, Journal of Hydrogen Energy (36) (2011) 4800-4813.

[39] R.A Mott, C.E. Spooner, The calorific value of carbon in coal: the Dulong relationship, Fuel (19) (1940) 242-251.

[40] D. Lozano-Castello, D. Cazorla-Amoros, A. Linares-Solano, Usefulness of CO_2 adsoprtion at 273 K for the characterization of porous carbons, Carbon (42) (2004) 1231-1236.

[41] R.A. Meyers, Coal structure, Academic Press, U.S.A., pp61-62.

[42] J. Landers, G.Y. Gor, A.V. Neimark, Density functional theory methods for characterization of porous materials, Colloids and Surfaces A: Physicochemical and Engineering Aspects (437) (2013) 3-32.

[43] N.A. Seaton, J.P.R.B Walton, N. Quirke, A new analysis method for the determination of the pore size distribution of porous carbons from nitrogen adsorption measurements, Carbon (27) (1989) 853-861.

[44] S.A. Channiwala, P.P. Parikh, A unified correlation for estimating HHV of solid, liquid and gaseous fuels, Fuel (81) (2002) 1051-1063.

[45] Exxon Mobil (2015, October), Product safety summary: Isopar G fluid [pdf], Available: www.exxonmobilchemical.com

[46] D.J. Nowakowski, A.V. Bridgwater, D.C. Elliot, D. Meier, P. de Wild, Lignin fast pyrolysis: Results from an international collaboration, Journal of Analytical and Applied Pyrolysis (88) (2010) 53-72.

[47] Kurose R, Ikeda M, Makino H. Combustion characteristics of high ash coal in a pulverized coal combustion. Fuel 2001; 80: 1447-1455.

[48] Jayanti S, Maheswaran K, Saravanan V. Assessment of the effect of high ash content in pulverized coal combustion. Applied Mathematical Modelling 2007; 31: 934-953.

Table 7-1. Physico-chemical characterisation of LAPWS and HAPWS, and its fermentation residues, LAFR and HAFR

	LAPWS	HAPWS	LAFR	HAFR
Moisture content (wt.%)	20.9	4.9	4.3	2.6
Ash (525 °C)	3.1	27.9	4.1	41.3
Proximate Analysis (df, wt.%)				
Volatile Matter	82.3	62.1	79.5	50.9
Fixed Carbon	14.6	9.5	16.5	6.5
Ash (900 °C)	3.1	21.1	4.0	31.0
Lignocellulosic composition (daf, wt.%)[a]				
Extractives	3.7	8.6	14.0	23.1
Cellulose	57.4	57.8	32.4	28.3
Hemicelluloses	17.3	19.4	15.2	14.0
Lignin	21.6	14.2	38.4	34.6
Ultimate Analysis (daf, wt.%)				
C	49.6	43.8	47.9	49.6
H	7.3	6.5	6.1	7.3
N	0.9	0.2	0.8	0.9
O + S (by difference)	51.2	49.5	45.2	42.2
HHV (MJ/kg)	18.8	13.1	18.0	11.3

[a] Boshoff *et al.* [34]

Table 7-2. Inorganic composition of LAFR and HAFR from XRF analysis

	Inorganic content (wt.%)										
	Al_2O_3	CaO	Cr_2O_3	Fe_2O_3	K_2O	MgO	MnO	Na_2O	P_2O_5	SiO_2	TiO_2
LAFR	0.64	0.41	0.01	0.19	0.05	0.14	0.01	0.35	0.07	1.83	0.05
HAFR	5.69	12.1	0.00	0.35	0.14	0.62	0.00	0.19	0.16	8.4	0.9

Table 7-3. Conversion of energy from PWS into products using either pyrolysis or integrated fermentation and pyrolysis processing

		PWS – pyrolysis ECs[a] (%)				FR - integrated process ECs (%)					
		RT	**EC_{char}**	**$EC_{bio\text{-}oil/tarry}$**	**EC_{pyro}**	**RT**	**EC_{char}**	**$EC_{bio\text{-}oil/tarry}$**	**EC_{pyro}**	**EC_{ferm}**	**$EC_{ferm\text{-}pyro}$**
Low ash	VP	300	31.5	21.5	53.0	300	32.9	13.1	46.0	31.3	77.3
		425	34.2	18.3	52.5	425	24.8	11.6	36.4	31.3	67.7
		550	27.5	16.9	44.3	550	25.4	12.9	38.2	31.3	69.5
	SP	340	38.0	-	38.0	300	33.9	-	33.9	31.3	65.2
		460	35.1	-	35.1	425	34.4	-	34.4	31.3	59.0
		580	32.3	-	32.3	550	27.7	-	27.7	31.3	65.7
	FP	300	41.3	35.9	77.2	300	43.7	13.5	57.2	31.3	88.4
		425	30.4	39.1	69.4	425	22.4	20.8	43.2	31.3	74.5
		550	29.9	29.3	59.2	550	23.8	28.3	52.1	31.3	83.4
High ash	VP	300	-	11.7	11.7	300	-	8.8	8.8	32.8	41.6
		425	-	11.7	11.7	425	-	9.7	9.7	32.8	42.5
		550	-	11.7	11.7	550	-	8.9	8.9	32.8	41.7
	SP	340	-	-	-	300	-	-	-	32.8	32.8
		460	-	-	-	425	-	-	-	32.8	32.8
		580	-	-	-	550	-	-	-	32.8	32.8
	FP	290	-	31.8	31.8	300	-	8.0	8.0	32.8	40.8
		340	-	37.5	37.5	425	-	15.0	15.0	32.8	47.8
		390	-	25.2	25.2	550	-	8.1	8.1	32.8	40.9

[a] Ridout *et al.* [23]; RT: reactor temperature (°C); VP: vacuum pyrolysis; SP: slow pyrolysis; FP: fast pyrolysis; EC: energy conversion; FR: fermentation residue.

Table 7-4. Yield of chemicals from vacuum, slow and fast pyrolysis of LAFR and HAFR at different reactor temperatures

			Chemical yields (daf, wt.%)														
			Lignin-derived compounds									Carbohydrate-derived compounds					
		RT	4-vinylguaicol	Eugenol	Apocycnin	Phenol	Guaiacol	2,3-Dimethyl phenol	2,6-Dimethyl phenol	1st Lignin	2nd Lignin	2-Furanmethanol	2(5H)-Furanone	5-Hydroxymethyl furfural	Levoglucosan	Glycolaldehyde	2-Cyclopenten-1-one
LAFR	VP	300	0.137	0.093	0.021	0.016	0.057	0.007	0.005	0.252	0.085	0.049	0.075	0.019	0.427	0.256	0.000
		425	0.083	0.094	0.023	0.023	0.049	0.007	0.006	0.201	0.085	0.045	0.079	0.017	0.379	0.129	0.000
		550	0.103	0.088	0.023	0.030	0.075	0.007	0.007	0.213	0.120	0.064	0.109	0.023	0.311	0.213	0.001
	SP	300	0.003	0.002	0.007	0.009	0.034	0.001	0.001	0.011	0.044	0.022	0.049	0.020	0.332	0.213	0.031
		425	0.004	0.003	0.009	0.009	0.043	0.001	0.002	0.016	0.055	0.040	0.062	0.029	0.286	0.236	0.021
		550	0.002	0.001	0.005	0.007	0.030	0.000	0.001	0.009	0.038	0.029	0.042	0.018	0.225	0.162	0.022
	FP	300	0.015	0.018	0.027	0.009	0.026	0.002	0.005	0.060	0.043	0.029	0.159	0.093	0.628	0.301	0.019
		425	0.025	0.051	0.042	0.022	0.059	0.007	0.008	0.118	0.096	0.049	0.155	0.065	0.694	0.194	0.029
		550	0.007	0.007	0.020	0.013	0.016	0.001	0.001	0.034	0.031	0.028	0.090	0.046	1.044	0.439	0.022
HAFR	VP	300	0.026	0.035	0.020	0.020	0.011	0.005	0.006	0.081	0.042	0.019	0.053	0.000	0.297	0.000	0.002
		425	0.036	0.034	0.020	0.031	0.015	0.007	0.009	0.089	0.063	0.023	0.074	0.000	0.313	0.009	0.002
		550	0.023	0.021	0.015	0.019	0.011	0.004	0.007	0.059	0.040	0.017	0.052	0.000	0.249	0.000	0.000
	SP	300	0.002	0.001	0.004	0.004	0.009	0.000	0.002	0.007	0.015	0.012	0.037	0.005	0.109	0.095	0.038
		425	0.002	0.001	0.004	0.007	0.008	0.000	0.003	0.007	0.019	0.015	0.047	0.003	0.193	0.066	0.043
		550	0.001	0.000	0.003	0.005	0.006	0.000	0.002	0.004	0.013	0.009	0.030	0.002	0.092	0.099	0.034
	FP	300	0.007	0.011	0.016	0.018	0.021	0.003	0.005	0.034	0.046	0.020	0.069	0.017	0.393	0.143	0.010
		425	0.012	0.017	0.022	0.028	0.030	0.004	0.005	0.051	0.066	0.039	0.097	0.012	0.571	0.220	0.017
		550	0.004	0.005	0.011	0.013	0.010	0.001	0.001	0.020	0.025	0.021	0.066	0.000	0.445	0.024	0.011

RT: reactor temperature (°C); VP: vacuum pyrolysis; SP: slow pyrolysis; FP: fast pyrolysis.

Table 7-5. DFT surface areas ($m^2.g^{-1}$) of PWS and FR-derived chars from vacuum, slow and fast pyrolysis.

Feedstock	VP	SP	FP
LAPWS[a]	286.8 [b]	244.3[c]	240.2[b]
LAFR	353.1 [b]	254.2 [b]	257.4 [b]
HAPWS[a]	55.2 [b]	65.7 [c]	46.2[d]
HAFR	75.9 [b]	103.8 [b]	70.3 [b]

[a] Ridout *et al.* [29]; [b] 425 °C; [c] 460 °C; [d] 390 °C

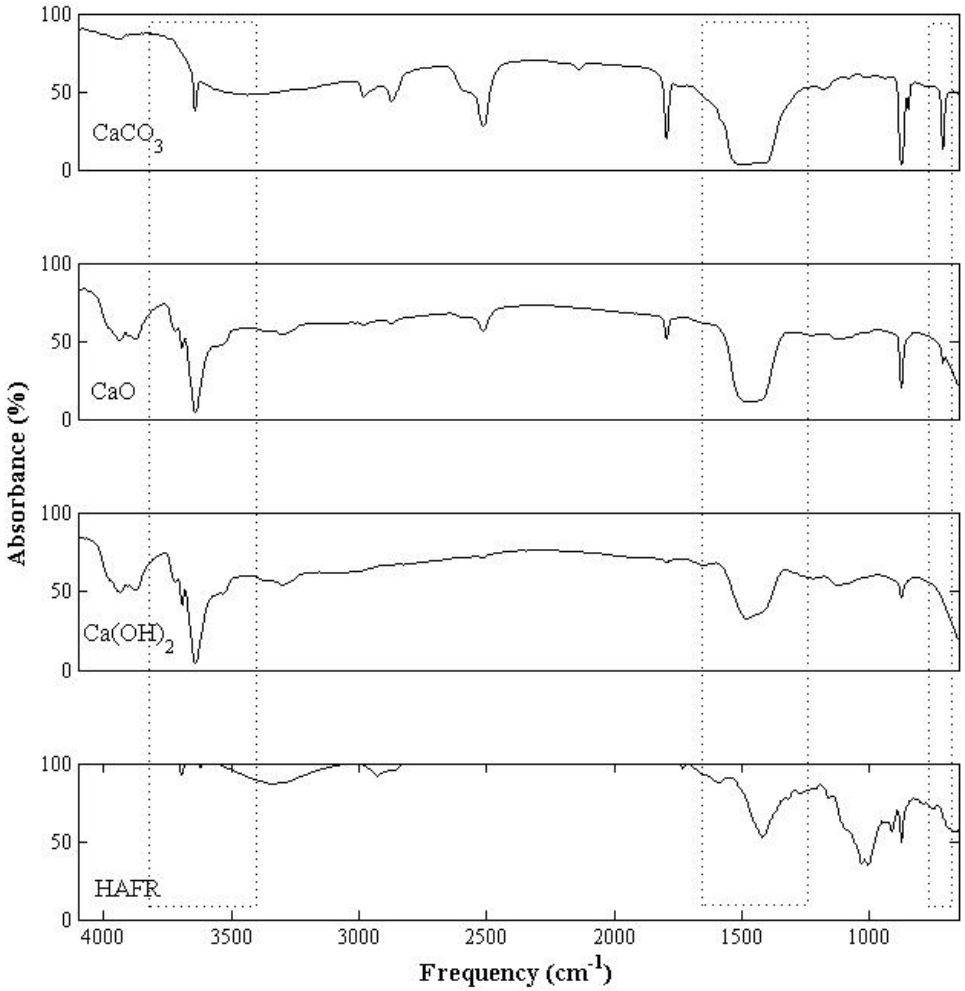

Figure 7-1. IR spectra of $CaCO_3$, CaO, $Ca(OH)_2$ and HAFR.

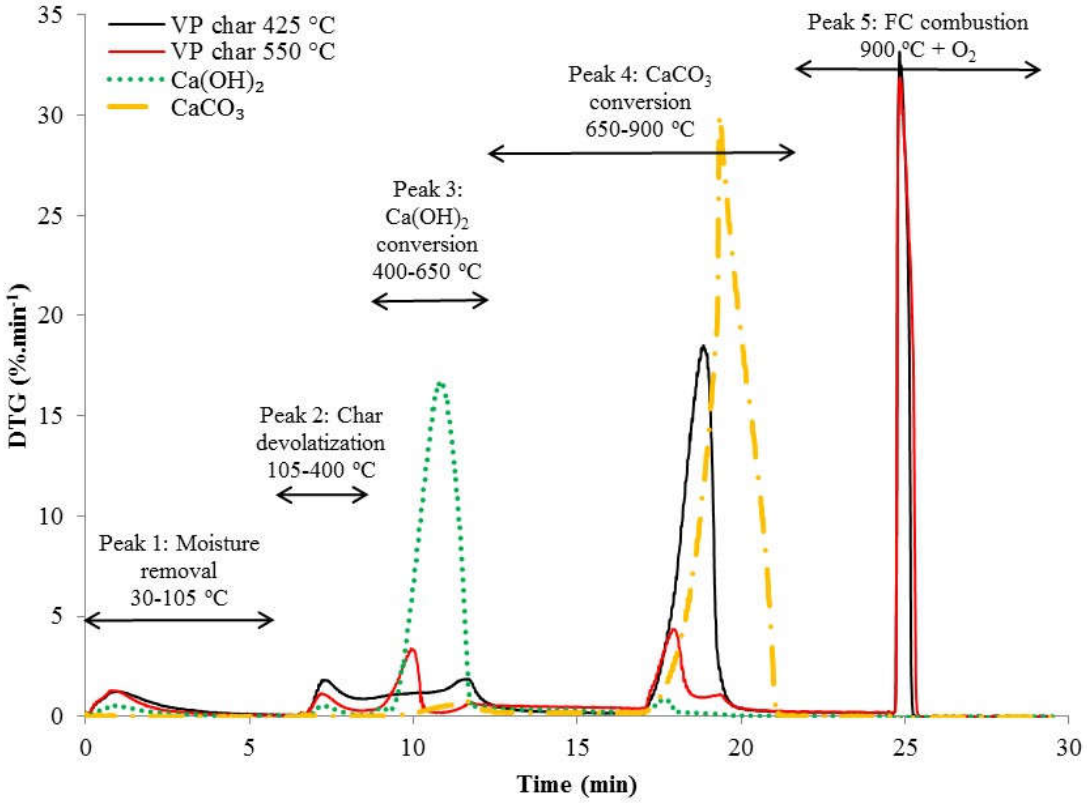

Figure 7-2. Altered proximate analysis DTG curves of char obtained from vacuum pyrolysis of HAFR, as well as $Ca(OH)_2$ and $CaCO_3$.

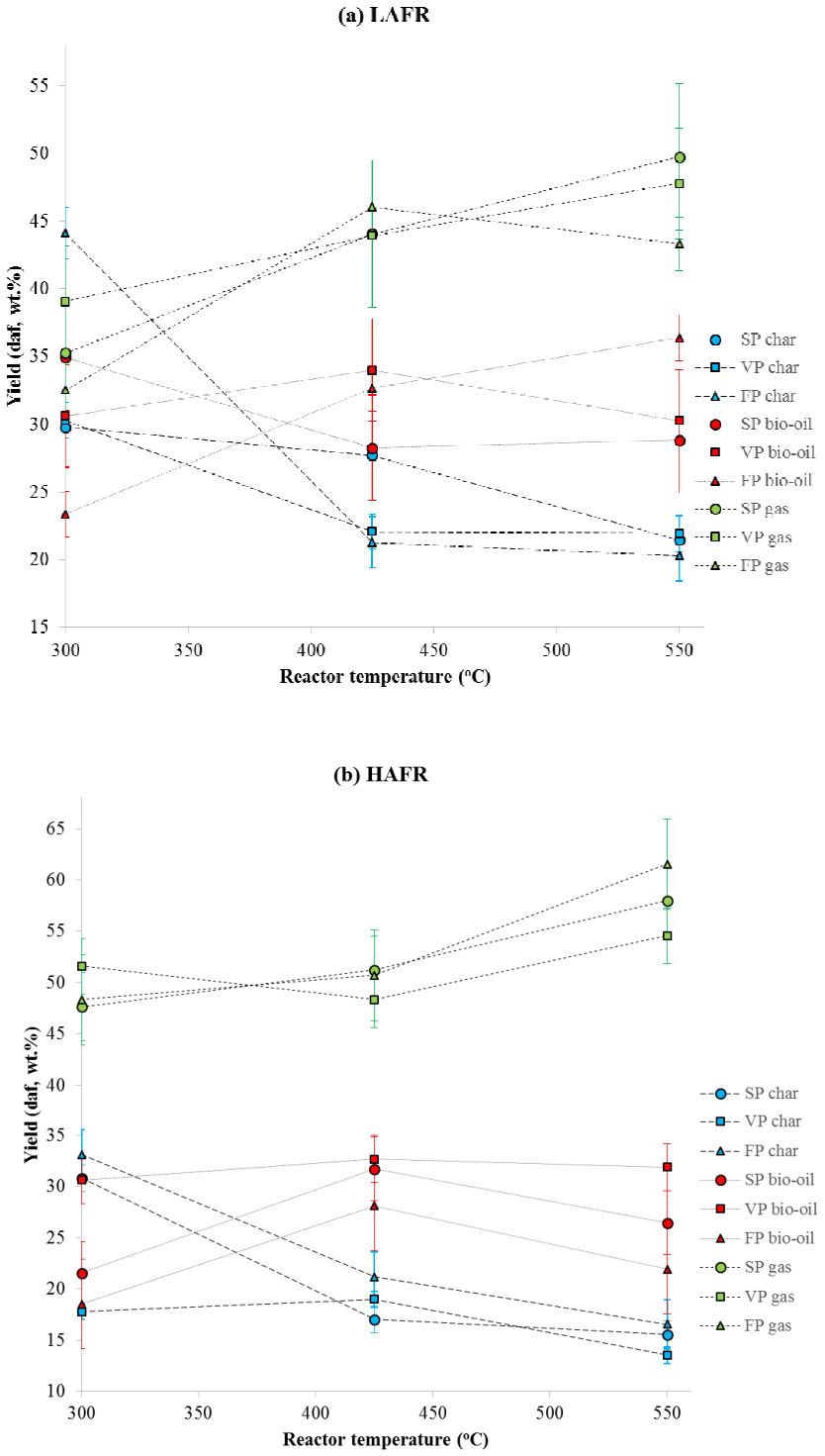

Figure 7-3. Yield of char, bio-oil and non-condensable gas from vacuum, slow and fast pyrolysis conversion of LAFR (a) and HAFR (b) at different reactor temperatures.

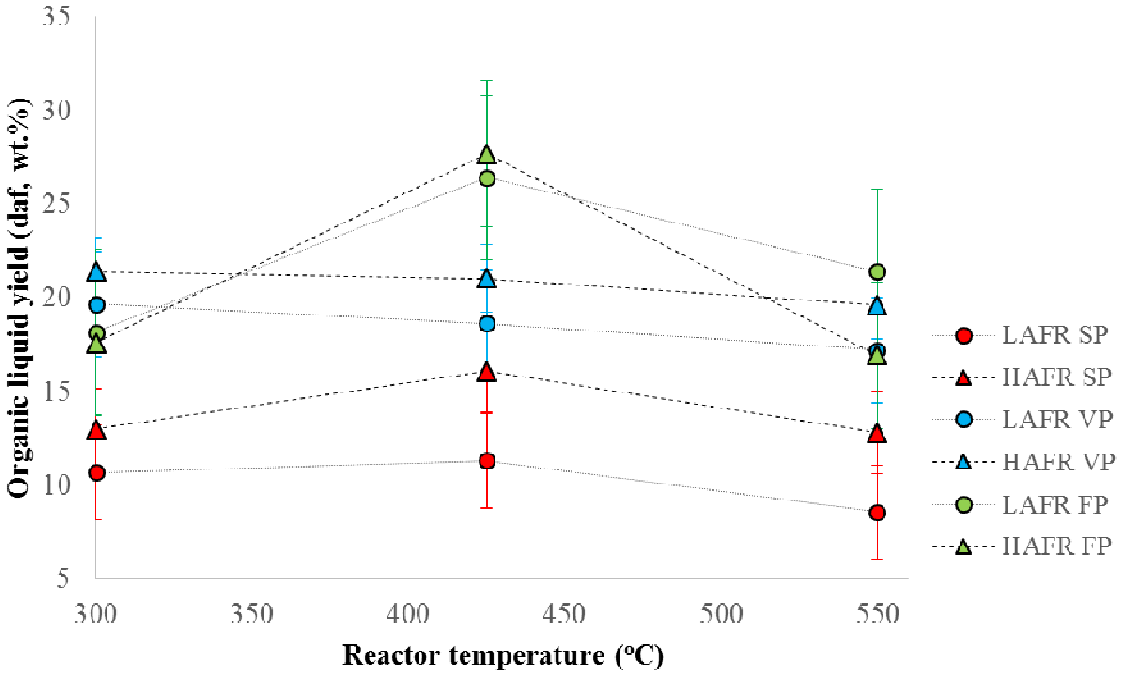

Figure 7-4. Yield of organic liquid from vacuum, slow and fast pyrolysis conversion of LAFR and HAFR at different reactor temperatures.

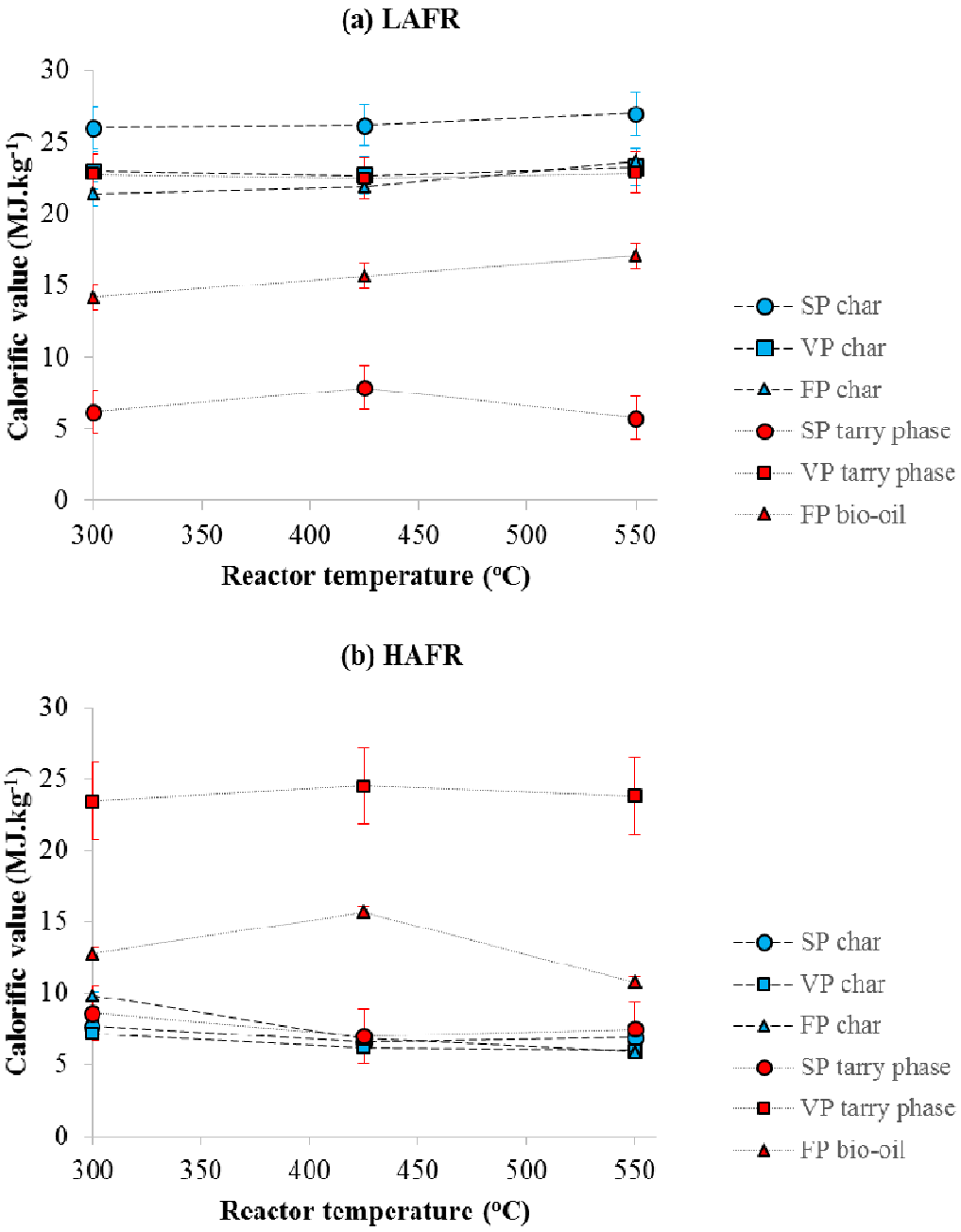

Figure 7-5. Calorific values of chars and bio-oil/tarry phases produced during slow, vacuum and fast pyrolysis of LAFR (a) and HAFR (b) at various reactor temperatures.

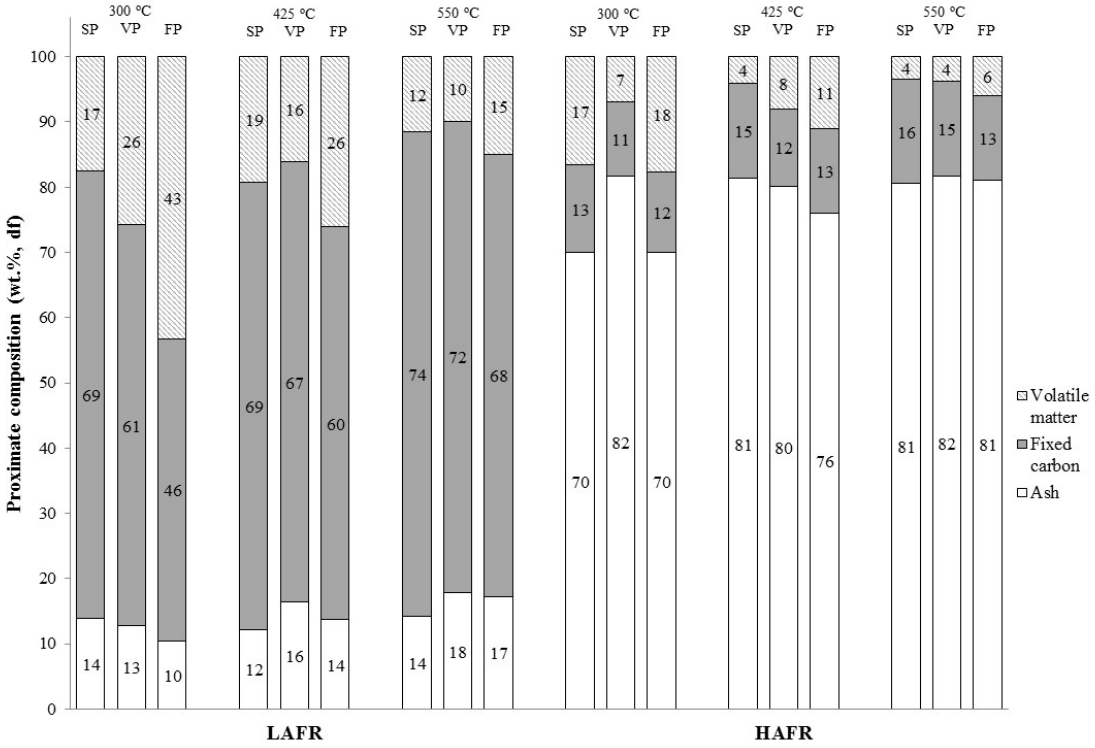

Figure 7-6. Proximate composition of chars generated during vacuum, slow and fast pyrolysis of LAFR and HAFR at different reactor temperatures.

CHAPTER 8: SUMMARY OF MAIN FINDINGS

The global aim of this dissertation was to investigate the full potential of various pyrolysis processes as part of a biorefinery to convert PWS and its FR into energy, chemical and biomaterial products. This chapter summarises the most significant findings of the results in Chapters 4 to 7.

8.1 PYROLYSIS OF PAPER WASTE SLUDGE

This section presents the results on stand-alone pyrolysis of paper waste sludge (**Chapters 4 to 6**). Low and high ash paper waste sludge were subjected to vacuum, slow and fast pyrolysis, at various key operating conditions, to maximise the yield of liquid and solid products, as well the energy recovery thereof. Furthermore, the potential the liquid and solid products for energy, chemical and biomaterial production was investigated. Product yields and physico-chemicals characteristics were also compared to reveal new thermodynamic and chemical mechanisms.

8.1.1 Maximisation of liquid and solid pyrolysis product yields

The low and high ash PWS (8.5 and 46.7 wt.%) were subjected to fast pyrolysis (fluidised bed) to maximise the bio-oil yield by optimising the reactor temperature and pellet size using a 2-way linear and quadratic model (**Chapter 4**). The optimal reactor temperatures for maximisation of the bio-oil yields were 400 ºC and 340 ºC for LAPWS and HAPWS (see Figure 4-2), respectively, and were significantly lower than reported optima for other lignocellulosic biomass (450 to 550 ºC). These low temperatures were attributed to the catalytic effect of calcium on primary reactions. At the pellet size of ~5 mm and respective optimum reactor temperature, maximum bio-oil yields of 44.5 daf, wt.% for LAPWS and above 50 daf, wt.% for HAPWS were attained (see Figure 4-2).

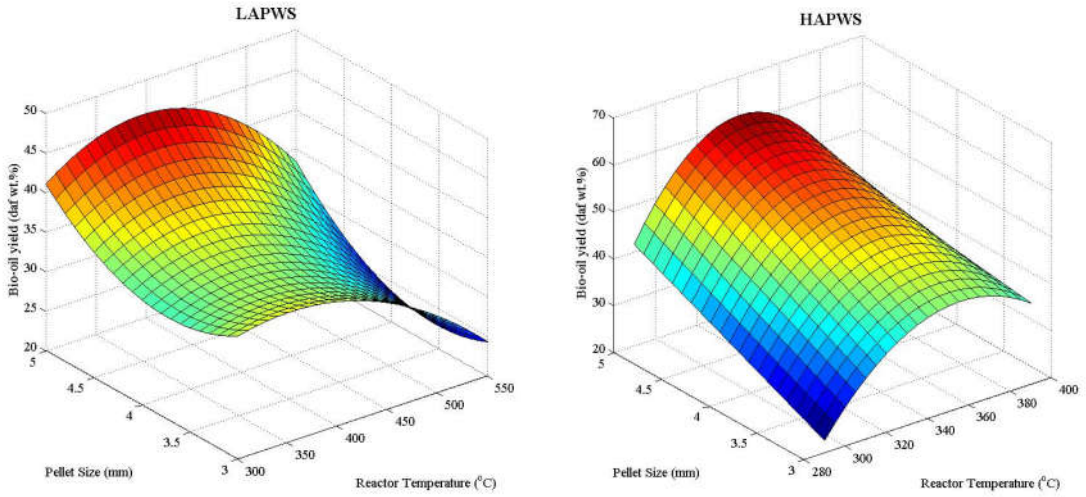

Figure 4-2. Evolution of bio-oil product yields (daf, wt.%) from fast pyrolysis conversion of LAPWS and HAPWS for different reactor temperatures and pellet sizes.

Comparison of the fast pyrolysis char and bio-oil yields to that obtained during vacuum and slow pyrolysis revealed interesting results (**Chapter 5**). On a similar temperature range for both PWSs, the char yields displayed by SP were highest, followed by FP then VP (see Figure 5-2), due to the promotion of secondary formation reactions by longer vapour residence times. For both PWSs, the maximum VP bio-oil yields were lower than those of SP and FP (see Figure 5-7). Unlike most studies that report higher bio-oil yields for FP, SP and FP displayed similar bio-oil yields for both PWSs. This observation can be explained by differences in the pyrolytic water yield, whereby SP had the highest and FP the lowest (see Figure 5-8). The large production of pyrolysis water during SP was attributed to the increased occurrence of dehydration reaction during char formation

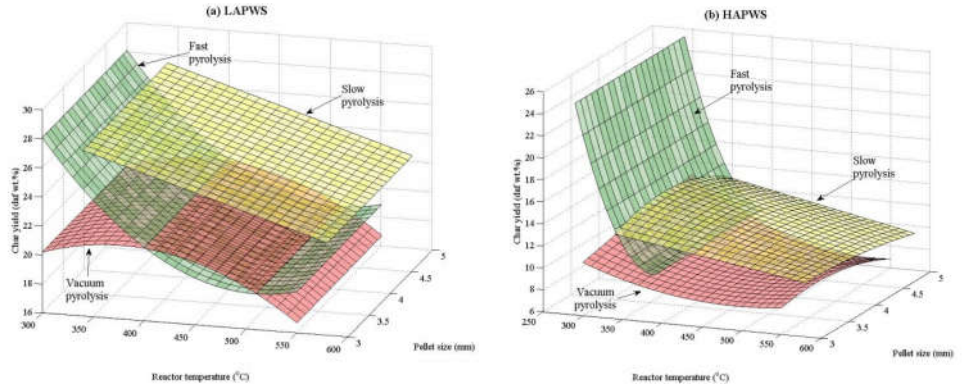

Figure 5-2. Dependence of char yield on reactor temperature and pellet size during vacuum, slow and fast pyrolysis conversion of LAPWS (a) and HAPWS (b).

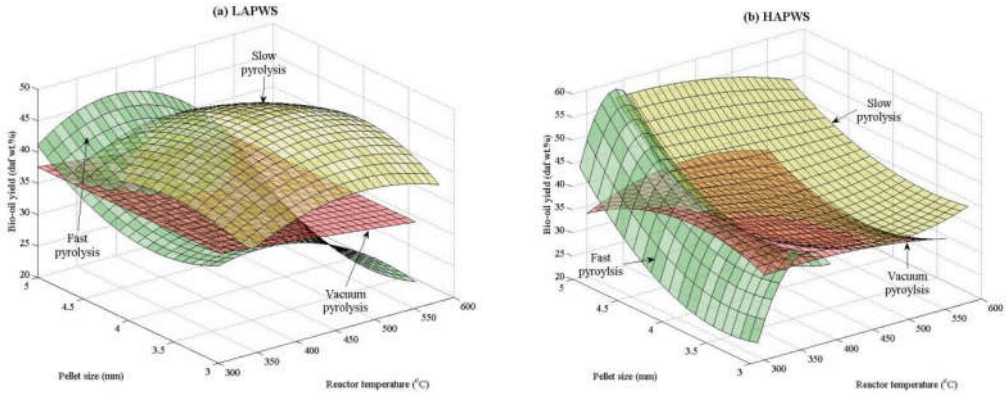

Figure 5-7. Dependence of bio-oil yield on reactor temperature and pellet size during vacuum (a-b), slow (c-d) and fast (e-f) pyrolysis of LAPWS (a,c,e) and HAPWS (b,d,f).

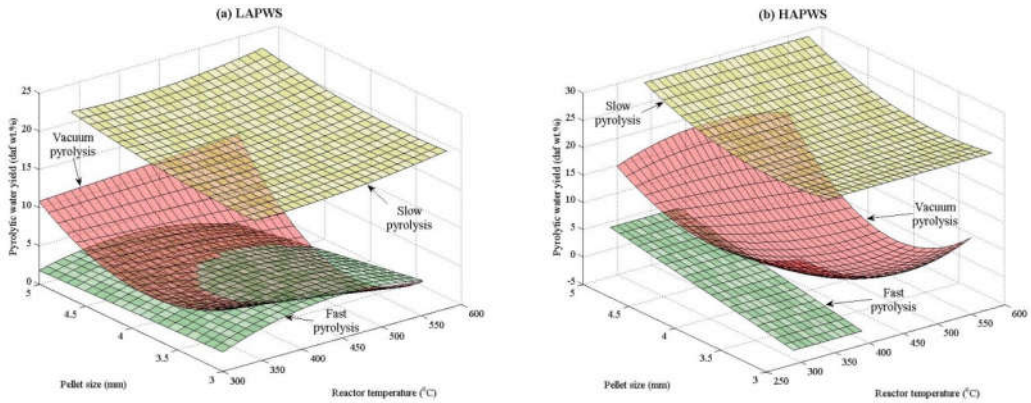

Figure 5-8. Evolution of pyrolytic water from vacuum, slow and fast pyrolysis of LAPWS (a) and HAPWS (b) for different reactor temperatures and pellet sizes.

8.1.2 Thermogravimetric study

In general, the use of a small particle sizes promote the production of bio-oil during fast pyrolysis (**Chapter 4**) by allowing for a regime in which the kinetics are predominantly controlled by chemical reactions, rather than heat and mass transfer. This general trend was not applicable to FP of PWS, since the highest bio-oil yields were attained with an intermediate pellet size range of ~5 to 6 mm (see Figure 4-3). Subsequently, a thermogravimetric analysis (TGA) was implemented to investigate the pyrolytic mechanisms behind the increase in bio-oil yield with intermediate pellets sizes (**Chapter 4**). The TGA indicated that the decrease in the bio-oil yield at smaller particle sizes was due to an increase in non-condensable gas yield (see Figure 4-9). This increase in non-condensable gas yield was associated with an increase in exothermic secondary reactions for high heating rates using smaller pellet sizes, and was apparently catalysed by the presence of inorganics in PWS (see Figure 4-10). At higher pellet sizes of ~6 mm, mass and heat transfer limitations were more significant resulting in lowered bio-oil yields and increased char formation explaining the optimum observed in the pellet size (~5 to 6 mm) (Figure 4-3).

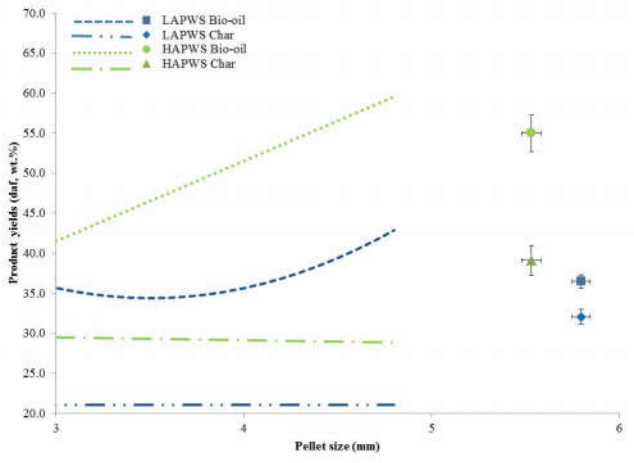

Figure 4-3. Experimental product yields (daf, wt.%) (dots) and model data points (curves) at optimal reactor temperatures for LAPWS (400 °C) and HAPWS (340 °C) for different pellet sizes.

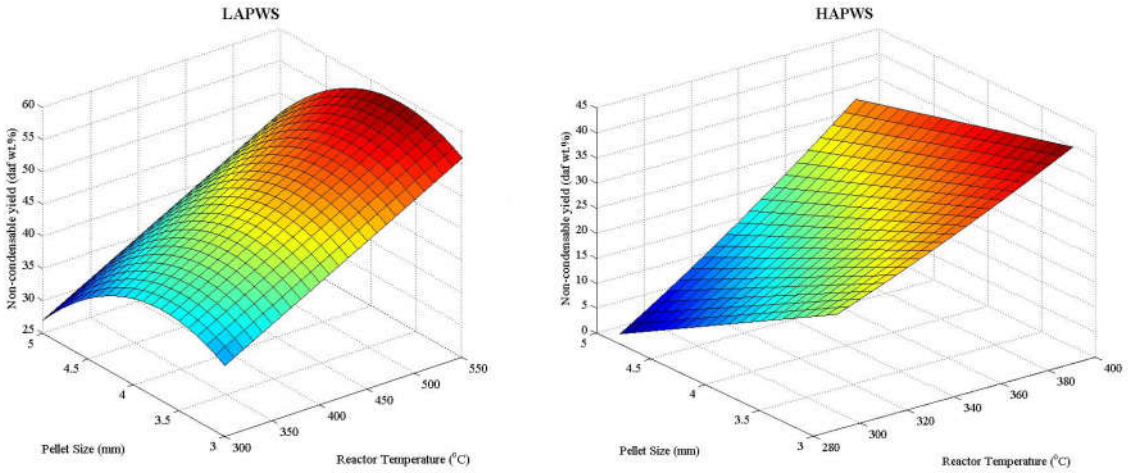

Figure 4-9. Evolution of non-condensable gas product yields (daf, wt.%) from fast pyrolysis conversion of LAPWS and HAPWS for different reactor temperatures and pellet sizes.

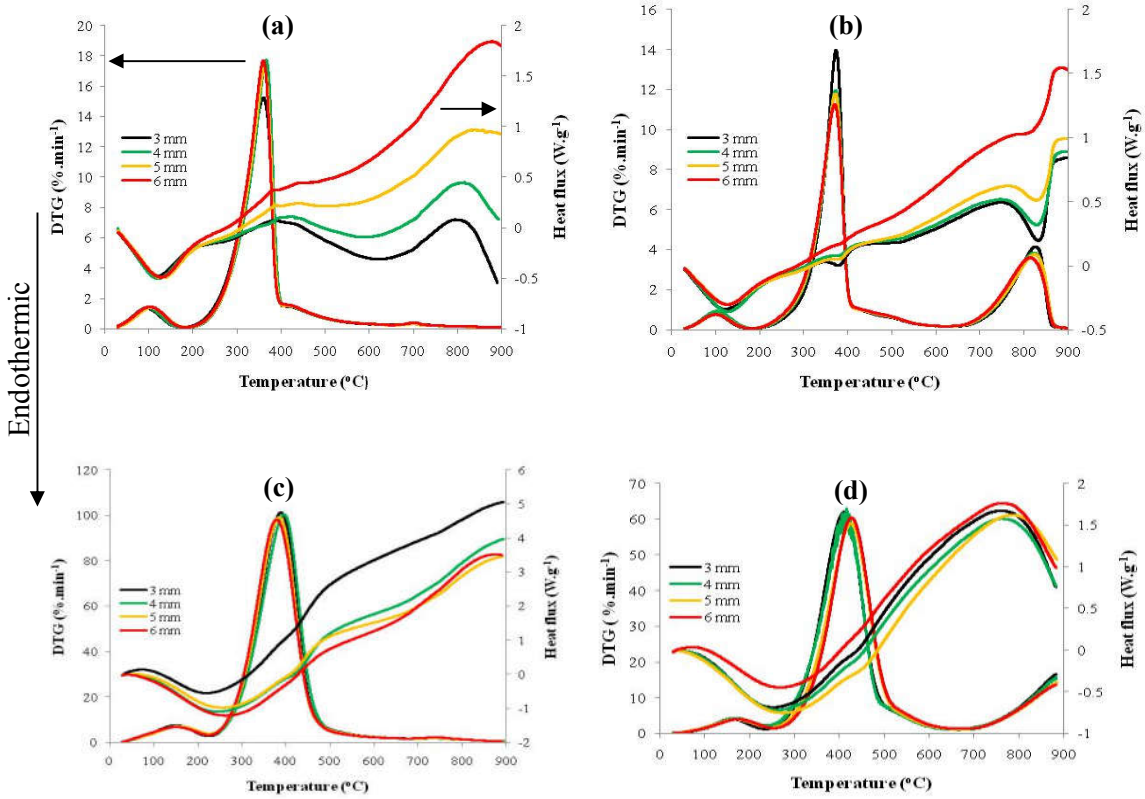

Figure 4-10. DTG and heat flux curves for LAPWS (a-c) and HAPWS (b-d) obtained at heating rates of 20 °C.min^{-1} (a-b) and 150 °C.min^{-1} (c-d) for different pellet sizes.

8.1.3 Energy conversion assessment

An energy assessment based on gross energy conversion of vacuum, slow and fast pyrolysis at varying reactor temperatures and pellet sizes was performed to compare performances (**Chapter 5**). Moreover, the suitability of the liquid and solid products for industrial energy applications was assessed. Comparison of the $EC_{sum\text{-}max}$ between the pyrolysis processes indicated that FP was highest at between 18.5 to 20.1 % for LAPWS, and 18.4 to 36.5 % for HAPWS when compared SP and VP (see Figure 5-6). This finding was mainly attributed to higher production of organic condensable compounds during FP for both PWSs (see Figures 5-7 and 5-8).

The LAPWS-derived char calorific values, which were enhanced at higher temperatures, were high at between ~21 to 23 $MJ.kg^{-1}$ (independently of process type) making them promising for industrial energy applications such as coal substitution (see Figure 5-3). On the other hand, due to an inherently large presence ash content (> 80 wt.%), HAPWS-derived char caloric values were low (~3 to 7 $MJ.kg^{-1}$ independently of process type) making them unsuitable for industrial application due to possible slagging and fouling during combustion. Thus, it was recommended that HAPWS should rather be converted to FP bio-oil to maximise the recovery of usable energy products. The VP tarry phase displayed slightly higher calorific values (19.9 to 22.3 $MJ.kg^{-1}$ for LAPWS; 22.5 to 24.4 $MJ.kg^{-1}$ for HAPWS) when compared to the FP bio-oil (17.6 to 22.2 $MJ.kg^{-1}$ for LAPWS; 14.4 to 19.7 $MJ.kg^{-1}$ for HAPWS) for both PWSs, due to a lower water content (~3 to 7 wt.% for VP; ~40 to 58 wt.% for FP). On the contrary, due to the high water content (~40 to 58 wt.%) in the SP tarry phases, calorific values were significantly lower (7.5 to 9.5 $MJ.kg^{-1}$ for LAPWS; 8.2 to 13.0 $MJ.kg^{-1}$ for HAPWS) making them unsuitable for industrial energy applications. Both the SP and VP aqueous phases contained a high water content (~75 wt.%) and thus were not considered for energy applications.

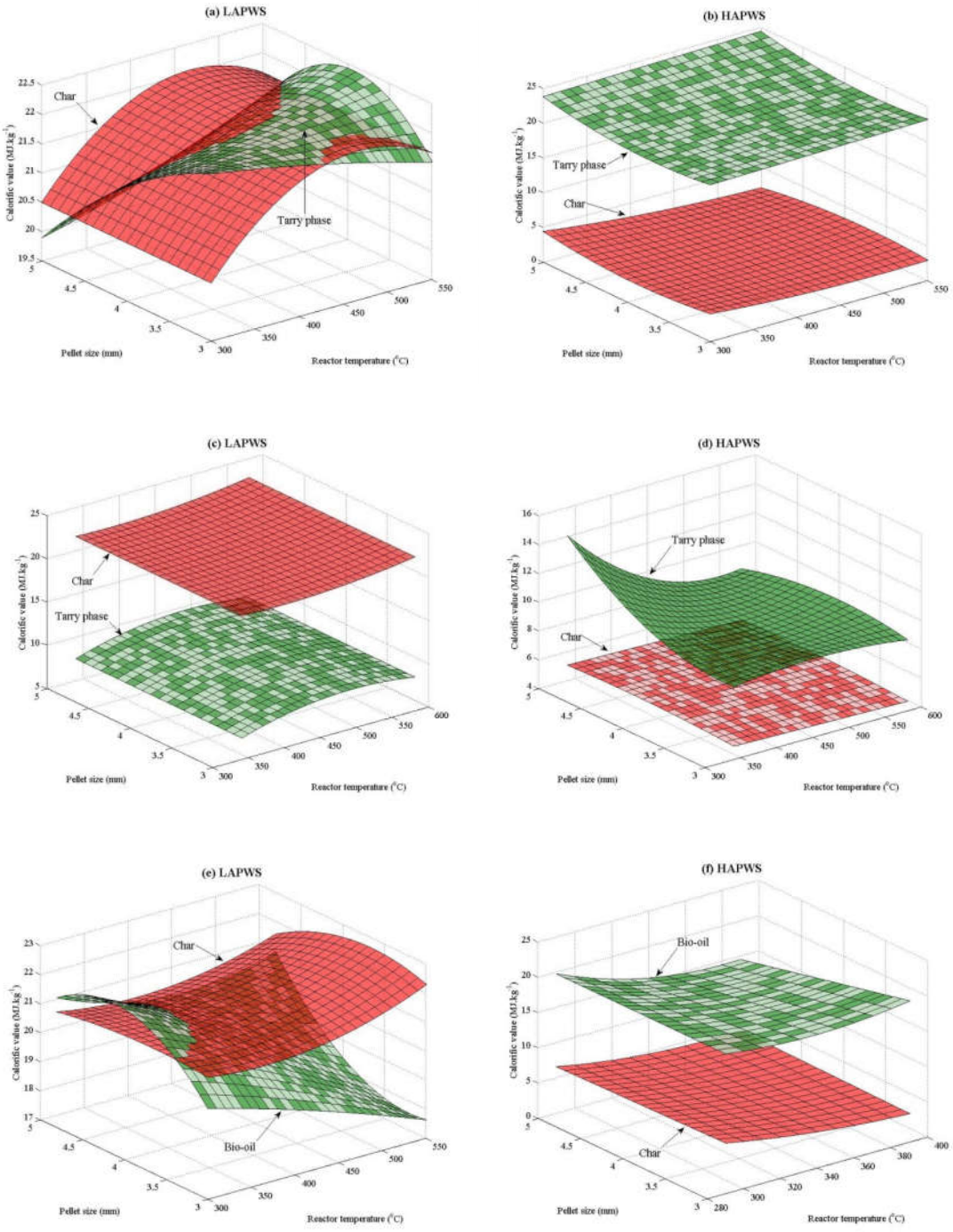

Figure 5-3. Calorific values of chars and bio-oil/tarry products obtained from the vacuum (a-b), slow (c-d) and fast (e-f) pyrolysis of LAPWS (a,c,f) and HAPWS (b,d,f) according to reactor temperature and pellet size.

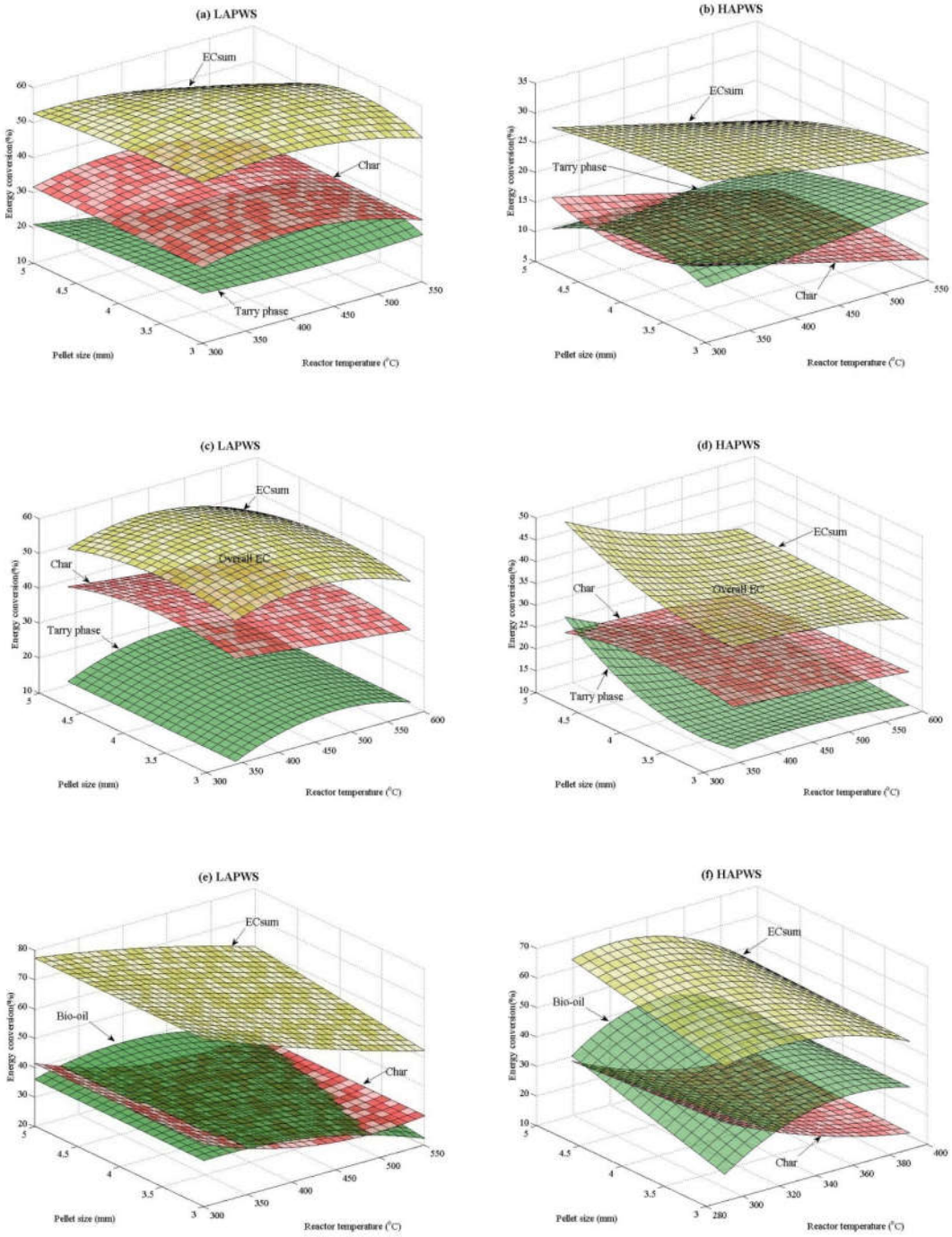

Figure 5-6. Dependence of energy conversion from PWS to its vacuum (a-b), slow (c-d) and fast (e-f) pyrolysis bio-oil/tarry and char products on reactor temperature and pellet size. (EC_{sum}: Sum of char and bio-oil/tarry EC)

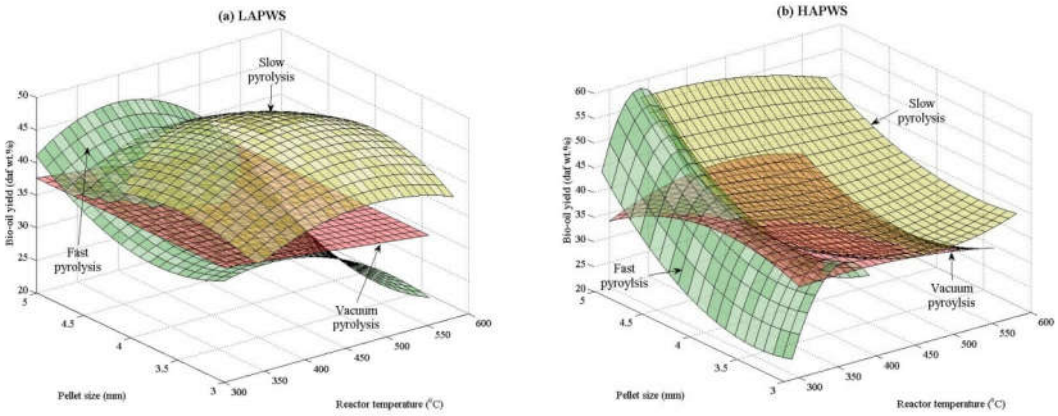

Figure 5-7. Dependence of bio-oil yield on reactor temperature and pellet size during vacuum (a-b), slow (c-d) and fast (e-f) pyrolysis of LAPWS (a,c,e) and HAPWS (b,d,f).

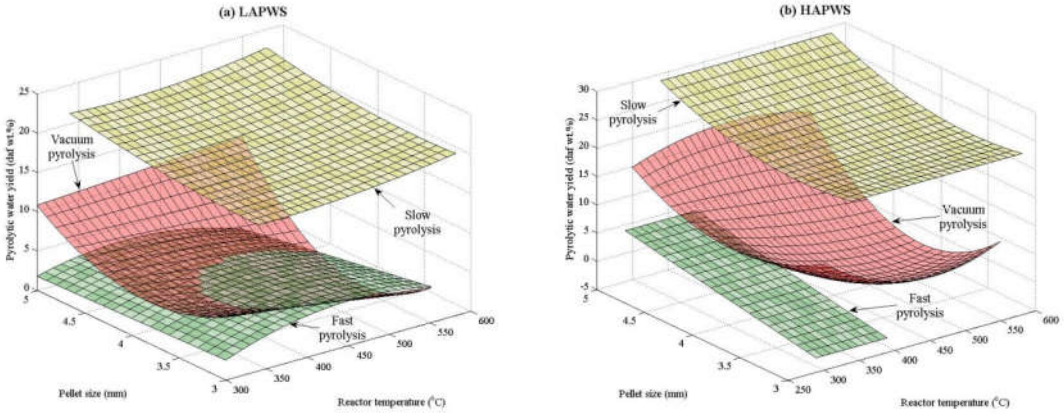

Figure 5-8. Evolution of pyrolytic water from vacuum, slow and fast pyrolysis of LAPWS (a) and HAPWS (b) for different reactor temperatures and pellet sizes.

8.1.4 Chemicals and biomaterials production

Vacuum, slow and fast pyrolysis technologies were evaluated at varying key operating conditions, reactor temperature and pellet size, for their ability to selectively drive the conversion of low and high PWS into renewable chemicals and biomaterials (**Chapter 6**). To do this, product

yields were optimised according to the reactor temperature and pellet size using a statistical design of experiments, and their variability quantified using principal component analysis (PCA).

The type of pyrolysis technology was found to have a greater influence on the selectivity of chemicals than the reactor temperature and pellet size. In particular, the heating rate employed during fast pyrolysis enhanced glycosidic bond cleavage resulting in large levoglucosan yields for both PWSs. In addition to the heating rate, the catalytic effect of inorganics during FP of HAPWS was prevalent, whereby higher yields of levoglucosan (3.7 daf, wt.%, 340 ^{o}C), at lower temperatures, were attained when compared to LAPWS (1.5daf, wt.%, 430 ^{o}C) (see Figure 6-3). Furthermore, the production of furans, phenols and glycolaldehyde was also promoted during FP of HAPWS.

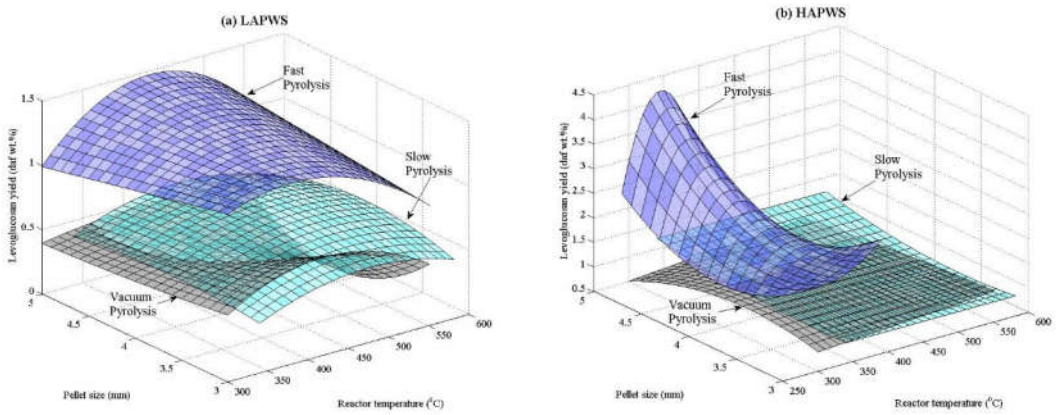

Figure 6-3. Production of levoglucosan from vacuum, slow and fast pyrolysis conversion of LAPWS (a) and HAPWS (b) at different reactor temperatures and pellet sizes.

The biomaterials displayed by both PWSs were found to be ultra-microporous (> 1 nm), and could have promising applications in areas such as gas separation (carbon molecular sieve) and pollutant removal from contaminated water. An increase in temperature led to greater CO_2 volumes adsorbed and microporous development leading to higher DFT surface area for both PWSs (see

Figure 6-6). For LAPWS, the promotion of devolatilization during vacuum pyrolysis resulted in chars that exhibited the highest DFT surface areas (281 to 344 $m^2.g^{-1}$) when compared to SP (200 to 309 $m^2.g^{-1}$) and FP (157 to 236 $m^2.g^{-1}$). For HAPWS however, the application of VP showed no significant differences in DFT surface area when compared to SP and VP. The DFT surface area displayed by HAPWS-derived chars (28 to 66 $m^2.g^{-1}$ independently of process type) where significantly lower than LAPWS, possibly due to the filling of pores with inorganics and/or lower organic content (see Figure 5-5).

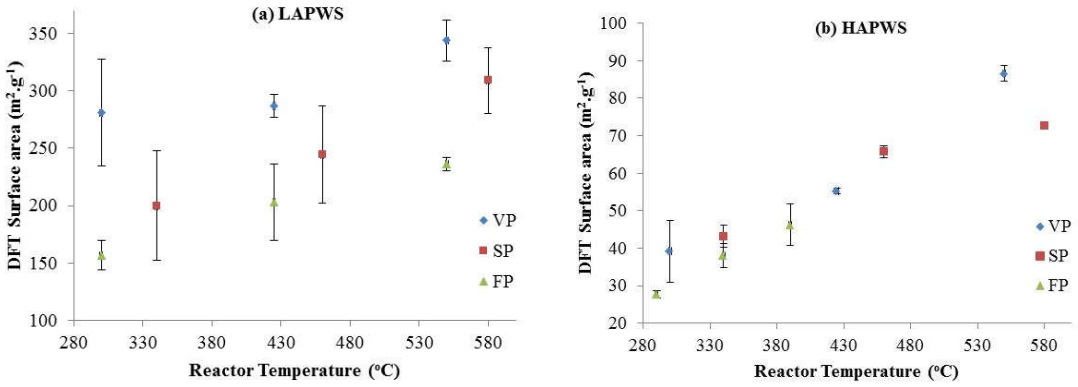

Figure 6-6. DFT pore surface areas of LAPWS (a) and HAPWS (b) vacuum, slow and fast pyrolysis chars at different reactor temperatures.

8.2 PYROLYSIS OF FERMENTATION RESIDUE

This section presents the results on the sequential fermentation and pyrolysis processing of paper waste sludge (**Chapter 7**). The fermentation residues from the fermentation of low and high ash paper waste sludge were converted into energy, chemicals and biomaterials (i.e., sorbent, biochar) products using vacuum, slow and fast pyrolysis. Furthermore, the effect of the

fermentation on the pyrolysis product yields and properties, as well as on the recovery of energy, was investigated by comparing results to stand-alone pyrolysis of PWS (**Chapter 4 to 6**).

8.2.1 Effect of fermentation pre-treatment

Fermentation of PWS significantly reduced cellulose content resulting in FRs that displayed higher levels of lignin (~35 daf, wt.%). Larger average char yields (independent of pyrolysis process and temperature) were obtained for LAFR (26.3 daf, wt%) and HAFR (20.4 daf, wt%) when compared to LAPWS (21.7 daf, wt%) and HAPWS (11.7 daf, wt%). This observation was attributed to the higher lignin content in the FRs, a constituent known to promote chars yields due to the greater availability of benzene rings, which form the char complex. On the contrary, the LAPWS (37.5 daf, wt.%) and HAPWS (44.3 daf, wt.%) displayed higher average bio-oil yields when compared to LAFR (31.0 daf, wt.%) and HAFR (27.1 daf, wt.%), thus confirming the key role of the carbohydrate fraction in the production of condensable volatiles. The greater availability of lignin in FR, after fermentation pre-treatment of PWS, led to phenols-rich bio-oil products. The DFT surface areas displayed by the FR chars were slightly higher than those of PWS.

8.2.2 Energy conversion assessment

To enhance the energy recovery of fermentation processes, the fermentation residues were converted into usable solid and liquid energy products using vacuum, slow and fast pyrolysis at varying reactor temperatures. An energy conversion assessment was performed considering only the products that displayed potential for utilization in industrial energy applications.

The VP tarry phase and FP bio-oil of both FRs, as well as the LAFR char, displayed high calorific values (~15 to 27 $MJ.kg^{-1}$) and have potential for industrial energy applications. On the

other hand, the HAFR chars, SP tarry phase as well as the SP and VP aqueous phases were not suitable for energy application due to poor quality and low calorific values.

Comparison of the gross energy conversion (EC) between the pyrolysis processes for FR conversion, revealed that FP was highest at between ~43 and 57 % for LAFR, and ~8 and 15 % for HAFR when compared to VP (~36 and 46 % for LAFR; ~9 and 10 % for HAFR) and SP (~28 and 34 % for LAFR; ~0 % for HAFR) (see Table 7-3). The combination of fermentation of PWS and fast pyrolysis of FR resulted in the highest overall gross ECs of between ~75 and 88% for the LAPWS, and ~41 and 48 % for the HAPWS. Moreover, these latter gross ECs were up to ~10 % higher in comparison to the ECs obtained during stand-alone fast pyrolysis of PWS (see Table 7-3). This finding was attributed to an increased yield of both liquid and solid products during fermentation-fast pyrolysis conversion of PWS (~65 daf, wt.% average normalised to PWS), when those of stand-alone fast pyrolysis of PWS were lower (~60 daf, wt.% average normalised to PWS).

Table 7-3. Conversion of energy from PWS into products using either pyrolysis or integrated fermentation and pyrolysis processing

		PWS – pyrolysis ECs[a] (%)				FR - integrated process ECs (%)					
		RT	**EC_{char}**	**$EC_{bio\text{-}oil/tarry}$**	**EC_{pyro}**	**RT**	**EC_{char}**	**$EC_{bio\text{-}oil/tarry}$**	**EC_{pyro}**	**EC_{ferm}**	**$EC_{ferm\text{-}pyro}$**
Low ash	VP	300	31.5	21.5	53.0	300	32.9	13.1	46.0	31.3	77.3
		425	34.2	18.3	52.5	425	24.8	11.6	36.4	31.3	67.7
		550	27.5	16.9	44.3	550	25.4	12.9	38.2	31.3	69.5
	SP	340	38.0	-	38.0	300	33.9	-	33.9	31.3	65.2
		460	35.1	-	35.1	425	34.4	-	34.4	31.3	59.0
		580	32.3	-	32.3	550	27.7	-	27.7	31.3	65.7
	FP	300	41.3	35.9	77.2	300	43.7	13.5	57.2	31.3	88.4
		425	30.4	39.1	69.4	425	22.4	20.8	43.2	31.3	74.5
		550	29.9	29.3	59.2	550	23.8	28.3	52.1	31.3	83.4
High ash	VP	300	-	11.7	11.7	300	-	8.8	8.8	32.8	41.6
		425	-	11.7	11.7	425	-	9.7	9.7	32.8	42.5
		550	-	11.7	11.7	550	-	8.9	8.9	32.8	41.7
	SP	340	-	-	-	300	-	-	-	32.8	32.8
		460	-	-	-	425	-	-	-	32.8	32.8
		580	-	-	-	550	-	-	-	32.8	32.8
	FP	290	-	31.8	31.8	300	-	8.0	8.0	32.8	40.8
		340	-	37.5	37.5	425	-	15.0	15.0	32.8	47.8
		390	-	25.2	25.2	550	-	8.1	8.1	32.8	40.9

[a] Ridout *et al.* [23]; RT: reactor temperature (°C); VP: vacuum pyrolysis; SP: slow pyrolysis; FP: fast pyrolysis; EC: energy conversion; FR: fermentation residue.

CHAPTER 9: CONCLUSION AND RECOMMENDATIONS

This study has provided the groundwork for which the pulp and paper industry can develop a biorefinery strategy to valorise their paper waste sludge in a more environmentally way, with the potential to develop additional income from the pyrolysis products. From the experimental results presented in this dissertation, the main conclusion and the recommendations are discussed in this chapter.

9.1 CONCLUSIONS

9.1.1 Pyrolysis of paper waste sludge

For the first time, valorisation of a high and low ash PWS via fast pyrolysis has been performed. Maximum bio-oil yields of 44.5 daf, wt.% at 400 ^{o}C, and 54.5 daf, wt.% at 340 ^{o}C for an intermediate pellet size of 4.84 mm were attained for LAPWS and HAPWS, respectively. For HAPWS, this bio-oil yield was not only higher but was attained at lower temperature when compared to literature, certainly due to the catalytic effect of inorganics on primary reactions.

The application of various pyrolysis processes resulted in significant differences in the product distribution. The SP char yield was highest, followed by FP then VP for both PWSs, which was attributed to increased secondary recombination reactions by longer vapour residence times. On the other hand, the higher heating rates employed by FP significantly enhanced the production of condensable organic volatiles, whereas SP displayed the highest pyrolytic water yields.

The thermogravimetric study provided a new novel understanding on the thermodynamic mechanisms behind pyrolysis of PWS at varying pellet sizes. Intermediate pellet sizes maximised the bio-oil yield during FP, which is contrary to trends often observed in literature. This finding was

attributed to smaller pellet sizes promoting non-condensable gas production by enhancing the number of secondary exothermic cracking reactions, which were catalysed by inorganics.

An energy assessment of the three pyrolysis processes pointed out the potential of FP for energy production. Comparison of the gross ECs, as a combination of char and bio-oil/tarry phase, indicated that FP performance was between 18.5 and 20.1 % higher for LAPWS, and 18.4 and 36.5 % higher for HAPWS when compared SP and VP. This observation was mainly attributed to the enhanced production of condensable organic volatiles and lower water yields during FP.

The pyrolysis technology was shown to have a greater influence on chemical yields than the reactor temperature and pellet size. In particular, the high heating rates employed during FP enhanced glyosidic bond cleavage resulting in higher levoglucosan yields for both PWS. The presence of inorganics in HAPWS catalysed these reactions resulting in a higher yield and lower optimum temperature for levoglucosan (3.7 daf, wt.%, 340 ^{o}C) when compared to LAPWS (1.5 daf, wt.%, 430 ^{o}C). Furthermore, promotions were also observed in the production of phenols, furans and glycolaldehyde.

The utilization vacuum pyrolysis, as well as higher temperatures, promoted the char CO_2 adsorbed volume and micropore development leading to greater DFT surface areas for LAPWS. On the other hand, no significant differences were observed in the biomaterial adsorbent properties between SP, VP or FP for HAPWS. The DFT surface areas displayed by HAPWS (28 to 66 $m^2.g^{-1}$) were significantly lower than those of LAPWS (281 to 344 $m^2.g^{-1}$), due to the filling of pore with inorganics and/or due to lower organic content.

The PWS liquid and solid products that show promising potential as sources for energy, chemicals (bio-oil) and biomaterials (char) are summarised in Table 9-1. When considering energy content, the calorific values (~18 to 23 $MJ.kg^{-1}$) displayed by the VP tarry phase and FP bio-oil for

both PWSs, as well as the LAPWS char, were high making them suitable for industrial energy applications. The levoglucosan yields were moderate to high (~1 to 4 daf, wt.%) in comparison to literature (~0.1 to 6 daf, wt.%), and thus could be targeted when considering chemicals production. Due to the ultra-microporous nature of these chars, they could find potential biomaterial applications in gas separation or in water treatment for pollutant removal.

Table 9-1. Potential applications for char and bio-oil/tarry phase products generated during vacuum, slow and fast pyrolysis of PWS and FR

		Char		Bio-oil/tarry phase	
		Energy	**Biomaterials**	**Energy**	**Chemicals**
LAPWS	**VP**	Yes	Yes	Yes	Yes
	SP	Yes	Yes	No	Yes
	FP	Yes	Yes	Yes	Yes (ideal)
HAPWS	**VP**	No	Yes	Yes	Yes
	SP	No	Yes	No	Yes
	FP	No	Yes	Yes	Yes (ideal)
LAFR	**VP**	Yes	Yes	Yes	Yes
	SP	Yes	Yes	No	Yes
	FP	Yes	Yes	Yes	Yes
HAFR	**VP**	No	Yes	Yes	Yes
	SP	No	Yes	No	Yes
	FP	No	Yes	Yes	Yes

VP: vacuum pyrolysis; SP: slow pyrolysis; FP: fast pyrolysis.

9.1.2 Pyrolysis of fermentation residue

For the first time PWS-derived low and high ash fermentation residues have been converted using vacuum, slow and fast pyrolysis. The conversion of cellulose during fermentation resulted in heightened levels of lignin in FR. Subsequently this resulted in higher yields of char, and the production of phenols-rich bio-oil.

Fast pyrolysis of the fermentation residues offered the highest gross energy conversion of between ~43 and 57 % for LAFR, and ~8 and 15 % for HAFR when compared to VP and SP. The

combination of fermentation of the PWS followed by FR fast pyrolysis offered the highest overall gross ECs at between ~75 and 88% for the LAPWS, and ~41 and48 % for the HAPWS. In addition, these gross ECs were up to ~10 % higher in comparison to those obtained during stand-alone fast pyrolysis of PWS. This finding was mainly attributed to the higher production of both solid and liquid product during fermentation-fast pyrolysis conversion of PWS, when those of stand-alone fast pyrolysis of PWS were lower.

The potential of the FR pyrolysis products for sources of energy, chemicals and biomaterials are summarised in Table 9-1. The VP tarry phase and FP bio-oil, as well as the LAFR char, displayed high calorific values (~15 to 27 $MJ.kg^{-1}$) and have promising potential for industrial energy applications. High-value phenol compounds could be extracted when considering chemicals production from the FR bio-oil. The ultra-microporous nature of the FR char biomaterials could find application in gas separation or in water treatment (pollutant removal)

9.2 RECOMMENDATIONS

Considering the findings of this work, the following key focus areas are recommended for further research:

9.2.1 Overall process efficiency

While this study has recommended the preferred conditions for maximisation of the gross energy conversion during stand-alone pyrolysis or integrated fermentation and pyrolysis processing, additional modelling studies would be required, taking into account the energy inputs (heat energy for biomass drying, pyrolysis and ethanol distillation) in order to confirm the efficiency of the whole process.

9.2.2 Economic feasibility study

Although this study has pointed out the promising potential of each pyrolysis process in terms of chemicals, energy and/or biomaterials production from low and high PWS/FR, no definitive concept can be recommended. To confirm which concept, namely stand-alone pyrolysis or the integrated fermentation and pyrolysis, an economic feasibility should to be considered within the context of a biorefinery approach. Indeed, this work has provided enough technical data for a subsequent study on the economic feasibility.

9.2.3 Scaling up of fast pyrolysis

When scaling up fast pyrolysis the following needs to be taken into account. As most of the char (pellet form) remains behind (> 90 %) in the bubbling fluidised bed reactor during fast pyrolysis, an overflow off the top of the bed should be considered in the technical design, such that the char is continuously drawn off and transferred elsewhere.

9.2.4 Mathematical modelling study

The thermogravimetric study revealed interesting new mechanistic insights into PWS pyrolysis whereby secondary tar cracking reactions were promoted with smaller pellets sizes due to mass transfer limitations resulting in lower bio-oil yields. To further the understanding of this latter, a full comprehensive mathematical modelling study considering reaction kinetics as well as heat and mass transfer limitations is recommended.

9.2.5 Vacuum fast pyrolysis

The presence of a vacuum was found to enhance the quality of the tarry phase by lowering the water content during vacuum pyrolysis of PWS, while a high heating rate maximised the production of condensable organic compounds during fast pyrolysis of PWS. Considering this latter, it would make for an interesting study if both a vacuum and high heating rate where applied simultaneously to maximise the conversion of PWS into high quality bio-oil product.

APPENDICES

APPENDIX A: PYROLYSIS EXPERIMENTAL EQUIPMENT AND PROCEDURE

A.1 FAST PYROLYSIS

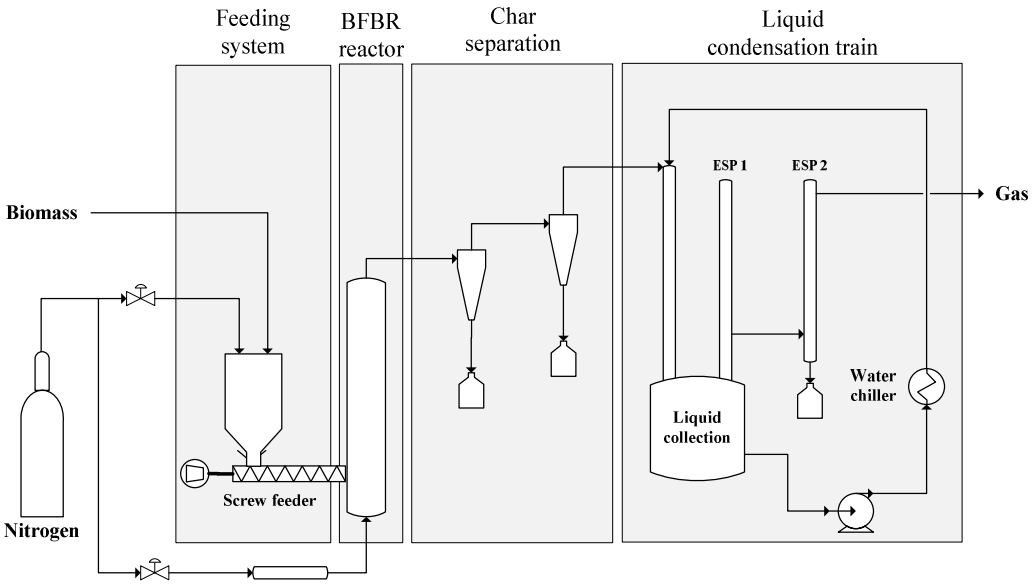

Figure A-1. Schematic diagram of fast pyrolysis unit. (BFBR: bubbling fluidised bed reactor; ESP: electrostatic precipitator)

Appendix A-2. Experimental procedure for fast pyrolysis experiments.

Before the run – Assembly of unit		
Steps	**Check**	**Notes**
Calibrate feeder for biomass with specific particle size, moisture content according to the feeder configuration	Run continuously for 5 minutes in triplicate and use average as flow rate	Avoid bridging
Sieve sand to size fraction of 0.4 - 0.6 mm	400 g per run	
Vacuum clean furnace		Take care to vacuum elements properly as carbon residue can cause hotspots and element melting
Weigh plant sections: • Reactor • Cyclones • Cooling tower • Electrostatic precipitators	Note the fittings included in original weighing of each unit	When equipment parts have an inconvenient shape, make use of bucket to weigh component. Weigh bucket, tare scale, and place equipment inside to determine weigh of equipment
Assemble plant sections and sensors	Fittings lubricated using Nickel spray	
Connect feeder	Gasket in place	
Test for leaks at Nitrogen flow rate of 8 $m^3.hr^{-1}$	Check for leaks at fittings and in piping	Ensures there are no leaks in the system
Assemble oven	Check that oven is sealed with fiber-glass insulation	Take precaution with outlet section
During the run		
Steps	**Check**	**Notes**
Start oven		Wait for oven to reach equilibrium (1 – 1.5 hours)
Add biomass to feeder	Seal rubber with Vaseline	Take sample for water and ash analysis
Flush system with N_2	3 minutes at 0.5 $m^3.hr^{-1}$	
When oven is close to set point temperature (approximately 30min before commencing with run or 100 ºC from set point)		
Open chiller water	Chiller hose should be in sink	
Switch on chiller	Values and leaks	4 ºC lowest temperature for water.
Once oven is a set temperature start N_2 flow	Set flow at 2.4 $m^3.hr^{-1}$	
Start isopar pump	Line pressure: 1.8 - 3 kPa	
Attach pipe heater for oven exit gas	Set temperature at T_3 if below 400 ºC, otherwise set at 400 ºC	Take precaution not to damage equipment
Monitor T_3 and T_4	Temperature (10 ºC)	

Appendix A-2. Continued…

During the run		
Steps	**Check**	**Notes**
Start electrostatic precipitators	Voltage 15 and 12 kV for ESP 1 and 2, respectively	Earth wire is connected
Start jacket cooling water	Ensure jacket hose is in sink	
Check for any problem in system: leaks, low/high pressure		
Insert flash disc for data capture		
Start feeder at calibrated feeding rate	Continuously check for bridging and flow obstruction	Ensure that feeder pressure is higher than reactor pressure
Monitor process during experiment		
Once all biomass fed, continue feeding for 10 minutes		
Reduce N_2 flow	0.5 $m^3.hr^{-1}$	Maintain inert atmosphere
Stop chiller	Close chiller tap	
Switch off ESP		
Redirect gas flow to vent		Maintain N_2 flow rate
Remove flash disc		
Remove oven top when temperature lower than 300 ^oC		Maintain N_2 flow rate
Stop jacket colling water		
Leave unit until cool enough to handle		Maintain N_2 flow rate
After the run		
Steps	**Check**	**Notes**
Dissemble and weigh cooling sections: • Cooling tower • Electrostatic precipitators.		Take care to correlate equipment with initial weighing configuration. These weights form part of the bio-oil yield. Clean section afterwards using acetone.
Collect bio-oil from reservoir		Allow isopar to separate out from the bio-oil. Weigh bio-oil and add to yield calculation.
Collect bio-oil residue from reservoir	Squirt acetone into reservoir and collect run-off in bucket.	Allow 2 days for acetone to evaporate. Add bio-oil reside weight to yield calculation.
Dissemble reactor and cyclones	Weight dirty reactor and cyclones.	Take care to correlate equipment with initial weighing configuration. These weights form part of char yield.

A.2 SLOW/VACUUM PYROLYSIS

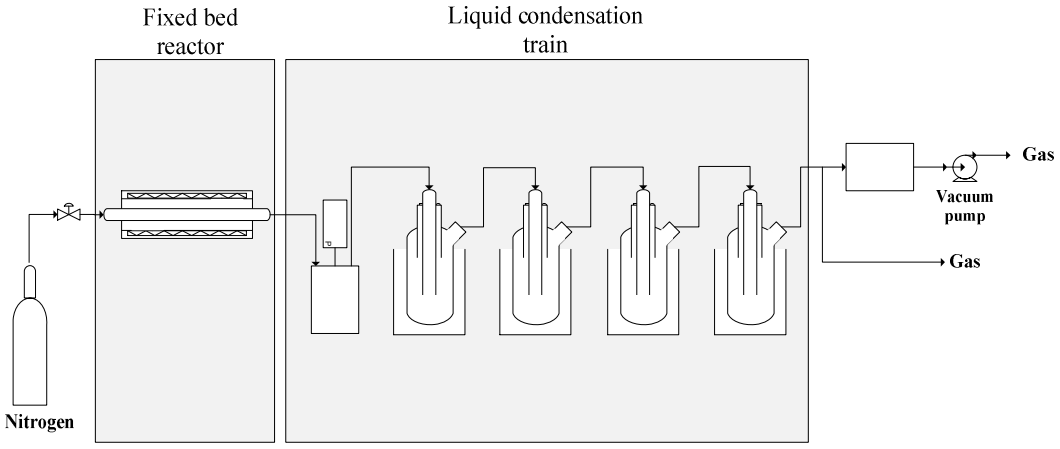

Appendix A-3. Schematic diagram of slow/vacuum pyrolysis unit.

Appendix A-4. Experimental procedure for slow/vacuum pyrolysis experiments.

Before the run – Assembly of unit		
Steps	**Check**	**Notes**
Weigh plant sections: • Condensers (1 x steel, 4 x glass) • Rubber connecting pipes • Pyrex reactor tube • Steel pipe • Reactor plate	Note the fittings included in original weighing of each unit	
Weigh out desired amount of sample and place on reactor plate	20 g per run	Ensure that sample centred and in a uniform shape
Place the reactor plate in the centre of the Pyrex reactor tube	Use baffle to move reactor plate to correct position in the Pyrex reactor tube	
Insert the Pyrex reactor tube into furnace	Ensure sample orientated in the middle of furnace	Take care when inserting the Pyrex reactor into the furnace as it breaks easily
Secure the end caps	Slide the metal flanges onto the Pyrex reactor tube followed by the Teflon seals and end caps	Tighten the bolts coupling the end caps and flanges in a star shape being careful not to over tighten
Assemble the steel condenser	Place the rubber seal between the condenser and top plate and bolt together in a star pattern.	
Attach steel pipe to steel condenser and Pyrex reactor tube		
Check for leaks	Attach vacuum pump to steel condenser	
Assemble the 4 glass condensers	Seal the tops with petroleum jelly between the glass component	Ensure that condensers arranged in waterfall formation
Connect all condensers using the rubber pipes		Gently fasten screw connections
Add cooling medium to glass condensers	Ice water (0 ^{o}C) for first two glass condensers Dry ice (-78 ^{o}C) for last two glass condensers	
Check for leaks	Attach vacuum pump to last glass condenser	

Appendix A-4. Continued…

During the run		
Steps	**Check**	**Notes**
Set the heating program and exit pipe temperature on the control panel		
For slow pyrolysis: Start N_2 flow For vacuum pyrolysis: Start vacuum pump	1 $L.min^{-1}$	
Start furnace		
Monitor process during experiment		
After the run		
Steps	**Check**	**Notes**
Switch off furnace		Maintain N_2 flow rate/vacuum
Leave unit to cool down to 120 ^oC		
Stop N_2 flow/vacuum		
Dissemble and weigh sections: • Condensers (1 x steel, 4 x glass) • Rubber connecting pipes • Pyrex reactor tube • Steel pipe • Reactor plate		Take care to correlate equipment with initial weighing configuration. These weights form part of the product yields. Clean section afterwards using boiling water followed by acetone.
Collect liquid from steel condenser		Tarry phase
Collect liquid from each glass condenser		Aqueous phase

APPENDIX B: PRE-SCREENING PYROLYSIS RUNS

B.1 FAST PYROLYSIS

As the objective of Chapter 4 was to maximise the fast pyrolysis bio-oil yield, pre-screening runs were required such that the correct reactor temperature range was selected for the design of experiments. In the case of LAPWS, a long reactor temperature range of between 300 to 550 °C was selected (Appendix B-1). On the other hand, the HAPWS reactor temperature range was lower and shorter than LAPWS at between 290 to 390 °C, as temperatures above 400 °C resulted in heightened levels non-condensable gas production probably due to the catalytic action of the inorganics. A pellet size range of between 3 to 5 mm was selected.

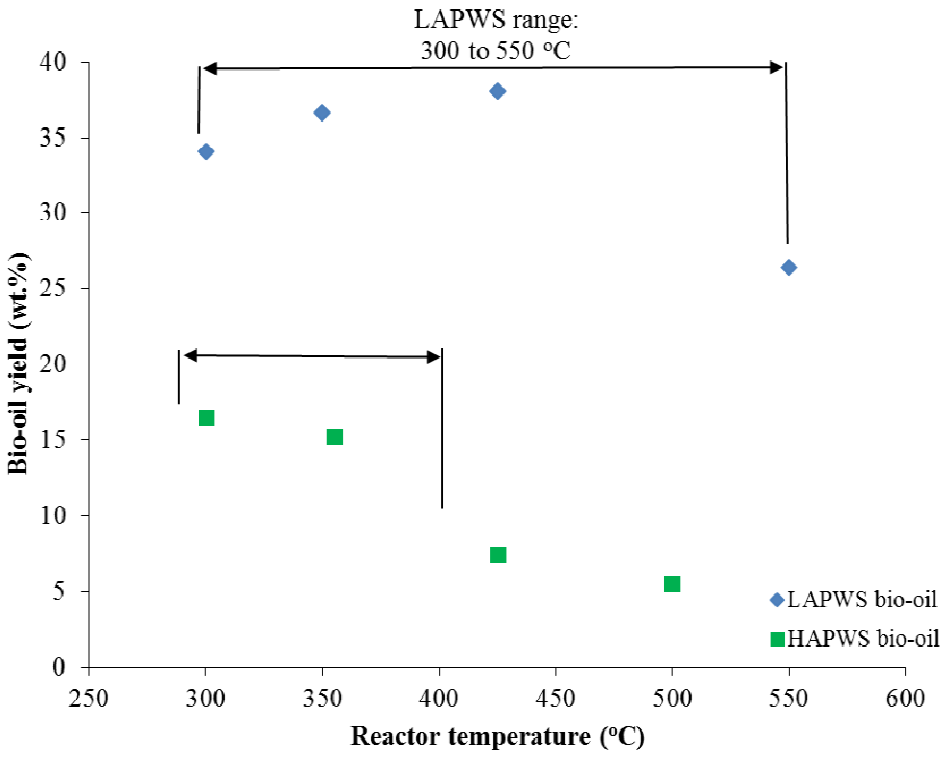

Figure B-1. Yield of bio-oil from fast pyrolysis of LAPWS (4 mm pellet size) and HAPWS (5 mm pellet size) at different reactor temperatures.

B.2 SLOW/VACUUM PYROLYSIS

Pre-screening slow and vacuum pyrolysis runs were performed over a range of reactor temperatures, pellet sizes and heating rates to determine appropriate operating conditions for the design of experiments (Appendix B-1). Subsequently, the reactor temperature levels of 340, 460 and 580 °C for slow pyrolysis, and 300, 425 and 550 °C for vacuum pyrolysis were selected. The heating rate was fixed at 30 °C.min^{-1} and the pellet size varied between 3 to 5 mm.

Appendix B-2. Slow and vacuum pyrolysis pre-screening runs

					Product yields (wt.%)		
		RT	PS	HR	$Y_{Bio-oil}$	Y_{Char}	Y_{Gas}
LAPWS	SP	260	4	20	26.9	29.1	44.0
		340	3	10	35.5	34.2	30.3
		340	5	10	35.4	33.3	31.3
		340	3	30	30.6	32.0	37.4
		340	5	30	32.3	30.6	37.1
		460	4	3.2	34.6	29.8	35.6
		460	4	20	33.3	30.3	36.4
		580	3	10	34.6	29.3	36.0
		580	5	10	28.9	29.9	41.2
		580	3	30	32.3	26.8	40.9
		580	5	30	33.4	28.1	38.5
	VP	260	4	20	30.9	32.6	36.5
		340	3	10	34.0	27.2	38.8
		340	5	10	35.7	30.4	33.9
		340	3	30	38.3	26.8	34.9
		340	5	30	41.2	23.8	34.9
		460	4	20	36.9	23.5	39.6
		580	3	10	32.0	22.9	45.1
		580	5	10	38.4	18.0	43.6
		580	3	30	35.8	22.4	41.7
		580	5	30	38.1	22.2	39.8
HAPWS	SP	300	5	20	16.4	59.6	24.0
		425	5	20	16.5	55.2	28.2
		550	5	20	20.7	49.3	30.0
	VP	300	5	20	16.4	59.5	24.0
		675	5	20	19.3	34.3	46.4

RT: reactor temperature (°C); PS: pellet size (mm); HR: heating rate (°C.min^{-1}).

APPENDIX C: EXPERIMENTAL RESULTS

C.1 PYROLYSIS PRODUCT YIELDS

Appendix C-1. LAPWS and HAPWS fast pyrolysis product yields at different reactor temperatures and pellet sizes

			Yield (wt.%)				Yield (daf, wt.%)			
	RT	PS	$Y_{Bio\text{-}oil}$	Y_{Char}	Y_{Gas}	$Y_{pyro\text{-}water}$	$Y_{Bio\text{-}oil}$	Y_{Char}	Y_{Gas}	$Y_{pyro\text{-}water}$
LAPWS	300	3	33.6	34.0	32.4	2.6	37.3	29.4	35.9	2.9
		4	27.2	33.2	39.6	-	30.9	29.0	45.0	-
		4 (R)	32.0	30.7	37.4	2.4	35.1	25.1	41.0	2.7
		4 (R)	29.9	30.8	39.3	2.2	32.9	24.9	43.3	2.4
		5	39.2	31.4	29.4	4.8	43.7	26.5	32.8	5.4
		5 (R)	35.8	32.7	31.5	2.0	40.4	26.6	35.5	2.3
	425	3	31.4	23.6	45.0	6.2	34.8	18.8	49.8	6.9
		4	32.8	25.1	42.1	2.7	36.0	18.6	46.2	3.0
		5	36.0	26.6	37.3	3.3	40.5	21.2	42.0	3.7
	550	3	21.6	24.9	53.5	3.6	23.8	19.5	59.0	4.0
		4	20.4	23.7	56.0	3.0	22.5	18.8	61.7	3.3
		5	25.4	24.4	50.2	0.0	28.8	19.0	56.9	0.0
	SD		2.4	1.4	1.2	0.2	2.1	2.3	2.0	1.5
HAPWS[a]	290	3	15.1	62.0	22.9	-1.4	30.0	45.7	45.4	-2.7
		4	15.1	55.4	29.5	0.1	29.8	46.5	58.2	0.2
		5	23.4	62.0	14.6	1.7	46.1	47.8	28.8	3.3
	340	3	18.4	55.1	26.4	-1.2	36.5	26.5	52.2	-2.3
		4	24.6	54.6	20.8	1.5	48.6	28.5	41.2	3.0
		5	28.4	54.7	16.9	1.7	56.2	26.6	33.4	3.3
		5 (R)	25.2	53.4	21.4	2.5	48.6	30.8	41.4	4.8
		5 (R)	28.3	51.2	20.4	1.3	56.3	22.0	40.6	2.6
	390	3	18.6	45.5	35.9	-1.3	36.8	20.5	70.9	-2.6
		4	18.0	46.8	35.2	1.8	35.5	21.3	69.4	3.5
		5	14.8	49.4	35.8	0.5	28.9	22.7	69.9	1.0
	SD		1.9	1.7	2.4	0.6	4.4	4.4	4.4	1.1

RT: reactor temperature (ºC); PS: pellet size (mm); SD: standard deviation; R: repeat; [a] isopar corrected bio-oil yield.

Appendix C-2. LAPWS and HAPWS slow pyrolysis product yields at different reactor temperatures and pellet sizes

			Yield (wt.%)						Yield (daf, wt.%)					
	RT	PS	$Y_{Bio-oil}$	Y_{tarry}	$Y_{aqueous}$	Y_{Char}	Y_{Gas}	$Y_{pyro-water}$	$Y_{Bio-oil}$	Y_{tarry}	$Y_{aqueous}$	Y_{Char}	Y_{Gas}	$Y_{pyro-water}$
LAPWS	340	3	30.6	26.1	4.5	32.0	37.4	16.4	34.9	29.8	5.1	28.2	36.9	18.7
		4	33.2	26.9	6.3	32.0	34.8	16.4	38.4	31.1	7.3	28.3	33.3	19.0
		5	32.3	24.6	7.7	30.6	37.1	18.8	36.2	27.5	8.6	24.8	39.0	21.1
	460	3	36.0	31.6	4.4	31.6	32.3	16.8	41.1	36.1	5.0	26.8	32.1	19.2
		4	40.8	35.3	5.5	28.7	30.4	21.0	46.4	40.1	6.3	24.9	28.7	23.9
		4 (R)	35.6	29.0	6.6	27.0	37.4	17.2	39.2	32.0	7.2	22.1	38.7	19.0
		4 (R)	36.5	29.9	6.6	27.5	36.0	22.9	40.2	32.9	7.3	22.4	37.4	25.3
		5	37.3	32.8	4.5	30.1	32.6	18.9	41.7	36.7	5.0	24.8	33.5	21.1
		5 (R)	35.2	27.6	7.5	30.8	34.1	18.3	39.9	31.3	8.5	24.5	35.6	20.8
	580	3	32.3	24.6	7.7	26.8	40.9	18.2	36.3	27.7	8.7	21.2	42.5	20.5
		4	37.8	32.6	5.2	28.2	34.0	18.7	42.9	36.9	5.9	23.0	34.1	21.2
		5	33.4	25.5	7.9	28.1	38.5	19.6	37.3	28.5	8.8	21.9	40.8	21.9
	SD		2.8	3.4	0.6	0.9	3.7	2.9	3.9	4.4	0.6	1.6	5.4	3.3
HAPWS	340	3	23.0	19.7	3.3	56.9	20.1	13.1	43.2	37.0	6.2	13.6	43.2	24.7
		4	22.5	19.0	3.6	56.6	20.9	11.9	42.6	35.9	6.7	14.7	42.8	22.6
		5	27.8	24.2	3.6	53.0	19.2	14.6	54.1	47.1	6.9	12.6	33.4	28.5
		5 (R)	24.8	21.0	3.8	53.7	21.5	8.9	48.1	40.6	7.4	13.4	38.5	17.2
		5 (R)	27.1	22.7	4.4	54.0	18.9	13.8	52.5	44.1	8.5	15.0	32.4	26.8
	460	3	20.8	18.2	2.6	55.2	24.0	11.7	39.0	34.1	4.9	12.4	48.6	22.0
		4	21.4	18.1	3.3	55.9	22.7	13.0	40.5	34.3	6.2	12.6	46.9	24.6
		5	26.4	22.6	3.8	52.1	21.5	14.5	51.3	43.9	7.4	11.5	37.1	28.2
	580	3	21.4	17.8	3.6	51.5	27.1	12.8	40.2	33.4	6.8	10.8	49.0	24.1
		4	22.5	19.1	3.5	48.0	29.4	12.5	42.6	36.1	6.5	10.3	47.1	23.7
		5	24.4	20.7	3.8	48.5	27.1	13.5	47.5	40.2	7.3	9.6	42.9	26.2
	SD		1.5	1.5	0.1	1.9	1.3	0.5	3.8	3.4	0.4	0.6	3.1	1.4

RT: reactor temperature (°C); PS: pellet size (mm); SD: standard deviation; R: repeat.

Appendix C-3. LAPWS and HAPWS vacuum pyrolysis product yields at different reactor temperatures and pellet sizes

			Yield (wt.%)						Yield (daf, wt.%)					
	RT	PS	$Y_{Bio\text{-}oil}$	Y_{tarry}	$Y_{aqueous}$	Y_{Char}	Y_{Gas}	$Y_{pyro\text{-}water}$	$Y_{Bio\text{-}oil}$	Y_{tarry}	$Y_{aqueous}$	Y_{Char}	Y_{Gas}	$Y_{pyro\text{-}water}$
LAPWS	300	3	32.6	17.1	15.5	27.2	40.2	6.6	37.1	19.5	17.6	19.8	43.2	7.5
		4	32.2	16.3	15.9	26.1	41.7	6.0	37.3	18.9	18.4	20.2	42.5	7.0
		5	33.6	16.5	17.1	27.7	38.7	7.3	38.1	18.7	19.4	20.5	41.4	8.2
	425	3	31.1	15.9	15.3	28.5	40.4	6.3	35.4	18.0	17.3	22.7	41.9	7.1
		4	27.9	14.7	13.3	25.8	46.2	2.9	32.4	17.0	15.4	20.0	47.6	3.3
		4 (R)	23.6	17.2	6.4	24.6	51.8	2.7	25.9	18.9	7.0	19.1	55.0	2.9
		4 (R)	31.1	20.5	10.5	23.3	45.7	5.6	34.2	22.6	11.6	17.5	48.3	6.1
		5	33.4	13.7	19.6	28.4	38.2	8.6	37.9	15.6	22.3	21.1	41.0	9.8
	550	3	29.5	17.0	12.4	23.0	47.5	3.9	33.5	19.4	14.1	16.9	49.7	4.4
		4	29.5	17.1	12.4	21.8	48.7	1.6	34.0	19.7	14.3	17.1	48.9	1.8
		5	29.6	11.9	17.8	23.0	47.3	8.1	33.6	13.5	20.1	16.1	50.3	9.2
	SD		3.8	2.9	3.5	1.3	3.4	1.6	4.3	2.8	4.2	1.3	4.1	1.8
HAPWS	300	3	19.4	7.8	11.6	55.1	25.5	7.0	38.6	15.5	23.1	11.2	50.2	13.9
		4	20.7	8.7	12.0	54.8	24.5	4.6	41.3	17.4	23.9	11.4	47.3	9.2
		5	18.0	5.7	12.3	53.2	28.7	6.7	35.1	11.2	23.9	13.2	51.8	13.0
	425	3	18.5	8.1	10.4	51.3	30.1	3.5	36.9	16.2	20.8	8.7	54.4	7.0
		4	20.5	9.4	11.1	52.3	27.3	2.0	40.8	18.6	22.2	9.3	49.9	3.9
		4 (R)	20.7	11.0	9.7	50.0	23.7	3.3	39.8	21.2	18.6	7.7	52.5	6.4
		4 (R)	19.0	8.1	10.9	50.1	30.0	2.1	36.4	15.5	20.9	8.4	55.2	4.1
		5	20.2	6.6	13.6	51.8	28.0	7.5	39.3	12.9	26.4	8.5	52.2	14.5
	550	3	18.1	9.5	8.6	37.1	44.8	4.7	36.1	18.9	17.2	8.5	55.4	9.4
		4	15.2	7.7	7.5	34.6	50.2	1.5	30.3	15.3	15.0	8.5	61.1	3.1
		5	17.3	5.7	11.5	45.3	37.4	6.2	33.6	11.2	22.5	7.4	59.0	12.0
	SD		0.9	1.5	0.8	1.3	3.2	0.7	2.3	2.8	1.8	0.8	2.7	1.4

RT: reactor temperature (°C); PS: pellet size (mm); SD: standard deviation; R: repeat.

C.2 PYROLYSIS PRODUCT CALORIFIC VALUES

Appendix C-4. LAPWS and HAPWS fast pyrolysis product yields at different reactor temperatures and pellet sizes

	Calorific value (MJ.kg^{-1})											
	Vacuum pyrolysis				Slow pyrolysis				Fast pyrolysis			
	RT	PS	Char	Tarry	RT	PS	Char	Tarry	RT	PS	Char	Bio-oil
LAPWS	300	3	20.0	20.0	340	3	21.8	7.7	300	3	21.1	19.6
		4	21.1	21.1		4	25.5	7.5		4	21.2	20.5
		5	20.3	20.3		5	21.4	7.3		4 (R)	21.4	20.2
	425	3	22.5	22.5	460	3	21.7	9.5		4 (R)	21.0	22.0
		4	21.9	21.9		4	20.7	9.2		5	21.2	20.4
		4 (R)	21.3	21.3		4 (R)	21.6	12.0		5 (R)	20.5	21.1
		4 (R)	19.4	19.4		4 (R)	23.6	9.5	425	3	21.6	18.7
		5	21.4	21.4		5	24.4	9.2		4	22.0	21.1
	550	3	21.5	21.5		5 (R)	21.8	9.8		5	20.1	20.4
		4	22.0	22.0	580	3	22.6	8.4	550	3	22.9	17.7
		5	21.5	21.5		4	23.1	9.4		4	22.6	18.0
	SD		1.3	1.3		5	22.6	22.6		5	21.3	21.3
					SD		1.5	1.5	SD		0.2	0.9
HAPWS	300	3	4.1	22.6	340	3	4.9	9.0	290	3	7.3	19.3
		4	3.2	21.7		4	5.3	10.4		4	5.6	20.0
		5	4.1	23.5		5	5.0	9.3		5	6.7	18.2
	425	3	2.8	22.7		5 (R)	5.1	13.2	340	3	4.9	19.4
		4	2.7	20.2		5 (R)	5.1	10.2		4	5.0	15.5
		4 (R)	2.9	25.5	460	3	4.8	9.5		5	6.1	16.8
		4 (R)	2.9	22.9		4	4.8	8.7		5 (R)	4.7	16.1
		5	2.7	22.2		5	5.0	9.1		5 (R)	5.7	16.0
	550	3	3.0	23.3	580	3	4.7	8.9	390	3	4.4	20.1
		4	3.0	22.6		4	4.9	9.3		4	5.0	17.3
		5	2.2	23.8		5	4.9	8.6		5	4.4	14.9
	SD		0.1	2.7	SD		0.1	2.0	SD		0.7	0.4

RT: reactor temperature (ºC); PS: pellet size (mm); SD: standard deviation; R: repeat.

APPENDIX D: RESULTS RELATED TO CHAPTER 5

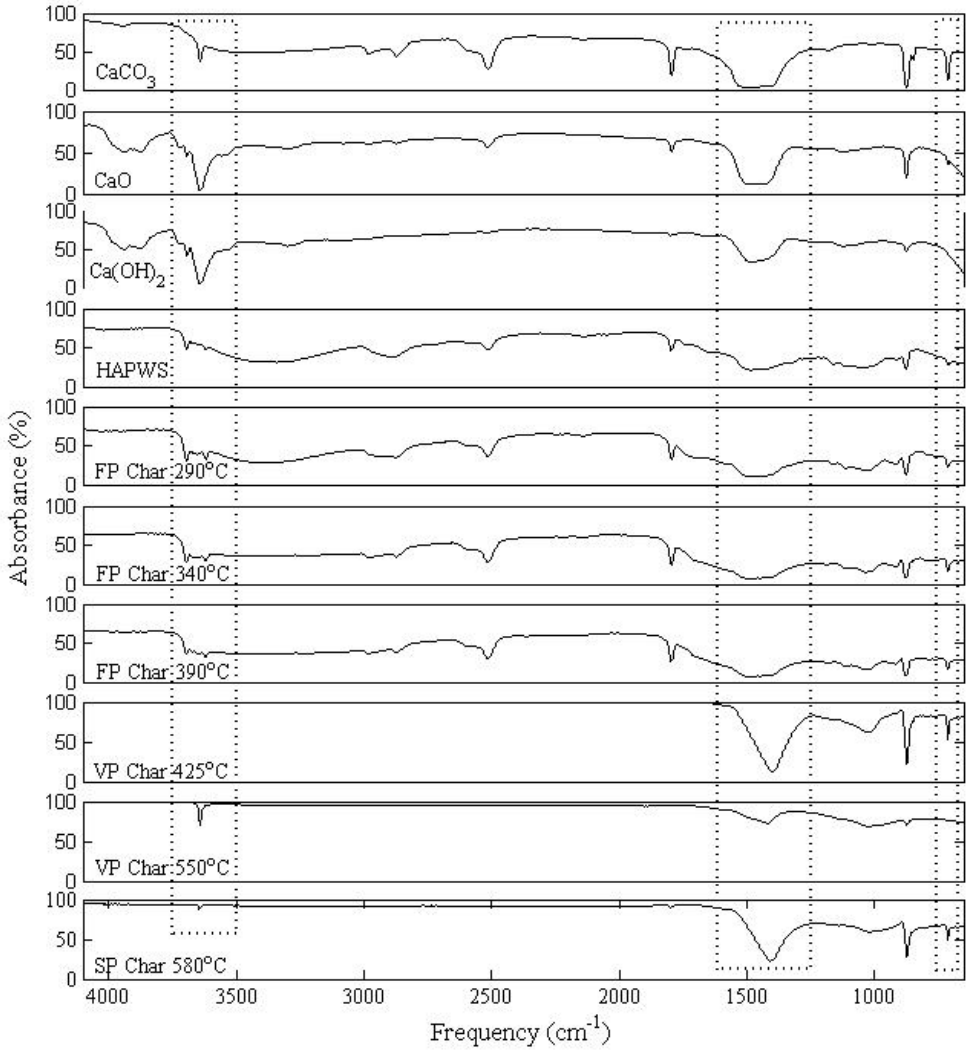

Appendix D-1. IR spectra of $CaCO_3$, CaO, $Ca(OH)_2$, HAPWS and its fast, vacuum and slow pyrolysis char (4 mm) produced at various reactor temperatures.

Appendix D-2. Statistical models fitted for the different product yields obtained from vacuum pyrolysis conversion of LAPWS and HAPWS

	Yield	Model									Statistics				
		Int.	β_1	β_2	β_3	β_4	β_5	β_6	β_7	β_8	R^2 (%)	R^2_{adj} (%)	P_{RT}	P_{PS}	Exp. E
LAPWS	$Y_{bio\text{-}oil}$	42.1	-0.02	-	-	-	-	-	-	-	73.4	70.0	0.00	-	3.8
	Y_{tarry}	95.7	-0.38	-17.9	$2.7*10^{-4}$	-	0.088	-	-	$-1.4*10^{-5}$	97.0	92.0	0.00	0.01	2.8
	Y_{char}	0.05	0.11	-	$-1.5*10^{-4}$	-	-	-	-	-	79.3	73.3	0.02	-	1.3
	$Y_{pyro\text{-}water}$	17.0	0.16	-1.59	-	-	-0.096	-	0.013	-	94.2	89.6	0.00	0.40	1.7
	$Y_{organic}$	120	-0.38	-48.1	$1.6*10^{-4}$	5.95	0.165	$-2.8*10^{-5}$	-0.020	-	99.9	99.9	0.00	0.00	2.8
HAPWS	$Y_{bio\text{-}oil}$	-230	0.63	149	-	-21.0	-0.350	-	0.054	$-1.0*10^{-5}$	90.3	71.1	0.06	0.06	2.3
	Y_{tarry}	-29.7	-	27.0	-	-3.81	-	-	-	-	85.5	80.7	-	0.01	2.8
	Y_{char}	17.6	-0.04	-	-	0.89	-	$2.4*10^{-5}$	-0.003	-	92.1	86.8	0.02	-	0.8
	$Y_{pyro\text{-}water}$	26.5	0.23	50.0	-	-11.6	-0.407	$3.2*10^{-4}$	0.078	$-7.0*10^{-5}$	99.8	99.1	0.05	0.06	1.4
	$Y_{organic}$	66.0	-0.82	-15.9	$1.3*10^{-3}$	-	0.385	$-6.2*10^{-4}$	-0.040	$6.6*10^{-5}$	99.7	98.6	0.01	0.05	1.8

Int: intercept; βn+1: model coefficients; R^2: coefficient of determination; R^2_{adj}: adjusted coefficient of determination; P_{RT}: p-value for reactor temperature; P_{PS}:p-value for pellet size; Exp. E: experimental error.

Appendix D-3. Statistical models fitted for the different product yields obtained from slow pyrolysis conversion of LAPWS and HAPWS

	Yield	Model									Statistics				
		Int.	β_1	β_2	β_3	β_4	β_5	β_6	β_7	β_8	R^2 (%)	R^2_{adj} (%)	P_{RT}	P_{PS}	Exp. E
LAPWS	$Y_{bio-oil}$	33.2	-0.14	-15.7	-	-	0.159	$-8.0*10^{-5}$	-0.011	-	92.7	83.6	0.02	0.02	3.9
	Y_{tarry}	-58.9	0.41	-	$-8.2*10^{-4}$	-	-	$-2.1*10^{-4}$	-	$-2.7*10^{-5}$	89.1	80.5	0.00	-	4.4
	Y_{char}	34.6	-0.02	-	-	-	-	-	-	-	73.6	69.9	0.00	-	0.4
	$Y_{pyro-water}$	9.79	0.04	4.07	-	-	-0.024	$1.1*10^{-5}$	0.002	-	92.6	83.3	0.05	0.05	3.3
	$Y_{organic}$	-112	0.57	19.7	$-8.1*10^{-4}$	-	-0.091	$2.0*10^{-4}$	-	$-1.3*10^{-5}$	97.7	93.2	0.03	0.10	2.5
HAPWS	$Y_{bio-oil}$	201	-0.19	-32.5	-	-	-0.158	$2.8*10^{-4}$	0.043	$-6.2*10^{-5}$	98.4	95.0	0.18	0.08	3.1
	Y_{tarry}	214	-	-99.5	$-4.7*10^{-4}$	13.6	-	2.5*10-	-	$-3.3*10^{-5}$	98.3	95.5	-	0.01	3.2
	Y_{char}	-28.2	0.06	24.3	-	-3.02	-0.038	-	0.005	-	99.8	99.5	0.03	0.00	1.3
	$Y_{pyro-water}$	58.9	-	-20.5	-	2.88	-	-	-	-	78.1	71.8	-	0.04	1.2
	$Y_{organic}$	-48.9	0.82	24.4	$-1.3*10^{-3}$	-	-0.406	$6.5*10^{-4}$	0.041	$-7.3*10^{-5}$	99.7	97.6	0.09	0.15	2.2

Int: intercept; βn+1: model coefficients; R^2: coefficient of determination; R^2_{adj}: adjusted coefficient of determination; P_{RT}: p-value for reactor temperature; P_{PS}:p-value for pellet size; Exp. E: experimental error.

Appendix D-4. Statistical models fitted for the different product yields obtained from fast pyrolysis conversion of LAPWS and HAPWS

	Yield	Model									Statistics				
		Int.	β_1	β_2	β_3	β_4	β_5	β_6	β_7	β_8	R^2 (%)	R^2_{adj} (%)	P_{RT}	P_{PS}	Exp. E
LAPWS	$Y_{bio\text{-}oil}$[a]	-123	-0.07	-56.8	-	5.04	0.10	$1.04*10^{-4}$	-	-	95.7	92.2	0.05	0.00	1.7
	Y_{char}[a]	75.5	-0.22	-	$2.2*10^{-4}$	-	-	-	-	-	87.0	84.1	0.01	-	1.9
	$Y_{pyro\text{-}water}$	-26.1	0.14	1.59	$-1.3*10^{-4}$	-	-0.007	-	-	-	82.4	68.4	0.02	0.90	0.2
	$Y_{organic}$[a]	55.5	-0.09	-16.6	-	-	0.08	$-8.0*10^{-5}$	-	-	89.6	83.7	0.05	0.03	1.4
HAPWS	$Y_{bio\text{-}oil}$	16.2	0.34	-173	-	7.93	0.768	$-1.2*10^{-3}$	-	-	89.7	79.5	0.16	0.02	4.4
	Y_{char}	234	-1.15	-	$-1.5*10^{-3}$	-	-	-	-	-	83.0	78.8	0.04	-	2.4
	$Y_{pyro\text{-}water}$	-12.1	-	3.22	-	-	-	-	-	-	89.6	88.4	-	0.00	1.1
	$Y_{organic}$	51.0	0.27	-166	-	8.64	0.666	$-1.06*10^{-3}$	-	-	95.6	90.0	0.07	0.00	3.9

Int: intercept; βn+1: model coefficients; R^2: coefficient of determination; R^2_{adj}: adjusted coefficient of determination; P_{RT}: p-value for reactor temperature; P_{PS}:p-value for pellet size; Exp. E: experimental error. [a] Ridout et al. [6].

Appendix D-5. Statistical model fitted for calorific values of the char and bio-oil/tarry phase products obtained from vacuum, slow an fast pyrolysis conversion of LAPWS and HAPWS

		Product	Model								Statistics				
			Int.	β_1	β_2	β_3	β_4	β_5	β_6	β_7	β_8	R^2 (%)	R^2_{adj} (%)	P_{RT}	P_{PS}	Exp. E
LAPWS	VP	Char	9.88	0.05	-	$-5.6*10^{-5}$	-	-	-	-	-	73.1	64.2	0.03	-	1.3
		Tar	27.8	-	-1.69	$-7.3*10^{-5}$	-	-	$2.4*10^{-5}$	-	$-3.6*10^{-6}$	81.0	65.8	0.01	0.04	1.4
	SP	Char	26.6	-0.03	-	$3.5*10^{-5}$	-	-	-	-	-	89.4	71.8	0.03	0.03	1.5
		Tar	-11.7	0.09	-	$-8.7*10^{-5}$	-	-	-	-	-	88.5	83.9	0.07	-	1.5
	FP	Char	25.7	-0.03	-	-	-	-	$-2.0*10^{-5}$	-	$-2.7*10^{-6}$	83.2	73.1	0.06	-	0.8
		Bio-oil	7.72	-0.15	4.69	$3.5*10^{-4}$	-	0.094	$-2.2*10^{-4}$	-0.015	$3.2*10^{-5}$	99.9	99.9	0.04	0.06	0.9
HAPWS	VP	Char	53.3	-0.13	-23.7	$2.9*10^{-5}$	3.09	0.054	-	-0.007	-	97.6	94.1	0.00	0.00	0.1
		Tar	36.7	0.002	-8.33	-	1.12	-	-	-	-	85.0	76.0	0.06	0.01	2.7
	SP	Char	2.43	-0.001	1.48	-	-0.2	-	-	$5.1*10^{-5}$	-	74.9	64.1	0.02	0.08	0.1
		Tar	-65.1	0.47	22.7	$-6.2*10^{-4}$	-	-0.18	$2.7*10^{-4}$	0.012	$-2.3*10^{-5}$	99.9	99.9	0.01	0.01	1.9
	FP	Char	21.3	-0.05	5.56	-	-	-0.04	$6.4*10^{-5}$	-	-	88.9	81.5	0.05	0.18	0.3
		Bio-oil	-4.57	0.084	22.7	-	-	-0.12	$-1.3*10^{-4}$	-	-	87.2	76.9	0.09	0.04	0.4

Int: intercept; $\beta n+1$: model coefficients; R^2: coefficient of determination; R^2_{adj}: adjusted coefficient of determination; P_{RT}: p-value for reactor temperature; P_{PS}:p-value for pellet size; Exp. E: experimental error.

Appendix D-6. Statistical model fitted for energy conversion obtained from vacuum, slow and fast pyrolysis conversion of LAPWS and HAPWS

		EC	Model									Statistics				
			Int.	β_1	β_2	β_3	β_4	β_5	β_6	β_7	β_8	R^2 (%)	R^2_{adj} (%)	P_{RT}	P_{PS}	Exp. E
LAPWS	VP	EC_{tarry}	147	-0.45	-61.6	$5.8*10^{-5}$	8.02	0.22	-	-0.029	-	99.0	97.0	0.01	0.02	2.0
		EC_{char}	-13.4	0.24	-	$-3.0*10^{-4}$	-	-	-	-	-	84.3	79.0	0.01	-	3.3
	SP	EC_{tarry}	-61.0	0.33	-	$-3.4*10^{-4}$	-	-	-	-	-	77.1	70.6	0.00	-	1.8
		EC_{char}	0.97	-0.02	26.0	-	-3.39	-	-	-	-	74.4	59.0	0.02	0.09	2.7
	FP	$EC_{bio-oil}$[a]	65.5	-0.10	-18.8	-	-	0.09	$-8.7*10^{-5}$	-	-	89.6	83.7	0.05	0.03	2.3
		EC_{char}	111	-0.33	-	$3.4*10^{-4}$	-	-	-	-	-	94.3	92.7	0.00	-	1.9
HAPWS	VP	EC_{tarry}	-67.0	-	43.6	$2.8*10^{-4}$	-5.66	-	$-1.4*10^{-4}$	-	$1.7*10^{-5}$	97.2	93.7	-	0.01	0.2
		EC_{char}	167	-0.31	-74.3	-	9.45	0.15	-	-0.019	-	96.4	92.9	0.04	0.04	0.1
	SP	EC_{tarry}	-110	1.02	36.8	$-1.4*10^{-3}$	-	-0.43	$-6.5*10^{-4}$	0.037	$-6.5*10^{-5}$	99.9	99.8	0.02	0.03	2.3
		EC_{char}	-62.6	0.15	48.9	-	-6.50	-0.09	-	0.012	$-1.1*10^{-6}$	99.8	99.5	0.00	0.00	0.5
	FP	$EC_{bio-oil}$	-13.9	0.39	-104	-	-6.74	0.42	$-7.5*10^{-4}$	-	-	97.1	93.4	0.01	0.00	3.1
		EC_{char}	131.9	-0.21	28.5	-	-	-0.21	$3.5*10^{-4}$	-	-	96.3	93.9	0.00	0.08	1.5

Int: intercept; $\beta n+1$: model coefficients; R^2: coefficient of determination; R^2_{adj}: adjusted coefficient of determination; P_{RT}: p-value for reactor temperature; P_{PS}:p-value for pellet size; Exp. E: experimental error, [a] Ridout *et al.* [6].

APPENDIX E: RESULTS RELATED TO CHAPTER 6

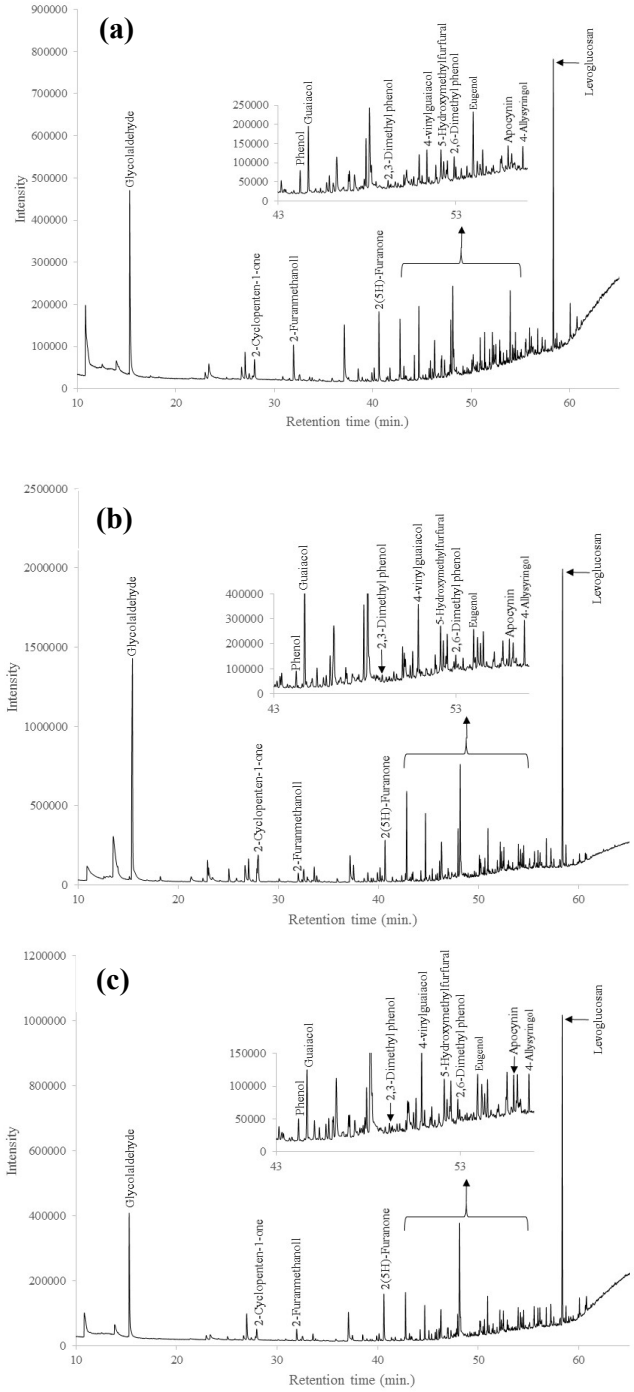

Appendix E-1. GC-MS chromatogram of the LAPWS vacuum (a) and slow (b) pyrolysis tarry phase, as well as FP bio-oil (c) with quantification of selected compounds.

Appendix E-2. Yield of chemicals from vacuum pyrolysis of LAPWS and HAPWS at different reactor temperatures and pellet sizes

			Chemical yields (daf, wt.%)												
			Lignin-derived compounds							Carbohydrate-derived compounds					
	RT	PS	4-vinylguaicol	Eugenol	Apocycnin	Phenol	Guaiacol	2,3-Dimethyl phenol	2,6-Dimethyl phenol	2-Furanmethanol	2(5H)-Furanone	5-Hydroxymethyl furfural	Levoglucosan	Glycolaldehyde	2-Cyclopenten-1-one
LAPWS	300	3	0.051	0.037	0.024	0.026	0.048	0.0052	0.0042	0.060	0.213	0.047	0.536	1.025	0.015
		4	0.071	0.031	0.020	0.018	0.043	0.0040	0.0037	0.083	0.197	0.040	0.447	1.003	0.014
		5	0.079	0.031	0.015	0.009	0.054	0.0026	0.0034	0.089	0.106	0.034	0.393	1.150	0.010
	425	3	0.091	0.041	0.026	0.009	0.037	0.0036	0.0049	0.088	0.184	0.048	0.609	0.801	0.004
		4	0.098	0.040	0.018	0.012	0.051	0.0040	0.0050	0.107	0.218	0.034	0.420	1.000	0.009
		5	0.107	0.043	0.020	0.010	0.033	0.0050	0.0054	0.070	0.146	0.035	0.463	0.768	0.000
	550	3	0.104	0.049	0.025	0.009	0.043	0.0040	0.0058	0.096	0.208	0.052	0.542	1.116	0.007
		4	0.104	0.050	0.028	0.018	0.037	0.0060	0.0059	0.104	0.188	0.059	0.636	0.952	0.003
		5	0.075	0.030	0.015	0.009	0.034	0.0026	0.0031	0.065	0.147	0.036	0.332	0.844	0.005
	SD		0.005	0.002	0.005	0.000	0.004	0.0004	0.0002	0.021	0.031	0.009	0.085	0.161	0.003
HAPWS	300	3	0.014	0.009	0.012	0.008	0.002	0.0026	0.0028	0.036	0.087	0.035	0.895	0.425	0.000
		4	0.018	0.014	0.016	0.006	0.003	0.0026	0.0033	0.045	0.113	0.043	1.001	0.400	0.000
		5	0.009	0.005	0.005	0.002	0.001	0.0007	0.0016	0.009	0.029	0.026	0.671	0.147	0.000
	425	3	0.013	0.008	0.010	0.005	0.000	0.0022	0.0021	0.032	0.065	0.037	0.976	0.522	0.000
		4	0.016	0.013	0.012	0.007	0.005	0.0029	0.0036	0.057	0.146	0.056	0.612	0.632	0.000
		5	0.010	0.009	0.012	0.004	0.000	0.0017	0.0026	0.028	0.068	0.031	0.690	0.319	0.000
	550	3	0.016	0.010	0.014	0.008	0.000	0.0029	0.0029	0.030	0.074	0.048	1.146	0.292	0.000
		4	0.008	0.007	0.009	0.004	0.000	0.0014	0.0026	0.033	0.096	0.037	0.994	0.531	0.000
		5	0.006	0.007	0.006	0.005	0.000	0.0013	0.0020	0.017	0.037	0.034	0.839	0.207	0.000
	SD		0.013	0.005	0.006	0.002	0.002	0.0007	0.0017	0.012	0.024	0.027	0.218	0.153	0.000

RT: reactor temperature (°C); PS: pellet size (mm); SD: standard deviation.

Appendix E-3. Yield of chemicals from slow pyrolysis of LAPWS and HAPWS at different reactor temperatures and pellet sizes

			Chemical yields (daf, wt.%)												
			Lignin-derived compounds							Carbohydrate-derived compounds					
	RT	PS	4-vinylguaicol	Eugenol	Apocycnin	Phenol	Guaiacol	2,3-Dimethyl phenol	2,6-Dimethyl phenol	2-Furanmethanol	2(5H)-Furanone	5-Hydroxymethyl furfural	Levoglucosan	Glycolaldehyde	2-Cyclopenten-1-one
LAPWS	340	3	0.003	0.002	0.007	0.016	0.025	0.0006	0.0020	0.004	0.085	0.020	0.369	0.371	0.048
		4	0.003	0.002	0.008	0.008	0.027	0.0003	0.0019	0.010	0.087	0.022	0.480	0.503	0.050
		5	0.002	0.002	0.007	0.018	0.028	0.0006	0.0023	0.004	0.088	0.021	0.349	0.262	0.039
	460	3	0.009	0.009	0.016	0.012	0.047	0.0013	0.0049	0.011	0.137	0.057	0.569	0.602	0.046
		4	0.012	0.014	0.015	0.008	0.054	0.0011	0.0058	0.027	0.149	0.054	0.590	0.912	0.046
		5	0.009	0.011	0.015	0.011	0.048	0.0014	0.0051	0.014	0.145	0.054	0.604	0.696	0.043
	580	3	0.003	0.003	0.008	0.010	0.027	0.0007	0.0020	0.005	0.089	0.023	0.417	0.509	0.036
		4	0.006	0.003	0.013	0.008	0.039	0.0003	0.0042	0.010	0.140	0.046	0.615	0.681	0.040
		5	0.003	0.002	0.008	0.010	0.026	0.0003	0.0018	0.005	0.093	0.025	0.460	0.488	0.039
	SD		0.003	0.004	0.003	0.000	0.011	0.0003	0.0013	0.009	0.027	0.009	0.081	0.163	0.007
HAPWS	340	3	0.002	0.002	0.006	0.010	0.007	0.0010	0.0031	0.022	0.124	0.075	0.963	0.488	0.068
		4	0.003	0.002	0.006	0.012	0.008	0.0014	0.0039	0.021	0.145	0.098	0.956	0.570	0.062
		5	0.006	0.004	0.022	0.011	0.009	0.0012	0.0065	0.024	0.153	0.161	1.133	0.575	0.076
	460	3	0.002	0.001	0.005	0.012	0.008	0.0010	0.0030	0.022	0.134	0.071	0.873	0.456	0.054
		4	0.003	0.002	0.014	0.009	0.006	0.0009	0.0036	0.021	0.122	0.089	0.998	0.447	0.059
		5	0.004	0.002	0.010	0.010	0.005	0.0008	0.0030	0.020	0.133	0.077	1.141	0.536	0.067
	580	3	0.002	0.001	0.006	0.011	0.007	0.0006	0.0026	0.014	0.136	0.072	0.923	0.663	0.053
		4	0.002	0.001	0.005	0.013	0.009	0.0010	0.0036	0.019	0.144	0.081	0.939	0.536	0.062
		5	0.003	0.002	0.007	0.009	0.005	0.0008	0.0027	0.023	0.128	0.071	1.085	0.536	0.060
	SD		0.005	0.002	0.006	0.007	0.008	0.0004	0.0039	0.007	0.060	0.031	0.649	0.411	0.020

RT: reactor temperature (°C); PS: pellet size (mm); SD: standard deviation.

Appendix E-4. Yield of chemicals from fast pyrolysis of LAPWS and HAPWS at different reactor temperatures and pellet sizes

			Chemical yields (daf, wt.%)												
			Lignin-derived compounds							Carbohydrate-derived compounds					
	RT	PS	4-vinylguaicol	Eugenol	Apocynin	Phenol	Guaiacol	2,3-Dimethyl phenol	2,6-Dimethyl phenol	2-Furanmethanol	2(5H)-Furanone	5-Hydroxymethyl furfural	Levoglucosan	Glycolaldehyde	2-Cyclopenten-1-one
LAPWS	300	3	0.022	0.025	0.040	0.021	0.048	0.0062	0.0079	0.070	0.328	0.067	1.397	1.254	0.023
		4	0.018	0.019	0.031	0.033	0.035	0.0062	0.0057	0.061	0.219	0.071	1.120	1.050	0.028
		5	0.017	0.020	0.042	0.046	0.038	0.0084	0.0084	0.092	0.310	0.046	1.241	0.993	0.053
	425	3	0.015	0.016	0.038	0.021	0.048	0.0041	0.0073	0.037	0.243	0.033	1.270	0.561	0.038
		4	0.018	0.024	0.036	0.028	0.043	0.0063	0.0070	0.071	0.278	0.071	1.512	1.126	0.028
		5	0.010	0.011	0.037	0.029	0.031	0.0047	0.0064	0.036	0.229	0.053	1.409	0.952	0.036
	550	3	0.011	0.016	0.021	0.049	0.029	0.0056	0.0036	0.026	0.095	0.030	0.925	0.353	0.041
		4	0.011	0.013	0.020	0.027	0.028	0.0040	0.0033	0.025	0.103	0.024	0.903	0.391	0.032
		5	0.010	0.011	0.024	0.029	0.026	0.0049	0.0041	0.034	0.147	0.036	1.008	0.827	0.030
	SD		0.003	0.006	0.003	0.022	0.010	0.0015	0.0011	0.008	0.050	0.005	0.110	0.341	0.008
HAPWS	290	3	0.008	0.007	0.020	0.011	0.005	0.0014	0.0036	0.077	0.262	0.107	2.355	0.726	0.000
		4	0.005	0.006	0.017	0.005	0.003	0.0011	0.0029	0.049	0.081	0.018	1.870	0.182	0.000
		5	0.011	0.023	0.021	0.010	0.020	0.0041	0.0100	0.110	0.163	0.063	2.533	0.676	0.034
	340	3	0.006	0.009	0.018	0.005	0.003	0.0016	0.0046	0.091	0.227	0.100	2.332	0.635	0.000
		4	0.011	0.027	0.029	0.017	0.020	0.0054	0.0119	0.112	0.058	0.026	2.671	0.331	0.000
		5	0.023	0.039	0.036	0.015	0.041	0.0066	0.0099	0.124	0.167	0.084	3.717	0.608	0.000
	390	3	0.002	0.007	0.021	0.005	0.005	0.0022	0.0042	0.034	0.137	0.044	2.889	0.038	0.000
		4	0.005	0.009	0.012	0.004	0.005	0.0017	0.0029	0.028	0.027	0.030	1.863	0.174	0.000
		5	0.007	0.011	0.019	0.005	0.011	0.0024	0.0060	0.052	0.127	0.070	2.390	0.420	0.036
	SD		0.004	0.006	0.005	0.007	0.009	0.0005	0.0030	0.013	0.025	0.036	0.360	0.186	0.000

RT: reactor temperature (°C); PS: pellet size (mm); SD: standard deviation.

Appendix E-5. Concentration of chemicals from vacuum pyrolysis of LAPWS and HAPWS at different reactor temperatures and pellet sizes

			Chemical concentrations (wt.%)												
			Lignin-derived compounds							Carbohydrate-derived compounds					
	RT	PS	4-vinylguaicol	Eugenol	Apocycnin	Phenol	Guaicaol	2,3-Dimethyl phenol	2,6-Dimethyl phenol	2-Furanmethanol	2(5H)-Furanone	5-Hydroxymethyl furfural	Levoglucosan	Glycolaldehyde	2-Cyclopenten-1-one
LAPWS	300	3	0.261	0.188	0.123	0.132	0.247	0.0270	0.0218	0.306	1.097	0.241	2.752	5.266	0.079
		4	0.375	0.164	0.105	0.095	0.229	0.0214	0.0195	0.440	1.043	0.212	2.369	5.311	0.075
		5	0.421	0.167	0.082	0.048	0.288	0.0137	0.0180	0.476	0.564	0.180	2.099	6.150	0.052
	425	3	0.506	0.230	0.146	0.052	0.203	0.0200	0.0269	0.490	1.023	0.265	3.380	4.443	0.025
		4	0.576	0.238	0.105	0.071	0.298	0.0237	0.0292	0.627	1.280	0.197	2.468	5.877	0.050
		5	0.684	0.276	0.131	0.064	0.213	0.0323	0.0346	0.451	0.936	0.223	2.972	4.926	0.000
	550	3	0.537	0.252	0.131	0.049	0.223	0.0207	0.0299	0.498	1.076	0.270	2.799	5.768	0.034
		4	0.528	0.253	0.141	0.089	0.187	0.0307	0.0299	0.528	0.952	0.298	3.224	4.830	0.014
		5	0.555	0.222	0.113	0.067	0.252	0.0194	0.0232	0.484	1.090	0.267	2.471	6.272	0.039
	SD		0.070	0.025	0.010	0.008	0.038	0.004	0.003	0.067	0.077	0.016	0.116	0.557	0.020
HAPWS	300	3	0.089	0.060	0.078	0.049	0.011	0.0166	0.0178	0.232	0.561	0.224	5.779	2.743	0.000
		4	0.101	0.078	0.093	0.037	0.018	0.0151	0.0187	0.256	0.650	0.248	5.742	2.293	0.000
		5	0.082	0.048	0.041	0.014	0.007	0.0065	0.0143	0.083	0.258	0.230	6.021	1.315	0.000
	425	3	0.078	0.050	0.065	0.034	0.000	0.0137	0.0130	0.198	0.401	0.229	6.032	3.230	0.000
		4	0.088	0.072	0.064	0.037	0.026	0.0157	0.0195	0.307	0.782	0.298	3.283	3.392	0.000
		5	0.080	0.070	0.091	0.034	0.000	0.0134	0.0200	0.218	0.525	0.238	5.367	2.481	0.000
	550	3	0.087	0.053	0.074	0.042	0.000	0.0151	0.0151	0.157	0.390	0.255	6.065	1.547	0.000
		4	0.053	0.045	0.062	0.029	0.000	0.0093	0.0169	0.216	0.627	0.242	6.489	3.463	0.000
		5	0.057	0.060	0.058	0.048	0.000	0.0114	0.0179	0.153	0.333	0.303	7.499	1.855	0.000
	SD		0.050	0.015	0.019	0.008	0.008	0.002	0.006	0.034	0.135	0.093	1.350	0.786	0.000

RT: reactor temperature (°C); PS: pellet size (mm); SD: standard deviation.

Appendix E-6. Concentration of chemicals from slow pyrolysis of LAPWS and HAPWS at different reactor temperatures and pellet sizes

			Chemical concentrations (wt.%)												
			Lignin-derived compounds							Carbohydrate-derived compounds					
	RT	PS	4-vinylguaicol	Eugenol	Apocycnin	Phenol	Guaicaol	2,3-Dimethyl phenol	2,6-Dimethyl phenol	2-Furanmethanol	2(5H)-Furanone	5-Hydroxymethyl furfural	Levoglucosan	Glycolaldehyde	2-Cyclopenten-1-one
LAPWS	340	3	0.009	0.006	0.024	0.054	0.084	0.0022	0.0067	0.014	0.286	0.067	1.236	1.244	0.163
		4	0.010	0.007	0.025	0.027	0.086	0.0010	0.0062	0.032	0.279	0.072	1.541	1.616	0.160
		5	0.008	0.007	0.026	0.066	0.100	0.0020	0.0082	0.013	0.321	0.075	1.267	0.950	0.143
	460	3	0.025	0.024	0.045	0.033	0.131	0.0036	0.0136	0.031	0.379	0.158	1.577	1.666	0.128
		4	0.030	0.034	0.037	0.021	0.135	0.0028	0.0144	0.068	0.373	0.135	1.472	2.276	0.114
		5	0.024	0.029	0.041	0.029	0.132	0.0038	0.0138	0.039	0.395	0.146	1.645	1.894	0.116
	580	3	0.011	0.012	0.031	0.037	0.097	0.0025	0.0072	0.018	0.323	0.083	1.506	1.837	0.131
		4	0.017	0.007	0.036	0.021	0.105	0.0008	0.0113	0.028	0.380	0.124	1.665	1.842	0.109
		5	0.011	0.006	0.029	0.036	0.090	0.0011	0.0063	0.016	0.327	0.088	1.614	1.712	0.136
	SD		0.008	0.009	0.007	0.003	0.034	0.001	0.004	0.019	0.103	0.018	0.050	0.543	0.025
HAPWS	340	3	0.007	0.004	0.015	0.028	0.018	0.0028	0.0083	0.060	0.334	0.202	2.602	1.319	0.183
		4	0.009	0.005	0.018	0.034	0.023	0.0038	0.0110	0.059	0.405	0.273	2.665	1.590	0.172
		5	0.013	0.008	0.047	0.023	0.018	0.0025	0.0137	0.050	0.325	0.342	2.405	1.220	0.161
	460	3	0.007	0.004	0.015	0.034	0.022	0.0029	0.0088	0.063	0.392	0.207	2.560	1.336	0.158
		4	0.009	0.006	0.042	0.025	0.019	0.0026	0.0104	0.062	0.355	0.261	2.911	1.379	0.172
		5	0.008	0.003	0.024	0.022	0.012	0.0019	0.0068	0.045	0.303	0.175	2.597	1.220	0.153
	580	3	0.006	0.004	0.017	0.033	0.022	0.0019	0.0078	0.043	0.409	0.216	2.763	1.514	0.158
		4	0.007	0.003	0.014	0.036	0.024	0.0028	0.0100	0.054	0.400	0.224	2.605	1.485	0.171
		5	0.007	0.004	0.017	0.023	0.013	0.0021	0.0068	0.057	0.318	0.176	2.697	1.331	0.150
	SD		0.014	0.006	0.012	0.019	0.021	0.001	0.011	0.022	0.174	0.099	1.777	1.114	0.053

RT: reactor temperature (°C); PS: pellet size (mm); SD: standard deviation.

Appendix E-7. Concentration of chemicals from fast pyrolysis of LAPWS and HAPWS at different reactor temperatures and pellet sizes

			Chemical concentrations (wt.%)												
			Lignin-derived compounds							Carbohydrate-derived compounds					
	RT	PS	4-vinylguaicol	Eugenol	Apocycnin	Phenol	Guaicaol	2,3-Dimethyl phenol	2,6-Dimethyl phenol	2-Furanmethanol	2(5H)-Furanone	5-Hydroxymethyl furfural	Levoglucosan	Glycolaldehyde	2-Cyclopenten-1-one
LAPWS	300	3	0.059	0.066	0.107	0.057	0.128	0.0165	0.0211	0.189	0.880	0.181	3.749	3.365	0.061
		4	0.058	0.063	0.099	0.107	0.114	0.0200	0.0185	0.197	0.708	0.229	3.620	3.395	0.089
		5	0.038	0.046	0.096	0.105	0.086	0.0193	0.0193	0.211	0.710	0.106	2.839	2.271	0.122
	425	3	0.042	0.046	0.111	0.059	0.137	0.0118	0.0211	0.107	0.699	0.096	3.652	1.612	0.109
		4	0.050	0.065	0.100	0.078	0.119	0.0173	0.0192	0.197	0.767	0.196	4.167	3.102	0.077
		5	0.025	0.027	0.091	0.073	0.077	0.0116	0.0159	0.089	0.564	0.130	3.478	2.350	0.090
	550	3	0.048	0.068	0.088	0.207	0.122	0.0234	0.0152	0.109	0.398	0.127	3.884	1.481	0.171
		4	0.047	0.058	0.089	0.122	0.125	0.0178	0.0148	0.109	0.458	0.108	4.018	1.738	0.142
		5	0.036	0.040	0.082	0.101	0.091	0.0170	0.0143	0.119	0.511	0.125	3.497	2.868	0.103
	SD		0.008	0.016	0.008	0.067	0.027	0.005	0.003	0.013	0.103	0.027	0.363	0.830	0.027
HAPWS	290	3	0.026	0.024	0.066	0.035	0.017	0.0048	0.0120	0.258	0.872	0.356	7.848	2.418	0.001
		4	0.017	0.021	0.057	0.017	0.010	0.0035	0.0099	0.165	0.273	0.062	6.287	0.611	0.000
		5	0.023	0.050	0.046	0.022	0.044	0.0090	0.0216	0.239	0.354	0.137	5.498	1.468	0.073
	340	3	0.016	0.025	0.048	0.013	0.009	0.0044	0.0127	0.250	0.624	0.274	6.395	1.741	0.000
		4	0.023	0.055	0.061	0.035	0.040	0.0111	0.0245	0.230	0.118	0.054	5.494	0.680	0.000
		5	0.028	0.049	0.058	0.048	0.046	0.0103	0.0230	0.246	0.224	0.081	7.546	0.719	0.000
	390	3	0.004	0.018	0.053	0.014	0.013	0.0056	0.0106	0.086	0.346	0.112	7.324	0.097	0.000
		4	0.017	0.033	0.040	0.012	0.018	0.0060	0.0101	0.096	0.094	0.104	6.457	0.603	0.000
		5	0.020	0.031	0.052	0.014	0.030	0.0068	0.0170	0.145	0.356	0.198	6.731	1.183	0.103
	SD		0.006	0.010	0.005	0.011	0.014	0.001	0.004	0.013	0.064	0.080	1.043	0.441	0.000

RT: reactor temperature (°C); PS: pellet size (mm); SD: standard deviation.

APPENDIX F: RESULTS RELATED TO CHAPTER 7

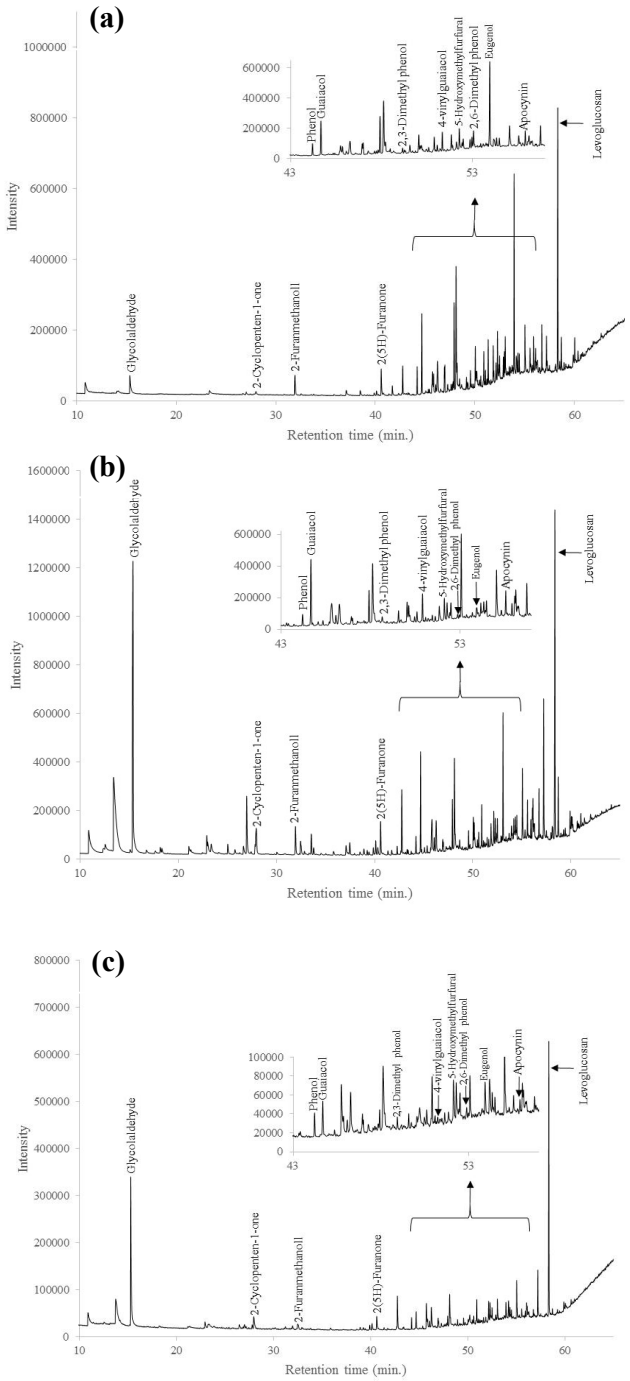

Appendix F-1. GC-MS chromatograms of the LAFR vacuum (a) and slow (b) pyrolysis tarry phase, as well as FP bio-oil (c) with corresponding selected compounds.